The *Aspergillus nidulans* Gal*f* biosynthesis pathway is a promising drug target

A Thesis Submitted to the College of

Graduate Studies and Research

in Partial Fulfillment of the Requirements

for the Degree of Doctor of Philosophy

in the Department of Biology

University of Saskatchewan

Saskatoon

Saskatchewan, Canada

By

Amira Mohamed Mohamed Ali El-Ganiny

PERMISSION TO USE

In presenting this thesis in partial fulfillment of the requirements for a Postgraduate degree from the University of Saskatchewan, I agree that the Libraries of this University may make it freely available for inspection. I further agree that permission for copying of this thesis/dissertation in any manner, in whole or in part, for scholarly purposes may be granted by the professor or professors who supervised my thesis/dissertation work or, in their absence, by the Head of the Department or the Dean of the College in which my thesis work was done. It is understood that any copying or publication or use of this thesis/dissertation or parts thereof for financial gain shall not be allowed without my written permission. It is also understood that due recognition shall be given to me and to the University of Saskatchewan in any scholarly use which may be made of any material in my thesis.

Requests for permission to copy or to make other uses of materials in this thesis in whole or part should be addressed to:

Head of the Department of Biology
University of Saskatchewan
Saskatoon, Saskatchewan S7N 5E2
Canada

Dedication

This Ph.D. thesis is dedicated to the memory of my parents

Everything I did in my life would not be possible without their guidance and support

ABSTRACT

Human systemic fungal infections are increasing, and causing high morbidity and mortality. Treatment is challenging because fungi share many metabolic pathways with mammals. Current antifungals are losing effectiveness due to drug resistance. In immunocompromised patients *Aspergillus fumigatus* causes systemic aspergillosis, the most important airborne fungal disease. Mortality from aspergillosis exceeds 50% even with aggressive treatment. We need novel antifungal drug targets. Fungal cell wall components are promising targets for antifungal therapy as they are essential for fungi and absent from humans.

The sugar galactofuranose (Gal*f*) is a 5-memberd ring form of galactose that is found in the cell walls of many fungi, but not in mammals. I used molecular biology and microscopy techniques to characterize Gal*f* biosynthesis enzymes in the model species *A. nidulans*. I studied three enzymes that catalyze sequential steps in Gal*f* biosynthesis: UgmA, UgtA and UgeA. UDP-galactopyranose mutase (UgmA) creates UDP-galactofuranose (UDP-Gal*f*) from UDP galactopyranose (UDP-Gal*p*) in the cytoplasm. The UDP-Gal*f* transporter (UgtA) moves UDP-Gal*f* into membrane bound organelles for incorporation into cell wall compartments. Upstream of UgmA, UDP-glucose/galactose epimerase (UgeA) interconverts UDP-glucose into UDP-Gal*p*, the UgmA substrate. Neither UgmA nor UgtA has a human counterpart; UgeA is in the Leloir galactose metabolism pathway that found in many organisms from bacteria to humans.

None of UgeA, UgmA and UgtA is essential for viability of *A. nidulans*, but deleting any one of them substantially reduces colony growth and sporulation (Figure i). Wild type and Gal*f* defective strains (*ugeA*Δ, *ugmA*Δ and *ugtA*Δ) were quantified for colony growth, cell morphometry, spore formation and germination, as well as wall architecture. The abundance of these proteins was regulated using the *alcA* promoter. Gal*f* content was assessed by immunolocalization in the Gal*f* defective strains, showing that those strains lacked immunodetectable Gal*f*. Gene products were localized with fluorescent protein tags; both UgmA and UgeA were cytoplasmic, whereas UgtA was Golgi localized. Wall surfaces were imaged and force-probed using transmission electron microscopy and atomic force microscopy. Overall, Gal*f* deletion strains had aberrant wall maturation, and poorly consolidated surfaces. Our results indicate that Gal*f* is necessary for abundant sporulation, wild type growth and full maturation of *Aspergillus* cell wall.

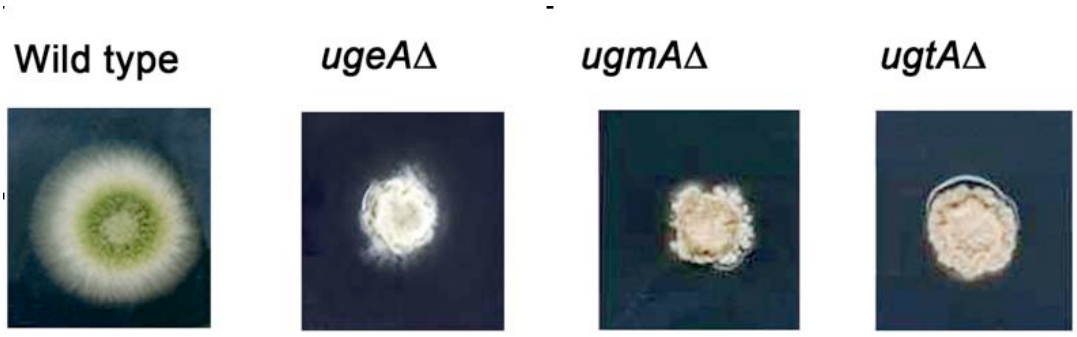

Figure i: Colony morphology of wild type and Gal*f*-defective strains: wild type strain has large abundantly sporulating colonies, whereas Gal*f*-defective strains (*ugeA*Δ*, ugmA*Δ*,* and *ugtA*Δ*)* have compact colonies with reduced sporulation.

Gal*f* deletion strains were assessed for sensitivity to antifungal agents in clinical use. They were significantly more sensitive to caspofungin and amphotericin B that target cell wall synthesis and cell membrane chemistry, respectively. Thus, anti-Gal*f* drugs (once created) may be useful in combination with existing antifungal drugs. In summary, Gal*f* biosynthesis pathway appears to be promising as an antifungal drug development target.

ACKNOWLEDGEMENTS

I am deeply thankful to my supervisor Prof. Susan Kaminskyj, for everything she taught me during the time I spend in her lab. She gave me great support and constant enthusiasm, which was truly inspiring and motivating. Also I am greatly thankful to my co-supervisor Dr. David Sanders (Chemistry Department) for giving me part of his time and supporting my research by valuable advices.

I would like to express my great appreciation to my committee members Dr. Ed Krol (College of Pharmacy & Nutrition), Dr. Yangdou Wei and Dr. Chris Todd (Biology Department). Thanks for being part of this work, for your valuable suggestions during my research, and also for critical reviewing of thesis drafts. Also I would like to thank Dr. Sijmen Schoustra for serving as my external examiner.

I would like to express my great thanks to my country Egypt, for sponsoring my 4-year scholarship and giving me a great chance to be here in Canada to do my PhD research. Also I am greatly thankful to Dr. Mayson Omar the council of the Egyptian Bureau of Cultural and Educational Affairs in Montréal for her support and accepting to extend my scholarship for extra 3 months to be able to finish my thesis.

During the time I spent in Canada, I get great help and support from many people from different Departments at the University of Saskatchewan. I would like to thank Dr. Peta Bonham-Smith and Chad Stewart for helping with qRT-PCR, Guosheng Liu for technical assistance microscopy work. Tom Bonli in Geology Department for giving permission to use Geology SEM. Dr. Jo-Anne Dillon and Dr. Mingmin Liao in VIDO for giving permission to use their level II biosafety cabinet. I really appreciate what everyone did to support my research.

I would like also to thank Dr Tanya Dahms and Biplab Paul, University of Regina for doing the atomic force microscopy for my strains. I am greatly thankful to all the members of Kaminskyj lab, especially Sharmin Afroz for being part of this team and working together on UgtA. The research in our lab was funded by the Canadian Institutes of Health Research Program (CIHR) and the Natural Sciences and Engineering Research Council (NSERC) which are gratefully acknowledged.

Finally I would like to express my thanks to my husband Dr. Khaled Gemail and my kids Abdel-rahman, Omar and Jannah, for their support, co-operation and patience during this work.

TABLE OF CONTENTS

LIST OF TABLES

LIST OF FIGURES

LIST OF ABBREVIATTIONS

AfGlfA	*Aspergillus fumigatus* UDP-galactopyranose mutase
AfGlfB	*Aspergillus fumigates* UDP-galactofuiranose transporter
AFM	Atomic force microscopy
AfpyrG	*Aspergillus fumigatus* orotidine 5'-monophosphate decarboxylase
AfpyroA	*Aspergillus fumigatus* pyridoxine biosynthesis gene
AFST	Antifungal susceptibility testing
alcA(p)	Promoter of alcohol dehydrogenase A
AmB	Amphotericin B
BLAST	Basic Local Alignment Search Tool
Casp	Caspofungin
cDNA	Complementary DNA
CFW	Calcofluor White
CM	Complete medium
CM3G	Complete medium with 3% glucose
CMFT	Complete medium with fructose and threonine
CMT	Complete medium with threonine
CR	Congo Red
Gal*f*	Galactofuranose
gDNA	Genomic DNA
GFP	Green fluorescent protein
GPI	Glycophosphatidylinositol
nkuA	*Aspergillus nidulans* homolog of human KU70
qRT-PCR	Quantitative real time polymerase chain reaction
RFP	Red fluorescent protein
SEM	Scanning electron microscopy
swoA	*Aspergillus nidulans* O-mannosyltransferase
TEM	Transmission electron microscopy
UDP-Gal*f*	uridine diphoshate galactofuranose
UDP-Gal*p*	uridine diphoshate galactopyranose

UgeA	UDP- glucose/galactose 4-epimerase A
UgmA	UDP- galactopyranose mutase A
UgtA	UDP- Gal*f* transporter A

Chapter 1

General introduction

1.1. Biology of fungi

Fungi are a diverse group of organisms. Most fungi are microscopic, but some fungi are macroscopic, particularly the fruiting bodies of mushrooms. Fungi are common in the environment and have several key roles in the functioning of ecosystems (Newbound et al., 2010). The estimated number of fungal species is at least 1.5 million, although only 72,000 have been formally described (Hawksworth, 2001). Many fungi play key roles in recycling of nutrients through decomposition of dead plant biomass and bioremediation (Barr and Aust, 1994). Some species form symbiotic relationships with plants (Rodriguez and Redman, 2008) which are essential for their survival in terrestrial environments. Some fungi are food sources for humans or animals and others are used in industrial fermentation processes to produce useful biochemicals (Bennett, 1998). However, some fungi are harmful for plants, animals and humans (Monk and Goffeau, 2008; Cannon et al., 2009).

Fungi are eukaryotic, heterotrophic microorganisms. Fungi and animals are in neighbouring kingdoms in the domain Eukarya. An important difference between these groups is that fungal cells are supported externally by a strong and flexible cell wall, whereas animal cells are not. Regarding their growth form, fungi can be multicellular (filamentous), unicellular (yeasts) or dimorphic (able to switch between unicellular and multicellular forms) (Osiewacz, 2002). Yeasts are oval or round cells that undergo cytokinesis after each mitosis, whereas filamentous fungi do not. Budding yeasts produce a daughter cell as an outgrowth from a localized site (Herskowitz, 1988). Filamentous fungi (moulds) are composed of long tubular cells called hyphae that exhibit tip localized growth (Kaminskyj and Heath, 1996). Hyphae may be divided by cross walls (septa), although certain fungal groups are aseptate. Major groups of septate fungi are the Ascomycetes (e.g. *Aspergillus* and *Candida*) and the Basidiomycetes (e.g. *Cryptococcus*). The major aseptate group of filamentous fungi is the Zygoycetes (e.g. *Rhizopus*).

Hyphae of septate filamentous fungi can be uninucleate or multinucleate. In *Aspergillus*, the nuclei are typically haploid, except before sexual reproduction or during parasexual cycle. Most filamentous fungi produce specialized cells for dispersal, called spores. Fungal spores contain one or more nuclei and mitochondria, have limited nutrient reserves, and in many species

they can survive long periods of dorminancy. Many spores are dispersed by air. Some fungi produce both sexual spores (conidiospores, products of meiosis) and asexual spores (ascospores, products of mitosis) spores (Taylor et al., 1999). For many filamentous fungi including *Aspergillus* the predominant life cycle stage is asexual (Wearing, 2010). In addition, most filamentous fungi can produce colonies from hyphal fragments. Filamentous fungi acquire nutrients during vegetative growth, forming mycelial colonies that produce spores for dispersal, as well as being able to regrow from fragments if a colony is physically damaged.

1.2. *Aspergillus nidulans* as a model system

Aspergillus is a genus of filamentous fungi that has more than 200 species. *Aspergillus* has diverse ecological roles. Its habitat includes soil, dust, and living or dead plant materials (Latge and Steinbach, 2009). The genus *Aspergillus* includes human and plant pathogens as well as beneficial species used to produce foodstuffs and industrial enzymes. For example, *A. fumigatus* is a deadly pathogen of immunocompromised patients; *A. flavus* is an agriculturally important toxin producer; *A. niger* and *A. oryzae* are used in industrial processes (Kapoor et al., 1999). As discussed below *Aspergillus nidulans* is used as an experimental model species.

Aspergillus hyphae are septate and their cells are multinucleate. *Aspergillus nidulans* hyphae are ~2-3 μm in diameter, and for wild type cells the basal cell length is ~40 μm. Apical cells are usually much longer than 40 μm and have many evenly spaced nuclei (Figure 1). *Aspergillus nidulans* reproduces asexually to form conidiophores that produce long chains of spherical uninucleated spores. Figure 2 shows the stages of the asexual reproduction in *A. nidulans*. The asexual life cycle takes ~2-3 days to be completed (Adams et al., 1998) depending on genetic background, nutrition, and temperature.

Aspergillus nidulans has many advantages that make it an excellent experimental model system including:

1. It is safe to deal with in a biosafety level 1 facility, whereas in Canada most *Aspergillus* species must be handled in a biosafety level 2 cabinet (de Aguirre et al., 2004).
2. It possesses a tractable well-characterized sexual cycle and thus a well-developed genetics system. *Aspergillus nidulans* is the asexual stage of the sexual fungus *Emericella nidulans*. The *A. nidulans* sexual cycle is well studied and readily induced

so this species is easily manipulated using classical and molecular genetics (Todd et al., 2007).

3. It has many similarities with the pathogenic species *A. fumigatus*. Analysis of cell wall sugars of *A. fumigatus* and *A. nidulans* showed that both fungi have overall similar wall sugar composition (Guest and Momany, 2000).
4. The genome of *A. nidulans* was sequenced in 2005 (Galagan et al., 2005) and the sequence was updated in 2008 (Wortman et al., 2009). There are several extensively curated comparative databases of many *Aspergillus* species and easy-to-use web-based tools for accessing, analyzing and exploring these data. Together these resources facilitate and accelerate *Aspergillus* research (Rokas et al., 2007; Arnaud et al., 2010).
5. Studies in *A. nidulans* contributes significantly to understanding fundamental biological principles and are relevant for biotechnology and industrial applications, as well as human, animal and plant fungal pathogenesis (Tsitsigiannis and Keller, 2006; Panagiotou et al., 2009).

1.3. Human fungal pathogens including *Aspergillus*

Many fungi degrade plants and plant products. However, about 300 to 400 fungi are reported to be pathogenic to humans, where they cause a wide variety of diseases (Person et al., 2010; Moran et al., 2011). Fungi can cause superficial infections of skin and mucous membranes of healthy individuals, as well as subcutaneous infections that can be painful and disfiguring. Fungi can also penetrate tissues or into the blood system of immunocompromised patients to cause invasive fungal infections which are associated with high morbidity and mortality (Menzin et al., 2009). Systemic infections can be acquired by environmental exposure or by wounding.

Fungal infections cause a variety of symptoms depending on the species, type of infection and the affected area of the body. People at risk for fungal infections include: 1) people with weak immune systems, 2) very young and very old people, 3) diabetic patients, 4) patients taking steroid medication or antibacterial antibiotics for extended periods of time, and 5) patients on chemotherapy (Ringden et al., 1991; Perlroth et al., 2007). The most common systemic human fungal pathogens are species of *Candida, Aspergillus,* and *Cryptococcus* (Richardson, 2005).

Although *Candida* infections have recently shown a slight decrease in North America, *Aspergillus* infections are increasing (Erjavec et al., 2009).

Several species of *Aspergillus* are opportunistic human pathogens that can cause a systemic disease named aspergillosis. In 1939, aspergillosis was described as "being so rare as to be of little practical importance" (reviewed in Latgé and Steinbach, 2009). Much has changed in the past 70 years. *Aspergillus fumigatus* become one of the most common fungal pathogens (Lass-Florl, 2009). *A. fumigatus* is regarded as the most important airborne pathogenic filamentous fungus in developed countries (Latgé, 2001). Other *Aspergillus* species can also cause human infections, particularly *A. flavus, A. terreus*, and *A. niger*, but also to a lesser extent *A. nidulans* (Mirhendi et al., 2007).

The lungs are the most common site of *Aspergillus* infection, which can be acquired by inhaling spores that reach the lungs to cause localized non-invasive infection called a pulmonary aspergilloma that can develop in a preexisting cavity (Thornton, 2010), Aspergillomas can also form in the brain, kidneys or other organs. *Aspergillus* species can produce allergic conditions such as allergic sinusitis (Walsh et al., 2008). Aspergillomas and allergic conditions are usually associated with low morbidity, and are seldom life-threatening (Riscili and Wood, 2009). Invasive aspergillosis happens when *Aspergillus* reaches the blood and spreads into other organs. Central nervous system aspergillosis has been reported in organ transplantation patients (Nadkarni, 2010). Despite aggressive treatment, invasive aspergillosis is still associated with high morbidity and mortality (Menzin et al., 2009). Overall, the increase in the number of immunocompromised patients has led to increase in the incidence of the life threatening fungal infections, particularly including invasive aspergillosis. Treatment of these infections is problematic with the current antifungal therapies.

1.4. Antifungal drugs and their targets

The ideal antifungal agent should have a broad spectrum of activity, low host toxicity, flexible routes of administration, and reasonable cost (Chapman et al., 2008). It is recommended that an antifungal drug target be present in a broad spectrum of fungal pathogens, be essential for fungal cell viability or pathogenicity, but not be found in human cells to avoid toxicity problems (Carrillo-Muñoz et al., 2006). Finding such a universal target appears to be unrealistic due to the underlying physiological similarities between humans and fungi (Aimanianda and Latgé, 2010).

Invasive fungal infections are often difficult to diagnose because their symptoms can be non-specific, and may resemble bacteria or viral infections. Following diagnosis, there are only about two dozen antifungal drugs, which limit therapeutic options. Antifungal drugs can be grouped into the following classes according to their targets. Cell membrane targeting antifungals either bind directly to ergosterol (polyenes) or inhibit ergosterol biosynthesis (azoles, allylamines and morpholines). Cell wall targeting antifungals (echinocandins) inhibit wall synthesis. Other agents, including flucytosine and griseofulvin, target nucleic acid biosynthesis and mitosis respectively (Carrillo-Muñoz et al., 2006; Cannon et al., 2009). No single class of antifungal is effective against all invasive mycoses, and some are highly selective. Each class of drug has a specific mode of action (summarized in table 1) and a distinct role in the treatment of particular fungal pathogens (Chen and Sorrell, 2007).

1.4.1. Polyenes

The polyenes irreversibly bind to ergosterol (Figure 3). Ergosterol is the sterol component of the fungal cell membrane (Figure 3a). It is chemically similar to human cholesterol (Figure 3b), and this similarity causes toxicity reactions in human treatment. The structure of polyenes (Figure 3c) allows them to bind to ergosterol, resulting in formation of pores in the membrane (Figure 3d) and so leakage of ions and small molecules that leads to cell death (Bolard, 1986). In addition, polyenes can cause oxidative damage to fungal cell, shown by *in vitro* studies (Brajtburg et al., 1990).

1.4.1.1. Nystatin

Nystatin was the first polyene drug to be used clinically. It is active against *Candida* and *Aspergillus*. However, nystatin can only be used topically due to problems with its solubilization in injectable solvents, as well as its human toxicity (Carrillo-Munoz et al., 1999). Nystatin is the most common antifungal agent prescribed in dentistry (Martinez-Beneyto et al. 2010). Recent developments include trials with nystatin formulations (Nystatin-Intralipid) that can be used intravenously to treat certain systemic fungal infections (Semis et al., 2010).

1.4.1.2. Amphotericin B

Amphotericin B (AmB) is a polyene developed shortly after nystatin, that was essentially the only available antifungal drug until the late 1980s. AmB is still one of the most effective drugs for treating systemic mycoses. AmB has a broad spectrum of activity, and is used successfully to treat various yeast and mould infections (Gallis et al., 1990). Resistance to AmB is rare, apart from a few species that are intrinsically resistant, including *Aspergillus terreus* and *Candida glabrata* (Walsh et al., 2003; Rezusta et al., 2008). Unfortunately, AmB clinical use is hindered by its kidney toxicity and by the requirement for intravenous administration.

Three lipid-based formulations of amphotericin B have been developed in order to minimize toxicities associated with AmB. These include amphotericin B lipid complex (ABLC), amphotericin B colloidal dispersion (ABCD), and liposomal amphotericin B (L-AmB) Their development has substantially reduced, but did not eliminate the toxicity completely (Adler-Moore and Proffitt, 2008).

1.4.2. Azole antifungal agents

Azoles are the most widely used as well as the best-studied class of antifungal drugs (Sheehan et al., 1999). In addition, azoles are abundantly used in the environment as agricultural pesticides for plant fungal diseases (Verweij et al., 2009). Azoles act by inhibiting the fungal cytochrome P450 enzyme (also known as 14α-sterol demethylase or lanosterol demethylase) (Figure 3). This depletes cellular ergosterol and causes accumulation of toxic sterol intermediates (Sheehan et al., 1999). There are two groups of azoles in clinical use: imidazoles and triazoles. Azoles are generally fungistatic against yeast, although some triazoles have fungicidal activity against moulds (Francois, 2006).

1.4.2.1. Imidazoles

The imidazoles have a five membered ring that includes two nitrogen atoms. The imidazoles in clinical use include ketoconazole, miconazole, clotrimazole, and econazole. Except for ketoconazole, imidazoles can only be applied topically due to their human toxicity, so their use is limited to treating superficial mycoses (Zhang et al., 2007).

1.4.2.2. Triazoles

The triazoles have a five membered ring with three nitrogen atoms. There are two generations of triazoles: the first generation (fluconazole and itraconazole), and the extended-spectrum second generation (voriconazole and posaconazole), which have a more extensive range. Triazoles have greater affinity for fungal compared with mammalian cytochrome P450 enzymes, so their safety profile is significantly improved for systemic use. Fluconazole is active against yeast but not against *Aspergillus* and other moulds (Koltin, 1997), so it is mainly used for treating oral candidiasis. However, development of fluconazole-resistant *Candida* strains has become a major issue in treatment of many patients (Tumbarello et al., 2009). Voriconazole and posaconazole have broad-spectrum activity against yeasts and moulds, including *Aspergillus*. Voriconazole is currently the drug of choice for the management of invasive aspergillosis. Posaconazole is the only azole drug with activity against zygomycete fungi. In general, the triazoles are relatively safe, even when used for prolonged periods, although they can cause liver toxicity (Spanakis et al., 2006).

1.4.3. Allylamines

The allylamines inhibit an early stage of ergosterol biosynthesis by binding the enzyme squalene epoxidase (Figure 4). Terbinafine is the only allylamine in clinical use. As it accumulates in hair, nail and skin, topical and oral preparations of terbinafine are widely used to treat nail and skin infections such as tinea pedis. Terbinafine displays a primary fungicidal action against dermatophytes and filamentous fungi (Petranyi et al., 1987). There are also new reports of its value in certain invasive mould infections in combination with either a triazole or AmB formulation (Yu et al., 2008). Terbinafine is generally well tolerated, but may cause gastrointestinal upset and transient elevation of liver enzymes.

1.4.4. Morpholines

There is only one morpholine used clinically, amorolfine**.** It blocks two enzymes in ergosterol biosynthesis. These are the sterol C8-C7 isomerase and the C-14 sterol reductase (Figure 4), which result in ergosterol depletion. Amorolfine is active against dermatophytes and yeasts, but it can only be applied topically (Gauwerky et al., 2009).

1.4.5. Echinocandins

The echinocandins are the newest class of antifungals. These compounds target the cell wall by inhibiting β-1,3-glucan synthase. Caspofungin (Cancidas®) was the first echinocandin approved. Caspofungin was first used clinically in 2001, followed shortly by micafungin (Mycamine®) and anidulafungin (Eraxis®) (Morrison, 2006). Echinocandins are fungistatic rather than fungicidal *in vitro* against *Aspergillus* species, but have strong efficacy *in vivo.* Echinocandins show good activity against *Candida* and *Aspergillus*, but they are not effective against *Cryptococcus neoformans* or non-*Aspergillus* moulds. Echinocandins are fungicidal against most ascomycete yeasts, but are fungistatic against most moulds (Bowman, 2002)**.** Because echinocandin action is specific to fungal cell walls, human toxicity associated with echinocandins is limited (Gauwerky et al., 2009). However, all echinocandins require injection, as there are no oral preparations available (Kauffman and Carver, 2008).

1.4.6. Flucytosine

Flucytosine (5-fluorocytosine; 5-FC) is a fluorinated analogue of the nucleotide base cytosine. It was synthesized in 1957 as a potential antitumor agent, but it was also used in 1968 for treatment of human candidiasis and cryptococcosis (Vermes et al., 2000). 5-FC is imported into cells by the action of the enzyme cytosine permease. In the cell, 5-FC is converted into the metabolically active nucleoside analogue 5-fluorouracil, which inhibits RNA and DNA synthesis. 5-FC should not be administered as a single agent because of rapid development of resistance (Barchiesi et al., 2000). Also, 5-FC should be used with caution in patients with renal insufficiency. 5-FC has very limited spectrum of activity (*Candida* species*, Cryptococcus neoformans*, some moulds). Its role is clinically limited to use in combination with AmB for treating cryptococcal meningitis (Patel, 1998).

1.4.7. Griseofulvin

Griseofulvin is an oral antifungal agent that was first used to treat superficial fungal infections of hair, nail and skin (Bedford et al., 1960). Griseofulvin has been the treatment of choice for the skin infection *tinea capitis* (ringworm) for more than 40 years (Gupta et al., 2008). Griseofulvin binds to microtubules where it acts mainly by inhibiting mitosis. Notably, the griseofulvin concentration required to inhibit the growth of fungal cells is much lower than that

required to inhibit the mammalian cells due to its higher affinity for fungal tubulin (Panda et al., 2005). Griseofulvin has recently been shown to inhibit proliferation of various types of cancer cells and to inhibit tumor growth (Rathinasamy et al., 2010).

In summary, AmB was one of the first therapeutic agents for treatment of fungal infection, but its use is limited due to human toxicity. Although azoles are less toxic, they are not effective against all fungi. In addition, the extensive use of azoles in agriculture as well as medicine has led to the development of resistance, as well as to the development of cross-resistant strains. Recent significant advances in antifungal therapy include: the development of lipid formulation of AmB, and the broad-spectrum triazoles (voriconazole and posaconazole). The newest class of antifungals, the echinocandins have relatively low human toxicity, however they are not active against *Cryptococcus* and Zygomycetes and also require injection. Overall, our current selection of antifungal drugs is insufficient given that each has limitations and that patient populations are increasing.

1.5. Problems associated with antifungal therapy

Despite the availability of effective antifungal agents including echinocandins and second-generation triazoles, therapy failure is a clinical problem with all invasive fungal infections. Therapy failure was reported in 40–70% of patients with invasive aspergillosis (Nucci and Perfect, 2008). Management of fungal infections is limited by problems of drug safety, fungal resistance and restricted effectiveness profiles (Chapman et al., 2008).

1.5.1. Toxicity and adverse reactions

Polyenes are the most toxic antifungal drugs. Amphotericin B toxicity results from the chemical similarity between ergosterol in fungal cell and cholesterol in mammalian cell. The major effect of AmB toxicity is nephrotoxicity, which is observed in approximately one third of patients. Other adverse effects of AmB include headache, chills, fever and intestinal problems (Worth et al., 2008). Recently-developed lipid-based formulations of amphotericin B are less toxic.

Azole drugs have relatively minor adverse effects, for example rashes are associated with fluconazole, gastrointestinal symptoms are observed with itraconazole, and eye symptoms are

reported in patients who receive voriconazole (Herbrecht et al., 2002; Chapman et al., 2008). Two relatively common adverse effects are associated with 5-FC: bone marrow suppression and hepatic dysfunction (Smith, 2008). In contrast, the echinocandins have a low frequency of toxicity. The most common adverse effects reported with echinocandin use are infusion reactions and elevations of liver enzyme levels (Denning, 2003).

1.5.2. Emerging resistance

Intrinsic and acquired antifungal resistance is a growing clinical problem with many fungal pathogens. Antifungal drug resistance can be caused by: 1) mutation or overexpression of the drug target, 2) biofilm formation, 3) drug efflux by upregulation of the efflux pumps, 4) stress-related tolerance that enhances short-term survival, or 5) modification of chromosomal ploidy (Monk and Goffeau, 2008; Marie and White, 2009). The extensive prophylactic use of fungistatic azole derivatives, especially fluconazole, is associated with the emergence of resistant fungal pathogens (Canuto and Rodero, 2002). Furthermore the use of azoles in agriculture has led to development of cross-resistance to related azoles that are used as drugs. This was recently found in *A. fumigatus* clinical isolates (Verweij et al. 2009). Resistance to azoles is an important factor in treatment failure. Some filamentous fungi can cause infections that are unresponsive to current therapies and so can be lethal. Antifungal drug resistance also has striking economic consequences. For example, a conservative estimate of the annual cost of evolution of resistance in the United States is US$33 billion (Cowen, 2008).

1.5.3. Low efficacy

A narrow spectrum of activity against some fungal pathogens is related to some classes of antifungals. 5-FC is active against yeasts such as *Candida* and *Cryptococcus* but has limited activity against moulds. Terbinafine is the drug of choice for treatment of dermatophyte infections but it has limited activity against invasive fungal infections. Echinocandins are effective against *Candida* and *Aspergillus* species, but not against *C. neoformans* or non-*Aspergillus* moulds (Denning and Hope, 2010).

Overall, numerous problems are associated with current antifungal therapies. The main problems are host toxicity, narrow activity spectra, and evolved resistance. Collectively these lead to high economic costs for treatment of fungal infections, as well as to increase in the

mortality rate. The problems associated with current antifungal drugs demand the development of new antifungal therapeutics.

1.6. The fungal cell wall as target for antifungal drugs

An ideal antifungal drug target should be widely distributed amongst fungal species, important for fungal cell viability or pathogenicity, but not found in humans (Carrillo-Muñoz et al., 2006). Although these general criteria may seem overly optimistic, fungal cell wall components can potentially fulfill at least some of them (Aimanianda and Latgé, 2010). The fungal wall functions include: 1) environment sensing and protection from certain environmental stressors, 2) adhesion to and penetration of host tissues, and 3) mediating secretion of pathogenicity factors and hydrolytic enzymes. Disruption of the cell wall renders the fungus susceptible to lysis or death (Aimanianda and Latge, 2010).

The fungal cell wall is a three-dimensional mesh work composed of several types of polysaccharide and glycoprotein. Despite decades of effort to characterize the composition and architecture of fungal cell walls (Bowman and Free, 2006), many details remain poorly understood. In part, this is because analysis of biologically distinctive carbohydrates is hampered by their similar chemistry. In filamentous fungi, the polysaccharides form about 90 % of the cell wall, which consists mainly of glucans, chitin and galactomannan (Gastebois et al., 2009).

Glucans are the major fungal cell wall polysaccharides, constituting about 50-60 % of the wall dry weight. Amongst these, β-1,3-glucan predominates, with β-1,6-glucans and α-1,3-glucans also present in lower amounts. Chitin, a β-1,4 polymer of N-acetylglucosamine, accounts for 10-20 % of fungal cell wall mass. In *Aspergillus* cell walls, galactomannan (GM) accounts for 20-25 % of the polysaccharides (Gastebois et al., 2009). The composition of filamentous fungi wall polysaccharides is summarized in table 2.

Galactomannans (GMs) are branched polymers composed of a linear core of α-mannans with short side chains of β-1,5-galactofuranose (Gal*f*). GMs are found in many fungi including *Aspergillus* (Latge et al., 2005). As well as being a part of the fungal cell wall, GM is the major antigen found in the bodies of patients suffering from aspergillosis (Leitao, 2003). The immunodominant epitope in the GM molecule is galactofuranose. This has been the basis of the

development of a monoclonal antibody that detects GM presence in the biological fluids of patients with invasive aspergillosis (Mennink-Kersten et al., 2004).

The cell wall is about one quarter of fungal cell biomass (Gastebois et al., 2009), and about one third of the fungal genome (~ 4000 genes) is involved in cell wall biosynthesis and maintenance (de-Groot et al., 2009). Fungal genomes typically have suites of genes with partially redundant and overlapping functions that encode synthetic enzymes for wall formation and others for its maintenance (Latge, 2007). As a result of the fungal cell wall complexity and its ability to be remodeled as growth conditions change, walls are dynamic structures that display ongoing changes in cell wall composition during growth and development, as well as in response to changing environmental conditions (Momany et al., 2004). The composition of the cell wall can be different between genera, between species of the same genus (Latge, 2007), and between disseminated growth and biofilms (Gastebois et al., 2009).

Due to the above mentioned reasons, development of compounds targeting the cell wall is challenging (Aimanianda and Latge, 2010). To date only the echinocandins are used clinically to target the fungal cell wall; these block β-1, 3-glucan synthesis (Kamigiri et al., 2004). In contrast, although inhibitors of chitin (Nikkomycin Z and Calcofluor White, CFW) and mannan (Pradimicin) synthesis have been identified, they are not clinically effective (Kim et al., 2002). Due to the importance of cell wall components for fungal growth and host invasion, and the lack of conservation with animal cell components, the cell wall could be extremely rich source of potential antifungal targets (Aimanianda and Latgé, 2010). However, each potential target pathway must be investigated individually, because of the adaptability of the fungal wall to respond to environmental stressors such as wall-targeting compounds.

The research presented in this thesis provides a comprehensive study of the biological roles of three sequential enzymes in the Gal*f* biosynthesis pathway. As will be discussed, this pathway appears to be a chink in the fungal armour that could be used as a drug development target.

1.7. Gal*f* biosynthesis as a potential drug target

Gal*f* is the 5-membered ring form of galactose that is found in several pathogenic microorganisms but not in humans (Figure 5). Gal*f* is usually found in glycoconjugates that are essential for survival or virulence of many pathogenic microorganisms including bacteria, protozoa and some fungi (Weston et al., 1998; Beverley et al., 2005; Kleczka et al., 2007; Schmalhorst et al., 2008; Lamarre et al., 2009). Gal*f* is a major carbohydrate in *A. fumigatus* walls, said to account for about 5% of the total wall dry weight of (Lamarre et al., 2009). Gal*f* is reported from four different molecules in *A. fumigatus*: galactomannans, glycoproteins, several sphingolipids and lipophosphogalactomannan (Latge, 2009). Research into Gal*f* roles in fungal cell wall structure and function has been hampered in part by analytical factors.

Gal*f* is absent from higher eukaryotes including humans, but is required for survival or virulence in many types of pathogenic microorganism. Thus the Gal*f* biosynthesis pathway (Figure 5) is thought to be a promising drug target (Pedersen and Turco, 2003; Scherman et al., 2003; Urbaniak et al., 2006; Dureau et al., 2010). Enzymes in the Gal*f* pathway have been well studied in prokaryotes (Weston et al., 1998; Mikusova et al., 2006). These include UDP-galactopyranose mutase (UGM) that catalyzes the inter-conversion between UDP-Gal*p* and UDP-Gal*f* (Weston et al., 1998) and galactofuranosyl transferase(s) that transfer Gal*f* moieties from UDP-Gal*f* to glycoconjugate molecules (Belanova et al., 2008).

In eukaryotes Gal*f* biosynthesis and incorporation in the cell wall is a multistep process that can be summarized in the following steps (Figure 5).

1) The synthesis of UDP-galactopyranose (UDP-Gal*p*) from UDP-glucose, upstream of UDP-Gal*f* biosynthesis. This step is catalyzed by the enzyme UDP-glucose/galactose epimerase (Singh et al., 2007).
2) The synthesis of UDP-Gal*f* from UDP-Gal*p*, catalyzed by UDP-galactopyranose mutase, an enzyme located in the cytoplasm (Kleczka et al., 2007). These are the 5-member and 6-member ring forms of galactose, respectively, that interconvert spontaneously in solution unless conjugated at carbon 1, such as with UDP.
3) Transport of UDP-Gal*f* into a membrane bound organelle (Golgi or endoplasmic reticulum) by the action of a UDP-Gal*f* transporter (Engel et al., 2009).
4) Incorporation of Gal*f* into glycoconjugates by the action of galactofuranosyl transferase(s). These have not yet been identified in fungi.

1.7.1. UDP-glucose-4-epimerase

UDP-glucose/galactose 4-epimerase (named *UGE*, *GalE, Gal10* in various systems) catalyzes the synthesis of UDP-galactopyranose from UDP-glucose. This is a step in the Leloir pathway of galactose metabolism that is highly conserved in species ranging from bacteria to humans (Allard et al., 2001; Holden et al., 2003)**.** In *Saccharomyces cerevisiae*, galactose metabolism enzymes are encoded by *GAL1* (galactokinase)*, GAL7* (galactose-1-phosphate uridylyltransferase)*,* and *GAL10* (a combined mutarotase and UDP-glucose/galactose-4-epimerase) (Holden et al., 2003). The GAL10 enzyme dual-activity is restricted to *S. cerevisiae* and a few other yeasts including *Kluyveromyces fragilis*, *Schizosacchromyces pombe and Candida albicans* (Scott and Timson, 2007, Brahma et al., 2009). The crystal structure of *ScGal10* shows an N-terminal epimerase domain and a C-terminal mutarotase domain joined by a short linker (Thoden and Holden, 2005). In most organisms, UGE is encoded by a gene distinct from that encoding the mutarotase (Singh et al., 2007).

UGE interconverts UDP-galactopyranose (UDP-Gal*p*) and UDP-glucopyranose (UDP-Glc). This may be the only source of providing galactose to the cell if it is not present in the environment (Singh et al., 2007). In some organisms including *Trypanosoma* species, hexose transporters are unable to uptake galactose directly from the media. Instead the parasite must generate galactose via UGE (MacRae et al., 2006). Human GalE not only contributes to Leloir pathway galactose metabolism, but can also interconvert UDP-N-acetylglucosamine and UDP-N-acetylgalactosamine which are important for glycosylation of some macromolecules in humans (Schulz et al., 2005).

Fungi including *C. neoformans, S. pombe* and some *Aspergillus* species have two genes that both encode functional UDP-glucose/galactose epimerases (Moyrand, 2008; Suzuki et al., 2009), whereas other organisms (e.g. *C. albicans*) have only one (Singh et al., 2007). *Arabidopsis thaliana* has five genes encoding UDP-glucose/UDP-galactose 4-epimerases (named *UGE1* to *UGE5*), that function in different metabolic situations (Barber et al., 2006).

Loss of GalE activity in humans causes a metabolic disorder called galactosemia (Openo et al., 2006). Epimerase deficiency galactosemia (galactosemia type III) can be benign or with symptoms that can be controlled by restricting lactose or galactose in the diet (Wohlers et al., 1999). Mutations of *GalE* in *S. cerevisiae* cause galactose sensitivity: the mutants cease growth in response to trace quantities of galactose, even in the presence of other carbon sources

(Wasilenko and Fridovich-Keil, 2006). *CaGAL10 (C. albicans* glucose / galactose-4-epimerase) was found to be essential for growth on galactose. Even if Ca*GAL10Δ* cells are grown on glucose they show some phenotypic defects. *CaGAL10* was found to be important for cell wall integrity and resistance to stress, which can affect cell permeability and sensitivity to antibiotics (Singh et al., 2007). *Cryptococcus neoformans* epimerases *UGE1* and *UGE2* have distinct roles in *C. neoformans* physiology. *UGE1* is essential for capsule formation and virulence, whereas *UGE2* was necessary for the cells to utilize galactose as a carbon source at 30ºC but is not required for virulence (Moyrand et al., 2008). In the protozoan, *Trypanosoma. brucei,* galactose metabolism mediated by UDP-glucose-4-epimerase is essential for parasite growth and survival (Roper et al., 2002).

UDP-glucose/galactose epimerase is well characterized both structurally and kinetically (Holden et al., 2003). Epimerases from *E. coli* (Thoden et al., 1996)*, S. cerevisiae* (Thoden and Holden, 2005) and human sources (Thoden et al., 2000) have been cloned and sequenced, and their X-ray crystallographic structures are solved (Thoden and Holden, 2005). Epimerases from *E. coli*, yeast and human are functional as dimers. Understanding the structure of UGE from different organisms could help in designing inhibitors that are selective for UGEs from microorganisms.

Some inhibitors of UGE were discovered from a directed library screen (Winans and Bertozzi, 2002). Inhibitors for TbGalE have been tested *in vivo*, and display some selectivity between human and *Trypanosoma* enzymes (Urbaniak et al., 2006). Although UgeA is highly conserved amongst diverse organisms, it may be possible to find compounds that selectively inhibit its function in specific organisms.

In summary, UDP-glucose/galactose-4-epimerase catalyzes a step in galactose metabolism that is highly conserved. UgeA activity is encoded by single gene in some organisms or multiple genes in others. UDP-glucose/galactose 4-epimerase appears to have distinct roles in different systems. For example UGE is essential for survival of the protozoan *Trypanosoma*. However its deletion only causes galactose sensitivity in yeast, and leads to metabolic disorder in human. Despite the crystal structure of different UGE(s) have been solved, few specific inhibitors are reported in the literature. More work could be done to find inhibitors that are selective for UGE in specific types of pathogenic microorganism.

1.7.2. UDP-galactopyranose mutase

UDP-galactopyranose mutase (UGM, also called GLF in some species) is the key enzyme in the Gal*f* biosynthesis pathway. UGM was first identified in *E. coli* (Nassau et al., 1996), followed shortly thereafter by its identification in *Klebsiella pneumoniae* and *Mycobacterium tuberculosis* (Köplin, 1997; Weston et al., 1998). UGM has also been identified in eukaryotes including *A. fumigatus, C. neoformans* and *L. major* (Bakker et al., 2005; Beverley et al., 2005; Schmalhorst et al., 2008). There is only about 15% - 20% amino acid sequence identity between the prokaryotic and the eukaryotic UGMs, which is restricted to its active site. In contrast, eukaryotic UGMs are more closely related to each other than to prokaryotes. For example, *A. fumigatus* and *L. major* UGM share 51 % amino acid sequence identity (Beverley et al., 2005).

The genes encoding UGM (*ugm* or *glf*) have been studied in several microorganisms. Those genes have consistently been shown to be important for survival, growth, and / or pathogenicity. Deletion of *glf* from *M. smegmatis* showed that it was essential for growth and survival (Pan et al., 2001). Targeted replacement of *GLF* in *L. major* (the causative agent of leishmaniasis) caused attenuation of virulence (Kleczka et al., 2007). Deletion of *glf-1* from the nematode *Caenorhabditis elegans* caused a significant late embryonic and larval lethality due to defective surface coat formation (Novelli et al., 2009).

Aspergillus species including *A. fumigatus* and *A. nidulans* contain only a single copy of the gene encoding UGM. However, Damveld *et al* (2008) reported that *A. niger* has two genes that encode putative UDP-galactopyranose mutase (*ugmA* & *ugmB*). Deletion of *A. niger ugmA* impaired the colony growth and produced a Calcofluor-sensitive phenotype, whereas deletion of *ugmB* did not create any observable changes in phenotype (Damveld et al., 2008).

Schmalhorst et al. (2008) reported that deletion of *A. fumigatus glfA* led to hyphae with thinner cell walls, as well as reduced colony growth, attenuated virulence, and increased susceptibility to antifungals. Lamarre *et al* (2009) created an *A. fumigatus* strain that lacked Af*UGM1*, another name for Af*glfA*. Their mutant lacked Gal*f*, had reduced growth and a hyper adhesive phenotype but it was as pathogenic as the wild type strain. Disparities between Schmalhorst et al (2008) and Lamarre et al (2009) results particularly regarding the pathogenicity of the deletion strains must be resolved.

UGM overexpression in *M. bovis* increases resistance to isoniazid, an important drug used to treat tuberculosis (Richards and Lowary, 2009). Because UGM is essential for survival in bacteria and for virulence of protozoa and fungi, it is thought to be good target for antimicrobial therapy.

Rational drug design of UGM inhibitors requires understanding its structure and catalytic mechanism. The first crystal structure of UGM was reported in 2001 from *E. coli* (Sanders et al., 2001a; Sanders et al., 2001b), followed by the crystal structure in *M. tuberculosis* and *K. pneumonia* (Beis et al., 2005). While many studies have been done on the prokaryotic UGM, little is known about eukaryotic UGM. Preliminary mechanistic studies of UGMs from *A. fumigatus* and *T. cruzi* were reported last year (Oppenheimer et al., 2010). Future work in this field should include a high-resolution crystal structure of UGM alone and bound to substrate, which will guide further efforts to design inhibitors. Several groups have designed inhibitors for UGM that mimic its substrate. Some of these inhibitors are active against mycobacteria (Scherman et al., 2003; Soltero-Higgin et al., 2004; Dykhuizen et al., 2008). Synthetic UDP-furanoses are reported to be active against *L. donovani* (Dureau et al., 2010).

Taken together, UGM is a key enzyme in Gal*f* biosynthesis, since it catalyzes the interconversion of UDP-Gal*p* and UDP-Gal*f*. UGM has been found in many microorganisms, but it is absent from mammals. Deletion of the gene encoding UGM showed that it is essential for survival of bacteria and for virulence of protozoa and the growth of fungi. Importantly, *Aspergillus fumigatus* has only one UGM encoding gene. Several inhibitors of bacterial UGM have been reported, but no inhibitor has been developed that is effective against fungal UGM.

1.7.3 UDP-Gal*f* transporter

The cell surface glycoconjugates are fundamental components of many organisms including fungi (Pinto et al., 2008). Approximately 80% of secreted proteins are covalently linked to a sugar (Caffaro and Hirschberg, 2006). Glycosylation of these compounds depends on a sugar donor that is typically a nucleoside diphosphate sugar (NDP-sugar), although a few are nucleoside monophosphate sugars (Handford et al., 2006). Many nucleotide sugars are synthesized in the cytosol, then translocated to the lumen of Golgi or ER by the action of the nucleotide-sugar transporters (NSTs) (Handford et al., 2006). NSTs translocate cytosolic nucleotide-sugars to the endomembrane system using luminal UMP as an antiporter substrate,

where the entrance of NDP-sugar is coupled to the exit of NMP (Reyes and Orellana, 2008; Sesma et al., 2009).

NSTs are transporter proteins, typically with 6–10 transmembrane domains. They occur in all eukaryotes and are frequently located in the membrane of the Golgi apparatus, an organelle in the endomembrane system where the biosynthesis of glycoconjugates and polysaccharides occurs (Reyes and Orellana, 2008). NSTs are structurally conserved and can be identified from genome databases; however their substrate specificity cannot be predicted from the sequence (Berninsone and Hirschberg, 2000). A large number of NSTs have been identified; many of them are able to transport multiple substrates, although a few have been shown to be monospecific (Handford et al., 2006).

UDP-Gal*f* is an NDP-sugar that is synthesized in the cytosol and then translocated into the organelles of the secretory pathway prior to incorporation into glycoconjugates. A transporter for UDP-Gal*f* has been identified in the genome of *A. fumigatus*, and named GlfB (Engel et al., 2009). *A. fumigatus* GlfB was found to be localized in Golgi. *In vitro* transport assays established binding of UDP-Gal*f* to GlfB and excluded transport of several other nucleotide sugars, which indicates that GlfB is specific for UDP-Gal*f* transportation (Engel et al., 2009).

In summary, the UDP-Gal*f* transporter actively translocates the nucleotide sugar UDP-Gal*f* from cytosol into Golgi equivalent in fungi. It was recently characterized in *Aspergillus fumigatus*. To our knowledge this is the only studied UDP-Gal*f* transporter till now.

1.7.4. Galactofuranosyl transferases

For production of Gal*f*-containing glycoconjugates, additional processing steps are required to conjugate Gal*f* subunits to other cell wall components and to each other (Chen and Okayama, 1988). These glycosylation steps take place in one or more compartments of the endomembrane system, and involve enzymes called galactofuranosyl transferases. In general, glycosyltransferases are specific enzymes that catalyze the transfer of monosaccharides to proteins, lipids or carbohydrates to produce glycoconjugates. Glycoconjugates are often vital for survival or virulence of many organisms (Breton et al., 2001, Deshpande et al., 2008). Many glycosyltransferases have been identified in fungi including glucan synthases, chitin synthases, and mannosyltransferses (Klutts et al., 2006).

Galactofuranosyl transferases were first characterized in prokaryotes. A bifunctional galactofuranosyl transferase (WbbO) was identified in *Klebsiella pneumoniae*. WbbO can transfer both Gal*p* and Gal*f* residues to form galactan molecules (Guan et al., 2001). Two galactofuranosyl transferases were identified in *Mycobacterium*, GlfT1 (Rv3782) and GlfT2 (Rv3808c) (Belanova et al., 2008). GlfT1 initiates the first step of galactan synthesis, whereas GlfT2 is a bifunctional enzyme responsible for the majority of galactan polymerization (Szczepina et al., 2010). GlfT2 was identified as essential for growth of *Mycobacterium* (Pan et al., 2001). GlfT1 was identified by its sequence similarity to GlfT2 and its location within the "possible galactan biosynthetic gene cluster" (Mikusova et al., 2006). A putative *E. coli* galactofuranosyl transferase, WbbI was partially characterized *in vitro* (Wing et al., 2006).

In eukaryotes, sequence analysis of parasitic protozoa shows that there are at least six putative UDP-Gal*f* transferases in the *Leishmania* genome and more than 20 related genes in *Trypanosoma cruzi* (Zhang et al., 2004; Wing et al., 2006). However, to date only one galactofuranosyl transferase has been identified and characterized in the *Leishmania*, LPG1 (Novozhilova and Bovin, 2010). Beverly *et al* (2005) note that no candidate UDP-Gal*f* transferases have so far been reported in fungi. Deshpande *et al* (2008) tried to identify a putative Gal*f* transferase in filamentous fungi using homology searches and applying hidden Markov model (HMM) techniques, but could not find any possible hits. However Gal*f* transferases should exist given the number of Gal*f* containing glycoconjugates reported in fungi (Latge, 2009).

Synthetic UDP-furanoses were identified recently as potent drugs against *Mycobacterium.* These synthetic furanoses are inhibitors for GlfT1 (Peltier et al., 2010). More research needs to be done to understand the structure of galactofuranosyl transferases and hence design inhibitors for them. In summary galactofuranosyl transferases are a specific type of glycosyl transferases that incorporates Gal*f* residues into glycoconjugates. They have been identified in bacteria and protozoa but not in fungi.

1.8. Assessment of antifungal drugs efficiency

Antifungal susceptibility testing (AFST) is an *in vitro* method used to assess the response of a fungus to a drug or drug combination. AFST was less well developed and utilized than

antibacterial testing (Lass-Flörl, 2006). The requirement for accurate and predictive susceptibility testing of fungi did not become a major issue until the start of the AIDS era, which caused dramatic increase in the incidence of fungal infections (Johnson, 2008). Recently, AFST has been standardized for both yeasts and filamentous fungi. Two international standard methodologies are available: the Clinical and Laboratory Standards Institute (CLSI) method (Espinel-Ingroff et al., 2005), and European Committee for Antimicrobial Susceptibility Testing (EUCAST) method (Lass-Flörl, 2006). Both of these methods are broth-microdilution based assays and both have good inter- and intra-laboratory reproducibility (Lass- Flörl et al., 2010).

Broth dilution methods use the minimum inhibitory concentrations (MICs) of antifungal drugs as an endpoint to define an appropriate dose. MIC is defined as the lowest concentration of the drug that inhibits the growth of fungi within a defined period of time. MIC is expressed as mg/L and must be observed visually (Subcommittee on Antifungal Susceptibility Testing (AFST) of EUCAST, 2008).

Assessment of *in vitro* activity of echinocandins against *Aspergillus spp*. is complicated because of the phenomena of trailing endpoints and the fact that MIC values are usually higher than the allowed treatment doses, which makes MICs for *Aspergillus* poorly reproducible. In order to deal with these difficulties, the minimum effective concentration (MEC) is used as an end point for echinocandins, since it generates more consistent susceptibility results than MIC. MEC is defined as the lowest drug concentration at which short, stubby, highly branched hyphae are observed by microscopic examination (Espinel-Ingroff et al., 2007).

Besides broth-microdilution methods, agar-based testing methods can be used for AFST, including agar diffusion, disc diffusion and E-test (Lass-Florl et al., 2010). Disc-based methods are convenient, simple and economical, with easy to read end points. A CLSI reference method (M 44A) was established for AFST in *Candida* species (Pfaller et al., 2005). Recently a disc-based assay for susceptibility testing of dermatophytes has been developed (Nweze et al., 2010).

Several studies have compared the results of AFST using disc diffusion and standardized broth microdilution method (Espinel-Ingroff et al., 2007; Messer et al., 2007; Maida et al., 2008). These studies tried to correlate inhibition zone diameter with MIC values and they suggest that the agar-based methods hold promise as simple and reliable method for AFST, once they are standardized. The CLSI has proposed a standardized disc diffusion method for mould

susceptibility testing (M51-P, under development) (Espinel-Ingroff et al., 2009). Overall, AFST is a method to predict the response of fungi to certain drugs. The broth-based AFST have been standardized for yeast and mould. The disc-based methods are easy and economical, but they are waiting for standardization.

1.9. Towards more effective antifungal therapy (drug combination)

The high rate of mortality from mould infections and the relatively limited number of effective antifungal drugs have produced pressing needs for new therapeutic options. This has led to the use of drug combination, especially to treat intractable infections (Kontoyiannis and Lewis, 2004). There are several possible benefits for using two or more antifungal drugs, instead of monotherapy. Combination therapy may achieve fungicidal activity that is not possible with only one agent. Drug combinations may be effective at lower drug dosages, thus reducing toxic side-effects while also increasing efficacy. Combination therapies may delay or possibly prevent the emergence of drug-resistant mutants. In addition, combination therapy may provide broader spectrum coverage for seriously ill patients (Wirk and Wingard, 2008).

When two drugs are used together, drug interaction can be classified as synergistic, additive/indifferent or antagonistic on the basis of the fractional inhibitory concentration (FIC) index. The FIC index is the sum of the FICs for each drug. The combined FIC is defined as the MIC of each drug when used in combination divided by the MIC of the drug when used alone (Te Dorsthorst et al., 2002). In case of synergism, the combined effect of two drugs is greater than the sum of the individual effects. Additive interaction means the effect of two drugs is equal to the sum of the effect of them when taken separately. In case of antagonism the combined effect is less than the sum of the effects produced by each drug separately (Kontoyiannis and Lewis, 2003).

Numerous *in vitro* investigations of various combinations of antifungal agents and trials in animal models of fungal infection have been performed (Johnson and Perfect, 2010). However, most of these antifungal combinations have not been evaluated in large clinical trials, in part because of the time and expense involved (Marr, 2004**,** Ashley and Johnson, 2011). To date, it has been shown that toxicity of amphotericin B can be reduced in combination with echinocandins (Caillot et al., 2007; Mihu et al., 2010). Also, use of flucytosine in combination

with many other drugs helps in preventing the rapid development of resistance (Johnson et al., 2004).

A problem with combination therapy is lack of generality of effect: combinations that prove successful with certain infections may not be broadly effective in improve the therapeutic outcome in others. For example, combination therapy can successfully treat cryptococcal meningitis where 5-FC used in combination with polyenes or azoles (Van et al., 1997). However, the same combinations don't work as well in treatment of invasive candidiasis, aspergillosis and zygomycoses (Chen et al., 2010). Additional clinical trials should be performed to support the use of combination therapy for different fungal infections, but again these are extremely expensive.

Recently there is a new trend toward developing methods to exploit chemosensitization to antifungal drugs (Kim et al., 2008). The chemicals used for chemosensitization do not have antifungal activity but can augment the efficacy and lower dosage of antifungals. HSP90 inhibitors, calcineurin inhibitors and fungal efflux pump inhibitors are examples of chemicals that are used in combination with antifungals to give better outcome (Onyewu et al., 2003; Cernicka et al., 2007; Cowen, 2008).

Overall, there are several trials to apply the idea of combination therapy in management of fungal infections. Combination therapy has been used successfully for treatment of cryptococcal infections. Several *in vitro* and *in vivo* studies tested different combination of antifungal drugs towards various infections. However, they should be tested clinically before approval.

1.10. Summary

Life threatening fungal infections, including invasive aspergillosis, have increased dramatically in the last three decades, in part because the susceptible population is growing, and also as resistant fungal pathogen strains develop. Despite new and combination drug treatments, systemic fungal infections are associated with high morbidity and mortality. We are in critical need of new and validated targets for developing novel types of antifungal drug. Some cell wall components are promising targets for new drug development, since the cell wall is essential for fungi and it is not found in humans. Galactofuranose is a component of the fungal cell wall that

is important for normal growth in culture, and also plays a role in virulence in some fungal diseases.

Synthesis of Gal*f*-containing compounds for the cell wall is a multi-step process. UDP-galactopyranose mutase (UGM), the UDP-Galf transporter (UGT) and galactofuranosyl transferases are enzymes that catalyze sequential steps in Gal*f* biosynthesis. UDP-glucose/galactose-4-epimerase catalyzes the upstream step from UGM, and hence contributes to Gal*f* biosynthesis. Gal*f* biosynthesis enzymes are well studied in bacteria, and inhibitors of these enzymes show potent activity against *Mycobacterium*. None of these inhibitors is yet used clinically. The enzymes involved in Gal*f* biosynthesis in fungi are under investigation by many groups.

In our lab we are studying Gal*f* biosynthesis enzymes in a safe and experimentally tractable model fungus, *Aspergillus nidulans,* which is closely related to the pathogen species *A. fumigatus*. During my research, I characterized the biological function of Gal*f* biosynthesis enzymes in *A. nidulans* using gene deletion strategy, and by controlling gene expression with an inducible promoter to compare the effects of gene repression and induction. Phenotype characterization of the Gal*f*-defective strains in comparison to wild type strain used fluorescence microscopy, SEM, TEM, and AFM. Gene product localization used GFP tagging, and Gal*f* localization used immunofluorescence microscopy. To assess whether Gal*f*-targeting compounds (if and when created and validated) might be useful for combination therapy, I assessed the sensitivity of the Gal*f*-defective strains to commercially available antifungal drugs.

1.11. Outline and objectives

My thesis has seven chapters in total. The first chapter is the general introduction. Chapters 2-6 contain 5 manuscripts which discuss biological roles of UgmA (chapter 2), UgeA (chapter 3), and UgtA (chapter 4). Chapter 5 describes the cell wall surface characteristics of Gal*f* deletion strains. Chapter 6 discusses how changing the level of expression of *ugmA* alters antifungal drug sensitivity and morphogenesis. My roles and those of the other authors in these manuscripts are described on the first page of each chapter. Finally, in chapter 7, I discuss my research results in terms of its importance to understanding fungal growth, development and

pathogenicity, and whether Gal*f* should continue to be considered as an anti-fungal drug development target.

There general objectives for my research work are

1. Exploring the biological roles of Gal*f* biosynthesis enzymes in the model filamentous fungi *Aspergillus nidulans*

   Hypothesis: the strains that have a defect in Gal*f*-biosynthesis enzymes will lack Gal*f* which will result in a wall defect causing impaired growth
2. Assessing the sensitivity of Gal*f*-defective strains to available antifungal drugs

   Hypothesis: deletion strains will have a wall defect that will make them more sensitive to wall-targeting agents

References

Adams, T.H., Wieser, J.K., Yu, J., 1998. Asexual Sporulation in *Aspergillus nidulans*. Microbiol. Mol. Biol. Rev. 62, 35-54.

Adler-Moore, J.P., Proffitt, R.T., 2008. Amphotericin B lipid preparations: what are the differences? Clin. Microbiol. Infect. 14 Suppl 4, 25-36.

Aimanianda, V., Latge, J.P., 2010. Problems and hopes in the development of drugs targeting the fungal cell wall. Expert Rev. Anti Infect. Ther. 8, 359-364.

Allard, S.T., Giraud, M.F., Naismith, J.H., 2001. Epimerases: structure, function and mechanism. Cell Mol. Life Sci. 58, 1650-1665.

Arnaud, M.B., Chibucos, M.C., Costanzo, M.C., Crabtree, J., Inglis, D.O., Lotia, A., Orvis, J., Shah, P., Skrzypek, M.S., Binkley, G., Miyasato, S.R., Wortman, J.R., Sherlock, G., 2010. The *Aspergillus* Genome Database, a curated comparative genomics resource for gene, protein and sequence information for the *Aspergillus* research community. Nucleic Acids Res. 38, D420-427.

Ashley E.D., and Johnson M.D., 2011 Combination antifungal therapy. In *Essentials of clinical mycology*, Part 2, 153-163, DOI: 10.1007/978-1-4419-6640-7_10.

Bakker, H., Kleczka, B., Gerardy-Schahn, R., Routier, F.H., 2005. Identification and partial characterization of two eukaryotic UDP-galactopyranose mutases. Biol. Chem. 386, 657-661.

Barber, C., Rosti, J., Rawat, A., Findlay, K., Roberts, K., Seifert, G.J., 2006. Distinct properties of the five UDP-D-glucose/UDP-D-galactose 4-epimerase isoforms of *Arabidopsis thaliana*. J. Biol. Chem. 281, 17276-17285.

Barchiesi, F., Arzeni, D., Caselli, F., Scalise, G., 2000. Primary resistance to flucytosine among clinical isolates of *Candida* spp. J. Antimicrob. Chemother. 45, 408-409.

Barr, D.P., Aust, S.D., 1994. Pollutant degradation by white rot fungi. Rev. Environ. Contam. Toxicol. 138, 49-72.

Bartnicki-Garcia, 2002 Hyphal tip growth: outstanding questions. In Molecular biology of fungal development. New York. pp. 29-58.

Bedford, C., Busfield, D., Child, K.J., Macgregor, I., Sutherland, P., Tomich, E.G., 1960. Studies on the biological disposition of griseofulvin, an oral antifungal agent. Arch. Dermatol. 81, 735-745.

Beis, K., Srikannathasan, V., Liu, H., Fullerton, S.W., Bamford, V.A., Sanders, D.A., Whitfield, C., McNeil, M.R., Naismith, J.H., 2005. Crystal structures of *Mycobacterium tuberculosis* and *Klebsiella pneumoniae* UDP-galactopyranose mutase in the oxidised state and *Klebsiella pneumoniae* UDP-galactopyranose mutase in the (active) reduced state. J. Mol. Biol. 348, 971-982.

Belanova, M., Dianiskova, P., Brennan, P.J., Completo, G.C., Rose, N.L., Lowary, T.L., Mikusova, K., 2008. Galactosyl transferases in mycobacterial cell wall synthesis. J. Bacteriol. 190, 1141-1145.

Bennett, J.W., 1998. Mycotechnology: the role of fungi in biotechnology. J. Biotechnol. 66, 101-107.

Berninsone, P.M., Hirschberg, C.B., 2000. Nucleotide sugar transporters of the Golgi apparatus. Curr. Opin. Struct. Biol. 10, 542-547.

Beverley, S.M., Owens, K.L., Showalter, M., Griffith, C.L., Doering, T.L., Jones, V.C., McNeil, M.R., 2005. Eukaryotic UDP-galactopyranose mutase (*GLF* gene) in microbial and metazoal pathogens. Eukaryot. Cell. 4, 1147-1154.

Bolard, J., 1986. How do the polyene macrolide antibiotics affect the cellular membrane properties? Biochim. Biophys. Acta 864, 257-304.

Bowman, J.C., 2002. The antifungal echinocandin caspofungin acetate kills growing cells of *Aspergillus fumigatus in vitro.* Antimicrobial Agents Chemother. 46, 3001-3012.

Bowman, S. M., Free, S. J., 2006. The structure and synthesis of the fungal cell wall. BioEssays 28, 799-808.

Brahma, A., Banerjee, N., Bhattacharyya, D., 2009. UDP-galactose 4-epimerase from *Kluyveromyces fragilis* catalytic sites of the homodimeric enzyme are functional and regulated. FEBS J. 276, 6725-6740.

Brajtburg, J., Powderly, W.G., Kobayashi, G.S., Medoff, G., 1990. Amphotericin B: current understanding of mechanisms of action. Antimicrob. Agents Chemother. 34, 183-8.

Breton, C., Mucha, J., Jeanneau, C., 2001. Structural and functional features of glycosyltransferases. Biochimie 83, 713-718.

Caffaro, C.E., Hirschberg, C.B., 2006. Nucleotide sugar transporters of the Golgi apparatus: from basic science to diseases. Acc. Chem. Res. 39, 805-812.

Caillot, D., Thiebaut, A., Herbrecht, R., de Botton, S., Pigneux, A., Bernard, F., Larche, J., Monchecourt, F., Alfandari, S., Mahi, L., 2007. Liposomal amphotericin B in combination with caspofungin for invasive aspergillosis in patients with hematologic malignancies: a randomized pilot study (Combistrat trial). Cancer 110, 2740-6.

Cannon, R.D., Lamping, E., Holmes, A.R., Niimi, K., Baret, P.V., Keniya, M.V., Tanabe, K., Niimi, M., Goffeau, A., Monk, B.C., 2009. Efflux-mediated antifungal drug resistance. Clin. Microbiol. Rev. 22, 291,321.

Canuto, M.M., Rodero, F.G., 2002. Antifungal drug resistance to azoles and polyenes. The Lancet Infectious Diseases, 2, 550-563.

Carrillo-Muñoz, A.J., Giusiano, G., Ezkurra, P.A., Quindós, G., 2006. Antifungal agents: mode of action in yeast cells. Rev. Esp. Quimioter. 19, 130-139.

Carrillo-Munoz, A.J., Quindos, G., Tur, C., Ruesga, M.T., Miranda, Y., del Valle, O., Cossum, P.A., Wallace, T.L., 1999. *In-vitro* antifungal activity of liposomal nystatin in comparison with nystatin, amphotericin B cholesteryl sulphate, liposomal amphotericin B, amphotericin B lipid complex, amphotericin B desoxycholate, fluconazole and itraconazole. J. Antimicrob. Chemother. 44, 397-401.

Cernicka, J., Kozovska, Z., Hnatova, M., Valachovic, M., Hapala, I., Riedl, Z., Hajós, G., Subik, J., 2007. Chemosensitisation of drug-resistant and drug-sensitive yeast cells to antifungals. International Journal of Antimicrobial Agents, 29, 170-18.

Chapman, S.W., Sullivan, D.C., Cleary, J.D., 2008. In search of the holy grail of antifungal therapy. Trans. Am. Clin. Climatol. Assoc. 119, 197-216.

Chen, C.A., Okayama, H., 1988. Calcium phosphate-mediated gene transfer: a highly efficient transfection system for stably transforming cells with plasmid DNA. BioTechniques 6, 632-638.

Chen, S.C., Sorrell, T.C., 2007. Antifungal agents. Med. J. Aust. 187, 404-409.

Chen, S.C., Playford, E.G., Sorrell, T.C., 2010. Antifungal therapy in invasive fungal infections. Current Opinion in Pharmacology 10, 522-530.

Cowen, L.E., 2008. The evolution of fungal drug resistance: modulating the trajectory from genotype to phenotype. Nat. Rev. Microbiol. 6, 187-198.

Damveld, R.A., Franken, A., Arentshorst, M., Punt, P.J., Klis, F.M., van den Hondel, C.A., Ram, A.F., 2008. A novel screening method for cell wall mutants in *Aspergillus niger* identifies

UDP-galactopyranose mutase as an important protein in fungal cell wall biosynthesis. Genetics 178, 873-881.

de Aguirre, L., Hurst, S.F., Choi, J.S., Shin, J.H., Hinrikson, H.P., Morrison, C.J., 2004. Rapid differentiation of *Aspergillus species* from other medically important opportunistic molds and yeasts by PCR-enzyme immunoassay. J. Clin. Microbiol. 42, 3495-3504.

de Groot, P.J.W., Brandt, B.W., Horiuchi, H., Ram, A.F.J., De Koster, C.G. and Klis, F.M. 2009. Comprehensive genomic analysis of cell wall genes in *Aspergillus nidulans*. Fung. Genet. Biol. 46, S72-S81.

Denning, D.W., 2003. Echinocandin antifungal drugs. The Lancet 362, 1142-1151.

Denning, D.W., Hope, W.W., 2010. Therapy for fungal diseases: opportunities and priorities. Trends Microbiol. 18, 195-204.

Deshpande, N., Wilkins, M.R., Packer, N., Nevalainen, H., 2008. Protein glycosylation pathways in filamentous fungi. Glycobiology 18, 626-637.

Dureau, R., Robert-Gangneux, F., Gangneux, J.P., Nugier-Chauvin, C., Legentil, L., Daniellou, R., Ferrieres, V., 2010. Synthetic UDP-furanoses inhibit the growth of the parasite *Leishmania*. Carbohydr. Res. 345(10), 1299-1305

Dykhuizen, E.C., May, J.F., Tongpenyai, A., Kiessling, L.L., 2008. Inhibitors of UDP-galactopyranose mutase thwart mycobacterial growth. J. Am. Chem. Soc. 130, 6706-6707.

Engel, J., Schmalhorst, P.S., Dork-Bousset, T., Ferrieres, V., Routier, F.H., 2009. A single UDP-galactofuranose transporter is required for galactofuranosylation in *Aspergillus fumigatus*. J. Biol. Chem. 284, 33859-33868.

Erjavec, Z., Kluin-Nelemans, H., Verweij, P.E., 2009. Trends in invasive fungal infections, with emphasis on invasive aspergillosis. Clin. Microbiol. Infect. 15, 625-633.

Espinel-Ingroff, A., Fothergill, A., Ghannoum, M., Manavathu, E., Ostrosky-Zeichner, L., Pfaller, M., Rinaldi, M., Schell, W., Walsh, T., 2005. Quality control and reference guidelines for CLSI broth microdilution susceptibility method (M38-A Document) for amphotericin B, itraconazole, posaconazole, and voriconazole. J. Clin. Microbiol. 43, 5243-5246

Espinel-Ingroff, A., Arthington-Skaggs, B., Iqbal, N., Ellis, D., Pfaller, M.A., Messer, S., Rinaldi, M., Fothergill, A., Gibbs, D.L., Wang, A., 2007. A multicenter evaluation of a new disk agar diffusion method for susceptibility testing of filamentous fungi with voriconazole,

posaconazole, itraconazole, amphotericin-B and caspofungin. J. Clin. Microbiol 45, 1811-1820.

Espinel-Ingroff, A., Fothergill, A., Ghannoum, M., Manavathu, E., Ostrosky-Zeichner, L., Pfaller, M.A., Rinaldi, M.G., Schell, W., Walsh, T.J., 2007. Quality control and reference guidelines for CLSI broth microdilution method (M38-A document) for susceptibility testing of anidulafungin against molds. J. Clin. Microbiol. 45, 2180-2182.

Espinel-Ingroff, Ana, Canton, Emilia, Peman, Javie, 2009. Updates in antifungal susceptibility testing of filamentous fungi. Current Fungal Infection Reports 3, 133-141.

Francois, I.E.J.A., 2006. Azoles: mode of antifungal action and resistance development. Effect of miconazole on endogenous reactive oxygen species production in *Candida albicans*. Anti-Infective Agents in Medicinal Chemistry 5, 3-13.

Galagan, J.E., Calvo, S.E., Cuomo, C., Ma, L.J., Wortman, J.R., Batzoglou, S., Lee, S.I., Basturkmen, M., Spevak, C.C., Clutterbuck, J., Kapitonov, V., Jurka, J., Scazzocchio, C., Farman, M., Butler, J., Purcell, S., Harris, S., Braus, G.H., Draht, O., Busch, S., D'Enfert, C., Bouchier, C., Goldman, G.H., Bell-Pedersen, D., Griffiths-Jones, S., Doonan, J.H., Yu, J., Vienken, K., Pain, A., Freitag, M., Selker, E.U., Archer, D.B., Penalva, M.A., Oakley, B.R., Momany, M., Tanaka, T., Kumagai, T., Asai, K., Machida, M., Nierman, W.C., Denning, D.W., Caddick, M., Hynes, M., Paoletti, M., Fischer, R., Miller, B., Dyer, P., Sachs, M.S., Osmani, S.A., Birren, B.W., 2005. Sequencing of *Aspergillus nidulans* and comparative analysis with *A. fumigatus* and *A. oryzae.* Nature 438, 1105-1115.

Gallis, H.A., Drew, R.H., Pickard, W.W., 1990. Amphotericin B: 30 Years of Clinical Experience. Review of Infectious Diseases 12, 308-329.

Gastebois, A., Clavaud, C., Aimanianda, V., Latge, J.P., 2009. *Aspergillus fumigatus*: cell wall polysaccharides, their biosynthesis and organization. Future Microbiol. 4, 583-595.

Gauwerky, K., Borelli, C., Korting, H.C., 2009. Targeting virulence: a new paradigm for antifungals. Drug Discov. Today 14, 214-222.

Guan, S., Clarke, A.J., Whitfield, C., 2001. Functional analysis of the galactosyltransferases required for biosynthesis of D-galactan I, a component of the lipopolysaccharide O1 antigen of *Klebsiella pneumoniae*. J. Bacteriol. 183, 3318-3327.

Guest, G.M., 2000. Analysis of cell wall sugars in the pathogen *Aspergillus fumigatus* and the saprophyte *Aspergillus nidulans.* Mycologia 92, 1047-1050.

Gupta, A.K., Cooper, E.A., Bowen, J.E., 2008. Meta-analysis: griseofulvin efficacy in the treatment of *tinea capitis*. J. Drugs Dermatol. 7, 369-372.

Handford, M., Rodriguez-Furlan, C., Orellana, A., 2006. Nucleotide-sugar transporters: structure, function and roles *in vivo*. Braz. J. Med. Biol. Res. 39, 1149-1158.

Hawksworth, D.L., 2001. The magnitude of fungal diversity: the 1.5 million species estimate revisited. Mycol. Res. 105, 1422-1432.

Herbrecht, R., Denning, D.W., Patterson, T.F., Bennett, J.E., Greene, R.E., Oestmann, J.W., Kern, W.V., Marr, K.A., Ribaud, P., Lortholary, O., Sylvester, R., Rubin, R.H., Wingard, J.R., Stark, P., Durand, C., Caillot, D., Thiel, E., Chandrasekar, P.H., Hodges, M.R., Schlamm, H.T., Troke, P.F., de Pauw, B., Invasive fungal infections group of the European organization for research and treatment of cancer and the global *Aspergillus* study group, 2002. Voriconazole versus amphotericin B for primary therapy of invasive aspergillosis. N. Engl. J. Med. 347, 408-415.

Herskowitz, I., 1988. Life cycle of the budding yeast *Saccharomyces cerevisiae*. Microbiol. Mol. Biol. Rev. 52, 536-553.

Holden, H.M., Rayment, I., Thoden, J.B., 2003. Structure and function of enzymes of the Leloir pathway for galactose metabolism. J. Biol. Chem. 278, 43885-43888.

Johnson, E.M., 2008. Issues in antifungal susceptibility testing. Journal of Antimicrobial Chemotherapy 61, i13-i18.

Johnson, M.D., Perfect, J.R., 2010. Use of antifungal combination therapy: agents, order, and timing. Curr. Fungal Infect. Rep. 4, 87-95.

Johnson, M.D., MacDougall, C., Ostrosky-Zeichner, L., Perfect, J.R., Rex, J.H., 2004. Combination Antifungal Therapy. Antimicrob. Agents Chemother. 48, 693-715.

Kamigiri, K., Tanaka, K., Matsumoto, H., Nagai, K., Watanabe, M., Suzuki, K., 2004. YM-193221, a novel antifungal antibiotic produced by *Pseudallescheria ellipsoidea*. J. Antibiot. (Tokyo) 57, 569-672.

Kaminskyj S., Heath I.B., 1996. Studies on *Saprolegnia ferax* suggest the importance of the cytoplasm in determining hyphal morphology. Mycologia 88: 20-37

Kapoor, A., Viraraghavan, T., Cullimore, D.R., 1999. Removal of heavy metals using the fungus *Aspergillus niger*. Bioresour. Technol. 70, 95-104.

Kauffman, C.A., Carver, P.L., 2008. Update on echinocandin antifungals. Semin. Respir. Crit. Care. Med. 29, 211-219.

Kim, J., Campbell, B., Mahoney, N., Chan, K., Molyneux, R., May, G., 2008. Chemosensitization prevents tolerance of *Aspergillus fumigatus* to antimycotic drugs. Biochemical and Biophysical Research Communications, 372, 266-271.

Kim, M.K., Park, H.S., Kim, C.H., Park, H.M., Choi, W., 2002. Inhibitory effect of nikkomycin Z on chitin synthases in *Candida albicans*. Yeast 19, 341-349.

Kleczka, B., Lamerz, A.C., van Zandbergen, G., Wenzel, A., Gerardy-Schahn, R., Wiese, M., Routier, F.H., 2007. Targeted gene deletion of *Leishmania major* UDP-galactopyranose mutase leads to attenuated virulence. J. Biol. Chem. 282, 10498-10505.

Klutts, J.S., Yoneda, A., Reilly, M.C., Bose, I., Doering, T.L., 2006. Glycosyltransferases and their products: cryptococcal variations on fungal themes. FEMS Yeast Res. 6, 499-512

Koltin, Y., 1997. The search for new triazole antifungal agents. Curr. Opin. Chem. Biol. 1, 176-182.

Kontoyiannis, D.P., Lewis, R.E., 2003. Combination chemotherapy for invasive fungal infections: what laboratory and clinical studies tell us so far. Drug Resist Updat 6, 257-269.

Kontoyiannis, D.P., Lewis, R.E., 2004. Toward more effective antifungal therapy: the prospects of combination therapy. Br. J. Haematol. 126, 165-175.

Köplin, R. Brisson J. R., Whitefield C., 1997. UDP-galactofuranose precursor required for formation of the lipopolysaccharide O antigen of *Klebsiella pneumoniae* serotype O1 is synthesized by the product of the rfbDKPO1 gene. The Journal of biological chemistry 272, 4121-1428.

Lamarre, C., Beau, R., Balloy, V., Fontaine, T., Hoi, J.W., Guadagnini, S., Berkova, N., Chignard, M., Beauvais, A., Latge, J.P., 2009. Galactofuranose attenuates cellular adhesion of *Aspergillus fumigatus*. Cell. Microbiol. 11, 1612-1623.

Lass-Flörl C., Cuenca-Estrella, M., Denning, D. W., Rodriguez, J. L., 2006. Antifungal susceptibility testing in *Aspergillus* spp. according to EUCAST methodology. Medical mycology 44, 319-325.

Lass-Florl, C., 2009. The changing face of epidemiology of invasive fungal disease in Europe. Mycoses 52, 197-205.

Lass-Florl, C., Perkhofer, S., Mayr, A., 2010. *In vitro* susceptibility testing in fungi: a global perspective on a variety of methods. Mycoses 53, 1-11.

Latgé, J.P., 2009. Galactofuranose containing molecules in *Aspergillus fumigatus*. Med. Mycol. 47 Suppl 1, S104-109.

Latgé, J.P., 2007. The cell wall: a carbohydrate armour for the fungal cell. Mol. Microbiol. 66, 279-290.

Latgé, J.P., 2001. The pathobiology of *Aspergillus* fumigatus. Trends Microbiol. 9, 382-389.

Latgé, J.P., Steinbach, W.J., 2009. *Aspergillus fumigatus* and aspergillosis. ASM Press, Washington, DC.

Latgé, J.P., Mouyna, I., Tekaia, F., Beauvais, A., Debeaupuis, J.P., Nierman, W., 2005. Specific molecular features in the organization and biosynthesis of the cell wall of *Aspergillus fumigatus*. Med. Mycol. 43 Suppl 1, S15-22.

Leitao, E.A., 2003. {beta}-Galactofuranose-containing O-linked oligosaccharides present in the cell wall peptidogalactomannan of *Aspergillus fumigatus* contain immunodominant epitopes. Glycobiology 13, 681-692.

MacRae, J.I., Obado, S.O., Turnock, D.C., Roper, J.R., Kierans, M., Kelly, J.M., Ferguson, M.A., 2006. The suppression of galactose metabolism in *Trypanosoma cruzi* epimastigotes causes changes in cell surface molecular architecture and cell morphology. Mol. Biochem. Parasitol. 147, 126-136.

Maida, C.M., Milici, M.E., Trovato, L., Oliveri, S., Amodio, E., Spreghini, E., Scalise, G., Barchiesi, F., 2008. Evaluation of the disk diffusion method compared to the microdilution method in susceptibility testing of anidulafungin against filamentous fungi. J. Clin. Microbiol. 46, 4071-4074.

Marie, C., White, T.C., 2009. Genetic basis of antifungal drug resistance. Curr. Fungal Infect. Rep. 3, 163-169.

Martinez-Beneyto, Y., Lopez-Jornet, P., Velandrino-Nicolas, A., Jornet-Garcia, V., 2010. Use of antifungal agents for oral candidiasis: results of a national survey. Int. J. Dent. Hyg. 8, 47-52.

Marr, K., 2004. Combination antifungal therapy: where are we now, and where are we going? Oncology (Williston Park) 18, 24-29.

Mennink-Kersten, M.A., Donnelly, J.P., Verweij, P.E., 2004. Detection of circulating galactomannan for the diagnosis and management of invasive aspergillosis. The Lancet Infectious Diseases 4, 349-357.

Menzin, J., Meyers, J.L., Friedman, M., Perfect, J.R., Langston, A.A., Danna, R.P., Papadopoulos, G., 2009. Mortality, length of hospitalization, and costs associated with invasive fungal infections in high-risk patients. Am. J. Health. Syst. Pharm. 66, 1711-1717.

Messer, S.A., Diekema, D.J., Hollis, R.J., Boyken, L.B., Tendolkar, S., Kroeger, J., Pfaller, M.A., 2007. Evaluation of disk diffusion and E-test compared to broth microdilution for antifungal susceptibility testing of posaconazole against clinical isolates of filamentous fungi. J. Clin. Microbiol. 45, 1322-1324.

Mihu, C.N., Kassis, C., Ramos, E.R., Jiang, Y., Hachem, R.Y., Raad, I.I., 2010. Does combination of lipid formulation of amphotericin B and echinocandins improve outcome of invasive aspergillosis in hematological malignancy patients? Cancer 116, 5290-5296.

Mikusova, K., Belanova, M., Kordulakova, J., Honda, K., McNeil, M.R., Mahapatra, S., Crick, D.C., Brennan, P.J., 2006. Identification of a novel galactosyl transferase involved in biosynthesis of the mycobacterial cell wall. J. Bacteriol. 188, 6592-6598.

Mirhendi, H., Diba, K., Kordbacheh, P., Jalalizand, N., Makimura, K., 2007. Identification of pathogenic *Aspergillus species* by a PCR-restriction enzyme method. J. Med. Microbiol. 56, 1568-1570.

Momany M., Lindsey R., Hill T.W., Richardson E.A., Momany C., Pedeira M., Guest G.M., Fisher J.F., Hessler R.B., 2004. The *Aspergillus fumigatus* cell wall is organized in domains that are remodelled during polarity establishment. Microbiology 150: 3261-3268.

Monk, B.C., Goffeau, A., 2008. Outwitting multidrug resistance to antifungals. Science 321, 367-369.

Moran, G.P., Coleman, D.C., Sullivan, D.J., 2011. Comparative genomics and the evolution of pathogenicity in human pathogenic fungi. Eukaryotic Cell 10, 34-42.

Morrison, V.A., 2006. Echinocandin antifungals: review and update. Expert Rev. Anti Infect. Ther. 4, 325-342.

Moyrand, F.**,** Lafontaine, I., Fontaine, T., Janbon, G.**,** 2008. UGE1 and UGE2 regulate the UDP-glucose/UDP-galactose equilibrium in *Cryptococcus neoformans*. Eukaryotic cell 7, 2069-2077.

Nadkarni, T., 2010. Aspergilloma of the brain: an overview. J. Postgrad. Med. 51, 37-41.

Nassau, P., Martin, S., Brown, R., Weston, A., Monsey, D., McNeil, M., Duncan, K., 1996. Galactofuranose biosynthesis in *Escherichia coli* K-12: identification and cloning of UDP-galactopyranose mutase. J. Bacteriol. 178, 1047-1052.

Newbound, M., Mccarthy, M.A., Lebel, T., 2010. Fungi and the urban environment: A review. Landscape Urban Plann. 96, 138-145.

Novelli, J.F., Chaudhary, K., Canovas, J., Benner, J.S., Madinger, C.L., Kelly, P., Hodgkin, J., Carlow, C.K.S., 2009. Characterization of the *Caenorhabditis elegans* UDP-galactopyranose mutase homolog *glf-1* reveals an essential role for galactofuranose metabolism in nematode surface coat synthesis. Dev. Biol. 335, 340-355.

Novozhilova, N.M., Bovin, N.V., 2010. Structure, functions, and biosynthesis of glycoconjugates of *Leishmania* spp. cell surface. Biochemistry (Mosc) 75, 686-694.

Nucci, M., Perfect, J.R., 2008. When primary antifungal therapy fails. Clin. Infect. Dis. 46, 1426-1433.

Nweze, E.I., Mukherjee, P.K., Ghannoum, M.A., 2010. An agar-based disk diffusion assay for susceptibility testing of dermatophytes. J. Clin. Microbiol. doi:10.1128/JCM.01357-10.

Onyewu, C., Blankenship, J.R., Del Poeta, M., Heitman, J., 2003. Ergosterol biosynthesis inhibitors become fungicidal when combined with calcineurin inhibitors against *Candida albicans, Candida glabrata,* and *Candida krusei.* Antimicrob. Agents Chemother. 47, 956-964.

Openo, K.K., Schulz, J.M., Vargas, C.A., Orton, C.S., Epstein, M.P., Schnur, R.E., Scaglia, F., Berry, G.T., Gottesman, G.S., Ficicioglu, C., Slonim, A.E., Schroer, R.J., Yu, C., Rangel, V.E., Keenan, J., Lamance, K., Fridovich-Keil, J.L., 2006. Epimerase-deficiency galactosemia is not a binary condition. The American Journal of Human Genetics 78, 89-102.

Oppenheimer, M.L., Blumer, A., Poulin, M. B., Helm, R. F., Lowary, T. L., Sobrado, P., 2010. Mechanistic studies on UDP-Galactopyranose mutases from *Aspergillus fumigatus* and *Trypanosoma cruzi.* The FASEB journal 24, (Meeting abstract supplement 513.2)

Osiewacz, H.D., 2002. Genes, mitochondria and aging in filamentous fungi. Ageing Res. Rev. 1, 425-442.

Pan, F., Jackson, M., Ma, Y., McNeil, M., 2001. Cell wall core galactofuran synthesis is essential for growth of mycobacteria. J. Bacteriol. 183, 3991-3998.

Panagiotou, G., Andersen, M.R., Grotkjaer, T., Regueira, T.B., Nielsen, J., Olsson, L., 2009. Studies of the production of fungal polyketides in *Aspergillus nidulans* by using systems biology tools. Appl. Environ. Microbiol. 75, 2212-2220.

Panda, D., Rathinasamy, K., Santra, M.K., Wilson, L., 2005. Kinetic suppression of microtubule dynamic instability by griseofulvin: Implications for its possible use in the treatment of cancer. Proceedings of the National Academy of Sciences of the United States of America 102, 9878-9883.

Patel, R., 1998. Antifungal agents. Part I. Amphotericin B preparations and flucytosine. Mayo Clin. Proc. 73, 1205-1225.

Pedersen, L.L., Turco, S.J., 2003. Galactofuranose metabolism: a potential target for antimicrobial chemotherapy. Cellular and molecular life sciences 60, 259-266.

Peltier, P., Belanova, M., Dianiskova, P., Zhou, R., Zheng, R.B., Pearcey, J.A., Joe, M., Brennan, P.J., Nugier-Chauvin, C., Ferrieres, V., Lowary, T.L., Daniellou, R., Mikusova, K., 2010. Synthetic UDP-furanoses as potent inhibitors of mycobacterial galactan biogenesis. Chem. Biol. 17, 1356-1366.

Perlroth, J., Choi, B., Spellberg, B., 2007. Nosocomial fungal infections: epidemiology, diagnosis, and treatment. Med. Mycol. 45, 321-346.

Person, A.K., Kontoyiannis, D.P., Alexander, B.D., 2010. Fungal infections in transplant and oncology patients. Infect. Dis. Clin. North Am. 24, 439-459.

Petranyi, G., Meingassner, J.G., Mieth, H., 1987. Antifungal activity of the allylamine derivative terbinafine *in vitro*. Antimicrob. Agents Chemother. 31, 1365-1368.

Pfaller, M.A., Boyken, L., Messer, S.A., Tendolkar, S., Hollis, R.J., Diekema, D.J., 2005. Comparison of results of voriconazole Disk diffusion testing for *Candida Species* with results from a central reference laboratory in the ARTEMIS Global Antifungal Surveillance Program. J. Clin. Microbiol. 43, 5208-5213.

Pinto, M.R., Barreto-Bergter, E., Taborda C.P., 2008. Glycoconjugates and polysaccharides of fungal cell wall and activation of immune system. Brazilian Journal of Microbiology 39,195-208

Rathinasamy, K., Jindal, B., Asthana, J., Singh, P., Balaji, P.V., Panda, D., 2010. Griseofulvin stabilizes microtubule dynamics, activates p53 and inhibits the proliferation of MCF-7 cells synergistically with vinblastine. BMC Cancer 10, 213-225. doi:10.1186/1471-2407-10-213

Reyes, F., Orellana, A., 2008. Golgi transporters: opening the gate to cell wall polysaccharide biosynthesis. Curr. Opin. Plant Biol. 11, 244-251.

Rezusta, A., Aspiroz, C., Boekhout, T., Cano, J.F., Theelen, B., Guarro, J., Rubio, M.C., 2008. Cholesterol dependent and Amphotericin B resistant isolates of a *Candida glabrata* strain from an Intensive Care Unit patient. Med. Mycol. 46, 265-268.

Richards, M.R., Lowary, T.L., 2009. Chemistry and biology of galactofuranose-containing polysaccharides. Chembiochem 10, 1920-1938.

Richardson, M.D., 2005. Changing patterns and trends in systemic fungal infections. Journal of Antimicrobial Chemotherapy 56, i5-i11.

Ringden, O., Meunier, F., Tollemar, J., Ricci, P., Tura, S., Kuse, E., Viviani, M.A., Gorin, N.C., Klastersky, J., Fenaux, P., 1991. Efficacy of amphotericin B encapsulated in liposomes (AmBisome) in the treatment of invasive fungal infections in immunocompromised patients. J. Antimicrob. Chemother. 28 Suppl B, 73-82.

Riscili, B.P., Wood, K.L., 2009. Noninvasive pulmonary *Aspergillus* infections. Clin. Chest Med. 30, 315-335.

Rodriguez, R., Redman, R., 2008. More than 400 million years of evolution and some plants still can't make it on their own: plant stress tolerance via fungal symbiosis. J. Exp. Bot. 59, 1109-1114.

Rokas, A., Payne, G., Fedorova, N.D., Baker, S.E., Machida, M., Yu, J., Georgianna, D.R., Dean, R.A., Bhatnagar, D., Cleveland, T.E., Wortman, J.R., Maiti, R., Joardar, V., Amedeo, P., Denning, D.W., Nierman, W.C., 2007. What can comparative genomics tell us about species concepts in the genus *Aspergillus*? Stud. Mycol. 59, 11-17.

Roper, J.R., Guther, M.L., Milne, K.G., Ferguson, M.A., 2002. Galactose metabolism is essential for the African sleeping sickness parasite *Trypanosoma brucei*. Proc. Natl. Acad. Sci. U. S. A. 99, 5884-5889.

Sanders, D.A., McMahon, S.A., Leonard, G.L., Naismith, J.H., 2001a. Molecular placement of experimental electron density: a case study on UDP-galactopyranose mutase. Acta Crystallogr. D Biol. Crystallogr. 57, 1415-1420.

Sanders, D.A., Staines, A.G., McMahon, S.A., McNeil, M.R., Whitfield, C., Naismith, J.H., 2001b. UDP-galactopyranose mutase has a novel structure and mechanism. Nat. Struct. Biol. 8, 858-863.

Scherman, M.S., Winans, K.A., Stern, R.J., Jones, V., Bertozzi, C.R., McNeil, M.R., 2003a. Drug targeting *Mycobacterium tuberculosis* cell wall synthesis: development of a microtiter plate-based screen for UDP-galactopyranose mutase and identification of an inhibitor from a uridine-based library. Antimicrob. Agents Chemother. 47, 378-382.

Schmalhorst, P.S., Krappmann, S., Vervecken, W., Rohde, M., Muller, M., Braus, G.H., Contreras, R., Braun, A., Bakker, H., Routier, F.H., 2008. Contribution of galactofuranose to the virulence of the opportunistic pathogen *Aspergillus fumigatus*. Eukaryot. Cell. 7, 1268-1277.

Schulz, J.M., Ross, K.L., Malmstrom, K., Krieger, M., Fridovich-Keil, J.L., 2005. Mediators of Galactose Sensitivity in UDP-Galactose 4′-Epimerase-impaired Mammalian Cells. Journal of Biological Chemistry 280, 13493-13502.

Scott, A., Timson, D.J., 2007. Characterization of the *Saccharomyces cerevisiae* galactose mutarotase/UDP-galactose 4-epimerase protein, Gal10p. FEMS Yeast Res. 7, 366-371.

Semis, R., Polacheck, I., Segal, E., 2010. Nystatin-intralipid preparation: characterization and *in vitro* activity against yeasts and molds. Mycopathologia 169, 333-341.

Sesma, J.I., Esther, C.R.,Jr, Kreda, S.M., Jones, L., O'Neal, W., Nishihara, S., Nicholas, R.A., Lazarowski, E.R., 2009. Endoplasmic reticulum/Golgi nucleotide sugar transporters contribute to the cellular release of UDP-sugar signaling molecules. J. Biol. Chem. 284, 12572-12583.

Sheehan, D.J., Hitchcock, C.A., Sibley, C.M., 1999. Current and emerging azole antifungal agents. Clin. Microbiol. Rev. 12, 40-79.

Singh, V., Satheesh, S.V., Raghavendra, M.L., Sadhale, P.P., 2007. The key enzyme in galactose metabolism, UDP-galactose-4-epimerase, affects cell-wall integrity and morphology in *Candida albicans* even in the absence of galactose. Fungal Genet. Biol. 44, 563-574.

Smith, J., David, A., 2008. Therapeutic drug monitoring of antifungals: pharmacokinetic and pharmacodynamic considerations. Ther. Drug Monit. 30, 167-172.

Soltero-Higgin, M., Carlson, E.E., Phillips, J.H., Kiessling, L.L., 2004. Identification of inhibitors for UDP-galactopyranose mutase. J. Am. Chem. Soc. 126, 10532-10533.

Spanakis, E.K., Aperis, G., Mylonakis, E., 2006. New agents for the treatment of fungal infections: clinical efficacy and gaps in coverage. Clin. Infect. Dis. 43, 1060-1068.

Subcommittee on Antifungal Susceptibility Testing (AFST) of the European Committee for Antimicrobial Susceptibility Testing (EUCAST), 2008. EUCAST definitive document EDef 7.1: method for the determination of broth dilution MICs of antifungal agents for fermentative yeasts. Clin. Microbiol. Infect. 14, 398-405.

Suzuki, S., Matsuzawa, T., Nukigi, Y., Takegawa, K., Tanaka, N., 2009. Characterization of two different types of UDP-glucose/-galactose 4-epimerase involved in galactosylation in fission yeast. Microbiology. 156, 708-718.

Szczepina, M.G., Zheng, R.B., Completo, G.C., Lowary, T.L., Pinto, B.M., 2010. STD-NMR studies of two acceptor substrates of GlfT2, a galactofuranosyltransferase from *Mycobacterium tuberculosis*: epitope mapping studies. Bioorg. Med. Chem. 18, 5123-5128.

Taylor, J., Jacobson, D., Fisher, M., 1999. The evolution of asexual fungi: reproduction, speciation and classification. Annu. Rev. Phytopathol. 37, 197-246.

Te Dorsthorst, D.T.A., Verweij, P.E., Meletiadis, J., Bergervoet, M., Punt, N.C., Meis, J.F.G.M., Mouton, J.W., 2002. *In vitro* interaction of flucytosine combined with amphotericin B or fluconazole against thirty-five yeast isolates determined by both the fractional inhibitory concentration index and the response surface approach. Antimicrob. Agents Chemother. 46, 2982-2989.

Thoden, J.B., Frey, P.A., Holden, H.M., 1996. High-resolution X-ray structure of UDP-galactose 4-epimerase complexed with UDP-phenol. Protein Sci. 5, 2149-2161.

Thoden, J.B., Holden, H.M., 2005. The molecular architecture of galactose mutarotase/UDP-galactose 4-epimerase from *Saccharomyces cerevisiae*. J. Biol. Chem. 280, 21900-21907.

Thoden, J.B., Wohlers, T.M., Fridovich-Keil, J.L., Holden, H.M., 2000. Crystallographic evidence for Tyr 157 functioning as the active site base in human UDP-galactose 4-epimerase. Biochemistry 39, 5691-5701.

Thornton, C.R., 2010. Detection of invasive aspergillosis. Adv. Appl. Microbiol. 70, 187-216.

Todd, R.B., Davis, M.A., Hynes, M.J., 2007. Genetic manipulation of *Aspergillus nidulans*: meiotic progeny for genetic analysis and strain construction. Nat. Protoc. 2, 811-821.

Tsitsigiannis, D.I., Keller, N.P., 2006. Oxylipins act as determinants of natural product biosynthesis and seed colonization in *Aspergillus nidulans*. Mol. Microbiol. 59, 882-892.

Tumbarello, M., Posteraro, B., Trecarichi, E.M., Sanguinetti, M., 2009. Fluconazole use as an important risk factor in the emergence of fluconazole-resistant *Candida glabrata* fungemia. Arch. Intern. Med. 169, 1444- 1445.

Urbaniak, M.D., Tabudravu, J.N., Msaki, A., Matera, K.M., Brenk, R., Jaspars, M., Ferguson, M.A.J., 2006. Identification of novel inhibitors of UDP-Glc 4′-epimerase, a validated drug target for african sleeping sickness. Bioorg. Med. Chem. Lett. 16, 5744-5747.

Van, D.H., Saag, M.S., Cloud, G.A., Hamill, R.J., Graybill, J.R., Sobel, J.D., Johnson, P.C., Tuazon, C.U., Kerkering, T., Moskovitz, B.L., Powderly, W.G., Dismukes, W.E., 1997. Treatment of Cryptococcal meningitis associated with the acquired immunodeficiency syndrome. N. Engl. J. Med. 337, 15-21.

Vermes, A., Guchelaar, H.J., Dankert, J., 2000. Flucytosine: a review of its pharmacology, clinical indications, pharmacokinetics, toxicity and drug interactions. J. Antimicrob. Chemother. 46, 171-179.

Verweij, P.E., Snelders, E., Kema, G.H., Mellado, E., Melchers, W.J., 2009. Azole resistance in *Aspergillus fumigatus*: a side-effect of environmental fungicide use? The Lancet Infectious Diseases 9, 789-795.

Walsh, T.J., Anaissie, E.J., Denning, D.W., Herbrecht, R., Kontoyiannis, D.P., Marr, K.A., Morrison, V.A., Segal, B.H., Steinbach, W.J., Stevens, D.A., van Burik, J.A., Wingard, J.R., Patterson, T.F., Infectious Diseases Society of America, 2008. Treatment of aspergillosis: clinical practice guidelines of the Infectious Diseases Society of America. Clin. Infect. Dis. 46, 327-360.

Walsh, T.J., Petraitis, V., Petraitiene, R., Field-Ridley, A., Sutton, D., Ghannoum, M., Sein, T., Schaufele, R., Peter, J., Bacher, J., Casler, H., Armstrong, D., Espinel-Ingroff, A., Rinaldi, M.G., Lyman, C.A., 2003. Experimental pulmonary aspergillosis due to *Aspergillus terreus*: pathogenesis and treatment of an emerging fungal pathogen resistant to amphotericin B. J. Infect. Dis. 188, 305-319.

Wasilenko, J., Fridovich-Keil, J.L., 2006. Relationship between UDP-galactose 4'-epimerase activity and galactose sensitivity in yeast. J. Biol. Chem. 281, 8443-8449.

Wearing, J., 2010. Fungi : Mushrooms, Toadstools, Molds, Yeasts, and Other Fungi. Crabtree Pub., c2010., St. Catharines, Ont.; New York.

Weston, A., Stern, R.J., Lee, R.E., Nassau, P.M., Monsey, D., Martin, S.L., Scherman, M.S., Besra, G.S., Duncan, K., McNeil, M.R., 1998. Biosynthetic origin of mycobacterial cell wall galactofuranosyl residues. Tubercle Lung Dis. 78, 123-131.

Winans, K.A., Bertozzi, C.R., 2002. An Inhibitor of the Human UDP-GlcNAc 4-Epimerase Identified from a Uridine-Based Library: A Strategy to Inhibit O-Linked Glycosylation. Chem. Biol. 9, 113-129.

Wing, C., Errey, J.C., Mukhopadhyay, B., Blanchard, J.S., Field, R.A., 2006. Expression and initial characterization of WbbI, a putative D-Galf:alpha-D-Glc beta-1,6-galactofuranosyltransferase from *Escherichia coli* K-12. Org. Biomol. Chem. 4, 3945-3950.

Wirk, B., Wingard, J.R., 2008. Combination antifungal therapy: from bench to bedside. Curr. Infect. Dis. Rep. 10, 466-472.

Wohlers, T.M., Christacos, N.C., Harreman, M.T., Fridovich-Keil, J.L., 1999. Identification and Characterization of a Mutation, in the Human UDP-Galactose-4-Epimerase Gene, Associated with Generalized Epimerase-Deficiency Galactosemia. The American Journal of Human Genetics 64, 462-470.

Worth, L.J., Blyth, C.C., Booth, D.L., Kong, D.C., Marriott, D., Cassumbhoy, M., Ray, J., Slavin, M.A., Wilkes, J.R., 2008. Optimizing antifungal drug dosing and monitoring to avoid toxicity and improve outcomes in patients with haematological disorders. Intern. Med. J. 38, 521-537.

Wortman, J.R., Gilsenan, J.M., Joardar, V., Deegan, J., Clutterbuck, J., Andersen, M.R., Archer, D., Bencina, M., Braus, G., Coutinho, P., von Dohren, H., Doonan, J., Driessen, A.J., Durek, P., Espeso, E., Fekete, E., Flipphi, M., Estrada, C.G., Geysens, S., Goldman, G., de Groot, P.W., Hansen, K., Harris, S.D., Heinekamp, T., Helmstaedt, K., Henrissat, B., Hofmann, G., Homan, T., Horio, T., Horiuchi, H., James, S., Jones, M., Karaffa, L., Karanyi, Z., Kato, M., Keller, N., Kelly, D.E., Kiel, J.A., Kim, J.M., van der Klei, I.J., Klis, F.M., Kovalchuk, A., Krasevec, N., Kubicek, C.P., Liu, B., Maccabe, A., Meyer, V., Mirabito, P., Miskei, M., Mos, M., Mullins, J., Nelson, D.R., Nielsen, J., Oakley, B.R., Osmani, S.A., Pakula, T., Paszewski, A., Paulsen, I., Pilsyk, S., Pocsi, I., Punt, P.J., Ram, A.F., Ren, Q., Robellet, X., Robson, G., Seiboth, B., van Solingen, P., Specht, T., Sun, J., Taheri-Talesh, N., Takeshita, N., Ussery, D., vanKuyk, P.A., Visser, H., van de Vondervoort, P.J., de Vries, R.P., Walton, J., Xiang, X., Xiong, Y., Zeng, A.P., Brandt, B.W., Cornell, M.J., van den Hondel, C.A.,

Visser, J., Oliver, S.G., Turner, G., 2009. The 2008 update of the *Aspergillus nidulans* genome annotation: a community effort. Fungal Genet. Biol. 46 Suppl 1, S2-13.

Yu, J., Li, R., Zhang, M., Liu, L., Wan, Z., 2008. *In vitro* interaction of terbinafine with itraconazole and amphotericin B against fungi causing chromoblastomycosis in China. Med. Mycol. 46, 745-747.

Zhang, A.Y., Camp, W.L., Elewski, B.E., 2007. Advances in topical and systemic antifungals. Dermatol. Clin. 25, 165,183.

Zhang, K., Barron, T., Turco, S.J., Beverley, S.M., 2004. The LPG1 gene family of *Leishmania major*. Mol. Biochem. Parasitol. 136, 11-23.

Table 1: Antifungal drug classes and their targets in fungal cell

Class	**Target**	**Examples**
Polyenes	Cell membrane ergosterol	Amphotericin B
Azoles	Ergosterol biosynthesis, lanosterol demethylase	Fluconazole, voriconazole
Allylamines	Ergosterol biosynthesis, squalene epoxidase	Terbinafine
Morpholines	Ergosterol biosynthesis, sterol C8-C7 isomerase and the C-14 sterol reductase	Amorofine
Echinocandins	Cell wall, β-1, 3-glucan synthesis	Caspofungin, micafungin
Fluorinated pyrimidines	RNA/DNA synthesis	Flucytosine
Others	Mitosis	Griseofulvin

Table 2: Typical polysaccharide composition of filamentous ascomycete cell walls.

Cell wall polymer	% composition
Glucans	50-60%
Chitin	10-20%
Galactomannans	20-25 %

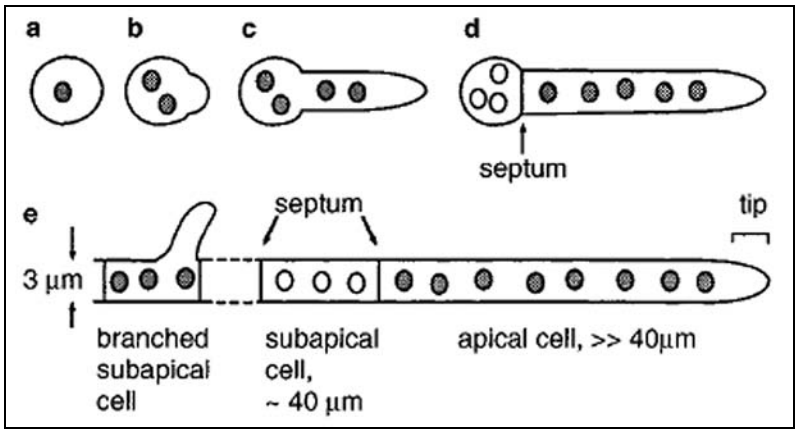

Figure 1. Germination and growth of wild type *Aspergillus nidulans* hyphae grown at 28℃ (not to scale), from Kaminskyj SGW and Hamer JE 1998 Genetics 148: 669-680, Fig 1 (reproduced with author's permission).

A conidium (a) germinates (b), and nuclei migrate into the germ tube as it grows (c). The first septum is deposited at the base of the germ tube when the germling has eight or more nuclei (d). Hyphae are tubular, ~ 3 μm in diameter, apical cells are variable in length and usually much longer than 40 μm. Apical cells contain many nuclei (circles) that are evenly spaced along the length of the cell (e).

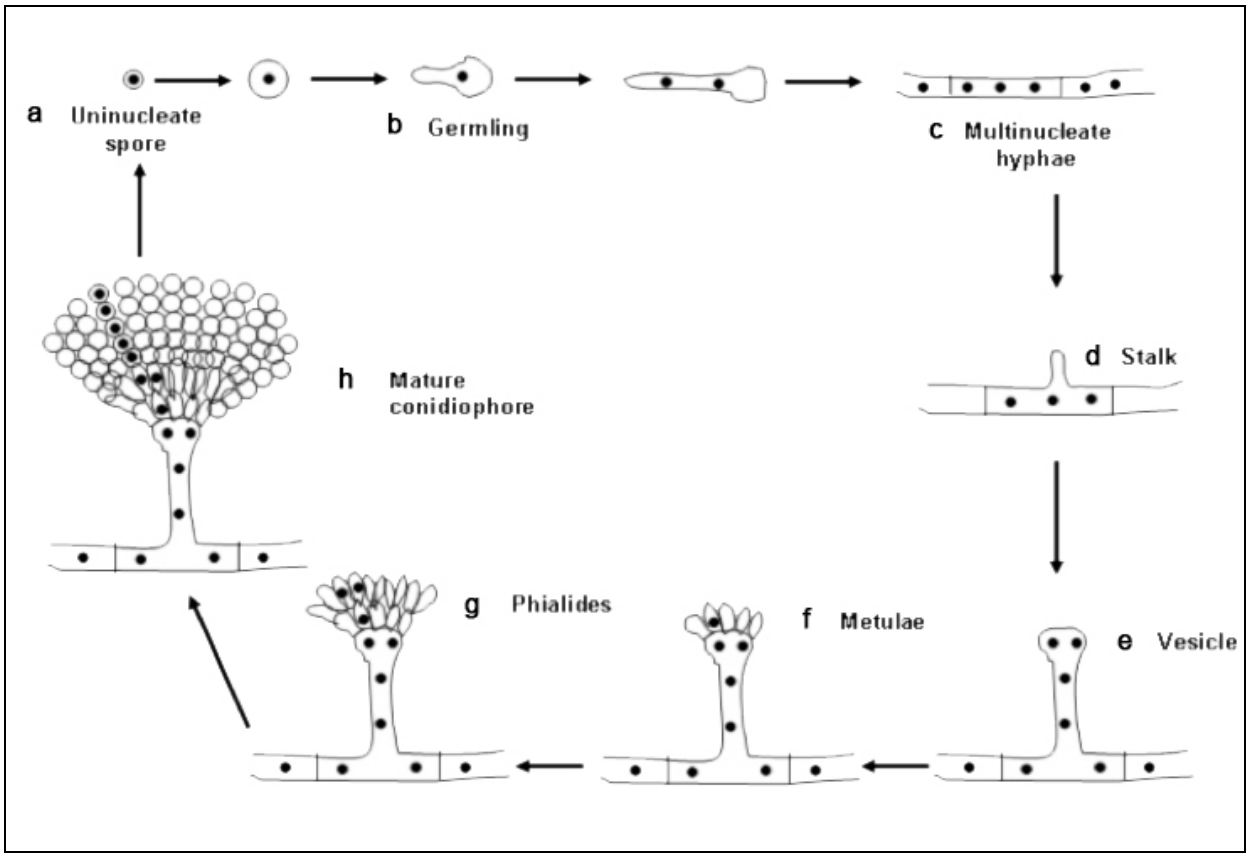

Figure 2. The asexual life cycle in *Aspergillus nidulans.* a-c) Germination and hyphal growth in *A. nidulans* leads to the formation of a vegetative colony. d) At the onset of spore development, a stalk forms. e) the stalk swells at its tip to form a vesicle. The vesicle produces two layers of specialized cells, f) metulae, and g) phialides. In wild type *A. nidulans*, each metula produces a pair of phialides. h) The mature conidiophore produces chains of uninucleate spores.

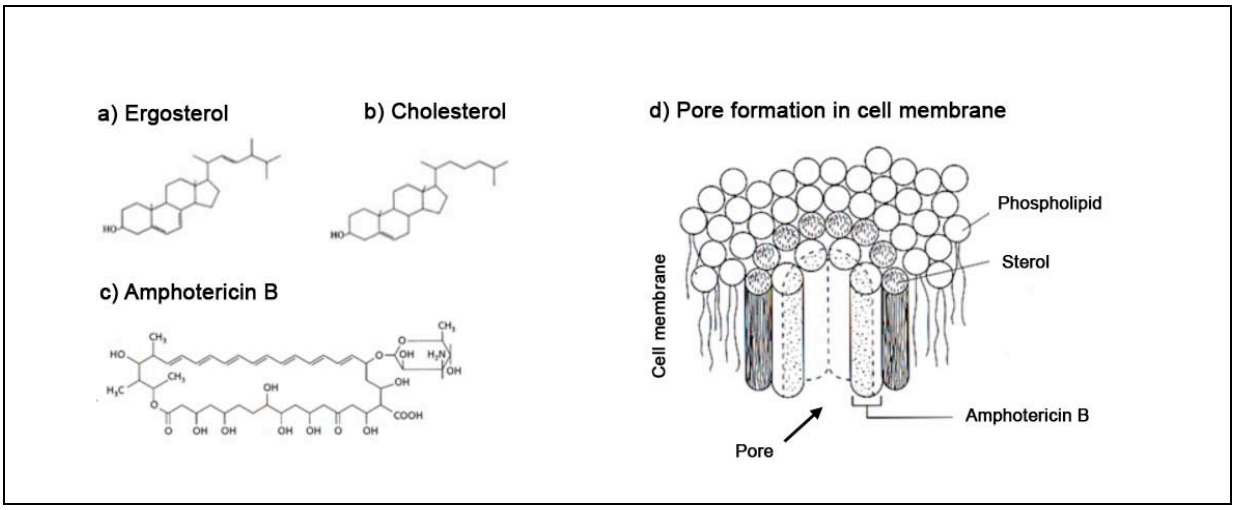

Figure 3. Target of polyene drugs. Structures of a) ergosterol, and b) cholesterol, which are found in fungi and mammals, respectively. c) Polyene drugs such as amphotericin B can span a membrane phospholipid bilayer. d) When polyenes are associated with cell membranes, they bind to sterols, and form transmembrane hydrophilic pores (part d was taken from www.biology.ed.ac.uk).

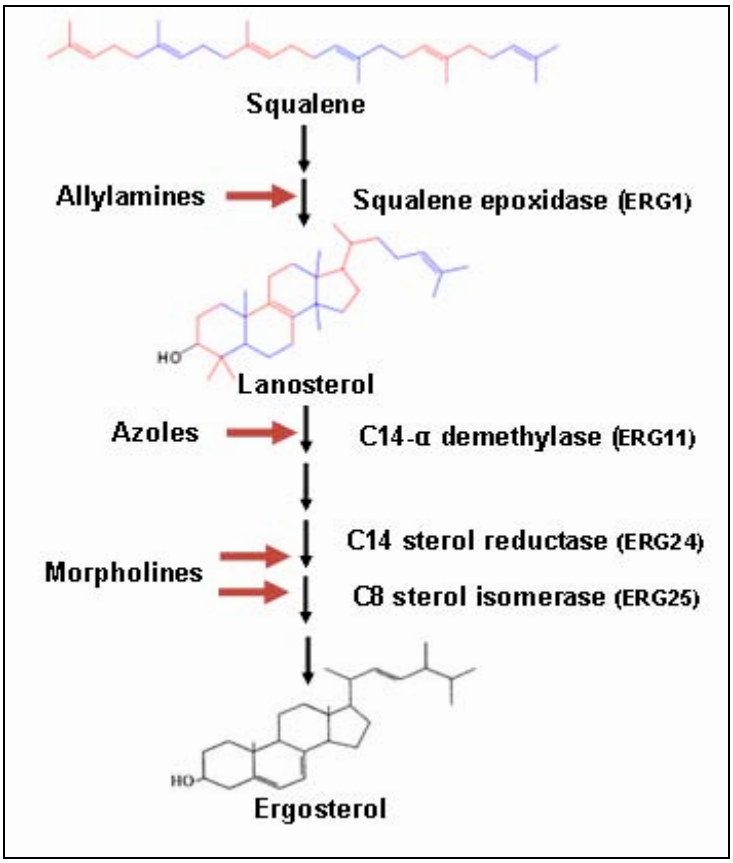

Figure 4. Antifungal drugs that target ergosterol biosynthesis. Allylamines, azoles and morpholines inhibite ergosterol biosynthesis at different steps. allylamines targets an early step in ergosterol biosynthesis by inhibiting the enzyme squalene epoxidase (ERG1). Azoles bind C14 α -demethylase (ERG11) while morpholines inhibit to enzymes C14 sterol reductase (ERG24) and C8 sterol isomerase (ERG 25).

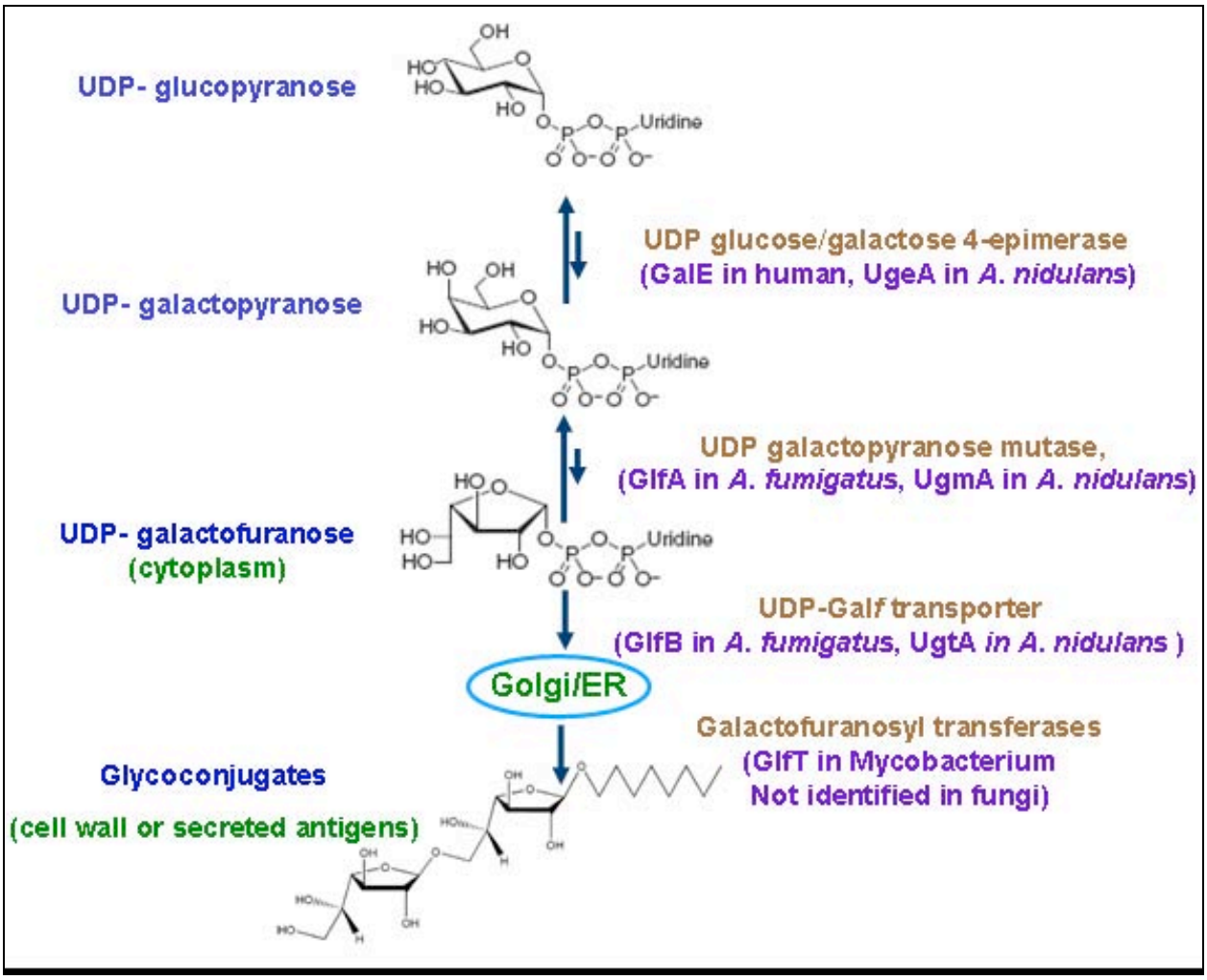

Figure 5. The galactofuranose (Gal*f)* biosynthesis pathway in *Aspergillus nidulans*, showing the steps of Gal*f* biosynthesis starting from UDP-glucose until the insertion of the Gal*f*-containing glycoconjugates in the cell wall. Enzymes are colored brown and the intermediates are colored blue.

Chapter 2

Characterization of *Aspergillus nidulans* UDP-galactopyranose mutase, UgmA

This chapter studies the biological roles of the key enzyme in Gal*f* biosynthesis pathway, UDP-galactopyranose mutase, UgmA. The manuscript has been published as "*Aspergillus nidulans* UDP-galactopyranose mutase, encoded by *ugmA* plays key roles in colony growth, hyphal morphogensis, and conidiation". In Fungal Genetics and Biology Journal, 45: 1533-1542. **El-Ganiny, Sanders and Kaminskyj, 2008.**

The objectives for the research work in this chapter were

1) To identify *A. nidulans* UDP- galactopyranose mutase (AnUgmA).
2) To determine whether UgmA is essential for viability of *A. nidulans.*
3) To quantify the effect of *ugmA* deletion on sporulation, colony and hyphal morphogenesis.
4) To examine the effect of *ugmA* deletion on Gal*f* localization and on the cell wall ultrastructure.
5) To investigate whether *A. fumigatus glfA* can complement the defects caused by *ugmA* deletion (homology of function).

The starting point of this project was the identification of *Aspergillus nidulans ugmA,* this part was done by Eshwari Addala, a former Ph.D. student that was working with my co-supervisor Dr. David Sanders. I performed all the experiments including: designing primers for gene deletion, deletion of *ugmA*, confirming the deletion of *ugmA*, characterization of *ugmA*Δ strains using confocal, SEM and TEM, Immunolocalization of Gal*f* in wild type and *ugmA*Δ strains, complementing *ugmA*Δ *strain* defects using Af*glfA* sequence and finally mating *ugmA*Δ strain *with swoA* strain. My supervisor Dr. Kaminskyj did the statistical analysis of the data and the editing of the final figures. I wrote the first manuscript of the paper which edited by my supervisor Dr. Kaminskyj prior to accepting it for publication.

Aspergillus nidulans UDP-galactopyranose mutase, encoded by *ugmA* plays key roles in colony growth, hyphal morphogenesis, and conidiation.

Amira M. El-Ganiny [a], David A.R. Sanders [b], Susan G. W. Kaminskyj [a, *]

[a] Department of Biology, University of Saskatchewan, 112 Science Place, Saskatoon SK S7N 5E2, Canada

[b] Department of Chemistry, University of Saskatchewan, 110 Science Place, Saskatoon SK S7N 5C9, Canada

[*] Author for Correspondence. Tel: 306 966 4422; Email Susan.Kaminskyj@usask.ca

Key words: *Aspergillus nidulans*, cell wall, galactofuranose, hyphal morphogensis, conidiation, UDP-galactopyranose mutase.

Abbreviations: Galactofuranose, Gal*f*; scanning electron microscopy, SEM; transmission electron microscopy, TEM; UDP-galactopyranose mutase, UGM; *Aspergillus nidulans* UGM-encoding gene, *ugmA*; *ugmA* deletion, *ugmA*Δ

Abstract

Growing resistance to current anti-fungal drugs is spurring investigation of new targets, including those in fungal wall metabolism. Galactofuranose (Gal*f*) is found in the cell walls of many fungi including *Aspergillus fumigatus*, which is currently the most prevalent opportunistic fungal pathogen in developed countries, and *A. nidulans,* a closely-related, tractable model system. UDP-galactopyranose mutase (UGM) converts UDP-galactopyranose into UDP-Gal*f* prior to incorporation into the fungal wall. We deleted the single-copy UGM sequence (AN3112.4, which we call *ugmA*) from an *A. nidulans nkuA*Δ strain, creating *ugmA*Δ. Haploid *ugmA*Δ strains were able to complete their asexual life cycle, showing that *ugmA* is not essential. However, *ugmA*Δ strains had compact colonial growth, which was associated with substantially delayed and abnormal conidiation. Compared to a wildtype morphology strain, *ugmA*Δ strains had aberrant hyphal morphology, producing wide, uneven, highly-branched hyphae, with thick, relatively electron-dense walls as visualized by transmission electron microscopy. These effects were partially remediated by growth on high osmolarity medium, or on medium containing 10 μg/mL Calcofluor, consistent with Gal*f* being important in cell wall structure and/or function.

1. Introduction

In the last decades there has been an increase in the incidence of fungal infections due to immunocompromising conditions such as AIDS and organ transplantation, and perhaps also to overuse of broad-spectrum antibiotics (Loeffler and Stevens, 2003; Garcia-Ruiz *et al.,* 2004). Mortality in patients with systemic fungal infections is high even with aggressive therapy (Randhawa and Sharma, 2004). *Aspergillus fumigatus* is the most common opportunistic fungal pathogen in industrialized countries, due to their relatively large populations at risk (Arathoon, 2001). *Aspergillus fumigatus* is common in the environment (where it contributes to recycling), has air-dispersed spores that are readily inhaled, and has a growth optimum near 37 ºC. Treatment of fungal infections is limited by problems of drug safety, effectiveness and fungal resistance. Polyene antifungals lack target specificity and have a high toxicity to humans; azoles are fungistatic, not fungicidal; echinocandins have a narrow spectrum of activity; and apart from polyenes, there is emerging antifungal drug resistance (Carrillo-Munoz *et al.,* 2006; Chamilos and Kontoyiannis, 2005). An anti-fungal drug target should be found in a broad spectrum of fungal pathogens, be important for infectivity, and not be found in humans. Fungal cell wall components, including chitin, β1-3 glucans, and galactofuranose (Notermans *et al.,* 1998; Leitao *et al.,* 2003) are obvious drug targets (Tawara *et al.,* 2000; Pederson and Turco, 2003, Schmalhorst *et al.*, 2008).

Genetic and biochemical studies of Gal*f* biosynthesis in prokaryotes show that UDP-Gal*f* (the five-membered ring form, Fig. 1) is formed from UDP-Gal*p* (the six-membered ring form) by UDP-galactopyranose mutase (UGM) (Nassau *et al*., 1996, Weston *et al*., 1998). UDP-Gal*f* is the precursor to Gal*f* residues found in the cell walls of many microorganisms. The gene encoding UGM has been identified in prokaryotes (Stevenson *et al*., 1996; Nassau *et al*., 1996; Koplin *et al*., 1997; Pan *et al*., 2001) and its crystal structure has been solved (Sanders *et al*., 2001).

Galactofuranose (Gal*f)* is an essential component of the bacterial cell wall (Whitfield *et al*., 1991; Nassau *et al*., 1996; Pan *et al*., 2001), and is important or essential for pathogencity of *Leishmania major* (Spath *et al*., 2000; Kleczka *et al.,* 2007), which causes leishmaniasis. Beta-linked Gal*f* chains are the immunodominant epitope in *Aspergillus* spp (Bennet *et al*., 1984; Leitao *et al*., 2003). In *A. niger*, *ugmA* contributes to cell wall integrity (Damveld *et al.,* 2008). In

A. fumigatus, the *ugmA* homologue *glfA* contributes to wildtype wall structure (Schmalhorst *et al.,* 2008). Gal*f* has been shown to be attached to linear mannan chains in the *A. fumigatus* cell wall, which are GPI-anchored to the cell membrane (Costachel *et al.*, 2005, Schmalhorst *et al.,* 2008). *Aspergillus fumigatus* and *A. nidulans* hyphal walls have similar galactose content (Guest and Momany, 2000). The Gal*f* monoclonal antibody EBA2 has been used for diagnosis of aspergillosis and to monitor therapy effectiveness (Stynen *et al*, 1992, Wallis *et al*., 2001, Maertens *et al*. 2007).

Beverly *et al*. (2005) identified eukaryotic UGM genes in protozoa (*L. major* and *Trypanosoma cruzi*) and the fungus (*Cryptococcus neoformans*). Beverly *et al*. (2005) found that eukaryote UGM amino acid sequences are closely related to each other but distantly related to prokaryote UGMs. *Aspergillus fumigatus* and *L. major* UGM shared 51 % sequence identity, but were less than 20 % identical to their prokaryotic orthologues, with the region of identity/similarity confined to the catalytic site (Bakker *et al*. 2005). Eukaryote UGMs have four major insertions, which are thought to form loops that are important for protein regulation and interaction.

BLAST analysis with default parameters using *A. fumigatus* UGM (Afu3g12690, named Af*glfA* by Schmalhorst *et al.*, 2008) at www.broad.mit.edu/annotation/fungi/aspergillus/ showed a strong sequence alignment (98 % identity) to one locus in *A. nidulans*, AN3112.4, which we named *ugmA*. We are using *A. nidulans* as a safe and experimentally-tractable system for studying UGM function *in vivo*, in parallel with crystallization studies of *A. fumigatus glfA*. This study focuses on the effects of *UgmA* deletion in *A. nidulans*. We found that *ugmA* was not essential, but its deletion resulted in compact colonial growth, reduced sporulation, and hyphal morphological abnormalities, all of which can be attributed to wall defects.

2. Materials and methods

Biological materials and primers are given in Table 1. Chemicals were reagent grade and were purchased from VWR (www.vwrcanlab.ca) or Sigma (www.sigmaaldrich.com) unless stated otherwise. Vinoflow was purchased from Gusmer Enterprises (www.thewinelab.com). Water was 18 MΩ deionized, and sterilized as appropriate. *Aspergillus nidulans* strains were grown in complete media CM with nutritional supplements as required (Kaminskyj, 2001).

Statistical analysis used Statview SE+Graphics v1.02. Values are presented as mean ± standard error of the mean. Images were prepared with Adobe Photoshop 7.0.

2.1. Gene knockout

Aspergillus nidulans strain A1149 was used for AN3112 (*ugmA*) gene deletion, following the procedures described in Nayak *et al*. (2006) and Szewczyk *et al*. (2007), with *A. fumigatus pyrG* as the selectable marker (Fig. 2A-F). Experiments using *A. fumigatus pyroA* selection (not shown) gave comparable results. A1149 was also transformed to pyrimidine prototrophy as described in Yang *et al.* (2008), creating AAE1, a wildtype phenotype *pyrG*+, *nkuA*Δ strain used for phenotype comparison. Following transformation, putative *ugmA*Δ colonies were able to conidiate on selective media. These conidia were inoculated onto selective and non-selective media to assess whether *ugmA* was essential (Osmani *et al*., 2006). Spores were also grown on selective media to examine hyphal and colony morphology under different growth conditions, and to generate mycelium for genomic DNA extraction, as described in Yang *et al.* (2008). PCR comparing A1149 genomic DNA with that from three *ugmA*Δ deletion strains used the primers described in Fig. 2 and Table 1.

2.2. Microscopical methods

2.2.1. Confocal Microscopy

Aspergillus nidulans wildtype and *ugmA*Δ strains were grown at 28 ºC, then samples were fixed and stained with Calcofluor to visualize walls and Hoechst 33258 to visualize nuclei, as described in Kaminskyj and Hamer (1998). Confocal imaging used a Zeiss META510 confocal microscope with a 63 X, 1.2 N. A. multi-immersion objective, a 405 nm diode at 20 % power, and a 420-480 nm emission filter. Fluorescence and transmitted light images were collected simultaneously.

For morphometry, hyphal width was measured at septa (50 per strain), and basal cell length was measured between adjacent septa (50 per strain) as previously described in Kaminskyj and Hamer (1998). Total hyphal length per germling was measured using Zeiss LSM software, by adding the lengths of all branches (30 germlings per strain). The number of tips per germling was counted.

For immunofluorescence microscopy, samples were prepared as described in Kaminskyj and Heath (1995). EBA2 monoclonal antibody originally raised against *A. fumigatus* galactomannan, which contains Gal*f* (Wallis *et al*., 2001), was eluted from a BioRad Platelia ELISA kit using TBS, and concentrated with a 10 kDa Microcon centrifugal concentration column (Millipore). EBA2 binding was localized using FITC-conjugated goat-anti-rat IgG (Sigma) that had been affinity purified against lyophilized *ugmA*Δ mycelium as described in Kaminskyj and Heath. Confocal imaging used 488 nm excitation, 5–10 % power from an argon multispectral laser operated at 5.9 A, with emission controlled by a BP505-530 filter.

2.2.2. Electron microscopy

For scanning electron microscopy (SEM), AAE1 and *ugmA*Δ strains were grown on dialysis tubing overlying selective media for 3 d at 28 ºC. Isolated colonies were fixed at 100 % relative humidity over 4 % aqueous OsO4 for 2 h, frozen to -80 ºC, and lyophilized overnight. Samples were mounted on SEM stubs, gold sputter coated for 6 min, and examined with scanning electron microscope JEOL model JSM840A. The accelerating voltage was 20 kV. The beam current for sample examination was 1.5 nA, and for image acquisition was 50 pA.

For transmission electron microscopy (TEM), AAE1 and *ugmA*Δ strains were grown on dialysis tubing overlying selective media (CM, CM + 1 molar sucrose, or CM + 10 µg/mL Calcofluor) for 16 h at 28 ºC. Samples were prepared and imaged as described in Kaminskyj (2000).

3. Results

3.1. UDP-galactopyranose mutase deletion

To test whether *ugmA* was essential, we deleted the AN3112.4 coding sequence in the *nkuA*Δ strain A1149 (Fig. 2A-F). The knockout construct was generated using fusion PCR: the selectable marker *A. fumigatus pyrG* was flanked by predicted 5' and 3' untranslated regions for AN3112. The deletion cassette was transformed into A1149 protoplasts as described in Nayak *et al.* (2006) and Szewczyk *et al.* (2007). Transformants were selected on CM lacking pyrimidines, containing 1 M sucrose as osmoticum. Conidia produced by these primary transformants were

able to germinate and formed sporulating colonies when streaked on growth medium lacking exogenous pyrimidines, indicating that *A. nidulans ugmA* is not essential.

Ectopic integration of the knockout construct could potentially have contributed to the *ugmA*Δ phenotype. Morphometric characterization of three randomly-chosen putative *ugmA*Δ phenotype colonies are given in Table 2. Deletion experiments using *A. fumigatus pyroA* as a selectable marker (not shown) gave comparable results regarding the phenotype of colonies produced by conidia from primary transformants. We interpret a high level of phenotype consistency at the colony and cellular level between multiple transformants from independent experiments, as being evidence of lack interference from ectopic integrants. Additional confirmatory studies are presented below.

Genomic DNA was extracted from A1149 and *ugmA*Δ strains, and used as template for PCR to test for the presence and location of AN3112 and Af*pyrG*. AN3112 is predicted to be 1.9 kb, and Af*pyrG* is predicted to be 0.9 kb. The 5' and 3' flanking regions were 1 kb and 1.1 kb respectively. PCR using P1 and P6 (to span AN3112 plus the 5' and 3' flanking regions) amplified a ~ 4 kb band from the A1149 parental strain, and a ~ 3 kb band with *ugmA*Δ strains (Fig 2G) consistent with replacement of AN3112 with Af*pyrG*. PCR using P1 and P8 (targeted to a flanking region and the middle of Af*pyrG*), produced bands of the 1.6 kb in *ugmA*Δ strains, and did not amplify a band for A1149 (Fig 2H). PCR using P21 and P23 (designed to amplify *ugmA*) gave no band with any of the *ugmA*Δ strains, and 1.9 kb band with A1149 (Fig. 2I). Additional studies re genetic segregation following mating, and complementation of the *ugmA*Δ defect with the *A. fumigatus* homologue are presented below. Three knockout strains, *ugmA*Δ*1*, *ugmA*Δ*2*, and *ugmA*Δ*3*, gave comparable results in all studies. We designated *ugmA*Δ*1* as AAE2.

Protoplasts were generated from *A. nidulans* AAE2 germlings, transformed with pET22b containing Af*glfA* (which encodes functional *A. fumigatus* UGM: Bakker et al., 2005), and incubated at 37 ºC for 3 d. The following data are presented in Supplemental figure 1. In addition to many *ugmA*Δ phenotype colonies that showed compact colony growth and limited sporulation, a putative *ugmA*Δ:Af*glfA* colony was generated that had wildtype growth and abundant conidiation (arrow in Suppl. Figure Aa). We named this strain AAE3. PCR of AAE3 genomic DNA using primers designed to amplify Af*glfA* showed a band comparable in size to the pET22b control (Suppl Fig Ab). Light microscopy of AAE3 revealed wildtype hyphal morphology (Suppl. Fig Ac), morphometry (Suppl. Fig Ad), and nuclear distribution unlike AAE2 (Fig. 4A,

and Table 2). Young AAE3 conidiophores had abundant metulae and synchronous phialide development (Suppl. Fig. Ac) unlike AAE2 (Fig. 3H).

AAE2 was mated to AOZ1 to determine whether the *ugmA*Δ defect segregated independently, and to create additional strains for future studies (Suppl. Fig. B). Independent assortment of the *ugmA*Δ phenotype following mating is evidence that the *ugmA*Δ knockout construct underwent homologous rather than ectopic integration. AAE2 mating efficiency is poor, matings with at least three other *A. nidulans* strains were not successful. Cleistothecium maturation was delayed (no outcrossed cleistothecia containing viable spores were isolated until three months), consistent with the suggestion by Adams *et al.* (1998) that mutations affecting conidiation also compromise sexual development. Both AOZ1 and AAE2 have reduced conidiation (Suppl. Fig. Ba). AOZ1 contains *swoA1,* which can be complemented by a protein O-mannosyl transferase (Shaw and Momany, 2002). Amongst 140 progeny from this cross were 43 with wildtype colony growth and sporulation, and equal numbers of green- and white-spored strains, consistent with independent assortment of *ugmA* and *swoA*. As expected, there were also [*ugmA*Δ, *swoA1*] progeny, with severe growth defects at permissive conditions (*e. g.* arrowheads in Suppl. Fig Ba).

Genomic DNA was prepared from six randomly-selected progeny that showed the *ugmA*Δ phenotype under the growth conditions shown in Suppl. Figure 2a. PCR with primers nkuAF and nkuAR, expected to amplify an band of 1981 bp in *nkuA*+ strains, amplified this band in three of these *ugmA*Δ progeny, as well as in wildtype strain A28 (Suppl. Fig. Bb). This is evidence that *ugmA* segregates independently of *nkuA*.

The phenotype consistency for multiple strains from independent knockout experiments using *pyrG* and *pyroA* as selectable markers; rescue of the *ugmA*Δ phenotype by Af*glfA*; and independent segregation of *ugmA* with *nkuA* and *swoA* is strong evidence that the AAE2 phenotype discussed below is due to the deletion of *ugmA,* and that *ugmA* encodes *A. nidulans* UGM.

3.2. Colony growth and sporulation

To characterize the effect of *ugmA*Δ on colony growth, AAE1 and AAE2 strains were grown for 3 d on CM lacking exogenous pyrimidines. AAE1 colonies had a wildtype phenotype, with a broad fringe of submerged hyphae extending into the growth medium (arrows in Fig. 3A),

whereas AAE2 colonies had a compact colonial morphology with little penetration of the medium. The AAE2 colonies also had reduced sporulation: the centres of AAE1 colonies had strong green pigmentation (Fig. 3A) whereas AAE2 colonies were pale (Fig. 3B). After 3 d growth at 28 ºC, isolated AAE1 colonies were about 50 % larger in diameter than those of AAE2, 6.0±0.8 mm *vs* 4.4±0.6 mm, respectively, even without considering the submerged hyphae at the AAE1 colony margins (arrows in Fig. 3A). Viewed from above at 50 x, the AAE1 colonies were sporulating abundantly at 3 d (Fig. 3C), with closely spaced conidiophores bearing pigmented conidia, whereas AAE2 conidiophores that produced pigmented spores were widely separated (*e. g.,* arrows in Fig. 3D).

The number of spores produced per colony was estimated for AAE1 and AAE2 strains. After 3 d, individual AAE1 colonies had produced an average of 1.0 ± 0.4 x 10^8 spores, compared to 2.2 ± 0.7 x 10^5 spores for AAE2 colonies. Thus, AAE2 had suffered a 500-fold reduction in sporulation compared to AAE1.

Viability of AAE1 and AAE2 spores was determined by plating similar numbers of conidia (~ 250, 125, or 60 per plate) and counting the number of colonies formed after 2 d incubation at 28 ºC. Plates inoculated with ~ 60 spores each produced 49 AAE1 and 48 AAE2 colonies, with comparable results for the higher inoculation densities, suggesting that spore viability was not compromised by *ugmA*Δ.

Conidiation in AAE1 and AAE2 was examined using SEM (Fig. 3E-H). By 3 d, AAE1 produced long chains of conidia (Fig. 3E, G), whereas AAE2 colonies (Fig. 3F, H) had relatively few conidiophores (arrows in Fig. 3F) with at most short chains of conidia (s in Fig. 3H), despite abundant sterile hyphae (Fig. 3F). Often, formation of metulae and phialides in AAE2 was arrested or aberrant.

3.3. Hyphal morphology and wall composition

The effect of *ugmA*Δ on hyphal morphogenesis is shown in Fig. 4. Unlike AAE1, which had a wildtype phenotype (Fig. 4 inset), AAE2 strains stained with Calcofluor (Fig. 4A) had wide, highly branched hyphae. The AAE2 and AAE1 hyphae in Fig. 4A were stained with the same solution of Calcofluor and Hoechst 33258, and imaged with the same confocal settings. Lateral walls, but few nuclei, were visible in the AAE2 hyphae, whereas the converse was true

for AAE1. We interpret this as meaning the AAE2 hyphal walls were relatively thicker than those of AAE1.

AAE1 and three *ugmA*Δ strains including AAE2 were compared by cell morphometry for hyphal width, basal cell length, total hyphal length per germling, and total tips per germling (Table 2A). Relative branching was quantified using the hyphal growth index described by Trinci (1974), as the total hyphal length of a germling divided by the number of tips for that germling. Compared to AAE1, all three *ugmA*Δ strains had more than two-fold lower hyphal growth index (Table 2A), indicating at least double the branching frequency.

Gal*f* can be immunolocalized with a monoclonal antibody, EBA2 (Wallis et al., 2001). We used EBA2 to compare Gal*f* content and distribution in AAE1 and AAE2 strains. EBA2 binding in AAE1 localized to mature conidia and phialides (Fig. 4B), and hyphae (Fig. 4B and C), but not to conidiophores and metulae (Fig. 4B and data not shown). Control AAE1 samples where EBA2 was omitted did not bind the FITC-conjugated secondary antibody. In contrast to AAE1, the spore and hyphal walls of the AAE2 strain did not bind EBA2 (Fig. 4D–G). Thus, AAE2 is depleted for Gal*f* in its walls, consistent with the expected function of the *ugmA* gene product.

Hyphal morphogenesis defects and branching abnormalities in the *ugmA*Δ strains in Table 2A suggested that *ugmA* deletion had impaired fungal wall formation and/or maturation. The growth morphology of AAE2 was assessed on CM containing sucrose and/or Calcofluor (Table 2B). Wildtype morphology strain A28, AAE1, and the three *ugmA*Δ strains for which data are provided in Table 2A were replica-plated on CM with or without sucrose or Calcofluor to assess colony phenotype at 2 d (Fig. 5A–E). Unexpectedly, the colony morphology of A28 and AAE1 strains differed on most media. AAE2 hyphae growing at the edges of the colonies were examined using transmitted light microscopy, directly on the plates to avoid damage from mounting on a microscope slide (Fig. 5F–O). Colonies of AAE1 and the three *ugmA*Δ strains grew differently on these media (Fig. 5A–E), consistent with Fig. 3A and B. Their hyphal morphologies also differed, consistent with Fig. 4A and described quantitatively in Table 2B.

AAE1 hyphae had wildtype morphology when grown on CM (Fig. 5F), whereas AAE2 hyphae had profuse apical branching (Fig. 5K). AAE1 hyphal morphology on CM containing 1 M sucrose was wildtype (Fig. 5G), substantially similar to Fig. 5F, whereas AAE2 grown on 1 M sucrose had a partially remediated hyphal phenotype (Fig. 5L) with reduced but still apical

branching. AAE1 hyphae grown on CM containing 10 µg/mL Calcofluor had a beaded morphology (Fig. 5H), whereas AAE2 hyphae grown on this medium had a partially remediated hyphal phenotype (Fig. 5M), reminiscent of AAE2 growth on 1 M sucrose (Fig. 5L). Like 10 µg/mL Calcofluor, AAE1 hyphae grown on CM containing 30 µg/mL Calcofluor had a beaded morphology (Fig. 5I), whereas AAE2 hyphae grown on this medium were highly branched (Fig. 5N). AAE1 hyphae grown on 30 µg/mL Calcofluor plus 1 M sucrose had a wildtype phenotype (Fig. 5J). Many AAE2 hyphae had a wildtype phenotype this medium, however, bursting was frequent (*e.g.,* arrow in Fig. 5O), despite being examined directly on the Petri plate, suggesting that their walls were fragile.

The effect of growth on CM containing 1 M sucrose or 10 µg/mL Calcofluor on the *ugmA*Δ strains was quantified morphometrically (Table 2B). AAE1 strains were slightly affected by growth on these media particularly regarding hyphal extension. For the *ugmA*Δ strains, growth on amended medium significantly reduced hyphal width, and had comparable relative effects on growth and branching (shown as hyphal growth index).

3.4. Hyphal wall ultrastructure

Relative hyphal wall thickness was inferred for wildtype AAE1 and *ugmA*Δ strain AAE2 using Calcofluor and Hoechst 33258 dual-stained samples (Fig. 4A). The same dye concentrations and imaging conditions were used for both strains. Lateral walls of AAE2 hyphae (Fig. 4A) stained brightly, but not those of AAE1 (inset). For the AAE2 hyphae, hyphal wall staining obscured visualization of all but a few nuclei (arrows in Fig. 4A), unlike AAE1 hyphae (arrows in Fig. 4A inset). For both strains, wall staining was evident at septa and in spore walls. We interpret this difference to mean that the lateral walls of the AAE2 hyphae are thicker than those of wildtype.

Transverse TEM sections of AAE1 and AAE2 hyphae (that is, with well resolved cell membrane bi-layers) were used to compare hyphal diameter and wall thickness. Hyphal diameters imaged with TEM (Fig. 6) were consistent with Calcofluor-stained samples imaged with fluorescence microscopy (Fig. 4A and Table 2). Both AAE1 and AAE2 hyphae imaged by TEM had abundant, well-preserved cytoplasmic organelles, suggesting that the hyphae were likely to have been growing at the time of fixation. The AAE2 walls grown on CM (Fig. 6A–D) were significantly thicker than those of AAE1 (Fig. 6E and F), or of AAE2 grown on 1 M

sucrose (Fig. 6G and H) or 10 µg/mL Calcofluor (Fig. 6I and J). Wall thicknesses in transverse TEM sections are shown in Table 2. Walls of AAE2 hyphae grown on CM had distinct layering of moderately electrondense material, compared to walls of AAE1 hyphae grown on CM, or walls of AAE2 hyphae grown on 1 M sucrose or 10 µg/mL Calcofluor (Fig. 6 and Table 2). The AAE2 walls appeared to be similar to wildtype when grown on CM containing 1 M sucrose or 10 µg/mL Calcofluor.

4. Discussion

The *A. nidulans* genome has a single sequence, AN3112.4, with high homology to UDP-galactopyranose mutase identified in other systems, which we call *ugmA*. Replacing the *ugmA* coding sequence with Af*pyrG* showed that *A. nidulans ugmA* is not essential. The *ugmA*Δ strains grew on medium lacking pyrimidines, and could complete their asexual life cycle, producing viable conidia. However, *ugmA*Δ strains had compact colonial growth, reduced conidiation, and aberrant hyphal morphology and wall structure. UGM is not essential in the protozoan *L. major*, but its deletion led to attenuated virulence (Kleczka et al., 2007). Studies on prokaryotic UGM showed it was essential for growth and viability in bacteria (Pan et al., 2001). Similarly, *A. fumigatus glfA* is not essential, but contributes to pathogenicity when tested in immunosuppressed mice (Schmalhorst et al., 2008).

Gal*f* has been found in *A. nidulans* cell walls (Bennett et al., 1984), consistent with results of Wallis et al. (2001) who used monoclonal antibody EBA2 to immunolocalize Gal*f* to conidia and conidiophores in *A. niger*. For strain AAE1, we had strong EBA2 localization to conidia and to a lesser extent to hyphae and phialides. Even with high-sensitivity confocal imaging settings, we had no immunofluorescent signal for AAE2 conidiophores and metulae, although perhaps this could be due to masking from outer wall layers. In contrast to AAE1, none of the AAE2 cell types bound EBA2, suggesting that they were indeed depleted for Gal*f*. Thus, the presence of Gal*f* in hyphal and conidial walls of *A. nidulans* appears to be due to the action of *ugmA*.

Damveld et al. (2008) screened for cell wall mutants in *A. niger*, using a constitutively activated stress response pathway to seek genes involved in cell wall integrity. They identified mutants in a UGM homologue, *A. niger ugmA*, and showed by sequence comparison that *A.*

niger and *A. nidulans ugmA* were closely related. Like *A. niger, A. nidulans ugmA* is predicted to have five introns (Damveld et al., 2008). Related *A. niger* sequences designated *ugmB* were present in at least two other *Aspergillus spp*, but not in *A. nidulans*. The *A. niger ugmB* sequence was full length, but *ugmB*Δ in a wildtype or in a *ugmA*Δ background did not generate an additional phenotype (Damveld et al., 2008). Unlike *ugmA*, *ugmB* function is unknown.

*Aspergillus niger ugmA*Δ strains showed increased sensitivity to Calcofluor compared to a wildtype strain (Damveld et al., 2008), consistent with results from Kim et al. (2008). Unexpectedly, the *A. nidulans* AAE2 hyphal phenotype was partially remediated on medium containing 10 µg/mL (but not 30 µg/mL) Calcofluor; this phenotype was reminiscent of growth on 1 M sucrose. This result is consistent with our TEM results showing that AAE2 cell wall thickness on CM containing 10 µg/mL Calcofluor was about a third as thick as on CM alone. *Aspergillus nidulans* mutants that are hypersensitive to growth on Calcofluor have been described previously (Hill et al., 2006), as has remediation on high osmolarity medium, but to our knowledge Calcofluor remediation has not. Damveld et al. (2008) assessed colony growth of *A. niger ugmA* mutants on medium containing 10 µg/mL Calcofluor, but did not examine them microscopically. Calcofluor treatment has been shown to increase chitin production in *Saccharomyces* (García-Rodriguez et al., 2000) but apparently that chitin is weaker, so the mechanism by which remediation occurs is unclear.

The *ugmA* deletion had a dramatic effect on *A. nidulans* hyphal walls imaged with TEM, and wall thicknesses measured with TEM were consistent with relative Calcofluor staining. Damveld et al (2008, and references therein) suggest that wall stress may induce compensatory synthesis of chitin and α-glucan. A comparable effect could account for the increased wall thickness in our AAE2 hyphal walls and changes in Calcofluor binding. Following partial remediation by growing AAE2 on 1 M sucrose or 10 µg/mL Calcofluor, hyphal wall cross-sections imaged by TEM resembled those of AAE1. Thus, at least some of the defects induced by deletion of *A. nidulans ugmA* can be remediated by treatments likely to have substantially different targets.

In contrast to our TEM results showing that AAE1 walls were significantly thinner than those of AAE2, Schmalhorst et al. (2008) found using freeze fracture SEM that wildtype *A. fumigatus* hyphal walls were substantially thicker than those of a Δ*glfA* strain. The *A. fumigatus* hyphae may have been older than ours (which were 16 h), since they lacked substantial

cytoplasm. In addition, TEM and SEM preparation techniques differ substantially. If the Δ*glfA* wall were as diffuse as that of AAE2 hyphae, it could have collapsed during drying. Given that walls of the wildtype *A. fumigatus* (Schmalhorst et al., 2008) and *A. nidulans* (this study) strains had substantially different thickness, even though they have similar overall composition (Guest and Momany, 2000), it will be important in the future to compare similar aged cells with both techniques.

In sum, we have shown that *A. nidulans ugmA* is important for wildtype growth, but is not essential for survival. The *ugmA*Δ phenotype is consistent with defects related in cell wall deposition and maturation. We are continuing to explore the biochemistry and ultrastructure of *A. nidulans ugmA*Δ strains.

Acknowledgments

This research was supported by Natural Science and Engineering Research Council of Canada Discovery grants and a Canadian Institutes of Health Research/Regional Partnership Program grant to SGWK and DARS, and by an Egyptian Ministry of Higher Education grant to A.M.E. We thank Tom Bonli (Department of Geological Sciences, University of Saskatchewan) for assistance with the scanning electron microscope (SEM), Dr. Robbert Damveld for providing a copy of their accepted manuscript prior to publication, and anonymous Reviewers for suggestions.

References

Adams, T.H., Wieser, J.K., Yu, J.-H., 1998. Asexual sporulation in *Aspergillus nidulans*. Microbiol. Mol. Biol. Rev. 62, 35–54.

Arathoon, E.G., 2001. Clinical efficacy of echinocandin antifungals. Curr. Opin. Infect. Dis. 14, 685–691.

Bakker, H., Kleczka, B., Gerardy-Schahn, R., Routier, F.H., 2005. Identification and partial characterization of two eukaryotic UDP-galactopyranose mutases. Biol. Chem. 386, 657–661.

Bennett, J.E., Bhattacharjee, A.K., Glaudemans, C.P.J., 1984. Galactofuranosyl groups are immunodominant in *Aspergillus fumigatus* galactomannan. Mol. Immunol. 22, 251–254.

Beverly, S.M., Owens, K.L., Showalter, M., Griffith, C.L., Doering, T.L., Jones, V.C., McNeil, M.R., 2005. Eukaryotic UDP-galactopyranose mutase (GLF gene) in microbial and metazoal pathogens. Eukaryot. Cell. 4, 1147–1154.

Carrillo-Munoz, A.J., Giusiano, G., Ezkurra, P.A., Quindos, G., 2006. Antifungal agents: mode of action in yeast cells. Rev. Esp. Quimioterap. 19, 130–139.

Chamilos, G., Kontoyiannis, D.P., 2005. Update on antifungal resistance mechanisms of *Aspergillus fumigatus*. Drug Resist. Updat. 8, 344–358. Costachel, C., Coddeville, B., Latge, J.-P., Fontaine, T., 2005. Glycosylphosphatidylinostol-anchored fungal polysaccharide in *Aspergillus fumigatus*. J. Biol. Chem. 280, 39835–39842.

Costachel, C., Coddeville, B., Latge, J.-P., Fontaine, T., 2005. Glycosylphosphatidylinostol-anchored fungal polysaccharide in *Aspergillus fumigatus*. J. Biol. Chem. 280, 39835–39842.

Cowen, L., 2008. The evolution of fungal drug resistance: modulating the trajectory from genotype to phenotype. Nat. Rev. Micro. 6, 187–198.

Damveld, R.A., Franken, A., Arentshorst, M., Punt, P.J., Klis, F.M., van den Hondel, C.A.M.J.J., Ram, A.F.J., 2008. A novel screening method for cell wall mutants in *Aspergillus niger* identifies UDP-galactopyranose mutase as an important protein in fungal cell wall biosynthesis. Genetics 178, 873–881.

García-Rodriguez, L., Durán, A., Roncero, C., 2000. Calcofluor antifungal action depends on chitin and a functional high-osmolarity glycerol response (HOG) pathway: evidence for a physiological role of the *Saccharomyces cerevisiae* HOG pathway under non-inducing conditions. J. Bacteriol. 182, 2428–2437.

García-Ruiz, J.C., Amutio, E., Pontón, J., 2004. Invasive fungal infection in immunocompromised patients. Rev. Iberoam. Micol. 21, 55–62.

Guest, G.M., Momany, M., 2000. Analysis of cell wall sugars in the pathogen *Aspergillus fumigatus* and the saprophyte *Aspergillus nidulans*. Mycologia 92, 1047–1050.

Hill, T.W., Loprete, D.M., Momany, M., Harsch, M., Livesay, J.A., Mirchandani, A., Murdock, J.J., Vaughan, M.J., Watt, M.B., 2006. Isolation of cell wall mutants in *Aspergillus nidulans* by screening for hypersensitivity to Calcofluor White. Mycologia 98, 399–409.

Kaminskyj, S.G.W., 2000. Septum position is marked at the tip of *Aspergillus nidulans* hyphae. Fungal. Genet. Biol. 31, 105–113.

Kaminskyj, S.G.W., 2001. Fundamentals of growth, storage, genetics and microscopy of *Aspergillus nidulans*. Fungal. Genet. Newsl. 48, 25–31.

Kaminskyj, S.G.W., Hamer, J.E., 1998. Hyp loci control cell pattern formation in the vegetative mycelium of *Aspergillus nidulans*. Genetics 148, 669–680.

Kaminskyj, S.G.W., Heath, I.B., 1995. Integrin and spectrin homologues, and cytoplasm-wall adhesion in tip growth. J. Cell Sci. 108, 849–856.

Kim, J., Campbell, B., Mahoney, N., Chan, K., Molyneux, R., May, G., 2008. Chemosensitization prevents tolerance of *Aspergillus fumigatus* to antimycotic drugs. Biochem. Biophys. Res. Commun. 372, 266–271.

Kleczka, B., Lamerz, A.-C., Zandbergen, G., Wenzel, A., Gerardy-Schahn, R., Wiese, M., Routier, F.H., 2007. Targeted gene deletion of *Leishmania major* UDPgalactopyranose mutase leads to attenuated virulence. J. Biol. Chem. 282, 10498–10505.

Koplin, R., Brisson, J.R., Whitfield, C., 1997. UDP-galactofuranose precursor required for formation of lipopolysaccharide O antigen of *Klebsiella* pneumoniae serotype O1 is synthesized by the product of the rfbDKPO1 gene. J. Biol. Chem. 272, 4121– 4128.

Latgé, J.-P., Kobayashi, H., Debeaupuis, J.-P., Diaquin, M., Sarfati, J., Wieruszeski, J.- M., Parra, E., Bouchara, J.-P., Fournet, B., 1994. Chemical and immunological characterization of the extracellular galactomannan of *Aspergillus fumigatus*. Infect. Immun. 62, 5424–5433.

Leitao, E.A., Bitte, V.C.B., Haido, R.M.T., Valente, A.P., Peter-Katalinic, J., Letzel, M., de Souza, L.M., Barreto-Bergter, E., 2003. b-Galactofuranose-containing O-linked oligosaccharides present in the cell wall peptidogalactomannan of *Aspergillus fumigatus* contain immunodominant epitopes. Glycobiology 13, 681–692.

Loffler, J., Stevens, D.A., 2003. Antifungal drug resistance. CID 36 (Suppl. 1), S31–S41.

Maertens, J., Theunissen, K., Lodewyck, T., Lagrou, K., Eldere, J., 2007. Advances in the serological diagnosis of invasive *Aspergillus* infections in patients with haematological disorders. Mycoses 50 (Suppl. 1), 2–17.

Nassau, P.M., Martin, S.L., Brown, R.E., Weston, A., Monsey, D., McNeil, M.R., Duncan, K., 1996. Galactofuranose biosynthesis in *Escherichia coli* K-12: identification and cloning of UDP-galactopyranose mutase. J. Bacteriol. 178, 1047–1052.

Nayak, T., Szewczyk, E., Oakley, C.E., Osmani, A., Ukil, L., Murray, S.L., Hynes, M.J., Osmani, S.A., Oakley, B.R., 2006. A versatile and efficient gene-targeting system in *Aspergillus nidulans*. Genetics 172, 1557–1566.

Notermans, S., Veeneman, G.H., van Zuylen, C.W.E.M., Hoogerhout, P., van Boom, J.H., 1998. (1→5)-linked β-D-galactofuranosides are immunodominant in extracellular polysaccharides of *Penicillum* and *Aspergillus species*. Mol. Immunol. 25, 975–979.

Osmani, A.H., Oakley, B.R., Osmani, S.A., 2006. Identification and analysis of essential *Aspergillus nidulans* genes using the heterokaryon rescue technique. Nat. Protoc. 1, 2517–2526.

Pan, F., Jackson, M., Ma, Y., McNeil, M., 2001. Cell wall core galactofuran is essential for growth of *Mycobacteria*. J. Bacteriol. 183, 3991–3998.

Pederson, L.L., Turco, S.J., 2003. Galactofuranose metabolism: a potential target for antimicrobial chemotherapy. Cell. Mol. Life Sci. 60, 259–266.

Randhawa, G.K., Sharma, G., 2004. Echinocandins: a promising new antifungal group. Indian J. Pharmacol. 36, 65–71.

Sanders, D.A.R., Staines, A.G., McMahon, S.A., McNeil, M.R., Whitfield, C., Naismith, J.H., 2001. UDP-galactopyranose mutase has a novel structure and mechanism. Nat. Struct. Biol. 8, 858–863.

Schmalhorst, P.S., Krappmann, S., Vervecken, S.W., Rohde, M., Müller, M., Braus, G.H., Contreras, R., Braun, A., Bakker, H., Routier, F.H., 2008. Contribution of galactofuranose to the virulence of the opportunistic pathogen *Aspergillus fumigatus*. Eukaryot. Cell 7, 1268–1277.

Shaw, B.D., Momany, M.M., 2002. *Aspergillus nidulans* polarity mutant *swoA* is complemented by protein O-mannosyltransferase *pmtA*. Fungal. Genet. Biol. 37, 263–270.

Shi, X., Sha, Y., Kaminskyj, S., 2004. *Aspergillus nidulans hypA* regulates morphogenesis through the secretion pathway. Fungal. Genet. Biol. 41, 75–88.

Spath, G.F., Epstein, L., Leader, B., Singer, S.M., Avila, H.A., Turco, S.J., Beverley, S.M., 2000. Lipophosphoglycan is a virulence factor distinct from related glycoconjugates in the protozoan parasite *Leishmania major*. Proc. Natl. Acad. Sci. USA 97, 9258–9263.

Stevenson, G.G., Andrianopoulos, K., Hobbs, M., Reeves, P.R., 1996. Organization of the *Escherichia* coli K-12 gene cluster responsible for production of the extracellular polysaccharide colonic acid. J. Bacteriol. 178, 4885–4893.

Stynen, D., Sarafati, J., Goris, A., Prevost, M-C., Lesourd, M., Kamphuis, H., Darras, V., Latgé, J.-P., 1992. Rat monoclonal antibodies against *Aspergillus* galactomannan. Infect. Immun. 60, 2237–2245.

Szewczyk, E., Nayak, T., Oakley, C.E., Edgerton, H., Xiong, Y., Taheri-Talesh, N., Osmani, S.A., Oakley, B.R., 2007. Fusion PCR and gene targeting in *Aspergillus nidulans*. Nat. Protoc. 1, 3111–3120.

Tawara, S., Ikeda, F., Maki, K., Morishita, Y., Otomo, K., Teratani, N., Goto, T., Tomishima, M., Ohki, H., Yamada, A., Kawabata, K., Takasugi, H., Sakane, K., Tanaka, H., Matsumoto, F., Kuwahara, S., 2000. *In vitro* activities of a new lipopeptide antifungal agent, FK463, against a variety of clinically important fungi. Antimicrob. Agents Chemother. 44, 57–62.

Trinci, A.P.J., 1974. A study of the kinetics of hyphal extension and branch initiation of fungal mycelia. J. Gen. Microbiol. 81, 225–236.

Wallis, G.L.F., Hemming, F.W., Peberdy, J.F., 2001. β-Galactofuranoside glycoconjygate on the conidia and conidiophores of *Aspergillus niger*. FEMS Microbiol. Lett. 201, 21–27.

Weston, A., Stern, R.J., Lee, R.E., Nassau, P.M., Monsey, D., Martin, S.L., Scherman, M.S., Besra, G.S., Duncan, K., McNeil, M.R., 1998. Biosynthetic origin of mycobacterial cell wall galactopyranosyl residues. Tuberc. Lung Dis. 78, 123–131.

Whitfield, C., Richards, J.C., Perry, M.B., Clarke, B.R., Maclean, L.L., 1991. Expression of two structurally distinct D-galactan O antigens in the lipopolysaccharide of *Klebsiella pneumoniae* serotype O1. J. Bacteriol. 173, 1420–1431.

Yang, Y., El-Ganiny, A.M., Bray, G.E., Sanders, D.A.R., Kaminskyj, S.G.W., 2008. *Aspergillus nidulans hypB* encodes a Sec7-domain protein important for hyphal morphogenesis. Fungal. Genet. Biol. 45, 749–759.

Tables

Table 1. Biological materials used in this study

Aspergillus nidulans

A1149 [a]	*pyrG89; pyroA4; nkuA*::*argB*
AAE1 [b]	*pyrG89*:*N. crassa pyr4*+; *pyroA4; nkuA*::*argB*
AAE2 (*ugmA*Δ) [b]	AN3112::Af*pyrG*; *pyrG89*; *pyroA4*; *nkuA*::*argB*
AAE3(*ugmA*Δ:Af*glfA*) [b]	AN3112::Af*pyrG*; *pyrG89*; *pyroA4*; *nkuA*::*argB*; Af*glfA*
AOZ1 [b]	*swoA1*; *wA3*, GFP-*tubA*

Plasmids

ARp1 [c]	AMA1, *Neurospora crassa pyr4*+, amp^R
pAO81 [a]	S-TAG, *A. fumigatus pyrG*, kan^R
pET22 [d]	*A. fumigatus glfA*, amp^R

Primers 5' → 3' [b]

P1	GACTCTTGAGATTTGCTTGGGTCTC
P2	CCTGGAGCATTCCTTGTCTG
P3	AATTGCGACTTGGACGACATAGAAGAGAGCGAAGCTGCAG
P4	GAGTATGCGGCAAGTCATGAAATAAAACTCTTCTGCGTGG
P5	CTGTTTGGCCGCCTAATAGC
P6	GTGTTTACCAAGAATATGTTCATCGA
P8	CACATCCGACTGCACTTCC
P21	ATGCTTAGTCTAGCTCGCAAGAC
P23	CTGCGCCTTATTCTTAGCAAA
AfpyrGF	ATGTCGTCCAAGTCGCAATT
AfpyrGR	TCATGACTTGCCGCATACTC
AfugmAF	CCCTCCAGCTCCGTCGAC
AfugmAR	CTGGGCCTTGCTCTTGGC
nkuAF	CCCCGTCCGTCTGCAG
nkuAR	AACTTCGTCTCAAGTAACTCCTCCAC

[a] www.fgsc.net

[b] This study

[c] Shi *et al.*, 2004

[d] Bakker *et al.*, 2005

Table 2. Morphometric comparison [a] of near-isogenic wildtype morphology (AAE1) and UDP-galactopyranose mutase deletion (*ugmA*Δ) strains [bc]

A. Growth on CM	**AAE1**	***ugmA*Δ*1***	***ugmA*Δ*2***	***ugmA*Δ*3***
Hyphal width (μm)	2.7±0.4 [d]	3.6±0.6 [e]	3.3±0.6 [f]	3.6±0.7 [e]
Basal cell length (μm)	26.9±1.2 [d]	14.9±0.7 [e]	19.5±0.9 [f]	15.3±0.6 [e]
Total colony length (μm)	252±25.7 [d]	317±27.3 [d]	378±79.5 [d]	348±25.0 [d]
Total tips per colony	2.4±0.2 [e]	7.6±0.5 [d]	8.3±1.4 [d]	8.2±0.4 [d]
Hyphal growth index (μm hypha/tip)	105	42	46	42
Wall thickness (nm)	54.0±2.4 [d]	204±10.5 [f]	n/a	n/a

B. Growth on amended CM	**CM + 1 M sucrose**		**CM+10 μg/mL calcofluor**	
	AAE1	**AAE2**	**AAE1**	**AAE2**
Hyphal width (μm)	2.4±0.1 [d]	3.1±0.1 [f]	2.6±0.0 [d]	3.1±0.0 [f]
Basal cell length (μm)	26.1±1.4 [d]	15.3±0.7 [e]	20.8±1.1 [f]	21.8±1.5 [f]
Total colony length (μm)	206±13.6 [e]	140±10.4 [f]	209±31.6 [e]	244±20.9 [d]
Total tips per colony	2.8±0.2 [d]	4.1±0.2 [e]	2.7±0.2 [d]	7.2±0.5 [f]
Hyphal growth index (μm hypha/tip)	73	32	77	34
Wall thickness (nm)	n/a	66.0±3.5 [de]	n/a	77.8±3.8 [e]

[a] Measurements are expressed as mean ± standard error, for 50 hyphae (width and basal cell length), 30 colonies (total colony length and total tips per colony), and 10 transmission electron micrograph near-median sections. n/a, not assessed.

[b] Strains were grown for 14 h at 28 ºC on dialysis tubing overlying agar-solidified medium. See Materials and Methods for details. AAE2 is *ugmA*Δ*1*.

[c] For each measurement type, values followed by different letters (d-f) are significantly different ($P<0.05$; ANOVA). Summary statistics: hyphal width ($P = 0.0001$; $F = 54.314$), basal cell length ($P = 0.0001$; $F = 38.772$); total colony length ($P = 0.082$; $F = 2.299$); tips per colony ($P = 0.0001$; $F = 27.115$).

Figures

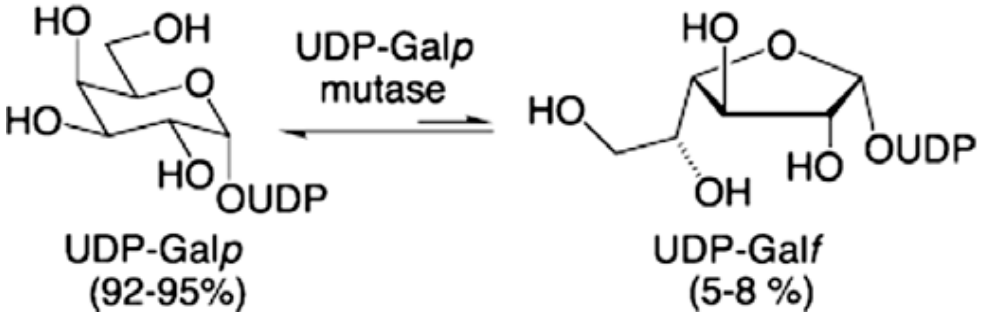

Fig. 1. Interconversion of UDP-galactopyranose (UDP-Gal*p*) and UDP-galactofuranose (UDP-Gal*f*) by UDP galactopyranose mutase. The equilibrium of this reaction is heavily in favour of UDP-Gal*p*.

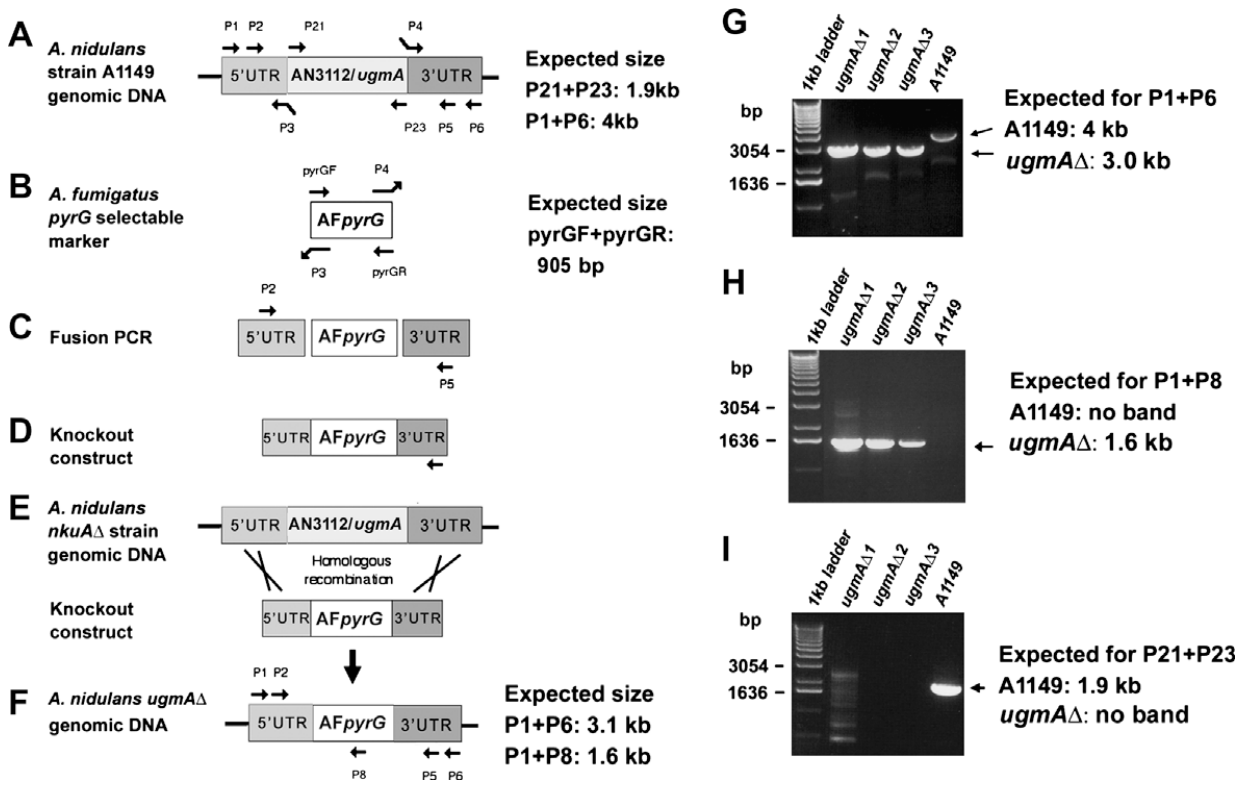

Fig. 2. Strategy for and results of deleting *Aspergillus nidulans* UDP-galactopyranose mutase (*ugmA*) to create *ugmA*Δ strains. (A–F) Deletion strategy. The 5' and 3' regions (5'UTR and 3'UTR, respectively) flanking AN3112 were amplified using P1 + P3 and P4 + P6, respectively, from strain A1149 (*nkuA*Δ*, pyrG89*) genomic DNA template. Primer sequences are in Table 1. P3 and P4 are bridging primers between the flanking regions and the selectable marker. (B) The selectable marker, *A. fumigatus pyrG*, was amplified from plasmid AO81 with pyrGF and pyrGR. (C) Fusion PCR (semi-nested, with P2 + P5) using mixed template (5'UTR, *AfpyrG*, 3'UTR), with complementary ends generated the bridging primers P3 and P4, created (D) the linear AN3112 knockout construct with AN3112 flanking regions. (E) A1149 protoplasts were transformed with the knockout construct. Homologous recombination between the flanking regions replaced AN3112 with *AfpyrG*, creating *ugmA*Δ. The flanking regions were not altered by the homologous recombination, so primer sites remain intact. (F) Predicted *ugmA*Δ genomic DNA. (G–I) PCR comparisons of genomic template from A1149 and *ugmA*Δ strains. (G) Using primers P1 + P6, to amplify *ugmA* plus flanking regions. (H) Using primers P1 + P8, to demonstrate that *AfpyrG* had integrated at the *ugmA* locus. (I) Using primers P21 + P23, to demonstrate the presence of *ugmA* in A1149, and its absence from the *ugmA*Δ strains.

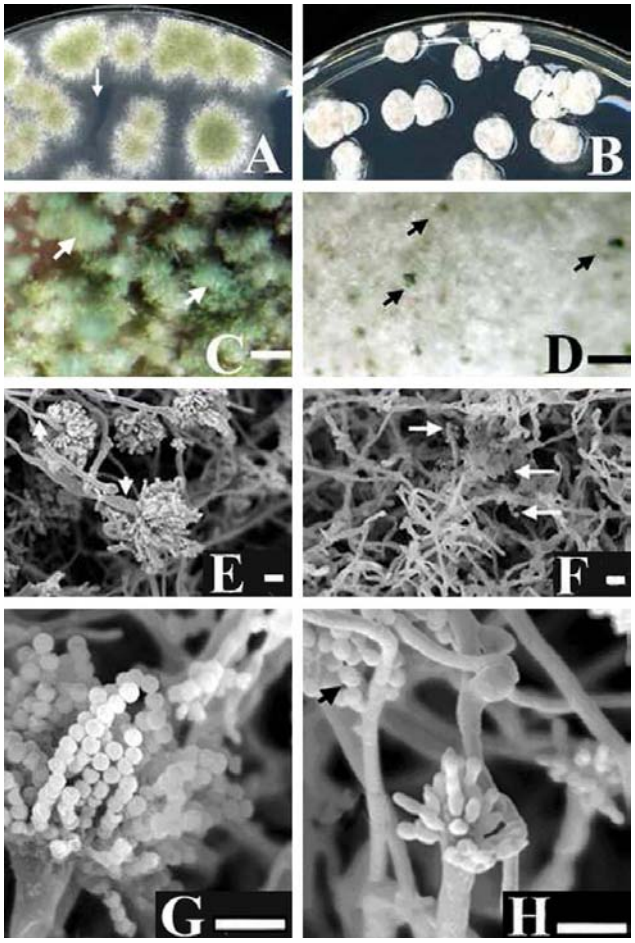

Fig. 3. Conidiation in *Aspergillus nidulans* wildtype AAE1 (A, C, E, and G), and UDP-galactopyranose mutase deletion strain AAE2 (B, D, F, and H), 3 d after inoculation. (A and B) Colony morphology of AAE1 and AAE2 strains. The centres of AAE1 colonies (A) have green conidia, whereas AAE2 colonies (B) have only faint pigmentation due to sparse conidiation. AAE1 colonies are surrounded by a fringe of hyphae extending into the medium (arrows in A) whereas these are lacking in AAE2 colonies. (C and D) A stereomicroscope images of the centres of colonies in A and B. Bars in C and D = 100 lm. As seen from above, an AAE1 colony (C) has closely packed conidial heads, whereas an AAE2 colony (D) has relatively few, widely separated, conidial heads that produced mature green conidia (e.g., arrows). (E–H) Scanning electron micrographs of AAE1 (E and G) and AAE2 colonies (F and H). Bars in E–H = 10 μ m. AAE1 colonies (E and G) produce conidiophores (arrowheads) with conidial heads bearing long chains of spores, whereas AAE2 colonies had sterile aerial hyphae with sparse conidiation (arrows in F). (H) An AAE2 colony showing chains of spores (arrow) on one conidial head, whereas others have abnormal or arrested development.

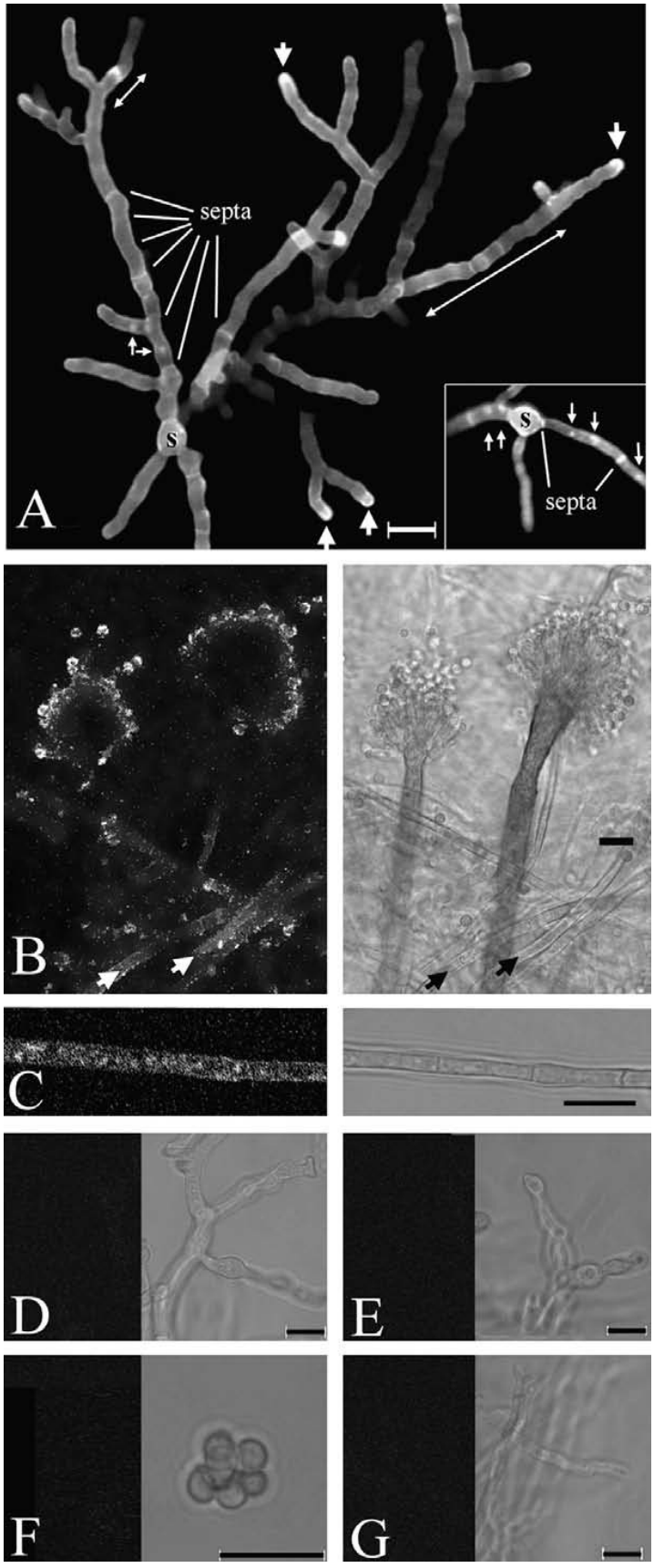
septa
s
A
s
septa
B
C
D
E
F
G

Fig. 4. Walls of *Aspergillus nidulans* AAE2 (*ugmA*Δ) and AAE1 (wildtype) strains following (A) Calcofluor staining at 16 h, or (B–F) Gal*f* immunolocalization at 36 h. Bars = 10 μm. (A) Germlings were stained with the same solution of Hoechst 33258 for nuclei and Calcofluor for cell walls, and visualized with confocal microscopy. The AAE2 hyphal walls are thick, and stain unevenly: double-headed arrows indicate hyphal walls with considerable variability in staining intensity despite being nearmedian optical sections. Some AAE2 hyphal tips stained intensely (large arrows) while other did not, even though both types were a similar optical section. Wildtype morphology AAE1 hyphal walls (A, inset) stained lightly compared to septa and spore (s) walls. Unlike the wildtype strain, hyphal wall staining in the AAE2 strain often obscured visualization of nuclei (small arrows). (B–G) Paired immunofluorescence and transmitted images of Gal*f* localization using the EBA2 monoclonal antibody (see Section 2). (B) In the AAE1 strain, Gal*f* was present in hyphal walls (arrows), in spores, and to a slight extent in phialides. No localization was detected on the conidiophore or metula walls. (C) Gal*f* in hyphal walls of AAE1. The AAE2 conidiophores (D and E), spores (F), and hyphae (G) did not stain under the same preparation and imaging conditions as used for (B) and (C).

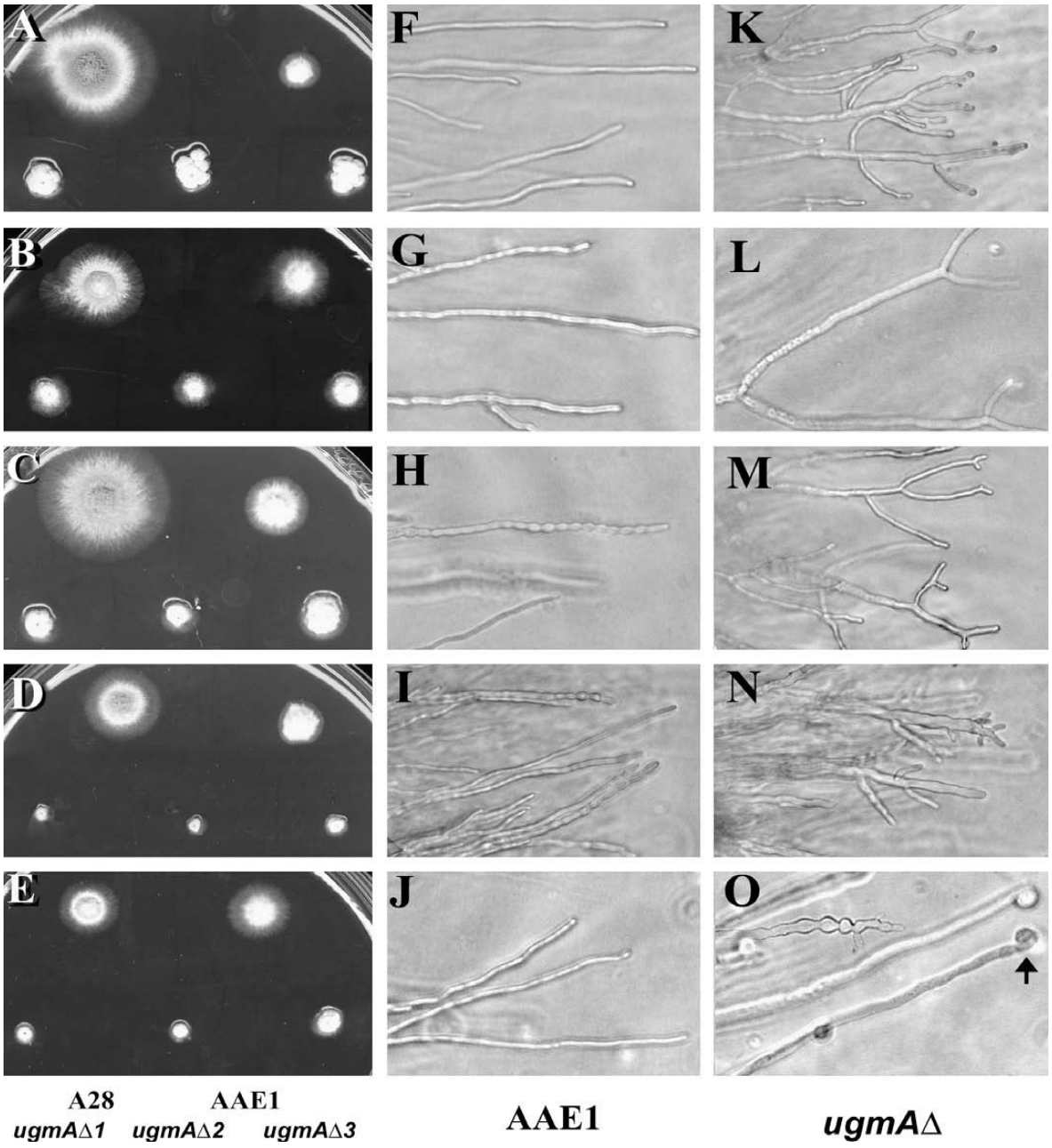

Fig. 5. Colony growth (A–E) and hyphal morphology for AAE1 (F–J) and *ugmA*Δ strains (K–O) after 2 d. Map to the inoculation pattern is at the bottom left. Strains were grown on complete medium, CM (A, F, and K); on CM + 1 M sucrose (B, G, and L); on CM + 10 µg/mL Calcofluor (C, H, and M); on CM + 30 µg/mL Calcofluor (D, I, and N); on CM + 1 M sucrose + 30 µg/mL Calcofluor (E, J, and O).

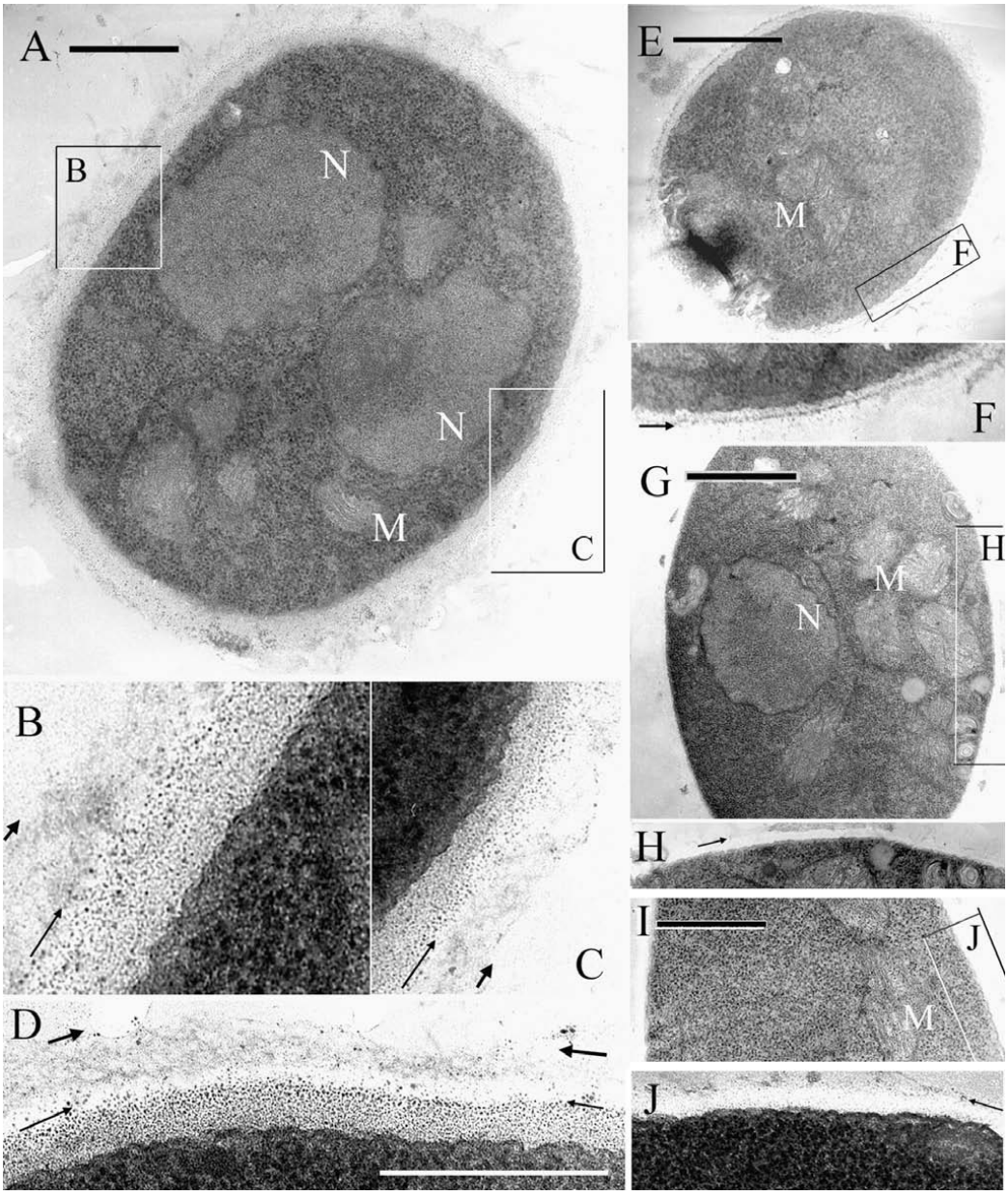

Fig. 6. Transmission electron micrographs of *Aspergillus nidulans ugmA*Δ strain AAE2 (A–D) and wildtype strain AAE1 (E–F) growing on complete medium (CM); AAE2 hyphae growing on CM containing 1 molar sucrose (G–H) or CM containing 10 µg/mL Calcofluor (I–J). Bars in A, E, G, I = 1 µm. Images in B–C, F, H, J are transverse sections that correspond to the boxed regions in A, E, G, I, respectively, and have been contrast-adjusted and magnified to highlight wall structure. Image D is a transverse section of another AAE2 hypha growing on CM for which a full cross section was not available. Arrows indicate the outer edge of the two prominent wall layers for AAE2 hyphae growing on CM (A–D), and the outer wall of hyphae in other samples (F, H, J). N, nucleus; M, mitochondrion.

Supplemental materials

Supplemental Figure A: Rescue of the *ugmAΔ* phenotype by complementation with Af*glfA*

a) AAE2 (*ugmAΔ*) colonies transformed with Af*glfA* protein expression plasmid pET22b. Af*glfA* from pET22b has been shown to mediate Gal*f*-Gal*p* conversion (Bakker *et al.* 2005 Biol Chem. 386, 657-662). After 4 d growth at 37 ºC, a single putative *ugmA*Δ:Af*glfA* colony with wildtype green conidia (black arrow) amongst many *ugmAΔ* colonies.

b) PCR of pET22b and of genomic DNA template extracted from the putative *ugmA*Δ:Af*glfA* colony shown in (a) using primers AfglfAF [CCCTCCAGCTCCGTCGAC] and AfglfAR [CTGGGCCTTGCTCTTGGC]. We believe that pET22b has integrated into the genome, since in six independent experiments we have been unable to rescue pET22b by transforming genomic DNA extracted from this strain into *E. coli* and selecting for ampicillin resistance. Differences in template concentration are consistent with the weak amplification of Af*glfA* from genomic DNA.

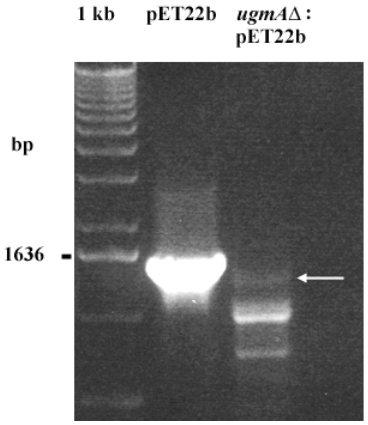

c) Hyphae (left) and a typical young conidiophore (right) of the *ugmA*Δ:Af*glfA* strain, which were stained with Calcofluor for septa and Hoechst 33258 for nuclei, and imaged with confocal epifluorescence microscopy. Nuclear morphology and spacing in the hyphae (left) is consistent with wildtype strains. Note synchronous development of metulae (m) and phialides (ph). Bars = 10 μm.

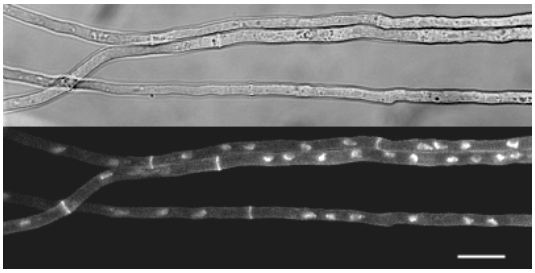

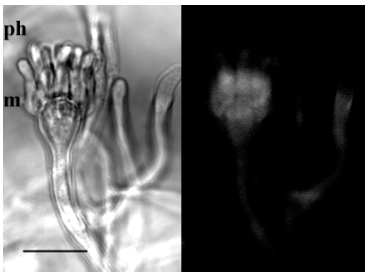

d)Morphometry of the *ugmA*Δ:Af*glfA* strain hyphae. Width: 3.0 ± 0.1 μm (n=50); basal cell length: 39.9 ± 2.9 μm (n=30). Compare with *ugmA*Δ strains (Table 2).

Supplemental Figure B: **Following mating, *ugmA* segregates independently of *nkuA* and *swoA*.**

AAE2 (*ugmΔ::AfpyrG*; *nkuA*Δ::*argB*; *pyroA1* and AOZ1 (*swoA1*^{ts}; *wA3*; *argB2*; GFP-*tubA*) were mated as described in Kaminskyj (2001). AOZ1 was created by mating *swoA1* strain AXL4 (a gift of Michelle Momany: Shaw and Momany 2002 Fung. Genet. Biol. 37: 263-270) and LO1022 (a gift of Liz and Berl Oakley: Horio and Oakley 2005 Molec. Biol. Cell 16: 918-926). Cleistothecia from the AAE2::AOZ1 cross containing viable spores were isolated only following extended incubation, ~3 months.

a) Independent inheritance of *ugmA*Δ and *swoA1*. Typical results are shown for single ascospore progeny from an AAE2::AOZ1 cross. Parental *swoA1* and *ugmA*Δ strains and their progeny were grown on fully supplemented medium at 37 ºC. Both *ugmA*Δ and *swoA1* have diminished sporulation at 37 ºC, but can be distinguished by their colony morphologies. Wildtype *vs* diminished sporulation was seen in 43:97 progeny, which is consistent with independent segregation of *ugmA*Δ and *swoA1*, and severely defective growth of [*ugmA*Δ *,swoA1*] double mutants (*e. g.,* arrowheads). For all single ascospore colonies showing wildtype sporulation, green : white = 22 : 21. Together, these data are consistent with independent inheritance of *ugmA*Δ and *swoA1*.

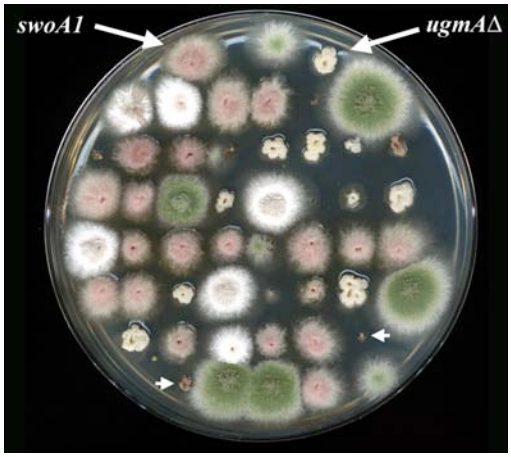

b) Independent inheritance of *ugmA* and *nkuA* in progeny from AAE2::AOZ1. Genomic DNA was extracted from six randomly-selected progeny with the *ugmA*Δ colony phenotype, and tested for the presence of *nkuA*$^{+}$ using PCR and primers nkuAF [CCCCGTCCGTCTGCAG], and nkuAR [AACTTCGTCTCAAGTAACTCCTCCAC], which are expected to amplify a 1981 bp fragment. Segregation of *nkuA*Δ and *nkuA*$^{+}$ (lanes ABC and DEF, respectively), independent of *ugmA*. The positive control template was *A. nidulans* A28 genomic DNA (lane G).

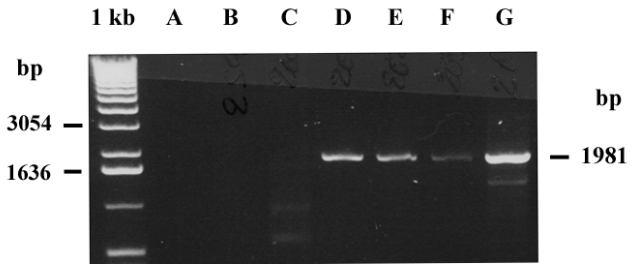

Chapter 3

Characterization of *Aspergillus nidulans* UDP-glucose -4-epimerase, UgeA

This chapter studies the biological roles of UgeA, the upstream enzyme of Gal*f* biosynthesis pathway, UgeA catalyze the reaction that create the substrate of UgmA. This manuscript has been published as "*Aspergillus nidulans* UDP-glucose-4-epimerase UgeA has multiple roles in wall architecture, hyphal morphogenesis, and asexual development" In Fungal Genetics and Biology 47: 629-635. **El-Ganiny, Sheoran, Sanders, and Kaminskyj, 2010.**

The objectives of the research in this chapter were

1) To identify putative UDP-glucose/galactose 4-epimerase in *A. nidulans*.
2) To determine if UgeA is essential for viability of *A. nidulans.*
3) To investigate the effects of *ugeA* deletion and [*ugeA, ugmA*] double deletion on colony growth, hyphal morphogenesis and cell wall ultrastructure.
4) To determine the subcellular localization of *A. nidulans* UgeA and UgmA

In this chapter, I have done the following part of the research: identification of *A. nidulans* UgeA, construction and validation of *ugeAΔ* and [*ugeAΔ, ugmAΔ*] strains, characterization of generated strains using fluorescence microscopy, SEM and TEM, comparing growth of wild type, *ugeAΔ*, *ugmAΔ* and [*ugeAΔ, ugmAΔ*] strains on glucose and galactose containing media, localization of UgeA and UgmA by C-terminus tagging with GFP and finally cloning of UgeA into expression vector. Inder Sheoran who was working in Dr. Sanders lab expressed UgeA in *E. coli*, purified the enzyme with affinity chromatography and tested its enzymatic activity *in vitro*. I wrote the first draft of the paper (excluding the *in vitro* enzymatic activity of UgeA). My supervisor Dr. Kaminskyj edited this draft, did the statistical analysis and the final processing of figures prior accepting it for publication.

Aspergillus nidulans UDP-glucose-4-epimerase UgeA has multiple roles in wall architecture, hyphal morphogenesis, and asexual development.

Amira M. El-Ganiny [a], Inder Sheoran [b], David A. R. Sanders [b], Susan G. W. Kaminskyj [a, *]

a Department of Biology, University of Saskatchewan, 112 Science Place, Saskatoon SK Canada S7N 5E2

b Department of Chemistry, University of Saskatchewan, 110 Science Place, Saskatoon SK Canada S7N 5C9

* Author for correspondence. Tel 1 306 966 4422; email susan.kaminskyj@usask.ca

Key Words: *Aspergillus nidulans*, galactofuranose, hyphal morphogenesis, hyphal wall architecture, UDP-glucose-4-epimerase, drug development target

Abbreviations: Gal*f*, galactofuranose; Gal*p*, galactopyranose; GFP, green fluorescent protein; UGE, UDP-glucose-4-epimerase; UGM, UDP-galactopyranose mutase

Abstract

Aspergillus nidulans UDP-glucose-4-epimerase UgeA interconverts UDP-glucose and UDP-galactose and participates in galactose metabolism. The sugar moiety of UDP-galactose is predominantly found as galactopyranose (Gal*p*, the six-membered ring form), which is the substrate for UDP-galactopyranose mutase (encoded by *ugmA*) to generate UDP-galactofuranose (Gal*f*, the five-membered ring form) that is found in fungal walls. In *A. fumigatus*, Gal*f* residues appear to be important for virulence. The *ugeA*Δ strain is viable, and has defects including wide, slow growing, highly branched hyphae and reduced conidiation that resemble the *ugmA*Δ strain. As for the *ugmA*Δ strain, *ugeA*Δ colonies had substantially reduced sporulation but normal spore viability. Conidia of the *ugeA*Δ strain could not form colonies on galactose as a sole carbon source, however they produced short, multinucleate germlings suggesting they ceased to grow from starvation rather than galactose toxicity. UgeA purified from an expression plasmid had a relative molecular weight of 40.6 kDa, and showed *in vitro* UDP-glucose-4-epimerase activity. Transmission electron microscope cross-sections of *ugeA*Δ hyphae had wild type appearance and distribution of organelles. The *ugeA*Δ walls were twice the thickness of wild type hyphae, but half the thickness of *ugmA*Δ walls. The outer wall appearance was similar for the *ugeA*Δ and *ugmA*Δ strains, and both strains showed increased substrate adhesion. Localization of UgeA-GFP and UgmA-GFP was cytoplasmic, and was similar on glucose and galactose. Neither gene product had a longitudinal polarized distribution and both were excluded from some organelles. The roles of UgeA in *A. nidulans* growth and morphogenesis are consistent with the importance of Gal*f*, and are related but not identical to the roles of UgmA.

1. Introduction

Fungi and protozoa are morphologically simple eukaryotes that are becoming increasingly important human pathogens. In 1939, *Aspergillus fumigatus* infections were considered to be 'so rare as to be of little practical importance' (reviewed in Latgé and Steinbach 2009), whereas now *A. fumigatus* is considered to be a predominant opportunistic and also a primary human fungal pathogen (Fedorova et al. 2008). Diseases caused by fungi and protozoa are often therapeutically intractable due to their underlying metabolic similarities with animal systems, and systemic fungal infections have high mortality even with aggressive treatment. There are relatively few antifungal drugs, most targeting ergosterol and its biosynthetic pathway (amphotericin B, azoles, allylamines) or more recently against fungal cell walls (echinocandins), but many of these are losing effectiveness due emerging fungal resistance (Cowen 2008).

About 20 % of fungal genome function relates to cell wall formation and maintenance (Lesage and Bussey 2006). The fungal cell wall comprises about 20 % of its biomass, and mediates interactions between the fungal organism and its environment, which is the host in the case of pathogenic species (Klis et al. 2007). Wall function is generally resilient to deletion of individual genes (de Groot et al. 2009) and to chemical stressors that trigger compensatory cell wall stress response pathways (Damveld et al. 2008). Fungal walls are remodeled during growth in culture (Momany et al. 2004) and in response to their environment (Gastebois et al. 2009, Hurtado-Guerrero et al. 2009). As with other human fungal pathogens, *A. fumigatus* forms biofilms in host tissue (Seidler et al. 2008, Loussert et al. 2009) that are more drug resistant than planktonic cultures (Seidler et al. 2008). Since fungal extracellular carbohydrates are not found in animal systems (Beverly et al. 2005), they and their biosynthetic pathways are drug development targets (Pederson and Turco 2003).

Gal*f* (the five-membered ring form of galactose) residues are found in the walls and extracellular carbohydrate sheaths of bacteria, protists, fungi, and plants, but not in animals (Beverly et al. 2005). The chemistry of Gal*f*-containing polysaccharides is reviewed in Richards and Lowary (2009). As summarized in Fig. 1, UDP-Gal*f* is formed from UDP-galactopyranose (UDP-Gal*p*, the six-membered ring form) by UDP-galactopyranose mutase (UGM) (Beverly et al. 2005) prior to incorporation in the extracellular carbohydrate-containing compounds. Gal*f* is essential in prokaryotes (Nassau et al. 1996, Sanders et al. 2001, Beverly et al. 2005) and some

protozoans (Roper et al. 2005, MacRae et al. 2006) but generally not so in fungi. Nevertheless, Gal*f* is important for wild type fungal growth, cell morphogenesis, wall architecture, and conidiation (Wallis et al. 2001, Damveld et al. 2008, El-Ganiny et al. 2008, Lamarre et al. 2009). Furthermore, Gal*f* is important for pathogenesis in fungi (Bar-Peled et al. 2004, Perfect 2005, Moyrand et al. 2007, Schmalhorst et al. 2008, Lamarre et al. 2009), and in protozoan parasites (Spath et al. 2000, Roper et al. 2005, MacRae et al. 2006).

The wall carbohydrate composition and architecture of *A. fumigatus* is the focus of intensive study, and was recently reviewed (Rementeria et al. 2005, Gastebois et al. 2009, Latgé and Steinbach 2009). *Aspergillus nidulans* and *A. fumigatus* cell walls have similar but not identical carbohydrate composition (Guest and Momany 2000). Although Gal*f* is not essential in *Aspergillus* (Damveld et al. 2008, El-Ganiny et al. 2008, Schmalhorst et al. 2008), it clearly has important roles in wild type growth and pathogenesis, and is a potential drug target for combination therapy. For example, deletion of *A. nidulans ugmA* (UDP-galactopyranose mutase), which is required for Gal*f* synthesis and so for wild type wall formation, causes compact colonial growth, abnormal hyphal wall structure and reduced conidiation (El-Ganiny et al. 2008).

In species ranging from *Escherichia coli* to human, UDP-glucose-4-epimerase (UGE, also called UDP-galactose-4-epimerase) catalyzes the inter-conversion of UDP-glucose and UDP-galactose (Fig. 1) (Allard et al. 2001, Holden et al. 2003). In various systems UGE is encoded by genes named *UGE*, *GalE, GAL10*. In *Saccharomyces cerevisiae*, galactose metabolism (Leloir pathway) enzymes are encoded by *GAL1* (galactokinase), *GAL7* (galactose-1-phosphate uridylyltransferase), and *GAL10* (combined mutarotase and UDP-glucose/galactose-4-epimerase) (Douglas and Hawthorne 1964). The *ScGAL10* epimerase function is essential for survival in the presence of traces of galactose, even if an alternate carbon source such as glycerol is available (Ross et al. 2004).

Some eukaryotes depend on UGE function for growth. *Trypanosoma cruzi* UGE (encoded by *TcGALE*) is the only source of galactose for its surface galactomannan synthesis, since its sole hexose transporter is unable to transport galactose (MacRae et al. 2006). *TcGALE* appears to be essential for *T. cruzi* survival in culture (MacRae et al. 2006). *Aspergillus nidulans* has 17 putative hexose transporters that are not yet fully characterized (Wei et al. 2004) and complex primary carbon metabolism (Flipphi et al. 2009). Nevertheless, deleting UDP-

galactopyranose mutase resulted in impaired cell growth, wild type morphogenesis, and sporulation (El-Ganiny et al. 2008). Thus *A. nidulans* galactose metabolism pathway appears to be a chink in its metabolic armour

Aspergillus nidulans ugeA (AN4727) encodes a UDP-glucose-4-epimerase. We present preliminary characterization of *A. nidulans ugeA* through analysis of the *ugeA*Δ deletion strain. Strains with single and double deletions of *ugeA* and *ugmA* produced phenotypically similar colonies. As expected, the *ugeA*Δ strain could not produce colonies on galactose as a sole carbon source, consistent with *in vitro* epimerase function of expressed UgeA.

2. Materials and methods

2.1 Strains and culture condition

Strains and plasmids are listed in Table 1, and primers in Supplemental Table A. *Aspergillus nidulans* strains were grown as described in El-Ganiny et al. (2008). DNA manipulations and transformations followed procedures in Osmani et al. (2006) and Szewczyk et al. (2007).

2.2 Strain construction

Strain construction followed procedures described in El-Ganiny et al. (2008) based on Osmani et al. (2006) and Szewczyk et al. (2007). AN4727 (*ugeA*) was deleted from *A. nidulan*s *nkuA*Δ strain A1147 using *AfpyrG* as a selectable marker (amplified from pAO18) to generate AAE4, and also from strain A1149 using the same marker to generate AAE5. Deletion of AN3112 (*ugmA*) from AAE5 used *AfpyroA* as a selectable marker (amplified from pTN1) to generate the [*ugeA*Δ, *ugmA*Δ] double deletion strain, AAE8. GFP-tagging constructs were amplified from pFNO3. Deletions and tagging were confirmed by PCR or gDNA template as shown in Supplemental Fig. A.

For long-term protoplast storage (Ken Bruno, *personal communication*), freshly made protoplasts were resuspended in STC buffer (1 M sorbitol, 50 mM Tris pH8, 50 mM $CaCl_2$) and adjusted to a concentration of at least 1.2 x 10^7/mL. The protoplast-STC suspension was mixed with a solution of 40 % (w/v) PEG_{4000}, at 1:4 (v/v) PEG:protoplast-STC. DMSO was added to a final concentration of 7 %. Aliquots of 200-300 µL protoplast-STC-DMSO suspension were

frozen to -80 °C. For transformation, the protoplast suspension was thawed on wet ice, mixed with DNA, and incubated for 20 min on wet ice. This was mixed with 1 mL of 40 % (w/v) PEG_{4000}, incubated at room temperature for 20 min, then spread on selective medium containing 1 M sucrose.

2.3 Microscopy, cell morphometry, and sporulation

Cell morphometry was characterized by fluorescence microscopy as described in El-Ganiny et al. (2008). Briefly, spores were germinated on dialysis tubing overlying CM agar or on coverslips, grown for 16 h, fixed in formalin, stained with Hoechst 33258, and examined using confocal laser fluorescence microscopy (CLSM) using a Zeiss META 510. Spore production and viability were determined as described previously (El-Ganiny et al. 2008). Hyphal widths and basal cell lengths were measured for 50 cells per strain. UgeA and UgmA were localized in growing hyphae of C-terminal GFP-tagged strains (Table 1).

SEM and TEM procedures were described previously (El-Ganiny et al. 2008). Hyphal wall thickness was measured on cross-sections of ten hyphae per strain where the cell membrane lipid bilayer was clearly resolved.

2.4 cDNA, recombinant UgeA production and activity

RNA was extracted using a Qiagen RNeasy kit, following manufacturer's instructions. Genomic DNA contamination was cleaned with DNaseI (Fermentas). cDNA was generated using an oligo-dt primer and RevertAid TM M-MulVRT (Fermentas) following manufacturer's instructions, and ligated into pCR4-TOPO. Constructs were confirmed by DNA sequencing at Plant Biotechnology Institute (PBI), NRC Saskatoon. The *ugeA* cDNA was subcloned into the pEHISTEV vector (Liu and Naismith, 2009) after PCR amplification with ugeAF and ugeAR primers that contained *Nco*1 and *Bam*H1 restriction sites, and *Nco*1 and *Bam*H1 digestion. The resultant plasmid was confirmed by DNA sequencing, then pHISTEV-UgeA was transfected into BL21-gold (DE3) (Novagen) expression cells. These were grown in LB-media with kanamycin at 37 ºC to OD 0.5, transferred to 15 ºC, then induced with 0.2 mM IPTG to express the recombinant protein. The His_6-UgeA was purified from cell lysate of induced cultures using Ni^{2+}-NTA affinity chromatography. Epimerase activity of the purified protein was assayed spectrophotometerically as described in Rosti et al. (2007) as conversion of UDP-galactose to

UDP-glucose, and confirmed with HPLC (Waters) using CarboPac PA1 (Dionex Inc). UDP-galactose and UDP-glucose and standards had retention times of 30.5 and 33.3 minutes respectively, when eluted with 0.2 M ammonium acetate buffer (pH 7.85).

3. Results

3.1 *Aspergillus nidulans* UDP-glucose/galactose-4-epimerase ugeA

The *A. nidulans* predicted amino acid sequence at the Broad Institute website was *Aspergillus nidulans* ANID4727.1 has 51 % homology to GalE, and was named UgeA. Amino acid identity with characterized fungal UGEs is shown in Table 2. UgeA is predicted to be 372 amino acids long, with a molecular weight of 40.6 kDa. The *ugeA* coding sequence was predicted to have four exons and three introns. This was confirmed by isolating and sequencing *ugeA* cDNA. The *ugeA* deletion strain was constructed and shown to be viable (Fig. 2A), but its hyphae was morphologically different from wild type (Fig. 2B) .The [*ugeA*Δ, *ugmA*Δ] double deletion strain was also viable (Fig. 2C). Confirmation of the *ugeA*Δ deletions used PCR of gDNA from these strains as described previously (El-Ganiny et al. 2008) and shown in Supplemental data Fig. A.

3.2 Characterization of the *Aspergillus nidulans ugeA*Δ and *[ugeA*Δ*, ugmA*Δ*]* strains

Strains were grown for 16 h at 28 °C, then fixed, stained with Hoechst 33258 to visualize nuclei (and lightly contrast cell walls), and examined with CLSM (Fig. 2). The *ugeA*Δ and [*ugeA*Δ, *ugmA*Δ] hyphae resembled those of the *ugmA*Δ strain (El-Ganiny et al. 2008): wide and highly branched, with short basal cells and abundant nuclei (Table 3).

The *ugeA*Δ and [*ugeA*Δ, *ugmA*Δ] strains were streaked for single colonies, and grown for 3 d at 28 °C until they produced pigmented conidia. Isolated colonies were assessed for conidium production as described in El-Ganiny et al. (2008). The *ugeA*Δ and [*ugeA*Δ, *ugmA*Δ] strains had substantially reduced sporulation (Table 3), comparable to the *ugmA*Δ strain. Spore viability was not affected by deleting either or both of *ugeA* and *ugmA*.

Scanning electron microscopy (SEM) of 3 d-old *ugeA*Δ colonies showed abundant aerial mycelium but few conidiophores (Suppl. data Fig. Ba arrows and box). The *ugeA*Δ strain conidiophores were morphologically aberrant (Suppl. data Fig. Bb). Conidium production by the

*ugeA*Δ strain was scant, consistent with conidiation rates shown in Table 3.

Transmission electron micrographs of cross-sectioned hyphae from 2 d-old colonies of wild type, *ugeA*Δ and *ugmA*Δ strains are shown in Supp. data Fig. Ca. The *ugeA*Δ hyphal walls were mostly electron-transparent and about twice as thick as wild type walls (Suppl. data Fig. Cb, Table 3). The *ugmA*Δ walls did not have a discrete electron-transparent inner layer (Suppl. data Fig. Cc). UgeA and UgmA appear to have different functions in hyphal wall formation.

3.3 Localization of UgeA and UgmA using GFP tagging.

Strains with UgeA-GFP and UgmA-GFP under the control of their wild type promoter were examined with confocal fluorescence microscopy. UgeA-GFP and UgmA-GFP strains were morphologically wild type. Both the UgeA-GFP and UgmA-GFP fluorescence patterns were cytoplasmic, and both lacked a pronounced longitudinal gradient of abundance (Fig. 3). Subcellular localization of UgeA-GFP and UgmA-GFP was similar when the strains were grown on glucose and galactose (UgeA-GFP Fig. 3b, cf Fig. 3A, B; UgmA-GFP Fig. 3c1, cf Fig. 3C). In addition, a UgmA-RFP strain that had the *ugmA*Δ morphology presumably due to impaired UgmA function also had a non-polarized cytoplasmic distribution (Fig. 3c2).

3.4 Growth of *ugeAΔ* and *ugmAΔ* strains on glucose and galactose as sole carbon sources

Wild type, *ugeA*Δ, and *ugmA*Δ, and double-deletion strains were grown on minimal medium containing 1 % glucose or 1 % galactose as sole carbon sources. All strains grew on glucose (Fig. 4A), and all grew faster at 37 °C (not shown). Wild type hyphal and colony morphology was not substantially reduced by growth on galactose, although colony growth was sparser and sporulation was somewhat delayed. The *ugmA*Δ hyphal morphogenesis defect was partly remediated on 1 % galactose. The *ugeA*Δ spores produced germ tubes that contained at least four nuclei (not shown) but they were unable to form colonies. The [*ugeA*Δ, *ugmA*Δ] spores produced cylindrical and sparsely branched germ tubes that did not form colonies (Fig. 4A).

Hyphal morphogenesis defects can frequently be remediated by growth on high osmolarity medium, which we also had shown for 10 µg/mL Calcofluor. Wild type, *ugeA*Δ, and *ugmA*Δ, and double-deletion strains were grown on minimal medium containing 1 % glucose amended with 1 M sucrose, or with 10 µg/mL or 30 µg/mL Calcofluor. Colonies and hyphae grown on these media are shown in Supplemental Fig. D and E, respectively. The 1 M sucrose

partly remediated the hyphal morphology but not the colony growth phenotypes of the single and double deletion strains. Growth and hyphal phenotypes of the single and double deletions strains were partly remediated on 10 µg/mL Calcofluor, but not on 30 µg/mL Calcofluor.

In wild type *A. nidulans*, Gal*f* localizes to conidial and hyphal walls (El-Ganiny et al. 2008). As with the *ugmA*Δ strain described in El-Ganiny et al. (2008), we were unable to immunolocalize Gal*f* in *ugeA*Δ strain hyphae or spores (not shown). This is consistent with the demonstrated function of UgeA, shown below (Fig. 4B-D).

3.5 In vitro enzymatic activity of UgeA

UgeA was expressed with an N-terminal His_6 tag, and purified using Ni^{2+}-NTA affinity chromatography. SDS-PAGE electrophoresis on a 10 % polyacrylamide gel showed that purified UgeA had an approximate molecular weight of 40.6 kDa (not shown) consistent with the expected translation product. UgeA was able to convert UDP-galactose to UDP-glucose *in vitro*, and *vice versa*, as tested with coupled reactions. Enzyme activity was linearly related to the amount of UgeA in the reaction mix (not shown). Using either UDP-galactose (Fig. 4B) or UDP-glucose (Fig. 4C) as substrates for UgeA resulted in two peaks in a 75:25 mixture of UDP-glucose:UDP-galactose (Fig. 4D). The data in Fig. 4D show the HPLC result with UDP-galactose as substrate. Similar results are seen with UDP-glucose as substrate (not shown).

4. Discussion

4.1 *Aspergillus nidulans* ugeA encodes a UDP-glucose-4-epimerase.

The *A nidulans* UgeA sequence was identified by its homology to human GalE (Daude et al. 1995). Galactose metabolism is mediated by enzymes in the Leloir pathway (Holden et al. 2003). These include galactose mutarotase (also called galactose-1-epimerase), galactokinase, galactose-1-phosphate uridylyltransferase, and UDP-glucose-4-epimerase. In fungi like *Saccharomyces cerevisiae* and *Candida albicans*, the UDP-glucose-4-epimerase and mutarotase functions are both encoded by GAL10, which has two domains (Ross et al. 2004, Singh et al. 2007). Other eukaryotes including fungi like *Aspergillus* have separate mutarotase- and epimerase-coding genes. *Aspergillus nidulans* UgeA was predicted to be a UDP-glucose-4-epimerase by sequence comparison. The *A. nidulans ugeA* sequence has similar

exon organization to that of the predicted *A. fumigatus* sequence afu5g10780, with which it shares 93 % sequence identity. The phenotype of the *ugeA*Δ strain is closely related to that of the *ugmA*Δ strain (El-Ganiny et al. 2008), suggesting that UgeA is the source of the UDP-Gal*p* that ultimately generates wall Gal*f* residues needed for wild type *A. nidulans* growth and development.

Hydropathy analysis of *C. neoformans* UGE1 and UGE2 (Moyrand et al. 2008) suggested these proteins each have a single membrane-spanning domain near their N-terminal. CnUGE1-RFP and CnUGE2-GFP distribution were associated with the cell membrane at 37 ºC, but only CnUGE2-GFP was cell membrane-associated at 25 ºC (Moyrand et al. 2008). Hydropathy analysis of *A. nidulans* UgeA shows that it lacks a predicted membrane-spanning domain. The cellular distribution of UgeA-GFP was cytoplasmic, like that of UgmA-GFP, and consistent with our expectation of their metabolic function. The lack of a longitudinal abundance gradient for UgeA-GFP and UgmA-GFP is consistent with the length of hypha required to support growth of the tip, and with relatively long-distance intracellular transport of wall-building components.

The UgeA-GFP and UgmA-GFP distributions were similar when wild type morphology tagged strains were grown on glucose and galactose. Also, a UgmA-RFP strain that appeared to have impaired UgmA function since grew with the *ugmA*Δ hyphal phenotype had a non-polarized cytoplasmic distribution, and was excluded from nuclei. Thus, localization of these gene products did not appear to be affected by nutrition or hyphal morphogenesis.

4.2 Galactose → glucose conversion in *Aspergillus nidulans* uses UgeA.

Wild type *A. nidulans* strains can grow on galactose as a sole carbon source. *Aspergillus nidulans* has 17 putative hexose transporters (Wei et al. 2004) and a primary carbon metabolism that permits nutritional flexibility (Flipphia et al. 2009). However, the *ugeA*Δ strain did not form colonies when grown on galactose. Galactose was toxic to an *S. cerevisiae GAL10*Δ (epimerase-mutarotase) strain (Mehta et al. 1999). Although *A. nidulans ugeA*Δ spores were unable to form colonies when grown on galactose, they produced multinucleate germlings so they were probably exhausting their endogenous reserves, rather than succumbing to toxicity. *A. nidulans* appears to lack the ability to import nutritionally significant amounts of galactose from its surroundings, so UgeA is likely the source for glucose to support metabolism during growth on

galactose. Consistent with these results, we have shown that expressed UgeA interconverts UDP-galactose and UDP-glucose *in vitro*, with an equilibrium in favour of UDP-glucose.

4.3 The phenotype of *ugeAΔ* and *[ugeAΔ, ugmAΔ]* strains.

The *ugeA*Δ strain cell morphometry, hyphal branching pattern, and sporulation resembled that of *ugmA*Δ strains described previously (El-Ganiny et al. 2008). The colony growth and hyphal morphogenesis defects of the single and double deletion strains were partially remediated by high osmolarity and by low levels of Calcofluor, consistent with results shown previously for the *ugmA*Δ strain (El-Ganiny et al. 2008). Cytoplasmic UDP-Gal*p* is needed to produce UDP-Gal*f* for the *A. nidulans* hyphal wall. In solution, Gal*p* and Gal*f* are naturally in equilibrium (95:5) so growing the *ugmA*Δ strain on galactose would have provided low-abundance Gal*f*, which could account for the partial remediation.

The organelle appearance and distribution in TEM cross-sections of *ugeA*Δ and *ugmA*Δ hyphae resembled wild type strains. The *ugeA*Δ hyphal walls were more than twice as thick as wild type strains, consistent with hyphal morphogenesis and wall defects in another *A. nidulans* mutant (Kaminskyj and Boire 2004). Compared to *ugeA*Δ strain, the *ugmA*Δ hyphae had a relatively poorly consolidated and more electron dense inner wall layer. Both deletion strains had a loose fibrillar outer wall layer, suggesting that *A. nidulans* Gal*f* is required for normal wall surface construction. Differences in the wall architecture of *ugeA*Δ and *ugmA*Δ strains, despite related functions of UgeA and UgmA, and similar colony phenotypes for the *ugeA*Δ and *ugmA*Δ strains, is consistent with the complexity of fungal cell wall formation. Lamarre et al. (2009) showed that some of the Gal*f* in the outer layer of the *A. fumigatus* wall is in the galactomannanan, and that *AfUGM1*Δ strains have exposed mannose on their cell wall surface that contributes to a morphologically altered and more adhesive wall surface. Consistent with this, *A. nidulans ugmA*Δ and *ugeA*Δ hyphae adhered more firmly to glass coverslips than do wild type strains. The electron dense material on the surface of *ugeAΔ* walls seen with TEM may be material that adhered during liquid shake culture. Taken together, Gal*f* residues appear to have roles in multiple aspects of *A. nidulans* hyphal wall structure and function, consistent with a large body of work on *A. fumigatus* (reviewed in Latgé 2009).

4.4 The Gal*f* synthesis pathway is expected to be therapeutically useful target.

We have shown that galactose metabolism mediated by UgeA and UgmA, which is required for deposition of Gal*f* residues in the wall, is not essential in *A. nidulans*. However, deleting *ugmA* or *ugeA* seriously perturbs cell growth and sporulation, reducing fitness of these strains. With the exception of polyenes that effectively target ergosterol in fungal cell membranes but have substantial human toxicity, antifungal drugs that target single aspects of fungal metabolism have proven repeatedly to lack durability (Cowen 2008). Inhibitors that target Gal*f* synthesis are expected to be therapeutically useful in combination with established antifungals.

Acknowledgements

This research was supported by Natural Science and Engineering Research Council of Canada Discovery grants, a Canadian Institutes of Health Research/Regional Partnership Program grant to DARS and SGWK, and by an Egyptian Ministry of Higher Education grant to AME. We thank Tom Bonli (Department of Geological Sciences, University of Saskatchewan) for technical assistance.

References

Allard, S.T.M., Giraud, M.F. and Naismith, J.H. 2001. Epimerases: structure, function and mechanism. Cell. Mol. Life Sci. 58, 1650-1665.

Bar-Peled, M., Griffith, C.L., Ory, J.J., and Doering, T.L. 2004. Biosynthesis of UDP-GlcA, a key metabolite for capsular polysaccharide synthesis in the pathogenic fungus *Cryptococcus neoformans*. Biochem. J. 381, 131-136.

Beverly, S.M., Owens, K.L., Showalter, M., Griffith, C.L., Doering, T.L., Jones, V.C. and McNeil, M.R. 2005. UDP-galactopyranose mutase (*GLF* gene) in microbial and metazoan pathogens. Euk. Cell 4, 1147-1154.

Cowen, L. 2008. The evolution of fungal drug resistance: modulating the trajectory from genotype to phenotype. Nat. Rev. Microbiol. 6, 187-198.

Damveld, R.A., Franken, A., Arenthorst, M., Punt, P.J., Klis, F.M., van den Hondel, C.A.M.J.J. and Ram, A.F.J. 2008. A novel screening method for cell wall mutants in *Aspergillus niger*

identifies UDP-galactopyranosemutase as an importent protein in fungal cell wall biosynthesis. Genetics 178, 873-881.

Daude, N., Gallaher, T.K., Zeschnigk, M., Starzinski-Powitz, A., Petry, K.G., Haworth, I.S. and Reichardt, J.K.V. 1995. Molecular-cloning, characterization, and mapping of a full-length cDNA encoding human UDP-galactose 4′-epimerase. Biochem. Molec. Med. 56, 1-7.

de Groot, P.J.W., Brandt, B.W., Horiuchi, H., Ram, A.F.J., De Koster, C.G. and Klis, F.M. 2009. Comprehensive genomic analysis of cell wall genes in *Aspergillus nidulans*. Fung. Genet. Biol. 46, S72-S81.

Douglas, H.C., and Hawthorne, D.C. 1964. Enzymatic expression and genetic linkage of genes controlling galactose utilization in *Saccharomyces*. Genetics 49, 837-844.

El-Ganiny, A.M., Sanders, D.A.R. and Kaminskyj, S.G.W. 2008. *Aspergillus nidulans* UDP-galactopyranose mutase, encoded by *ugmA* plays key roles in colony growth, hyphal morphogenesis, and conidiation. Fung. Genet. Biol. 45, 1533-1542.

Fedorova, N.D., Khaldi, N., Joardar, V.S., Maiti, R., Amedeo, P., Anderson, M.J., Crabtree, J., Silva, J.C., Badger, J.H., Albarraq, A., Angiuoli, S., Bussey, H., Bowyer, P., Cotty, P.J., Dyer, P.S., Egan, A., Galens, K., Fraser-Liggett, C.M., Haas, B.J., Inman, J.M., Kent, R., Lemieux, S., Malavazi, I., Orvis, J., Roemer, T., Ronning, C.M., Sundaram, J.P., Sutton, G., Turner, G., Venter, J.C., White, O.R., Whitty, B.R., Youngman, P., Wolfe, K.H., Goldman, G.H., Wortman, J.R., Jiang, B., Denning, D.W. and Nierman, W.C. 2008. Genomic islands in the pathogenic filamentous fungus *Aspergillus fumigatus*. PLoS Genetics 4, 1-13.

Flipphi, M., Sun, J., Robellet, X., Karaffad, L., Fekete, E., Zeng, A.-P. and Kubicek, C.P. 2009. Biodiversity and evolution of primary carbon metabolism in A*spergillus nidulans* and other *Aspergillus* spp. Fung. Genet. Biol 46, S19-S44.

Gastebois, A., Clavaud, C., Aimanianda, V. and Latge, J.-P. 2009. *Aspergillus fumigatus*: cell wall polysaccharides, their biosynthesis and organization. Fut. Microbiol. 4, 583-595.

Guest, G.M., and Momany, M. 2000. Analysis of cell wall sugars in the pathogen *Aspergillus fumigatus* and the saprophyte A*spergillus nidulans*. Mycologia 92, 1047-1050.

Holden, H.M., Rayment, I. and Thoden, J.B. 2003. Structure and function of enzymes of the Leloir pathway for galactose metabolism. J. Biol. Chem. 278, 43885-43888.

Hurtado-Guerrero, R., Schuttelkopf, A.W., Mouyna, I., Ibrahim, A.F.M., Shepherd, S., Fontaine, T., Latge, J.-P. and van Aalten, D.M.F. 2009. Molecular mechanisms of yeast cell wall glucan remodeling. J. Biol. Chem. 284, 8461-8469.

Kaminskyj, S. and Boire, M. 2004. Ultrastructure of the *Aspergillus nidulans hypA1* restrictive phenotype shows defects in endomembrane arrays and polarized wall deposition. Can. J. Bot. 82, 807-814.

Klis, F.M., Ram, A.F.J. and deGroot, P.W.J. 2007. A molecular and genomic view of the fungal cell wall. *In* The Mycota. *Edited by* R.J. Howard, and N.A.R. Gow. Springer-Verlag, Berlin. pp. 95-117.

Lamarre, C., Beau, R., Balloy, V., Fontaine, T., Hoi, J.W.S., Guadagnini, S., Berkova, N., Chignard, M., Beauvais, A. and Latge, J.-P. 2009. Galactofuranose attenuates cellular adhesion of *Aspergillus fumigatus*. Cell. Microbiol. 11, 1612-1623.

Latgé, J.-P. 2009. Galactofuranose containing molecules in *Aspergillus fumigatus*. Med. Mycol. 47 (Suppl): S104-S109.

Latgé, J.-P., and Steinbach, W.J. 2009. *Aspergillus fumigatus* and Aspergillosis.ASM Press, Washington DC.

Lesage, G., and Bussey, H. 2006. Cell wall assembly in *Saccharomyces cerevisiae*. Micro. Molec. Biol. Rev. 70, 317-343.

Liu, H. and Naismith, J.H. 2009. A simple and efficient expression and purification system using two newly constructed vectors. Prot. Expr. Purif. 63, 102-111.

Loussert, C., Schmitt, C., Prevost, M.-C.., Balloy, V., Fadel, E., Philippe, B., Kaufmann-Lacroix, C., Latge, J.-P. and Beauvais, A. 2009. *In vivo* biofilm composition of *Aspergillus fumigatus*. Cell. Microbiol. *in press*

MacRae, J.I., Obado, S.O., Turnock, D.C., Roper, J.R., Kierans, M., Kelly, J.M. and Ferguson, M.A.J. 2006. The suppression of galactose metabolism in *Trypanosoma cruzi* epimastigotes causes changes in cell surface molecular architecture and cell morphology. Molec. Biochem. Parasitol. 147, 126-136.

Mehta, D.V., Kabir, A., Bhat, P.J. 1999. Expression of human inositol monophosphate suppresses galactose toxicity in *Saccharomyces cerevisiae*: possible implications in galactosemia. Biochim. Biophys. Acta 1454, 217-226.

Momany, M., Lindsey, R., Hill, T.W., Richardson, E.A., Momany, C., Pedreira, M., Guest, G.M., Fisher, J.F., Hessler, R.B. and Roberts, K.A. 2004. The *Aspergillus fumigatus* cell wall is organized in domains that are remodelled during polarity establishment. Microbiology 150, 3261-3268.

Moyrand, F., Lafontaine, I., Fontaine, T. and Janbon, G. 2008. *UGE1* and *UGE2* regulate the UDP-glucose/UDP-galactose equilibrium in *Cryptococcus neoformans*. Euk. Cell 7, 2069-2077.

Moyrand, F. 2007. Systematic capsule gene disruption reveals the central role of galactose metabolism on *Cryptococcus neoformans* virulence. Mol. Microbiol. 64, 771-781.

Nassau, P.M., Martin, S.L., Brown, R.E., Weston, A., Monsey, D., McNeil, M.R. and Duncan, K. 1996. Galactofuranose biosynthesis in *Escherichia coli* K-12: identification and cloning of UDP-galactofuranose mutase. J. Bacteriol. 178, 1047-1052.

Osmani, A.H., Oakley, B.R. and Osmani, S.A. 2006. Identification and analysis of essential *Aspergillus nidulalns* genes using the heterokaryon rescue technique. Nat. Protoc. 1, 2517-2526.

Pederson, L.L., and Turco, S.J. 2003. Galactofuranose metabolism: a potential target for antimicrobial chemotherapy. Cell. Mol. Life Sci. 60, 259-266.

Perfect, J. 2005. *Cryptococcus neoformans*: a sugar-coated killer with designer genes. FEMS Immunol. Med. Microbiol. 45, 395-404.

Rementeria, A., López-Molina, N., Ludwig, A., Vivanco, A.B., Bikandi, J., Pontón, J. and Garaizar, J. 2005. Genes and molecules involved in *Aspergillus fumigatus* virulence. Rev. Iberoam. Micol. 22, 1-23.

Richards, M.R.l., and Lowary, T.L. 2009. Chemistry and biology of galactofuranose-containing polysaccharides. Chembiochem 10, 1920-1938.

Roper, J.R., Guther, M.L., MacRae, J.L., Prescott, A.R., Hallyburton, I., Acosta-Serrano, A. and Ferguson, M.A.J. 2005. The suppression of galactose metabolism in procyclic form

Trypanosoma brucei causes cessation of cell growth and alters procycloin glycoprotein structure and copy number. J. Biol. Chem. 280, 19728-19736.

Ross, K.L., Davis, C.N. and Fridovich-Keila, J.L. 2004. Differential roles of the Leloir pathway enzymes and metabolites in defining galactose sensitivity in yeast. Molec. Genet. Metab. 83, 116.

Rosti, J., Barton, C.J., Albrecht, S., Dupree, P., Pauly, M., Findlay, K., Roberts, K. and Seifert, G.J. 2007. UDP-glucose-4-epimerase isoforms *UGE2* and *UGE4* cooperate in providing UDP-galactose for cell wall biosynthesis and growth of *Arabidopsis thaliana*. The Plant Cell 19, 1565-1579.

Sanders, D.A.R., Staines, A.G., McMahon, S.A., McNeil, M.R., Whitfield, C. and Naismith, J.H. 2001. UDP-galactopyranose mutase has a novel structure and mechanism. Nat. Struct. Biol. 8, 858-863.

Schmalhorst, P.S., Krappmann, S., Vercecken, S.W., Rohde, M., Muller, M., Braus, G.H., Contreras, R., Braun, A., Bakker, H. and Routier, F.H. 2008. Contribution of galactopyranose to the virulence of the opportunistic pathogen *Aspergillus fumigatus*. Euk. Cell 7, 1268-1277.

Seidler, M.J., Salvenmoser, S. and Muller, F.-. 2008. *Aspergillus fumigatus* forms biofilms with reduced antifungal drug susceptibility on bronchial epithelial cells. Antimicrob. Agents Chemother. 52, 4130-4136.

Singh, V., Satheesh, S.V., Raghavendra, M.L. and Sadhale, P.P. 2007. The key enzyme in galactose metabolism, UDP-galactose-4-epimerase, affects cell-wall integrity and morphology in *Candida albicans* even in the absence of galactose. Fung. Genet. Biol 44, 563-574.

Spath, G.F., Epstein, L., Leader, B., Singer, A.M., Avila, H.A., Turco, S.J. and Beverly, S.M. 2000. Lipophosphoglycan is a virulence factor distinct from related glycoconjugates in the protozoan parasite *Leishmania major*. Proc. Natl. Acad. Sci. U. S. A. 97, 9258-9263.

Szewczyk, W., Nayak, T., Oakley, C.E., Edgerton, H., Xiong, Y., Taheri-Talesh, N., Osmani, S.A. and Oakley, B.R. 2007. Fusion PCR and gene targeting in *Aspergillus nidulans*. Nat. Protoc. 1, 3111-3120.

Wallis, G.L., Hemming, F.W. and Peberdy, J.F. 2001. β-Galactofuranoside glycoconjygate on the conidia and conidiophores of *Aspergillus niger*. FEMS Microbiol. Lett. 201, 21-27.

Wei, H., Vienken, K., Webera, R., Buntinga, S., Requeña, N. and Fischer, R. 2004. A putative high affinity hexose transporter, *hxtA*, of *Aspergillus nidulans* is induced in vegetative hyphae upon starvation and in ascogenous hyphae during cleistothecium formation. Fung. Genet. Biol 41, 148-156.

Tables

Table 1: Strains and plasmids used in this study

Aspergillus nidulans	
A1147 [a]	*pyrG89*; *argB2*; *pabaB22*; *nkuA*::*argB*; *riboB2*
A1149 [a]	*pyrG89; pyroA4; nkuA*::*argB*
AAE1 [b]	*pyrG89*::*Ncpyr4*$^{+}$ *; pyroA4; nkuA*::*argB*
AAE2 (*ugmA*Δ) [b]	AN3112::*AfpyrG; pyrG89; pyroA4; nkuA*::*argB*
AAE4 (*ugeA*Δ) [c]	AN4727::*AfpyrG; pyrG89; argB2; pabaB22; nkuA*::*argB; riboB2*
AAE5 (*ugeA*Δ) [c]	AN4727::AfpyrG; pyroA4, *nkuA*::*argB;*
AAE6 (*ugmA*-GFP) [c]	AN3112-GA_5-GFP + *Af pyrG; pyrG89; pyroA4; nkuA::argB*
AAE7 (*ugeA*-GFP) [c]	AN4727-GA_5-GFP + *Af pyrG; pyrG89; pyroA4; nkuA::argB*
AAE8 (*ugeA*Δ, *ugmA*Δ) [c]	AN4727::*AfpyrG;* AN3112::*AfpyroA; pyrG89; pyroA4; nkuA*::*argB*
Escherichia coli [d]	BL21-gold (DE3)
Plasmids	
pAO18 [a]	S-TAG, *AfpyrG,* Kan^R
pCR4-TOPO[e]	Kan^R, amp^R
pFNO3 [a]	GA5-GFP + *Af pyrG*, Kan^R
pTN1 [a]	*AfpyroA*, Amp^R
pHISTEV [f]	modified pET30a, Kan^R

a Fungal Genetics Stock Center www.fgsc.net

b El-Ganiny et al. (2008)

c This study

d Novagen

e Invitrogen

f Liu and Naismith (2009)

Table 2: Percent amino acid sequence identity of *Aspergillus nidulans* UgeA with selected fungal UDP-glucose-4-epimerases, and with the human and *A. fumigatus* sequences used in *ugeA* identification.

Organism	**Gene name**	**UGEAp amino acid identity**
Aspergillus fumigatus	afu5g10780	93
Candida albicans	*Gal10*	57
Cryptococcus neoformans	*UGE1*	47
C. neoformans	*UGE2*	45
Homo sapiens	*GalE*	51
Kluyveromyces lactis	*Gal10*	55
Pichia stipitis	*GALK*	61
Saccharomyces cerevisiae	*GAL10*	57
Schizosaccharomyces pombe	*uge1*	58
S. pombe	*gal10*	58

Table 3: Cell characteristics of *ugeA*Δ, *ugmA*Δ, and [*ugeA*Δ, *ugmA*Δ] and related strains [a]

	Hyphal width (μm)	Basal cell length (μm)	Nuclei/ basal cell	Wall thickness (nm)	Conidia / colony %
wildtype [b]	2.4 ± 0.0 [e]	26 ± 1 [e]	4.2 ± 1.1 [e]	54 ± 2 [e]	100
*ugeA*Δ [c]	3.6 ± 0.1 [f]	14 ± 1 [f]	3.2 ± 1.2 [f]	123 ± 4 [f]	4
*ugmA*Δ [d]	3.1 ± 0.1 [f]	15 ± 1 [f]	3.6 ± 1.0 [f]	204 ± 10 [g]	2
*ugeA*Δ, *ugmA*Δ [c]	3.2 ± 0.4 [f]	16 ± 5 [f]	3.5 ± 1.1 [f]	-- [h]	1

a In any one column, values followed by different letters (e-g) are significantly different (ANOVA, $P < 0.05$)

b AAE1 is near isogenic wild type to the transformant parent strain (El-Ganiny et al, 2008).

c This study

d AAE1 and *ugmA*Δ morphometry was originally presented in (El-Ganiny et al. 2008)

h Not quantified

Figures

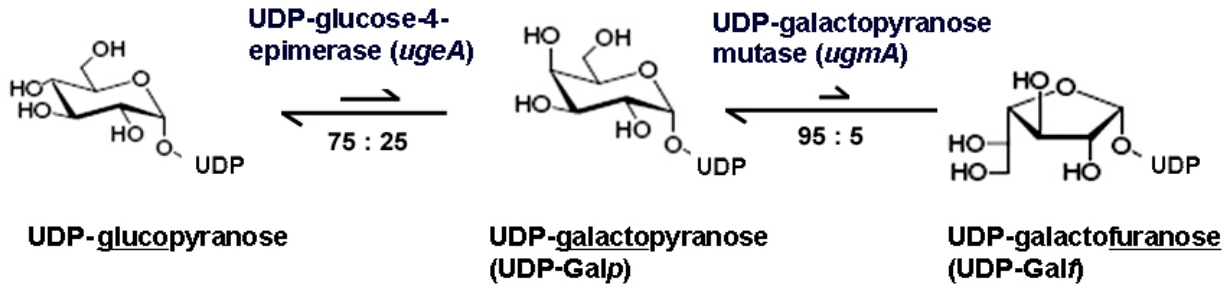

Fig. 1. UDP-galactofuranose synthesis in *Aspergillus nidulans*.

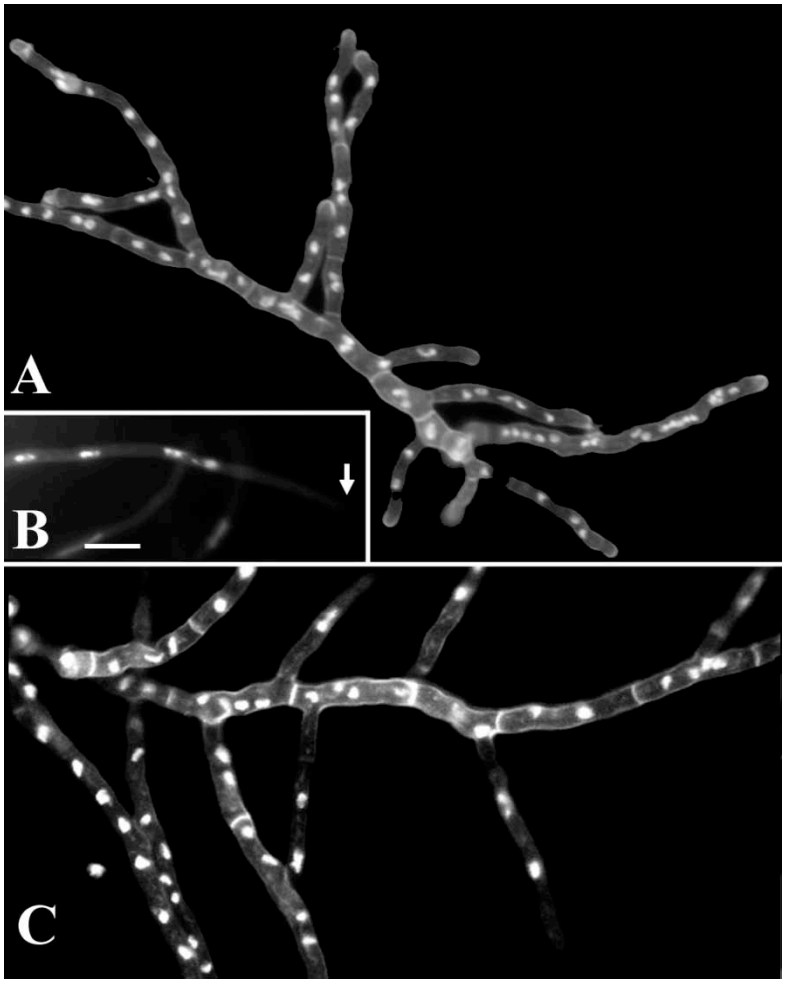

Fig. 2. Phenotype of (A) *ugeA*Δ, (B) wild type and (C) [*ugeA*Δ, *ugmA*Δ] germlings grown on 1 % glucose and stained with Hoechst 33258. Arrowhead in B indicates the end of the hyphal tip. Bar in B = 10 μm for all parts.

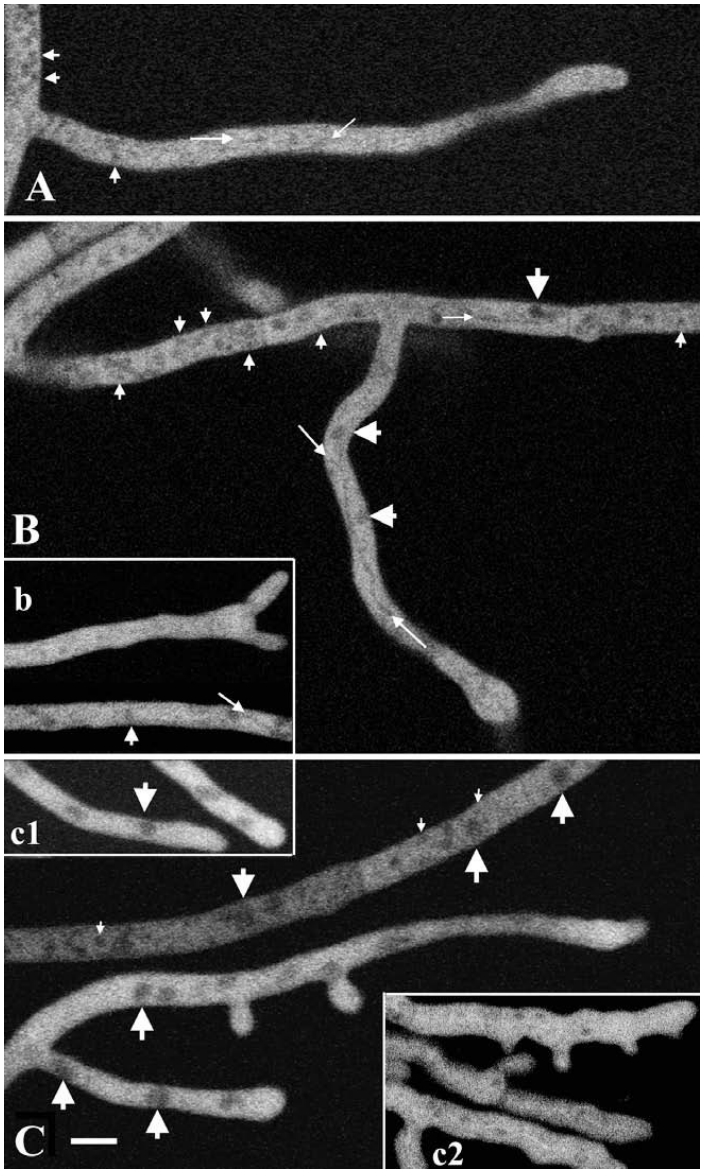

Fig. 3. UgeA (A, B) and UgmA (C) localization patterns on glucose and galactose. UgeA-GFP and UgmA-GFP were localized by confocal fluorescence microscopy in wild type phenotype hyphae. Both proteins were cytoplasmic, lacked pronounced longitudinal polarization, and had comparable localization patterns when grown on glucose (A–C) or galactose (insets b and c1). Areas of lower fluorescence intensity are indicated by small and large arrowheads and arrows. In contrast to the UgmAGFP strain, which had wild type hyphae, a UgmA-RFP strain had ugmAD phenotype hyphae (inset c2), suggesting that UgmA function had been compromised, however this did not noticeably affect protein distribution. Bar in C = 5 lm, for all parts.

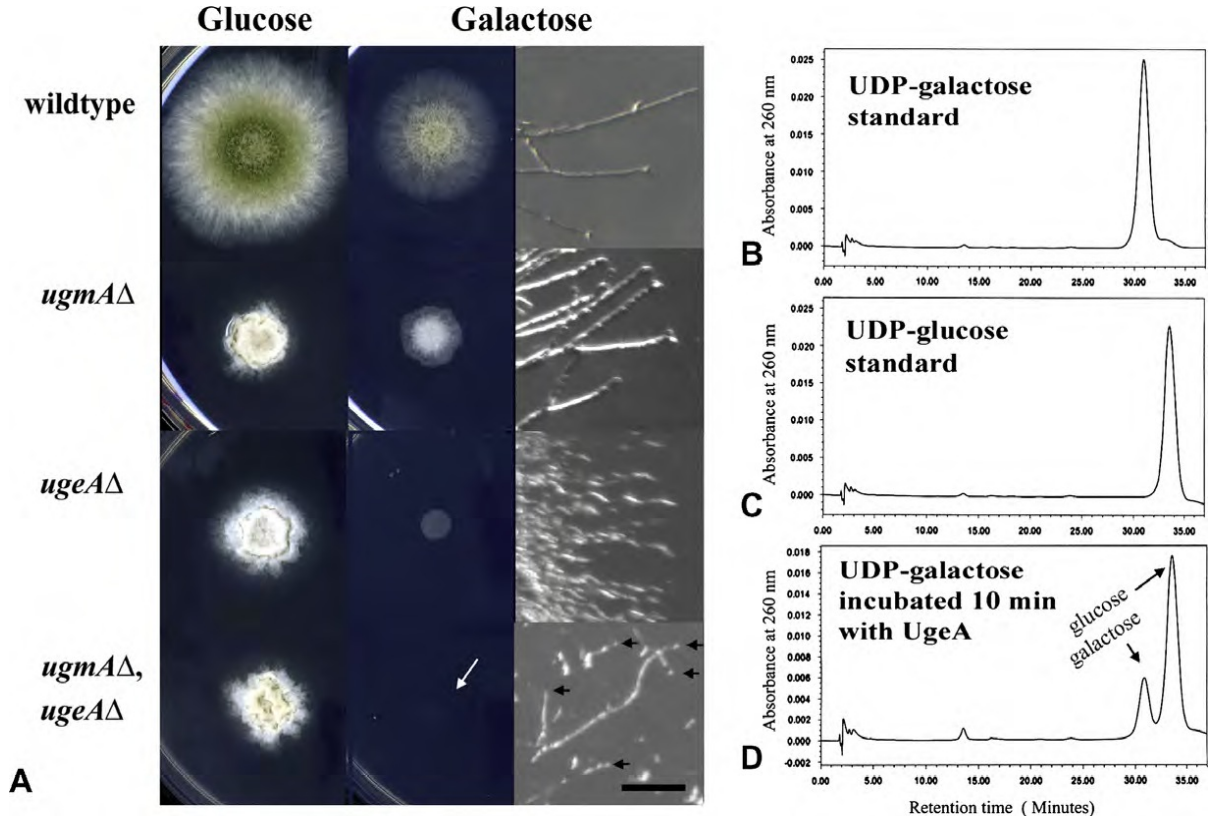

Fig. 4. *Aspergillus nidulans* UgeA converts UDP-galactose → UDP-glucose. (A) Growth of *A. nidulans* wild type, *ugmAΔ, ugeAΔ,* and double-deletion strains on minimal medium containing 1% glucose or 1% galactose, and micrographs of these strains grown on 1% galactose. Bar = 100 μm for all micrographs. When germinated on galactose, the wild type hyphal morphology was unaffected although colony growth and sporulation was sparse; the *ugmAΔ* hyphal phenotype was partly remediated; the *ugeAΔ* strain produced wild type germlings but failed to form colonies; the [*ugmAΔ, ugeAΔ*] strain produced short wild type germlings (arrowheads). (B–D) UgeA converts UDP-galactose to UDP-glucose in vitro. B) UDP-galactose standard (peak 1, at 30.5 min). C) UDP-glucose standard (peak 2, at 33.3 min). (D) A 10 min incubation of UDP-galactose with UgeA gives an mixture of UDP-galactose:UDP-glucose = 25:75. Comparable results (not shown) are seen when incubating UDP-glucose with UgmA for 10 min.

Supplementary materials

Supplementary table A: Primers used in this study

Primer name	sequence 5' → 3'	use
P1 AfpyrGF	ATGTCGTCCAAGTCGCAATT	*ugeA* deletion
P2 AfpyrGR	TCATGACTTGCCGCATACTC	*ugeA* deletion
P8 MidpyrGR	CACATCCGACTGCACTTCC	Confirmatory PCR
P9 AFpyroAF	ATGGCTTCCAACGGTACCA	*ugmA* deletion
P10 AFpyroAR	TTACCATCCTCTCTTGGCCA	*ugmA* deletion
P16 MidpyroAR	TCAACAACATCTCCGGTACC	Confirmatory PCR
P21 ugmAF	ATGCTTAGTCTAGCTCGCAAGAC	UgmA-GFP
P23 ugmAR	GCCTGCACCAGCTCCCTGCGCCTTATTCTTAGCAAA	UgmA-GFP
P24 DugmAF	AGTATGCGGCAAGTCATGAAATAAAACTCTTCTGCGTGGATG	UgmA-GFP
P26 DugmAR	GTGTTTACCAAGAATATGTTCATCGA	UgmA-GFP
P22 TugmAFuF	ATATCCTACAAGGCAGGATGACC	UgmA-GFP
P25 TugmAFuR	TGATCGTCCATCCCATACTTG	UgmA-GFP
P27 5GA-GFPF	GGAGCTGGTGCAGGC	UgmA-GFP & UgeA-GFP
P28 5GA-GFPR	TCATGACTTGCCGCATACT	UmgA-GFP & UgeA-GFP
P41 upugeAF	CTCCTATGGTATGTCTCTTCCAACTT	*ugeA* deletion
P43 upugeAR	AATTGCGACTTGGACGACATGGTGAATGTGAATTGAATGCAG	*ugeA* deletion
P44 dugeAF	GAGTATGCGGCAAGTCATGAATGGAAATCTTGAATGGATT	*ugeA* deletion & tagging
P46 DugeAR	AACTCGACTTTTCGCAGCTC	*ugeA* deletion & tagging
P42 FugeAdF	TCCTAACTTTTGTTACTTTAGGCCC	*ugeA* deletion
P45 FugeAdR	GGGTACAAAACCGCTACGC	*ugeA* deletion
P47 ugeAF	ATGCCTTCTGGATCTGTCCT	UgeA-GFP
P95 TugeAFusF	CAACACCAATAATTATTGACCCTTC	UgeA-GFP
P96 TugeAFusR	ACCGCTACGCACTCAAGC	UgeA-GFP
P104 ugeAR	GCCTGCACCAGCTCCTTTCTTGAGCTGTTCCAGC	UgeA-GFP
ugeAF (*Nco*I)	CGCATGCCATGGGAATGCCTTCTGGATCTGTCCTTG	*ugeA* cloning
ugeAR (*Bam*H1)	GCGCGCGGATCCTTATTTCTTGAGCTGTTCCAGC	*ugeA* cloning

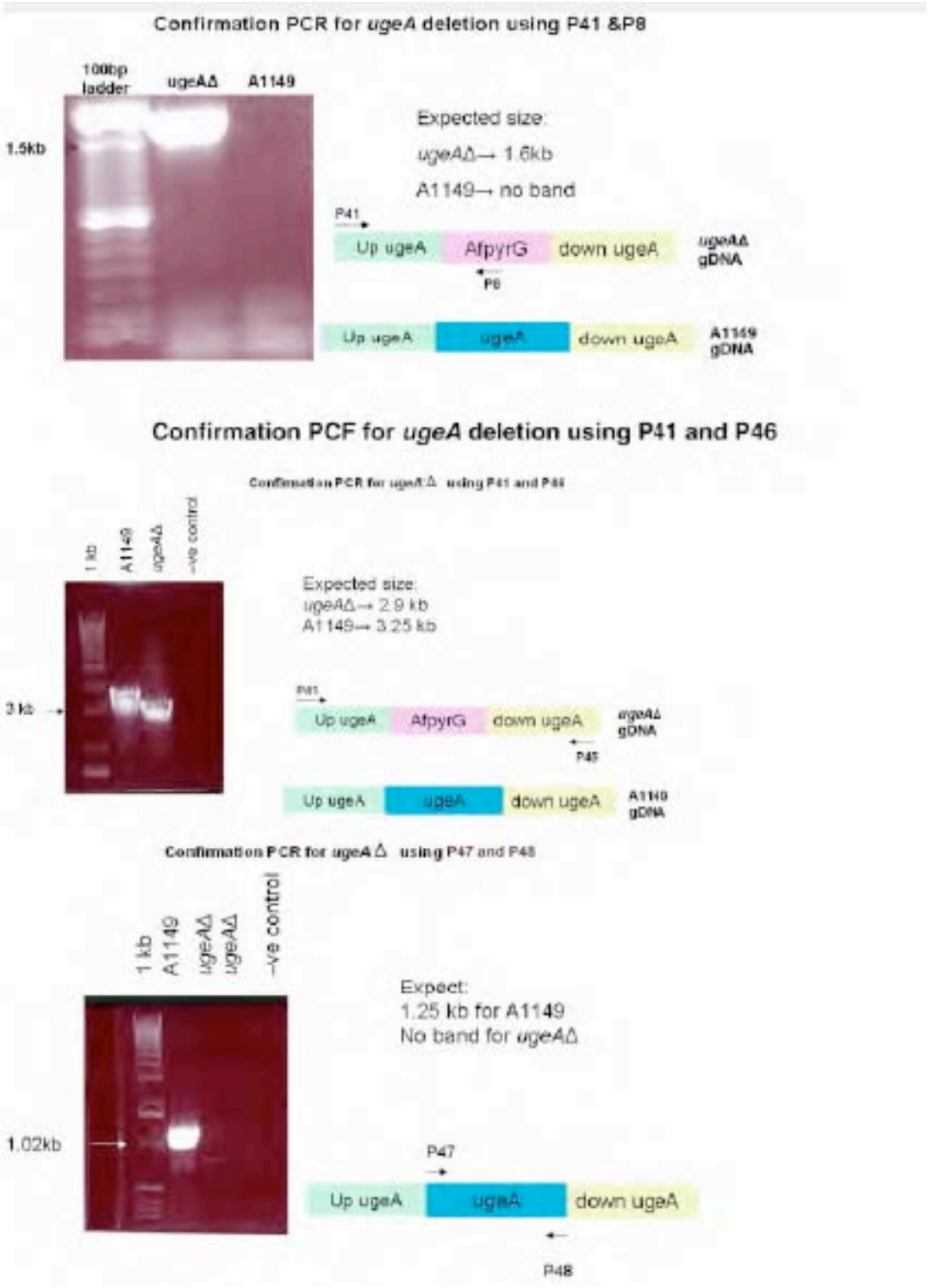
Confirmation PCR for ugeA deletion using P41 &P8
100bp ladder
ugeAΔ
A1149
1.5kb
Expected size:
ugeAΔ→ 1.6kb
A1149→ no band
P41
Up ugeA
AfpyrG
down ugeA
ugeAΔ gDNA
P8
Up ugeA
ugeA
down ugeA
A1149 gDNA
Confirmation PCF for ugeA deletion using P41 and P46
Confirmation PCR for ugeAΔ using P41 and P46
1 kb
A1149
ugeAΔ
-ve control
Expected size:
ugeAΔ→ 2.9 kb
A1149→ 3.25 kb
3 kb
P41
Up ugeA
AfpyrG
down ugeA
ugeAΔ gDNA
P46
Up ugeA
ugeA
down ugeA
A1149 gDNA
Confirmation PCR for ugeAΔ using P47 and P48
1 kb
A1149
ugeAΔ
ugeAΔ
-ve control
Expect:
1.25 kb for A1149
No band for ugeAΔ
1.02kb
P47
Up ugeA
ugeA
down ugeA
P48

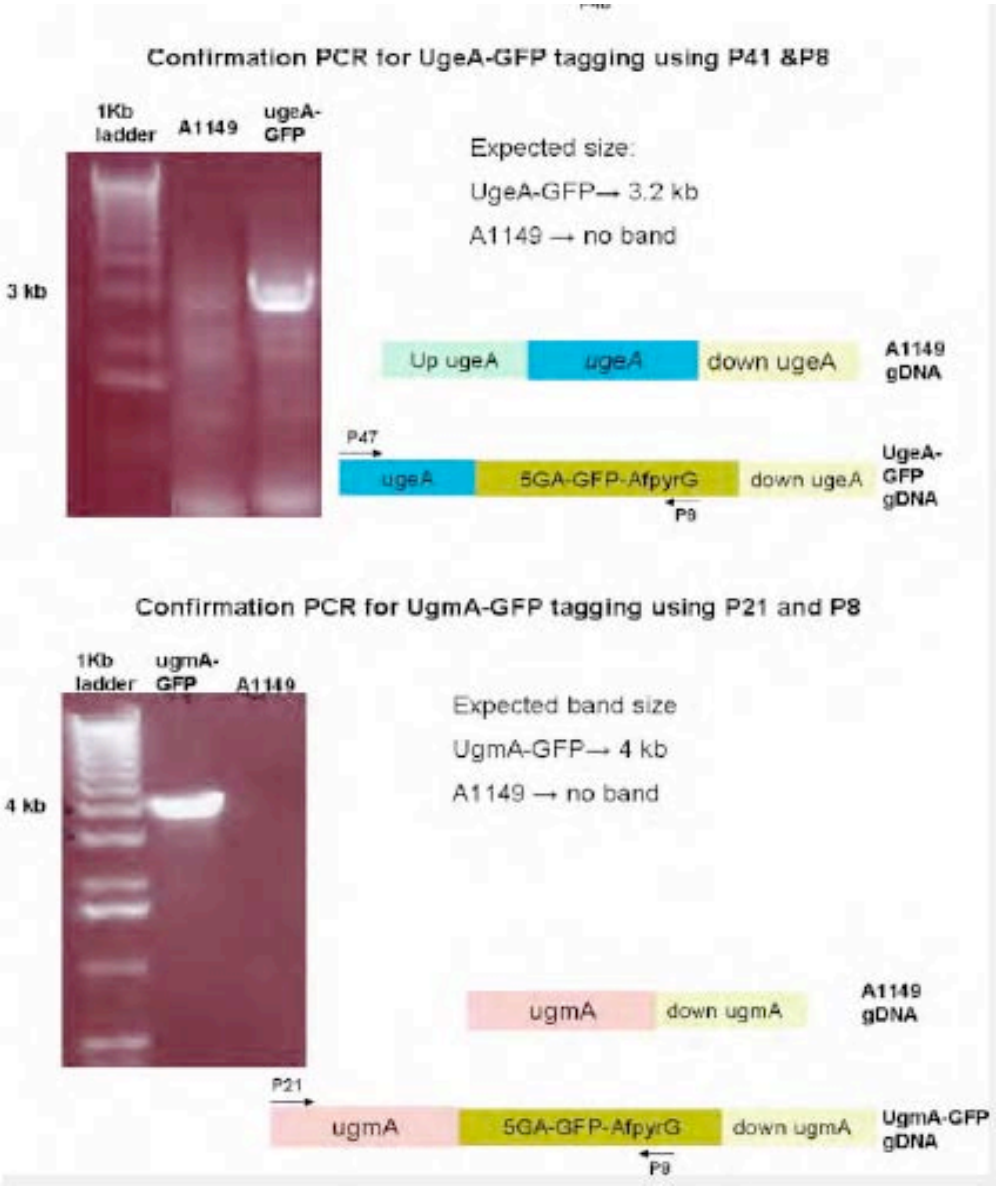

Supplementary Fig. A: **Confirmation PCRs.** The *ugeA*Δ strain was confirmed using wild type A1149 gDNA and *ugeA*Δ gDNA templates. These were amplified with P41 and P8 (*ugeA* upstream and midpyrG selectable marker), P41 and P46 (*ugeA* upstream and *ugeA* downstream), P47 and P48 (which amplify *ugeA*). The UgeA-GFP strain was confirmed using wild type A1149 gDNA and UgeA-GFP gDNA templates, amplified with P41 and P8 (*ugeA* upstream and midpyrG selectable marker). The UgmA-GFP strain was confirmed using wild type A1149 gDNA and UgmA-GFP gDNA templates, amplified with P21 and P8 (*ugmA* upstream and midpyrG selectable marker).

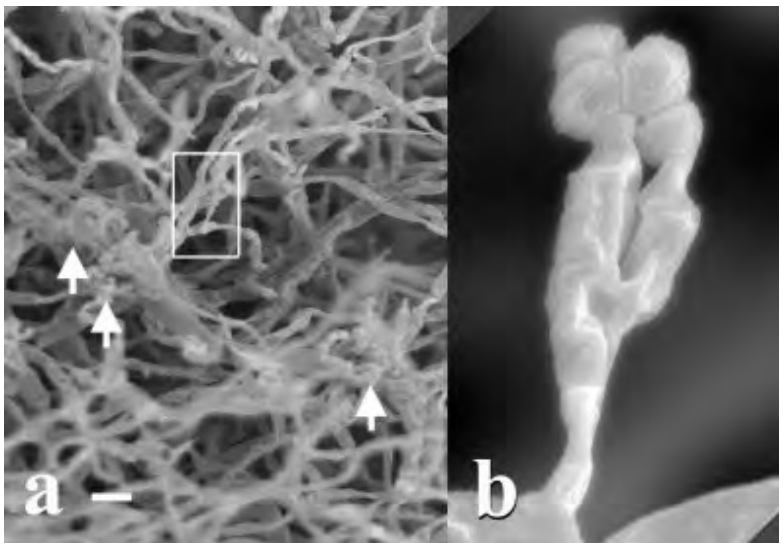

Supplementary Fig. B. Scanning electron micrographs of a 3 d old colony (a) and conidiophore (b) of a *ugeA*Δ strain. Bar in *A* = 10 μm.

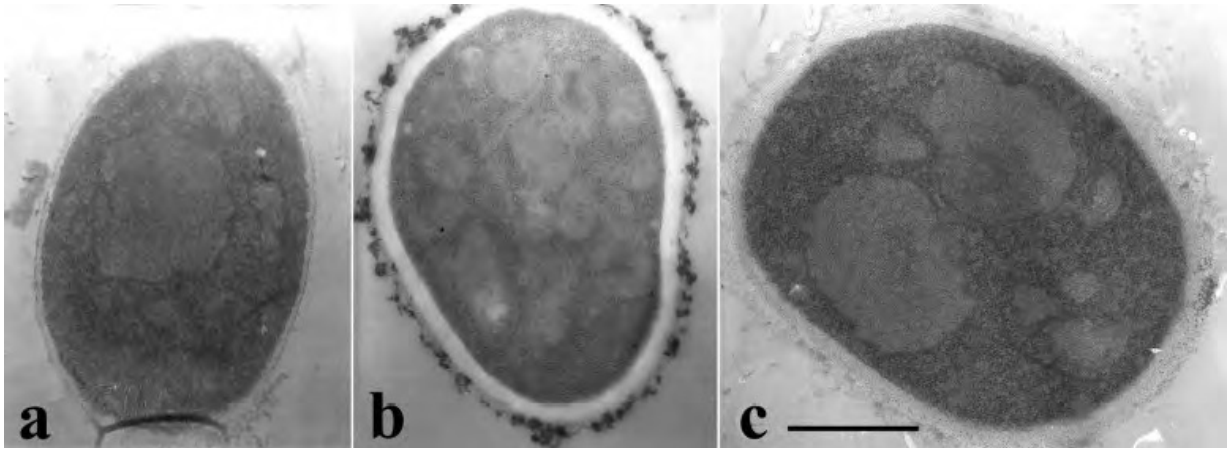

Supplementary Fig. C. Transmission electron micrographs of hyphal cross-sections of wild type (a), *ugeA*Δ (b), and *ugmA*Δ (c) strains. Boxed area in *A* is shown at higher magnification in C. Bar in *A* = 10 μm.

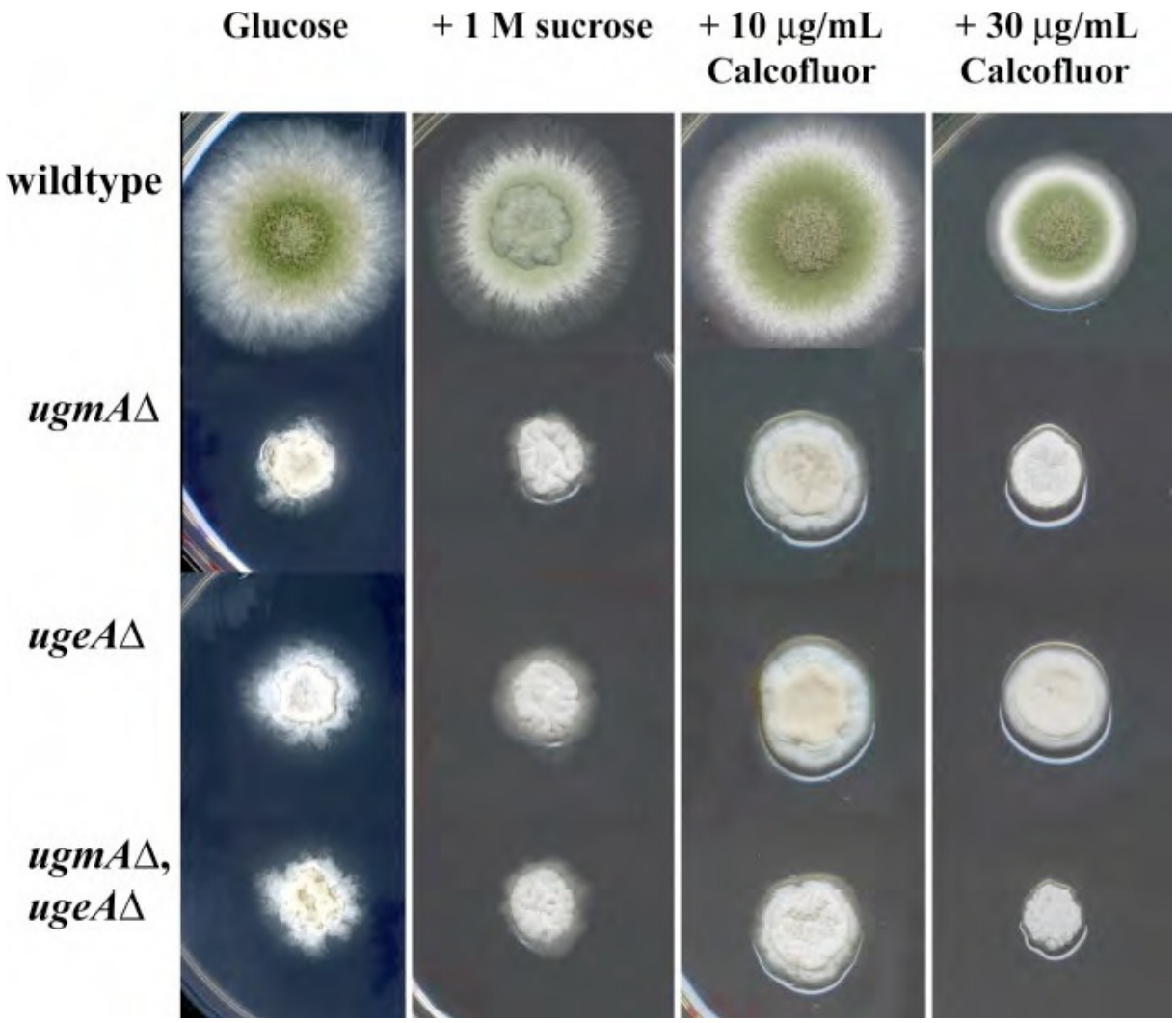

Supplementary Fig. D. Growth of *Aspergillus nidulans* strains on a variety of media. Wild type, *ugmA*Δ, *ugeA*Δ and double-deletion strains were grown on glucose supplemented with 1 M sucrose, 10 µg/mL Calcofluor, 30 µg/mL Calcofluor.

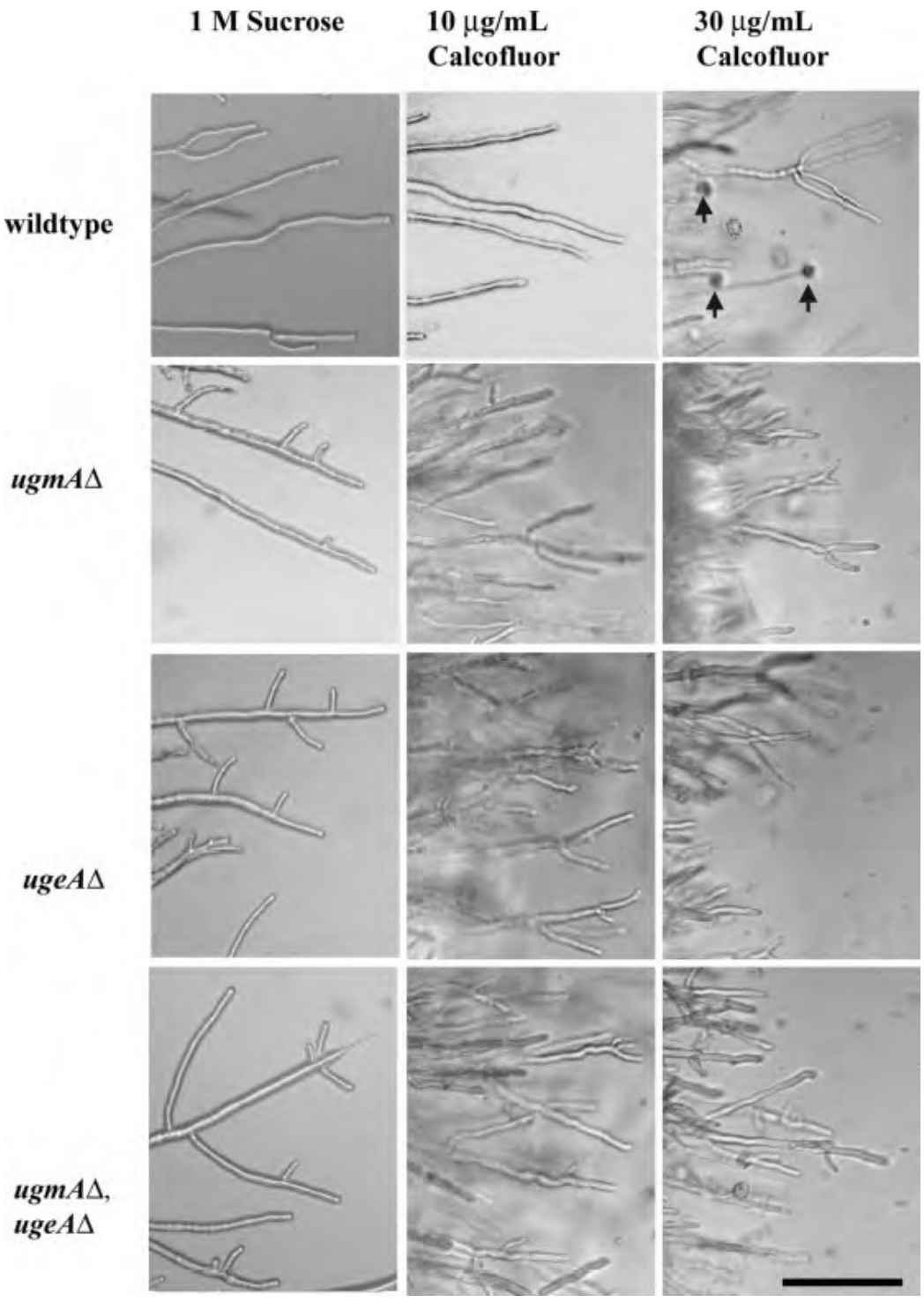

Supplementary Fig. E. Hyphal phenotype for the colonies shown in Supplementary Fig. D.

Chapter 4

Characterization of *Aspergillus nidulans* UDP-galactofuranose transporter, UgtA

This chapter study UgtA, the downstream enzyme to UgmA in the Gal*f* biosynthesis pathway. The function of UgtA is to transport UDP-Galf units from cytoplasm to membrane bound organelles for further processing. This chapter has been submitted to Fungal Genetics and Biology Journal as "Roles of the *Aspergillus nidulans* UDP-galactofuranose transporter, UgtA in wild type hyphal morphogenesis, conidiation, cell wall architecture and drug sensitivity". **Afroz, El-Ganiny, Sanders, and Kaminskyj** (accepted, 2011).

The objectives for the research in this chapter were

1) To find if the *A. nidulans* genome contains a potential UDP-galactofuranose transporter.
2) To determine if UgtA is essential for viability of *A. nidulans*.
3) To examine if *A. fumigatus glfB* and *A. nidulans ugtA* are functionally homologous.
4) To find if UgtA is also Golgi-localized, as *A. fumigatus* GlfB.
5) To characterize *ugtA* deletion on *A. nidulans* regarding morphogenesis and sporulation.
6) To determine *ugtA* deletion sensitivity towards wall targeting agents.

My roles in this paper: I identified the UgtA coding sequence in *A. nidulans* (AN3113), and did the hydropathy analysis of UgtA sequence. I trained and provided daily supervision and guidance to a newly arrived MSc candidate, Sharmin Afroz. I taught Sharmin how to grow and manipulate *A. nidulans* strains, how to design primers and access information from databases. I also taught her different technique like gDNA extraction, RNA extraction, cDNA synthesis, cloning, fusion PCR, protoplasting, transformation and antifungal susceptibility testing. Sharmin was involved in deletion of *ugtA* and characterization of the *ugtAΔ* strain, tagging of UgtA, complementation of *ugtAΔ* defects and the preliminary antifungal sensitivity testing. I did the statistical analysis of the data and wrote the first draft of the manuscript with input from Ms Afroz, we are listed as co-first authors on this manuscript. This manuscript was edited by Dr. Kaminskyj prior to submission and acceptance.

Roles of the *Aspergillus nidulans* UDP-galactofuranose transporter, UgtA in wild type hyphal morphogenesis, conidiation, cell wall architecture and drug sensitivity.

Sharmin Afroz[ab], Amira M. El-Ganiny[abc], David A.R. Sanders[d], Susan G.W. Kaminskyj[ae]

a Department of Biology, University of Saskatchewan, 112 Science Place, Saskatoon SK S7N5E2, Canada

b Contributed equally to the research

c Microbiology Department, Faculty of Pharmacy, Zagazig University, Egypt.

d Department of Chemistry, University of Saskatchewan, 110 Science Place, Saskatoon SK Canada S7N 5C9

e Author for correspondence: susan.kaminskyj@usask.ca; tel 306 966 4422

Key words: *Aspergillus nidulans*, galactofuranose, integral membrane protein, nucleotide sugar transporter, cell morphogenesis, cell wall

Abbreviations: Gal*f*, galactofuranose; Gal*p*, galactopyranose; GDP, guanidine diphosphate; GPF, green fluorescent protein; NDP, nucleotide diphosphate; NMP, nucleotide monophosphate; NST, nucleotide sugar transporter; RPMI, Rosewell Park Memorial Institute; UDP, uridine diphosphate

Abstract:

Galactofuranose (Gal*f*) is the 5-member-ring form of galactose found in the walls of fungi including *Aspergillus*, but not in mammals. UDP-galactofuranose mutase (UgmA, ANID_3112.1) generates UDP-Gal*f* from UDP-galactopyranose (UDP-Gal*p*, 6-member ring form). UgmA-GFP is cytoplasmic, so the UDP-Gal*f* residues it produces must be transported into an endomembrane compartment prior to incorporation into cell wall components. The adjacent gene, ANID_3113.1 (which we call UgtA) was identified as being likely to encode the *A. nidulans* UDP-Gal*f* transporter, based on its high amino acid sequence identity with its recently described orthologue in *A. fumigatus,* GlfB. The *ugtA* deletion (*ugtA*Δ) strain had a phenotype similar to that of *ugmA*Δ: compact colonies, wide, highly branched hyphae, and reduced sporulation. The *ugtA*Δ hyphal walls were more than three-fold thicker than wild type strains, accumulated exogenous material during submerged culture, and did not bind the EBA2 antibody. However, unlike the *ugmA*Δ strain, *ugtA*Δ metulae often produced triplets of phialides, rather than pairs, and *ugtA*Δ spore germination was substantially reduced. Af*glfB* restored wild type growth in the *ugtA*Δ strain, showing that these genes have homologous function. AfGlfB had been shown using density-gradient centrifugation to be associated with Golgi-derived membranes. Subcellular localization of UgtA-GFP under the control of its constitutive promoter showed a tip-high gradient of punctate GFP fluorescence in fungal hyphae, consistent with localization in fungal Golgi. Notably, the *ugtA*Δ strain was significantly more sensitive to Caspofungin, Calcofluor White, and Congo Red, all of which interfere with cell walls, suggesting that drugs targeting UgtA function could be useful in combination antifungal therapy.

1. Introduction

Cell walls support and protect fungal organisms, and are their interface with the environment. *Aspergillus nidulans* hyphal walls are about 20 % of cell dry weight (de Groot et al., 2009). A similar proportion of the fungal genome appears to relate to cell wall formation and maintenance (Harris, 2009). *Aspergillus* hyphal wall carbohydrates include chitin, glucans, and mannans (Leitao, 2003; Bowman and Free, 2006; Latgé, 2009). Some wall carbohydrates such as galactomannan contain a five-membered ring form of galactose called galactofuranose (Gal*f*) (Bernard and Latgé, 2001; Peltier et al., 2008). Gal*f* residues are reported to be about 5 % of the *A. fumigatus* wall (reviewed in Lamarre et al., 2009). Wild type *A. fumigatus* hyphal wall surfaces appear to have Gal*f* residues that mask a mannose-containing layer whose exposure contributes to enhanced substrate adhesion (Lamarre et al., 2009). Atomic force microscopy of wild type and Gal*f* biosynthesis enzyme deletion strains shows that Gal*f* is important for wall surface structure, strength, and adhesion (Paul et al., 2011). In addition, Gal*f* has been implicated in *A. fumigatus* pathogenicity (Latgé, 2009) although the mechanism is not yet understood.

Cell surface glycans and glycoconjugates are important for function of organisms including fungi. In addition, approximately 80 % of secreted proteins are covalently linked to a sugar prior to secretion (Caffaro and Hirschberg, 2006). Glycosylation requires a sugar donor that typically is a nucleoside diphosphate sugar (NDP-sugar) or nucleoside monophosphate sugar (Bakker et al., 2005; Handford et al., 2006). Many nucleotide sugars are synthesized in the cytosol, and then translocated to the lumen of Golgi or ER (Hirschberg, 1998) by nucleotide-sugar transporters (NSTs). NSTs translocate cytosolic nucleotide-sugars to the endomembrane system using luminal UMP as an antiporter substrate, so that the entrance of NDP-sugar is coupled to the exit of NMP (Reyes and Orellana, 2008, Sesma et al., 2009). Within the endomembrane compartment, nucleotide sugars serve as sugar donors for glycosyltransferase reactions, reviewed in Klutts et al. (2006).

Biosynthesis of glycoconjugates and polysaccharides takes place in the endomembrane system (Reyes and Orellana, 2008, Reyes et al., 2010). NSTs are integral proteins typically with six to ten transmembrane domains that frequently are located at the Golgi apparatus (Handford et al., 2006). NSTs are structurally conserved and can readily be identified from genome databases; however, their substrate specificity cannot be predicted from the sequence (Berninsone and

Hirschberg, 2000). Many NSTs have been shown to transport more than one type of substrate (Handford *et al.,* 2006).

UDP-Gal*f* is a nucleotide diphosphate sugar that is synthesized in the cytosol (El-Ganiny et al., 2010), so it must be translocated into a membrane-bound organelle prior to incorporation into glycoconjugates. The UDP-Gal*f* transporter identified in *A. fumigatus* was shown to localize to Golgi equivalents using both density-gradient centrifugation and immunolocalization (Engel et al., 2009).

We have characterized the *A. nidulans* UDP-galactofuranose transporter UgtA, whose deletion phenotype generally resembles that of the UgmA (El-Ganiny *et al.,* 2008) and UgeA (El-Ganiny *et al.,* 2010) deletion strains, although there were differences related to sporulation and germination. Af*glfB* restored wild type growth in the *ugtA*Δ strain, showing that these genes have homologous function. UgtA-GFP had a tip-high punctate distribution in hyphae, consistent with localization in fungal Golgi. Notably, the *ugtA*Δ strain was significantly more sensitive to caspofungin, suggesting that drugs that could be developed to target the Gal*f* biosynthesis pathway have potential for combination therapy.

2. Materials and Methods

2.1 Strains and culture conditions

Strains, plasmids and primers are listed in Supplemental Table A. *Aspergillus nidulans* strains were grown as described in (El-Ganiny *et al.,* 2008) on complete medium (CM) as described in (Kaminskyj, 2001). Some experiments used CM containing 1 % galactose (CM-Gal) rather than glucose. Protoplasting followed procedures in Osmani et al. (2006). Long-term storage of transformation-competent protoplasts is described in El-Ganiny et al. (2010).

2.2 Strain construction and validation

Construction of the *ugtA* deletion (*ugtA*Δ) strain ASA1 used the method described in El-Ganiny et al. (2010) based on Osmani et al. (2006) and Szewczyk et al. (2007). ANID_03113.1 was deleted from the wild type *A. nidulans* strain A1149 using Af*pyrG* as a selectable marker (amplified from pAO18). Confirmation was done by isolating gDNA from

putative knockout strains and using it as template for PCR with combinations of primers shown in Suppl. Table A and Suppl. Figure A.

The *ugtA* cDNA was prepared as described in El-Ganiny et al. (2010), and cloned into pCR4-TOPO. The positions and lengths of intron sequences predicted by the Broad website were confirmed by sequencing this cDNA at the Plant Biotechnology Institute (PBI), NRC, Saskatoon.

An *A. nidulans* strain that was C-terminal tagged UgtA (UgtA-GFP) under the control of its endogenous promoter, was generated as described in El-Ganiny et al. (2010) using a tagging construct (5GA-GFP-Af*pyrG*) amplified from plasmid pFNO3. Confirmation of GFP-tagged strains containing these constructs is shown in Suppl. Figure D.

A plasmid containing the Af*glfB* coding sequence (a generous gift of Francoise Routier) was transformed into *ugtA*Δ protoplasts to create a strain containing *ugtA*:Af*glfB* to test for functional homology between these genes. Transformation was confirmed by PCR using *ugtA*Δ:Af*glfB* gDNA template and primers SA72 and SA73 (Suppl. Table A and suppl. Figure E).

2.3 Microscopy, cell morphometry and sporulation, UgtA localization:

Strain morphometry followed procedures described in El-Ganiny et al. (2008). Freshly harvested spores were grown on coverslips for 16 h at 28 ºC in CM liquid, fixed in buffered 3.7 % formaldehyde, stained with 0.4 µg/mL Hoechst 33258 (for nuclei) and 0.2 µg/mL Calcofluor (for cell walls). Samples were imaged by confocal microscopy using a Zeiss META510 with 63 x N.A. 1.2 multi-immersion objective, or structured illumination microscopy using a Zeiss Apotome with a 60x N.A. 1.4 oil-immersion objective. For Hoechst 33258- and Calcofluor-stained samples, excitation used a 405 nm diode laser or 365 nm light emitting diode, and filters as described in El-Ganiny *et al.* (2008). Cell measurements used analysis software bundled with these systems. Some sporulating *ugtA*Δ cultures were imaged after Hoechst 33258 staining to examine nuclei in conidiophores. For morphometric analysis, hyphal width at septa and basal cell length (distance between adjacent septa) were measured for 50 cells per strain, and nuclei were counted in these cells.

To assess relative spore production, individual isolated wild type and *ugtA*Δ colonies grown 4 d at 37 °C were harvested to count their conidia. To assess spore viability, we counted the number of colonies that formed when equal numbers of freshly harvested spores (three replicate plates with about 200 spores per plate) were germinated at 28 °C for 24 h.

Scanning electron microscopy examined sporulating colonies that had grown for 4 d at 37 ºC (El-Ganiny et al. 2008). These were fixed by immersion in 1 % glutaraldehyde, dehydrated in acetone, frozen to -80 ºC, critical point dried (Polaron E3000, Series II), and sputter coated with gold (Edwards model S150B). Samples were imaged with a JEOL 840A scanning electron microscope.

Transmission electron microscopy examined hyphae that had grown overnight either submerged in liquid growth medium, or supported on dialysis tubing overlying agar, samples were prepared as described in (Kaminskyj, 2000). Cells were fixed for 1 h in 1 % glutaraldehyde in 50 mM phosphate buffer, pH 7, post-fixed for 1 h in 1 % osmium tetroxide in the same buffer, and dehydrated in a graded ethanol series. After transfer to 100 % anhydrous acetone, samples were embedded in Epon 812, which was polymerized at 60 ºC for 2 d. Silver sections (~ 75 nm thick) were collected on formvar-coated slot grids, stained with uranyl acetate and lead citrate, and imaged with a Philips CM10 operating at 60 kV. Films were digitized at 1200 dpi.

The UgtA product was C-terminal tagged with GFP, under control of its endogenous promoter, as described in El-Ganiny et al. (2010). Confirmation of this tagging construct is shown in Suppl Fig. D. GFP excitation used confocal fluorescence microscopy and an argon laser as described in El-Ganiny et al. (2010).

2.4. Antifungal susceptibility testing

Drug sensitivity of the wild type and *ugtA*Δ strains was compared using disc diffusion (Kontoyiannis et al, 2003; Rodriguez-Tudela et al, 2008). Briefly, 1 x 10^7 freshly-harvested spores were inoculated on plates containing 20 mL of RPMI agar (Rodriguez-Tudela et al, 2008). Sterile 6 mm-round filter paper discs were placed on the agar surface. Then, 10 µL of the following solutions were added to disc surfaces: Caspofungin (20 mg/mL, in water), Congo Red (10 mg/mL, in water), and Calcofluor White (10 mg/mL, in 25mM KOH) (Hill et al, 2006). The plates were incubated at 28 ºC for 24 h and 48 h. Four replicate plates were prepared for each strain, and examined at 24 h and 48 h. The radius of the zone of growth inhibition (no fungal growth) in mm was calculated as [Average inhibition diameter – 6 mm]/2.

3. Results

3.1 UgtA identification, deletion, and complementation

UDP-galactopyranose mutase (UgmA; ANID_3112) converts UDP-galactopyranose (UDP-Gal*p*) into UDP-Gal*f* (El-Ganiny et al., 2008), a process that occurs in the cytoplasm (El-Ganiny et al., 2010). Before Gal*f* can be incorporated into cell wall components, it must be transported into an endomembrane compartment, where it is expected to be a substrate for a glycosyltransferase (Berninsone and Hirschberg, 2000). *Aspergillus fumigatus* AFUA_3G12700 was recently characterized as a UDP-galactofuranose transporter by Engel et al. (2009) and named GlfB. BLAST comparison with the *A. nidulans* genome database showed that ANID_03113.1 had 88 % amino acid sequence identity with GlfB. We named the putative *A. nidulans* UDP-Gal*f* transporter UgtA.

ANID_3113.1 was deleted by replacing it with Af*pyrG* in strain A1149 (El-Ganiny et al., 2008; and Suppl Fig. A). Conidia from primary transformant colonies germinated and grew on selective medium, suggesting that UgtA is dispensable for viability. As shown in Suppl Fig. A, genomic DNA from *ugtA*Δ strains but not the wild type morphology parent strain A1149 contained Af*pyrG*. In contrast, the parental but not the deletion strains contained the *ugtA* coding sequence. Thus, UgtA is not essential for spore germination and growth.

A plasmid containing the Af*glfB* sequence was transformed into *ugtA*Δ protoplasts, creating a *ugtA*Δ:Af*glfB* strain, to test whether these sequences were functionally homologous. Af*glfB* fully complemented *ugtA*Δ defects and restored the wild type hyphal morphology and sporulation phenotypes (Fig. 1; Table 1).

The *ugtA* genomic sequence ANID_3113.3 is on chromosome 3. UgtA is predicted to be 400 amino acids (Suppl. Figure B). Hydropathy analysis using TMHMM2.0 suggests that it has 11 membrane-spanning regions (Suppl. Figure B). UgtA is predicted to be 1446 nucleotide bases and to have five exons, which we confirmed by isolating and sequencing the *ugtA* cDNA. The *ugtA* predicted gDNA and cDNA sequence shown in Suppl. Figure C agreed with those shown on the Broad *A. nidulans* genome database.

3.2 Roles of UgtA in *Aspergillus nidulans* morphogenesis and sporulation

Fig. 1 shows colony and hyphal phenotypes of wild type, *ugtA*Δ, and *ugmA*Δ, and *ugtA*Δ:Af*glfB* strains grown on CM and CM-Gal. The *ugtA*Δ strain had a compact colonial morphology unlike wild type, but similar to the *ugmA*Δ strain (El-Ganiny et al., 2008).

Sporulation was delayed and/or reduced in *ugtA*Δ colonies compared to wild type. The wild type and *ugtA*Δ:Af*glfB* colonies had begun to produce pigmented conidia by 2 d (Fig. 1A, H) and were sporulating abundantly by 3 d. In contrast at 3 d, the *ugtA*Δ and *ugmA*Δ colonies had barely begun to sporulate, so that the center of the colony was only faintly pigmented (Fig. 1B, C). Sporulation of *ugtA*Δ colonies was improved by growth on CM-Gal (Fig. 1F) compared to CM (Fig. 1B), although colony growth was not remediated. The morphology of hyphae at the margins of the colonies in Fig. 1 A-H is shown in Fig. 1 A'-H'. The wild type and *ugtA*Δ:Af*glfB* hyphae were slender and relatively unbranced, whereas the *ugtA*Δ strain hyphae resembled those of the *ugmA*Δ strain.

Fig. 2 shows typical cellular morphologies of the wild type, *ugtA*Δ, and *ugtA*Δ:Af*glfB* strains grown in liquid CM for 16 h at 28 °C. In this figure, the wild type and *ugtA*Δ:Af*glfB* cells were stained with Calcofluor and Hoechst 33258, but the *ugtA*Δ cells were stained only with Hoechst 33258. This stain accumulates non-specifically in cell walls (Kaminskyj and Hamer, 1998), suggesting that the *ugtA*Δ hyphal walls were considerably thicker than those of wild type strains. Staining *ugtA*Δ hyphae with Calcofluor and Hoechst 33258 together masked nucleus visibility due to intense wall staining (*data not shown*), consistent with their hyphal walls being thicker than wild type. A morphometric comparison of wild type, *ugtA*Δ and *ugtA*Δ:Af*glfB* hyphae is shown in Table 1.

The *ugtA*Δ strain was grown on dialysis tubing lying on agar medium for 4 d at 37 °C to examine conidiophore morphology using scanning electron microscopy (SEM) (Fig. 3A). The *ugtA*Δ conidiophore structures were smaller than wild type strains. In addition, whereas wild type *A. nidulans* metulae each produce two phialides (Mims et al., 1988), some *ugtA*Δ metulae produced three phialides (arrows in Fig. 3B, C). Each of these phialides was able to produce conidia (Fig. 3 B, C). Notably, unlike *ugmA*Δ (El-Ganiny et al., 2008) germination of the *ugtA*Δ conidia was only half that of wild type strains (Table 1).

Hyphal wall thickness and surface adhesion characteristics of wild type and *ugtA*Δ hyphae were examined using transmission electron microscopy (TEM) (Fig. 4). We used cross-sections

of near-apical regions of actively growing hyphae that contained organelle-rich cytoplasm. The organelle appearance and distribution were qualitatively similar between the wild type and *ugtA*Δ hyphae. Two growth conditions were compared: 16 h old cultures grown in liquid CM, and similar age cultures grown on dialysis tubing overlying solid CM. In both cases, the *ugtA*Δ near-apical hyphal walls were at least three-fold thicker than wild type strains (Table 1; Fig. 4). Also unlike wild type (Fig. 4B), *ugtA*Δ hyphae grown in liquid CM were thickly coated with material (Fig. 4D) that we attribute to exogenous components from growth in the culture medium adhering to the hyphal wall surfaces. Similar accumulations of material on *ugtA*Δ hyphae grown in liquid culture are seen in Fig. 2.

3.3 Localization of *Aspergillus nidulans* UgtA

Aspergillus nidulans UgtA was C-terminal tagged with GFP under the control of the endogenous *ugtA* promoter. The UgtA-GFP strain had wild type hyphae and colony morphology and sporulated abundantly, suggesting that the construct is fully functional. The UgtA-GFP localization pattern was punctate, and more abundant at hyphal tips (Fig. 5A) than basal regions (Fig. 5B), both consistent with Golgi distribution. These were motile, and moved in both directions. In conidiophores, UgtA-GFP also had a punctate distribution and was prominent in phialides and young conidia (data not shown).

3.4. Testing sensitivity to antifungal drugs

We used the radius of zone of inhibition as an end point to show the sensitivity of our strains towards the used wall targeting agents. Growth inhibition is defined as the clear zone where hyphae are unable to grow (see arrows in Fig. 6), rather than the surrounding region where growth is sparse. At 48 h (the standard time for drug sensitivity tests of this type), *ugtA*Δ strain was more sensitive than wild type strain to Caspofungin (Fig. 6).

4. Discussion

4.1 *Aspergillus nidulans* contains a putative galactofuranose nucleotide sugar transporter that is predicted to be a transmembrane protein.

NSTs are proteins that translocate sugars from their site of synthesis in the cytosol (Berninsone and Hirschberg, 2000) into the lumen of Golgi or ER (Kuhn and White, 1976;

Hirschberg, 1998; Eckhardt et al., 1999). BLAST comparison of *A. nidulans* predicted protein sequences with the recently characterized *A. fumigatus* UDP-galactofuranose transporter, GlfB (Engel et al., 2009) showed that the *A. nidulans* genome database had a single sequence (ANID_03113.1) with high homology, which we call UgtA. UgtA is immediately downstream of UgmA (ANID_3112.1), which encodes UDP-galactopyranose mutase (El-Ganiny et al., 2008) that makes the UgtA possible candidate. *ugmA* is on the (–) strand while *ugtA* is on the (+) strand, so each gene has its own promoter. The *A. fumigatus* genes encoding UDP-galactofuranose mutase (GlfA) and the UDP-galactofuranose transporter (GlfB) are adjacent in their genome (Engel et al., 2009). Similarly, galactose metabolism genes are clustered in other fungi (Moyrand et al., 2008).

Comparison of UgtA and related sequences showed that their identity is highest at the putative active site (Engel et al., 2009). Two lysine residues, positions 59 and 294 in *A. fumigatus* GalfB are predicted to be involved in substrate binding (Engel et al., 2009). The position of these residues is highlighted in Supplemental Fig. B. Neither is in a transmembrane domain, consistent with their expected function, K59 is luminal and K294 is cytoplasmic.

Nucleotide sugar transporters analyzed to date typically have 6–10 transmembrane domains (Handford et al., 2006). UgtA is predicted to have 11 transmembrane domains. Confirmation will require the UgtA crystal structure, which will be a challenging task. Currently, we are exploring interactions between UgmA and cytoplasmic loops of UgtA.

For production of Gal*f*-containing cell wall components (Latge, 2009), additional processing steps in one or more compartments of the endomembrane system involving glycosylation enzymes called galactofuranosyl transferases conjugate Gal*f* subunits to each other and to other cell wall components. Two galactofuranosyl transferases have been identified in the genome of *Mycobacterium* (Belanova et al., 2008; Szczepina et al., 2010), one in *Leishmania* (Gaur et al., 2009, Novozhilova and Bovin, 2010), but none in fungi (Deshpande et al., 2008).

4.2 Roles of *Aspergillus nidulans* UgtA in morphogenesis and development

Aspergillus nidulans UgtA is not essential for survival *in vitro*, however UgtA has important roles in wild type hyphal growth and sporulation. These results are consistent with our previous studies on UgmA (El-Ganiny et al., 2008) and UgeA (El-Ganiny et al., 2010), which catalyze reactions immediately upstream of UgtA. Notably, deletion of any of these three genes

caused substantially similar hyphal growth abnormalities. Thus, it appears that preventing Gal*f* biosynthesis or downstream stages in its incorporation into the *A. nidulans* cell wall is equally devastating to fungal vigour.

Nucleotide sugars are substrates for glycosylation reactions in the Golgi equivalent or endoplasmic reticulum. Inactivation of related transporters in mammals, yeast and protozoa has been shown to cause problems in morphology or/and virulence (Hirschberg, 1998, Arakawa et al., 2006)). *Cryptococcus neoformans* and *A. nidulans* both have two GDP-mannose transporters, called Gmt1/Gmt2 and GmtA/GmtB, respectively. Deletion of *C. neoformans* Gmt1 caused capsule integrity defects (Cottrell et al., 2007). Mutation of GmtA in *A. nidulans* caused hyphal morphology defects and hypersensitivity to Calcofluor (Jackson-Hayes et al. 2008, Liu et al., 2010). An *A. fumigatus* Gal*f* deficient strain *glfA*Δ, was found to be less virulent in animal model (Schmalhorst et al., 2008).

Lamarre et al. (2009) showed that the *A. fumigatus ugm1*Δ strain (called *glfA* in Schmalhorst et al., 2008) had increased the adhesion to surfaces including glass and latex, and other hyphae (Lamarre, 2009). Hyphal wall surface adhesion can be quantified using atomic force microscopy and spectroscopy: both *ugeA*Δ and *ugmA*Δ strains had increased adhesion to silicon nitride compared to wild type (Paul et al., 2011). In our current study, ASA1 grown in liquid CM became covered with extraneous material, also suggesting it had increased adhesiveness compared to wild type. Taken together, surface Gal*f* residues on *Aspergillus* hyphae appear to moderate hyphal adhesion, perhaps by masking a mannose-containing layer.

4.3 Subcellular localization of UgtA is consistent with its predicted protein function

The UgtA-GFP Golgi localization pattern shown in this study is consistent with density gradient centrifugation and immunofluorscence results for *A. fumigatus* GlfB (Engel et al., 2009). Golgi distribution in *A. nidulans* has previously been shown to be punctate, and more abundant near hyphal tips (Breakspear et al., 2007; Hubbard and Kaminskyj, 2008) Similarly, the GDP-mannose transporter (GMT) in *Saccharomyces cerevisiae* (Dean et al., 1997), *Candida albicans* (Nishikawa et al., 2002), and *A. nidulans* (Jackson-Hayes et al., 2008) localize to Golgi. In contrast, the UDP-glucose/galactose transporter in *Arabidopsis thaliana (*AtUTr1, AtUTr3) was found to localize the endoplasmic reticulum, perhaps due to its additional role in mediating

the unfolded protein response (Reyes et al., 2006; Rollwitz er al., 2006). We are actively studying interactions between UgtA and UgmA.

4.4 AfGlfB can restore the function of *A. nidulans* UgtA

After transforming the Af*glfB* containing plasmid into the *ugtA*Δ strain, the *ugtA*Δ:*AfglfB* colony has wild type morphology where the size of the colony and sporulatrion was similar to AAE1 strain. Morphometric analysis also showed that the hyphae of the *ugtA*Δ:Af*glfB* strain restore the wild type characters of AAE1 strain. This indicates that AfGlfB complemented the defects in the *ugtA*Δ as it performs the same function.

4.5. *ugtA*Δ is more sensitive to antifungal cell wall targeting agents than wild type strain.

The disc diffusion assay of Caspofungin, CR and CFW represents different sensitivity index. In the case of *ugtA*Δ strain more attenuation of growth was observed than wild type strain AAE1 after both 24 hrs and 48 hrs. As a cell wall defective strain, *ugtA*Δ was anticipated to be most sensitive to these antifungal agents. This anticipated result consistent with our experiment result.

Acknowledgements

SGWK is pleased to acknowledge funding from the Canadian Institutes of Health Research Regional Partnership Program, the Natural Sciences and Engineering Research Council (NSERC) of Canada Discovery Grant program, and the NSERC Research Tools and Instruments program. SA was supported by a University of Saskatchewan Graduate Scholarship and a Graduate Equity Scholarship. AME was supported by a fellowship from the Egyptian Ministry of Higher Education. We thank Francoise Routier for providing the pYEScupFLAGK Af*glfB* plasmid and Tom Bonli for technical assistance with SEM work.

References

Arakawa, K., Abe, M., Noda, Y., Adachi, H., Yoda, K., 2006. Molecular cloning and characterization of a Pichia pastoris ortholog of the yeast Golgi GDP-mannose transporter gene. The Journal of General and Applied Microbiology 52, 137-145.

Bakker, H., Routier, F., Oelmann, S., Jordi, W., Lommen, A., Gerardy-Schahn, R., Bosch, D., 2005. Molecular cloning of two *Arabidopsis* UDP-galactose transporters by complementation of a deficient Chinese hamster ovary cell line. Glycobiology 15, 193-201.

Belanova, M., Dianiskova, P., Brennan, P.J., Completo, G.C., Rose, N.L., Lowary, T.L., Mikusova, K., 2008. Galactosyl transferases in mycobacterial cell wall synthesis. J. Bacteriol. 190, 1141-1145.

Bernard, M., Latgé, J.P. 2001. *Aspergillus fumigatus* cell wall: composition and biosynthesis. Med. Mycol. 39: S9-S17.

Berninsone, P.M., Hirschberg, C.B., 2000. Nucleotide sugar transporters of the Golgi apparatus. Curr. Opin. Struct. Biol. 10, 542-547.

Bowman, S. M., Free, S. J., 2006. The structure and synthesis of the fungal cell wall. BioEssays 28, 799-808.

Breakspear, A., 2007. CopA:GFP localizes to putative Golgi equivalents in *Aspergillus nidulans*. FEMS Microbiol. Lett. 277, 90- 97.

Caffaro, C.E., Hirschberg, C.B., 2006. Nucleotide sugar transporters of the Golgi apparatus: from basic science to diseases. Acc. Chem. Res. 39, 805-812.

Cottrell, T.R., Griffith, C.L., Liu, H., Nenninger, A.A., Doering, T.L. 2007. The pathogenic fungus *Cryptococcus neoformans* expresses two functional GDP-mannose transporters with distinct expression patterns and roles in capsule synthesis. Eukaryot. Cell 6, 776-785.

Dean, N., Zhang, Y.B., Poster, J.B., 1997. The *VRG4* gene is required for GDP-mannose transport into the lumen of the Golgi in the yeast, *Saccharomyces cerevisiae*. J. Biol. Chem. 272, 31908-31914.

de Groot, P.W.J., Brandt, B.W., Horiuchi, H., Ram, A.F.J., de Koster, C.G., Klis, F.M., 2009. Comprehensive genomic analysis of cell wall genes in *Aspergillus nidulans*. Fungal Genet. Biol. 46, S72-S81.

Deshpande, N., Wilkins, M.R., Packer, N., Nevalainen, H., 2008. Protein glycosylation pathways in filamentous fungi. Glycobiology 18, 626-637.

Eckhardt, M., Gotza, B. Gerardy-Schahn, R. 1999. Membrane topology of the mammalian CMP-sialic acid transporter. J Biol. Chem. 274, 8779-8787.

El-Ganiny, A.M., Sanders, D.A.R., Kaminskyj, S.G.W., 2008. *Aspergillus nidulans* UDP-galactopyranose mutase, encoded by *ugmA* plays key roles in colony growth, hyphal morphogensis, and conidiation. Fungal Genet. Biol. 45, 1533-1542.

El-Ganiny, A., Sheoran, I., Sanders, D.A.R., Kaminskyj, S.G.W., 2010. *Aspergillus nidulans* UDP-glucose-4-epimerase UgeA has multiple roles in wall architecture, hyphal morphogenesis, and asexual development. Fungal Genet. Biol. 47, 629-635

Engel, J., Schmalhorst, P.S., Dörk-Bousset, T., Ferrières, V., Routier, F.H., 2009. A single UDP-galactofuranose transporter is required for galactofuranosylation in *Aspergillus fumigatus*. J Biol. Chem. 284, 33859-33868.

Gaur, U., Showalter, M., Hickerson, S., Dalvi, R., Turco, S.J., Wilson, M.E., Beverley, S.M., 2009. *Leishmania donovani* lacking the Golgi GDP-Man transporter LPG2 exhibit attenuated virulence in mammalian hosts. Exp. Parasitol. 122, 182-191.

Handford, M., Rodriguez-Furlán, C., Orellana, A., 2006. Nucleotide-sugar transporters: structure, function and roles *in vivo*. Braz. J. Med. Biol. Res. 39, 1149-1158.

Harris, S.D., Turner, G., Meyer, V., Espeso, E. A., Specht, T., Takeshita, N., Helmstedt, K., 2009. Morphology and development in *Aspergillus nidulans*: a complex puzzle. Fungal Genet. Biol. 46, S82-S92.

Hill, T.W., Loprete, D.M., Momany, M., Harsch, M., Livesay, J.A., Mirchandani, A., Murdock, J.J., Vaughan, M.J., Watt, M.B., 2006. Isolation of cell wall mutants in *Aspergillus nidulans* by screening for hypersensitivity to Calcofluor White. Mycologia 98, 399–409.

Hirschberg, C.B., 1998. Transporters of nucleotide sugars, ATP, and nucleotide sulfate in the endoplasmic reticulum and Golgi apparatus. Annu. Rev. Biochem. 67, 49-69.

Hubbard, M.A., Kaminskyj, S.G.W., 2008. Rapid tip-directed movement of Golgi equivalents in growing *Aspergillus nidulans* hyphae suggests a mechanism for delivery of growth-related materials. Microbiology 154, 1544-1553.

Jackson-Hayes, L., Hill, T.W., Loprete, D.M., Fay, L.M., Gordon, B.S., Nkashama, S.A., Patel, R.K., Sartain, C.V., 2008. Two GDP-mannose transporters contribute to hyphal form and cell wall integrity in *Aspergillus nidulans*. Microbiology 154, 2037-2047.

Kaminskyj, S.G.W., 2000. Septum position is marked at the tip of *Aspergillus nidulans* hyphae. Fungal Genet. Biol. 31, 105-113

Kaminskyj, S.G.W., 2001. Fundamentals of growth, storage, genetics and microscopy of *Aspergillus nidulans*. Fungal Genet. Newsl. 48, 25-31.

Kaminskyj S, Hamer J 1998 *hyp* Loci control cell pattern formation in the vegetative mycelium of *Aspergillus nidulans*. Genetics 148, 669-680.

Klutts, J.S., Yoneda, A., Reilly, M.C., Bose, I., Doering, T.L., 2006. Glycosyltransferases and their products: cryptococcal variations on fungal themes. FEMS Yeast Res. 6, 499-512.

Kontoyiannis, D. P,. Lewis, R. E., Osherov, N., Albert, N. D.. May, G. S., 2003. Combination of caspofungin with inhibitors of the calcineurin pathway attenuates growth *in vitro* in *Aspergillus* species. *Journal of Antimicrobial Chemotherapy.*51, 313–316.

Kuhn, N.J., White, A. 1976. Evidence for specific transport of uridine diphosphate galactose across the Golgi membrane of rat mammary gland. Biochem. J. 154, 243-244.

Lamarre, C., Beau, R., Balloy, V., Fontaine, T., Sak Hoi, J. W., Guadagnini, S., Berkova, N., Chignard, M., Beauvais, A., Latgé, J., 2009. Galactofuranose attenuates cellular adhesion of *Aspergillus fumigatus*. Cell. Microbiol. 11, 1612-1623

Latgé, J.P., 2009. Galactofuranose containing molecules in *Aspergillus fumigatus*. Med. Mycol. 47, S104-S109.

Leitao, E.A., , Bittencourt, V. C.B., Haido, R. M.T., Valente, A. P., Peter-Katalinic, J., Letzel, M., de Souza, L. M., Barreto-Bergter, E. 2003. β-Galactofuranose-containing O-linked oligosaccharides present in the cell wall peptidogalactomannan of *Aspergillus fumigatus* contain immunodominant epitopes. Glycobiology 13, 681-692.

Liu, L., Xu, Y.X., Hirschberg, C.B., 2010. The role of nucleotide sugar transporters in development of eukaryotes. Semin. Cell Dev. Biol. 21, 600-608.

Mims, C.W., Richardson, E.A., Timberlake, W.E., 1988 Ultrastructural analysis of conidiophore development in the fungus *Aspergillus nidulans* using freeze-substitution. Protoplasma 144, 132-141.

Moyrand, F., Lafontaine, I., Fontaine, T., Janbon, G. 2008. *UGE1* and *UGE2* regulate the UDP-glucose/UDP-galactose equilibrium in *Cryptococcus neoformans*. Eukaryot. Cell 7, 2069-2077.

Nishikawa, A., Poster, J.B., Jigami, Y., Dean, N., 2002. Molecular and phenotypic analysis of *CaVRG4*, encoding an essential Golgi apparatus GDP-mannose transporter. J. Bacteriol. 184, 29-42.

Novozhilova, N.M., Bovin, N.V., 2010. Structure, functions, and biosynthesis of glycoconjugates of *Leishmania* spp cell surface. Biochemistry 75, 686-694.

Osmani, A.H., Oakley, B.R., Osmani, S.A., 2006. Identification and analysis of essential *Aspergillus nidulans* genes using the heterokaryon rescue technique. Nat. Protocols 1, 2517-2526.

Paul, B., El-Ganiny, A.M., Abbas, M., Kaminskyj, S.G.W., Dahms, T.E.S., 2011. Quantifying the importance of galactofuranose in *Aspergillus nidulans* hyphal wall surface organization by atomic force microscopy. Eukaryotic Cell. 10,646-653

Peltier, P., Euzen, R., Daniellou, R., Nugier-Chauvin, C., Ferrières, V. 2008. Recent knowledge and innovations related to hexofuranosides: structure, synthesis and applications. Carbohydr. Res. 343, 1897-1923.

Reyes, F., Marchant, L., Norambuena, L., Nilo, R., Silva, H., Orellana, A., 2006. AtUTr1, a UDP-glucose/UDP-galactose transporter from *Arabidopsis thaliana*, is located in the endoplasmic reticulum and up-regulated by the unfolded protein response. J. Biol. Chem. 281, 9145-9151.

Reyes, F., Orellana, A., 2008. Golgi transporters: opening the gate to cell wall polysaccharide biosynthesis. Curr. Opin. Plant Biol. 11, 244-251.

Reyes, F., Leon, G., Donoso, M., Brandizzi, F., Weber, A.P., Orellana, A., 2010. The nucleotide sugar transporters AtUTr1 and AtUTr3 are required for the incorporation of UDP-glucose into the endoplasmic reticulum, are essential for pollen development and are needed for embryo sac progress in *Arabidopsis thaliana*. Plant J. 61, 423-435.

Rodriguez-Tudela. J. L., Arendrup, M. C., Arikan, S., Barchiesi, F., Bille, J.,Chryssanthou, E., Cuenca-Estrella, M., Dannaoui, E., Denning, D. W., Donnelly, J. P., Fegeler, W., Lass-Flörl11, C., Moore, C., Richardson, M., Gaustad, P., Schmalreck, A., Velegraki, A.. Verweij, P., 2008. EUCAST Definitive Document E. DEF 9.1: Method for the determination of broth dilution minimum inhibitory concentrations of antifungal agents for conidia forming moulds.

Rollwitz, I., Santaella, M., Hille, D., Flügge, U.I., Fischer, K., 2006. Characterization of AtNST-KT1, a novel UDP-galactose transporter from *Arabidopsis thaliana*. FEBS Lett. 580, 4246-4251.

Schmalhorst, P.S., Krappmann, S., Vervecken, W., Rohde, M., Muller, M., Braus, G.H., Contreras, R., Braun, A., Bakker, H., Routier, F.H., 2008. Contribution of galactofuranose to

the virulence of the opportunistic pathogen *Aspergillus fumigatus*. Eukaryot. Cell 7, 1268-1277.

Sesma, J.I., Esther, C.R., Kreda, S.M., Jones, L., O'Neal, W., Nishihara, S., Nicholas, R.A., Lazarowski, E.R., 2009. Endoplasmic reticulum/Golgi nucleotide sugar transporters contribute to the cellular release of UDP-sugar signaling molecules. J Biol. Chem. 284, 12572-83.

Szczepina, M.G., Zheng, R.B., Completo, G.C., Lowary, T.L., Pinto, B.M., 2010. STD-NMR studies of two acceptor substrates of GlfT2, a galactofuranosyltransferase from *Mycobacterium tuberculosis*: epitope mapping studies. Bioorg. Med. Chem. 18, 5123-5128.

Szewczyk, E., Nayak T., Oakley, C.E., Edgerton, H., Xiong, Y., Taheri-Talesh, N. Osmani, S.A., Oakley, B.R. 2007. Fusion PCR and gene targeting in *Aspergillus nidulans*. Nat. Protocols 1, 3111-3120.

Table 1. Hyphal morphometry, conidium production, germination, and wall thickness for wild type (AAE1), *ugtA*Δ (ASA1), and *ugtA*Δ:Af*glfB* (ASA3) strains.

	Wild type	*ugtA*Δ	*ugtA*Δ:Af*glfB*
Hyphal width (μm ± SE) [a]	2.2 ± 0.1[c]	3.5 ± 0.1 [d]	2.0 ± 0.0 [c]
Basal cell length (μm ± SE) [a]	24 ± 1 [c]	16 ± 1 [d]	22 ± 0.5 [c]
Nuclei per basal cell [a] (± SE)	4.3 ± 0.4 [c]	3.7 ± 1.0 [d]	3.6 ± 0.1 [d]
Spore production/colony (millions)	107 [c]	1.33 [d]	n/a
Germination efficiency	96 %	55 %	n/a
Wall thickness (nm ± SE) [b]	53 ± 0.1 [c]	183 ± 1 [d]	n/a

a For hyphal morphometry, values presentd are average of 50 measurment / strain (mean ± SE), from two independent expermints. For each measurement, values followed by different letters (c-d) are significantly different. Statistical analyasis was done using Graphpad Prism (ANOVA, $P \leq 0.05$)

b Wall thickness of 10 different hyphal sections per strain (typically three measurement sites), measured where the cell membrane was crisply focused.

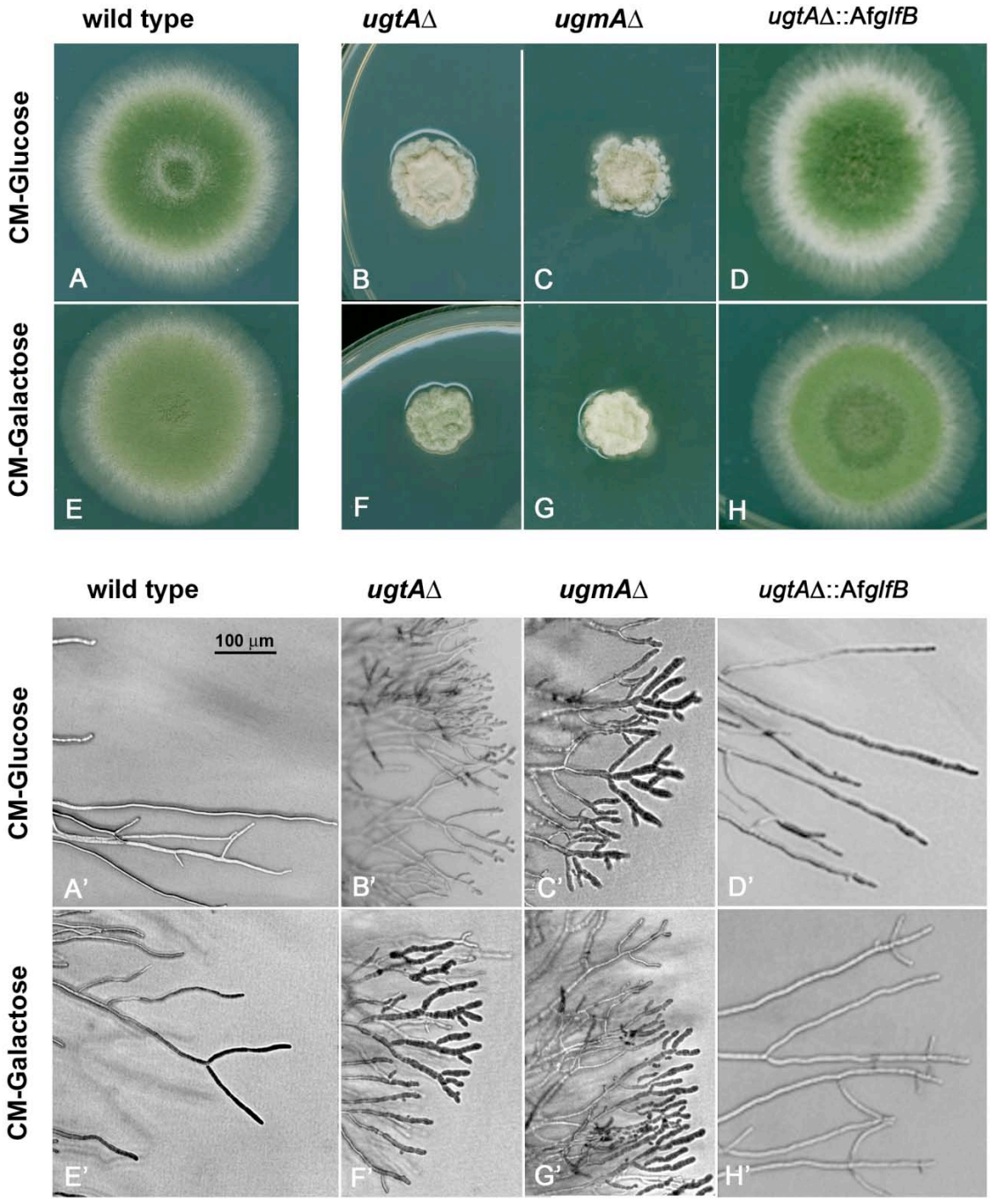

Figure 1: Effect of *ugtA* deletion on colony morphology (A-H) and on hyphal morphology at the edges of those colonies (A'-H'). Wild type (A, E, A', E'); *ugtA*Δ (B, F, B', F'), *ugmA*Δ (C, G, C', G'), and *ugtA*Δ:Af*glfB* (D, H, D', H') grown on complete medium containing 1 % glucose (A-D, A'-D') or 1 % galactose (E-H, E'-H'). Bar in A' represents 100 µm, for images A'-H'.

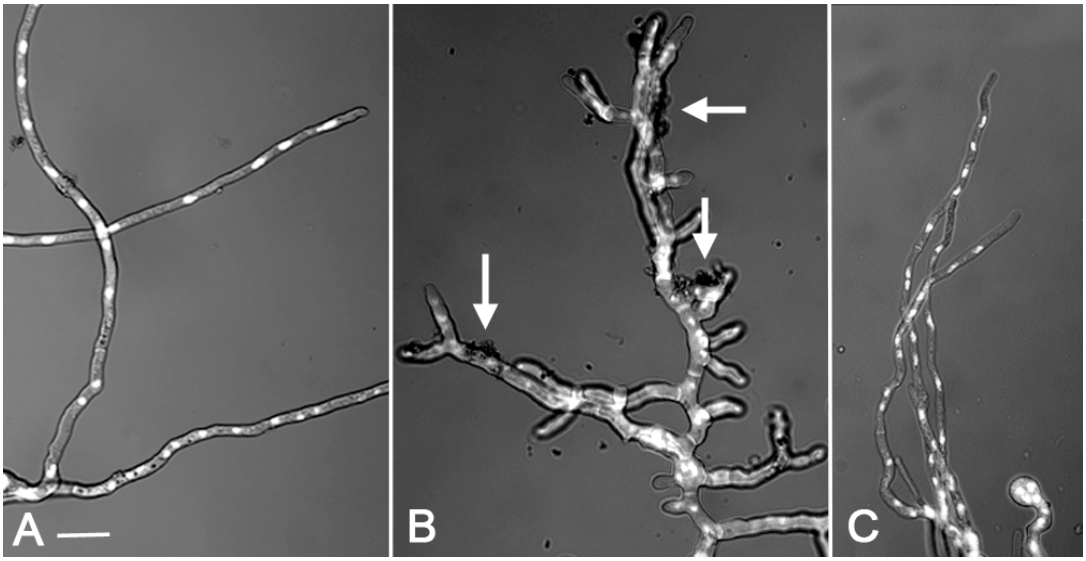

Figure 2: Hyphae of wild type (A), *ugtA*Δ (B), and *ugtA*Δ:Af*glfB* (C) strains grown in liquid medium and stained with Hoechst 33258. Pictures shown as merged confocal fluorescence and transmitted images. Arrows in (B) indicate detritus that has accumulated from the medium during culturing. Bar in (A) represents 10 µm, for A, B and C.

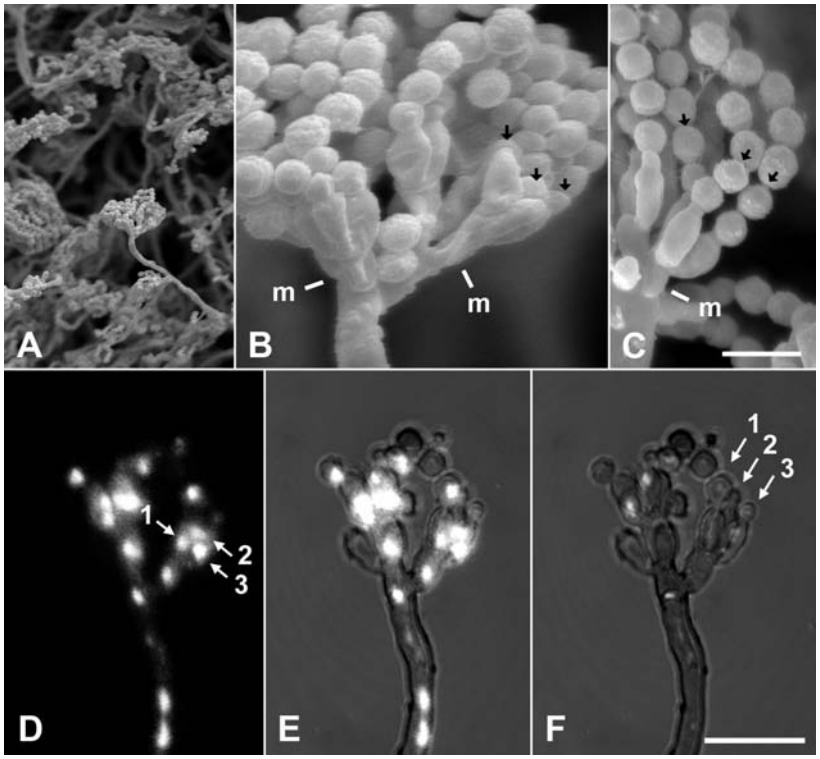

Figure 3. ***Aspergillus nidulans ugtA*Δ metulae occasionally bear phialide triplets.**

(A-C) Scanning electron microscopy of a four days-old *ugtA*Δ colony showing variable conidiophore maturation. Bar in C = 10 μm, for A-C. **A)** Conidiophore vesicles of *ugtA*Δ are typically smaller than those of wild type strains, so *ugtA*Δ has fewer metulae per conidiophore, and the conidial chains are splayed, not tightly packed. The conidiophore in the center of (A) is shown at higher magnification in (B). **B, C)** Some *ugtA*Δ metulae (m) bear phialide triplets. A chain of spores is produced by each phialide (*e. g.* black arrows in B, C).

(D-F) Confocal images of an *ugtA*Δ conidiophore stained with Hoechst 33258. Bar in F = 10 μm, for D-F. D) fluorescence, E) merged, F) transmitted. D) The metula on the right has produced three phialides, each of which has a single nucleus (1-3). F) Each of the phialides in D is sporulating (F), but only the spore on phialide 1 contains a nucleus.

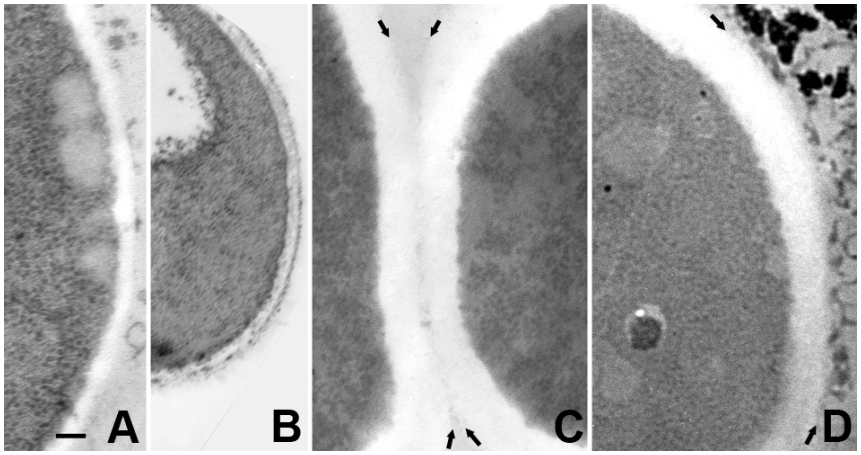

Figure 4. Transmission electron micrographs of cross-sections of wild type and ASA1 hyphae. A) Wild type grown on dialysis tubing, **B)** wild type grown in liquid medium, **C)** *ugtA*Δ grown on dialysis tubing, **D)** *ugtA*Δ grown in liquid medium.

The hypha in **A** was sectioned at an angle to the hyphal axis, so it is oval in profile. Wall thickness measurements were made where the cell membrane was crisply in focus (see Methods). Arrows indicate the outer surface of the *ugtA*Δ cell walls in C and D. Unlike the wildtype strain AAE1 (B), considerable material adhered to the ASA1 (*ugtA*Δ) hyphal surface during growth in liquid medium (D). Bar in A = 100 nm, for A-D.

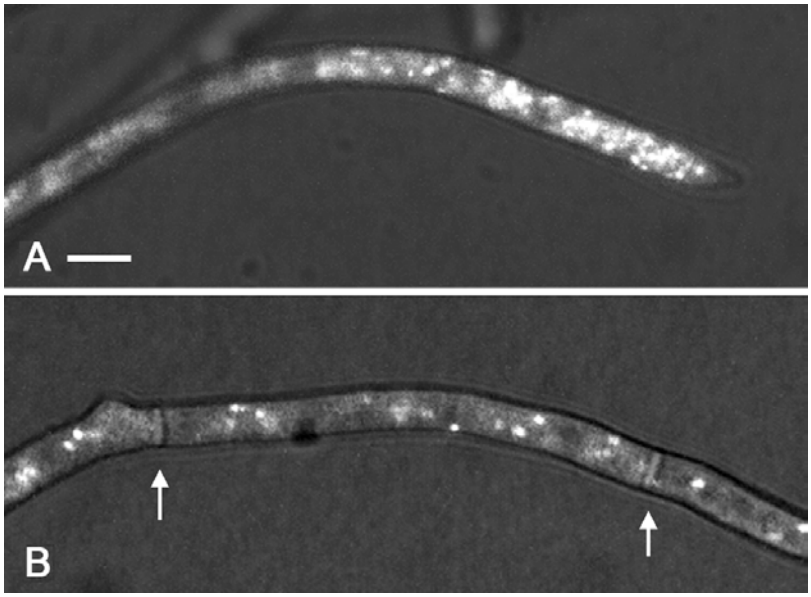

Figure 5. Localization of UgtA-GFP in (a) tip and (b) basal hyphal regions. Showing punctate patterns more abundant at the hypha tip, these are consistent with fungal Golgi equivalents. These images are merge of fluorescent and transmitted light. Septa, arrows in b. Bar in a = 5 μm, for a and b.

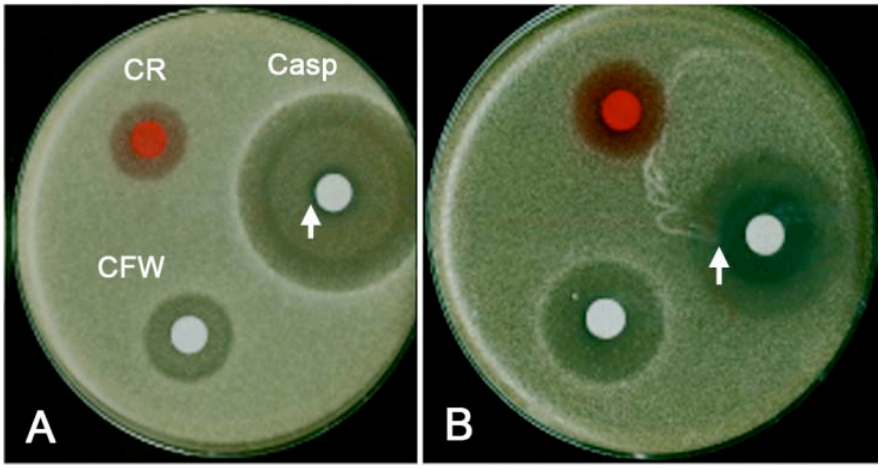

Figure 6. Sensitivity of wild type (A) and *ugtA*Δ (B) to antifungal agents. CR, Congo Red; CFW, Calcofluor White; Casp, Caspofungin. End point is zone of inhibition radius (zone with no visible growth, indicated by arrow).

Supplemental Table A. Strains, plasmids and primers used in this study

Strains	
A1149[a]	*pyrG89*; *pyroA4*; *nkuA*:: *argB*
AAE1[b]	*pyrG89*:: Nc*pyr4*$^{+}$; *pyroA4*; *nkuA*::*argB*
AAE2 (*ugmA*Δ)[b]	AN3112::Af*pyrG*; *pyrG89*; *pyroA4*; *nkuA* :: *argB*
ASA1 (*ugtA*Δ)[c]	AN3113::Af*pyrG*; *pyrG89*; *pyroA4*; *nkuA* :: *argB*
ASA2 (UgtA-GFP)[c]	AN3113-GA5-GFP-Af*pyrG; pyrG89; pyroA4; nkuA:: argB*
ASA3 (*ugtA*Δ:Af*glfB*)[c]	AN3113::Af*pyrG*: Af*glfB*; *pyrG89*; *pyroA4*; *nkuA*::*argB*
Plasmids	
pAO18 [a]	S-TAG, Af*pyrG*, Kan^{R}
pFNO3 [a]	GA5-GFP+ *AfpyrG*, Kan^{R}
pCR4-TOPO [d]	Kan^{R}, amp^{R}
pAf*glfB* [e]	pYEScupFLAGK amp^{R}
Primers (5' → 3')	
***ugtA* Deletion:**	
SA1, up ugtA F[c]	AAATAATATCTGCTTCGACCCACA
SA2, up ugtA pyrG, R[c]	AATTGCGACTTGGACGACATTTTGAGAGCGCGAGCTTG
SA3, dn ugtA pyrG, F[c]	GAGTATGCGGCAAGTCATGAATCAACCTTCGTGAGCAGTTTT
SA4, dn ugtA R[c]	TGCGCGACACTCCAAAT
SA5, Fus ugtA F[c]	ATAGTGACAATAATTTTCTCCAGAGAA
SA6, Fus ugtA R[c]	TATGCAGTTCTGCACTCCTATTC
Confirmatory PCR:	
Ame8, MidpyrG, R[b]	CACATCCGACTGCACTTCC
SA1, up ugtA F[c]	AAATAATATCTGCTTCGACCCACA
SA4, dn ugtA R[c]	TGCGCGACACTCCAAAT
SA7, ugtA amplif F[c]	ATGAGCAGCTCCGAAGAGAA
SA8, ugtA amplif R[c]	CTCCAGCGCCTGCACCAGCTCCAGCATTGCAGTACTGGCA
SA72 AfglfB F [c]	ATGAGTAACGAAGGAGAAAAAGCC
SA73 AfglfB R [c]	TTACGCATTCCCAGCAG T T
ugtA-GFP Tagging:	
Ame 27 tag cassette F [b]	GGAGCTGGTGCAGGC
Ame 28 tag cassette R [b]	TCATGACTTGCCGCATACT
SA43, ugtA amplif F[c]	TTGATCTGCGGTAACGTTACAT
SA36, ugtA amplif R[c]	GGCCTGCACCAGCTCCAGCATTGCCAGTACTGGCA
SA37, dn ugtA pyrG, F[c]	GAGTATGCGGCAAGTCATGAATCAACCTTCGTGAGCAGTTTT
SA4, dn ugtA R [c]	AGTATGCGGCAAGTCATGAATCAACCTTCGTGAGCAGTTTT
SA44, ugtA-GFP fus F[c]	AATGCTCAAGGTACGGACG
SA12, ugtA-GFP fus R[c]	TGCAGTTCTGCACTCCTATTC
***ugtA* cDNA cloning:**	
SA30 ugtA cloning F[c]	ATGAGCAGCTCCGAAGAGAA
SA31 ugtA cloning R[c]	TTAAGCATTGCCAGTACTGGC

a Fungal Genetics Stock Center, www.fgsc.net
b El-Ganiny et al. (2008)
c This study
d Invitrogen
e Engel et al. (2009)

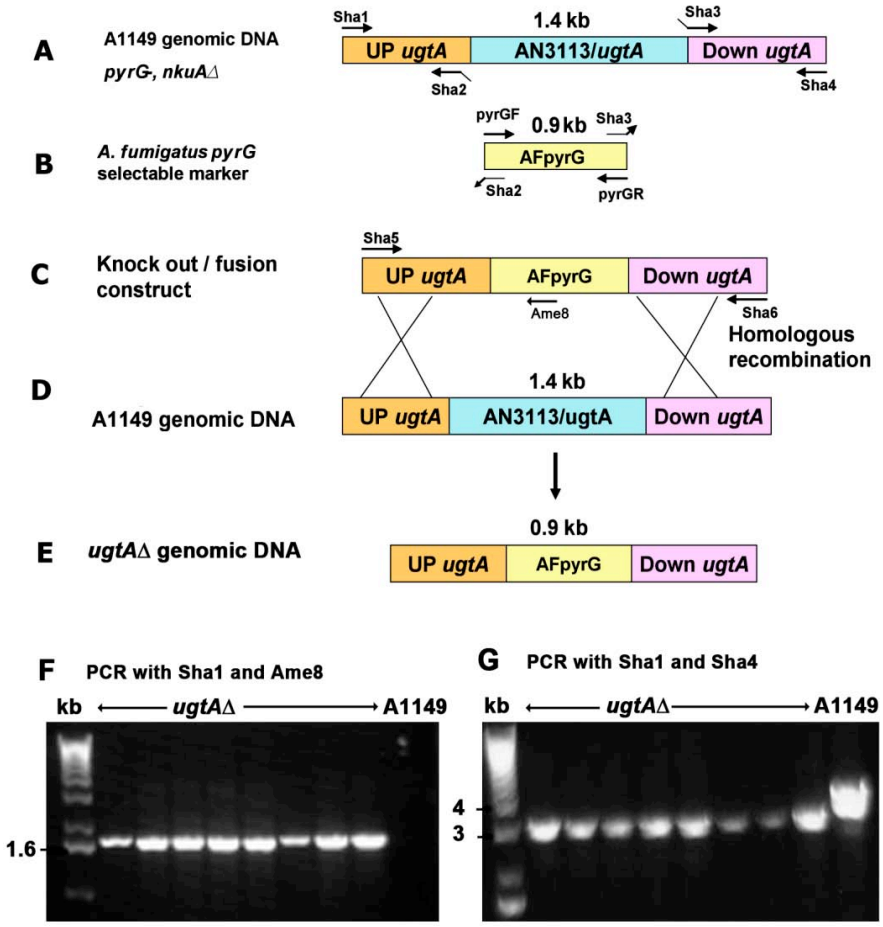

Supplemental Figure A. Strategy (A-E) and confirmation PCR (F, G) for *Aspergillus nidulans ugtA* deletion. The deletion strategy has previously been described in El-Ganiny et al. (2008). In addition to growth of conidium-derived colonies on selective media, confirmation of A3113.1 (*ugtA*) deletion used genomic DNA templates isolated from the transformation parent strain A1149 and 8 putative *ugtA* deletion strains (*ugtA*Δ). Primer binding sites are shown in A and B.

a.

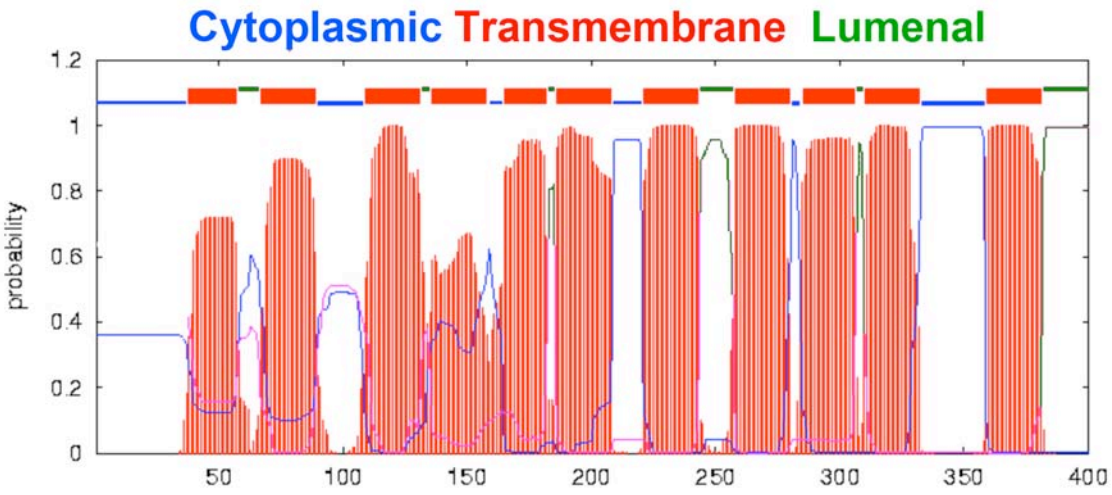

b.

Cytoplasmic Transmembrane Lumenal

```
MSSSEEKVRTSGEVSRPEPTLPTVNPAVDKPEPPKPTFHPAVYVTSWIAL     50
SSSVILFNKHILDYAQFRFPIILTTWHLAFATFMTQVLARTTTLLDGRKT    100
VKMTGRVYLRAIVPIGLFFSLSLICGNVTYLYLSVAFIQMLKATTPVAVL    150
LATWGMGMAPVNLKVLTNVSVIVFGVIIASFGEIKFVFIGFLFQIAGIIF    200
EATRLVMVQRLLSSAEYKMDPLVSLYYFAPVCAVMNGVTALFLEVPTLTM    250
DHIYNVGVWTLLANAMVAFMLNVSVVFLIGKTSSLVMTLCGVLKDILLVV    300
ASMVIWNTPVTALQFFGYSIALIGLVYYKLGGDKIKEYTSQANRAWAEYG    350
ATHPAQRRFVIIGAALLSFFLLVGSMAPSYAPDSVANVKGMLGGASTGNA    400
```

Supplemental Figure B: *Aspergillus nidulans* UgtA *in silico* analysis.

a. Predicted hydropathy (TMHMM2.0).

b. UgtA amino acid sequence, colour-coded to correspond with the hydropathy analysis. Lumenal amino acids are anticipated to be within the Golgi equivalent. The highlighted lysine residues are predicted by Engel et al. (2009) to be important for *A. fumigatus* UgtA function.

```
1     ATGAGCAGCTCCGAAGAGAAAGTAAGAACCTCCGGCGAGGTCTCTCGCCCGGAACCTACT
61    CTGCCTACCGTCAACCCTGCCGTCGACAAGCCAGAACCCCCGAAGCCGACCTTCCACCCT
121   GCCGTCTATGTTACgtgagtcgaccccgatcctatgcaattcaagacgattgtactaaac
181   ccgcgatgatttcagTTCCTGGATTGCCCTGAGTTCAAGTGTTATCCTGTTCAACAAGCA
241   CATCCTTGACTATGCTCAGTTCCgtgagtccactttgctccgcaagctgcaggctgtcaa
301   ttgaagcgaacgaggctgacttcgattcggttcagGATTCCCTATCATCCTTACAACATG
361   GCATCTGGCGTTCGCGACTTTCATGACGCAGGTTCTCGCTCGCACTACAACCCTCCTTGA
421   CGGCCGCAAGACCGTCAAGATGACTGGTCGTGTCTACCTCCGCGCCATTGTCCCTATCGG
481   TCTCTTCTTCAGTCTGAGTTTGATCTGCGGTAACGTTACATACCTGTACCTAAGTGTTGC
541   ATTTATCCAAATGCTCAAGgtacggacggacctctgtttgggattcgatgtggcataaac
601   taataaccgctatttagGCCACCACTCCTGTTGCTGTTCTGCTTGCCACTTGGGGTATGG
661   GCATGGCACCCGTCAACCTCAAGGTTCTTACAAACGTCAGCGTCATTGTCTTCGGTGTCA
721   TCATCGCCTCTTTCGGTGAGATCAAGTTTGTCTTCATCGGTTTCCTCTTCCAGATTGCCG
781   GTATCATCTTCGAGGCCACCCGATTGGTCATGGTGCAGCGCCTGCTCAGCTCCGCGGAGT
841   ACAAGATGGACCCTCTTGTCTCCCTTTACTATTTCGCTCCGGTCTGCGCTGTCATGAACG
901   GTGTCACTGCTCTGTTCCTTGAGGTTCCTACCCTGACTATGGACCACATCTACAACGTCG
961   GCGTCTGGACTCTCCTGGCCAACGCCATGGTCGCCTTCATGCTGAACGTCTCCGTTGTCT
1021  TCCTGgtaggtaatctccattttgagtactctactgttgcctaacagtcaattatagATC
1081  GGAAAGACTTCTTCTTTGGTCATGACCCTTTGCGGTGTCCTTAAGGATATCCTTCTTGTT
1141  GTCGCCTCCATGGTCATCTGGAACACTCCTGTCACCGCCCTCCAGTTCTTCGGTTACTCG
1201  ATTGCCCTCATTGGTCTCGTCTACTACAAGCTCGGTGGCGACAAGATCAAGGAATACACC
1261  AGCCAGGCTAACCGTGCCTGGGCTGAATACGGTGCCACTCACCCCGCTCAGCGCCGCTTT
1321  GTGATCATTGGTGCTGCTCTCCTTAGCTTCTTCTTGCTCGTTGGCTCCATGGCACCCAGC
1381  TACGCTCCCGATTCCGTTGCCAACGTCAAGGGCATGCTTGGCGGTGCCAGTACTGGCAAT
1421  GCTTAA
```

Supplemental Figure C: EXON-intron structure of *ugtA*. The cDNA sequence (UPPER case) was amplified from strain A1149; introns from the gDNA (lower case) sequence are from the Broad Institute, strain A4, which confirmed by sequencing at PBI, Saskatoon.

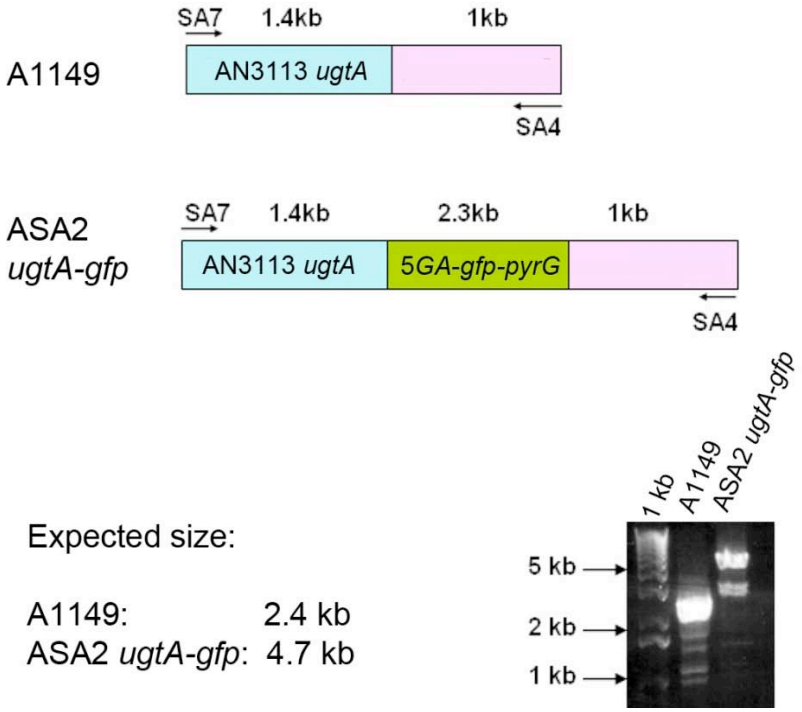

Supplemental Figure D: Confirmation of *ugtA-gfp* tagging. Using SA7 (ugtA F) and SA4 (down ugtA R) primers

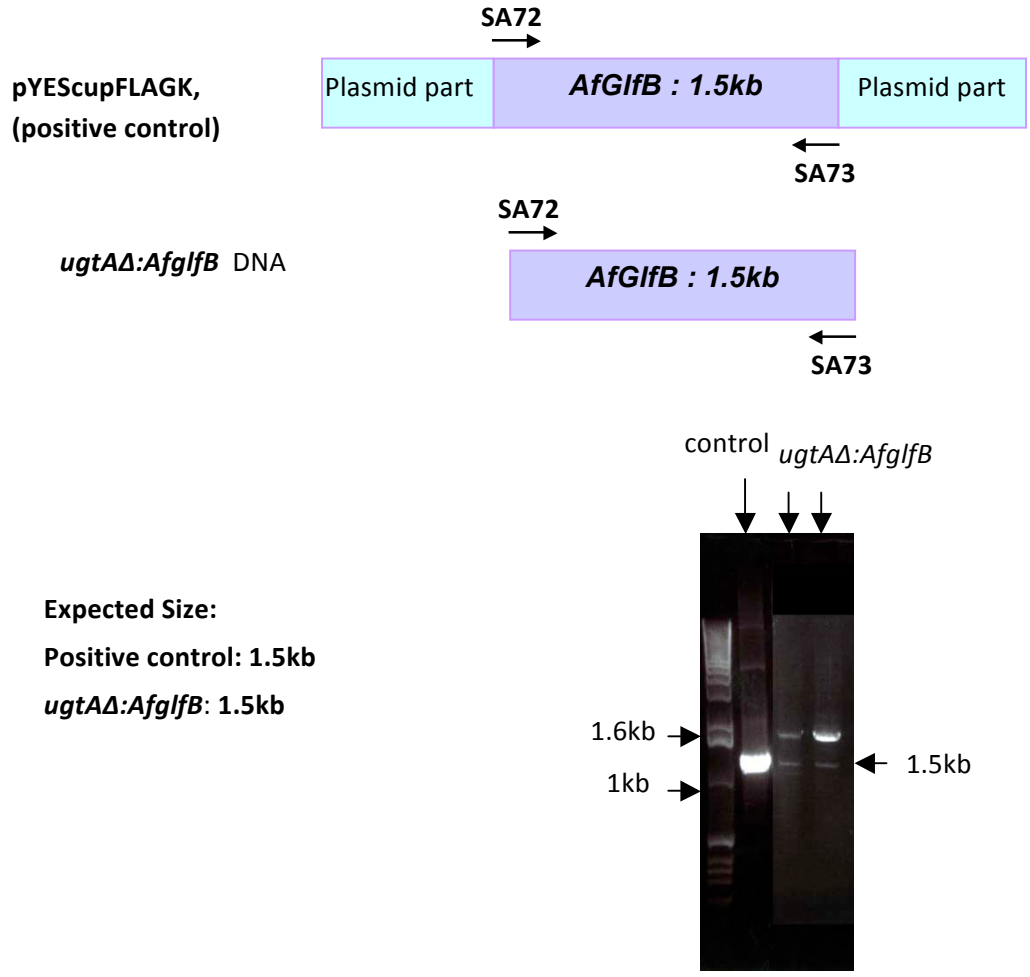

Supplemental Figure E: PCR confirming complementation of *ugtA*Δ with Af*glfB*. Using SA72 (AfglfB F) and SA73 (AfglfB R) primers.

Chapter 5

The importance of galactofuranose in *Aspergillus nidulans* hyphal wall surface characters

This chapter studied the effect of deletion of one or more of the Gal*f* biosynthesis genes on the cell wall surface characters in *A. nidulans*. This chapter was accepted for publication in Eukaryotic Cell 10(5), 646-653 as "Quantifying the importance of galactofuranose in *Aspergillus nidulans* hyphal wall surface organization by atomic force microscopy". **Paul, El-Ganiny, Abbas, Kaminskyj and Dahms, 2011.**

The objectives of the research in this chapter were

1) To determine the cell wall architecture of *A. nidulans* strains deleted for one or two of the Gal*f* biosynthesis genes
2) To investigate the effect of Gal*f* biosynthesis gene deletion strains on the organization and maturation of cell wall subunits, and their adhesion to hydrophilic surfaces.
3) To study the cell wall viscoelasticity and adhesion of Gal*f* biosynthesis gene deletion strain.

This work was based on some of the galactofuranose deletion strains that I generated during my PhD thesis project. I did all of the cell biological characterization of these strains, including confocal microscopy, and transmission electron microscopy. I also did the tagging and overexpression for UgeB. I was the direct supervisor of Mariam Abbas, who was a visiting summer student from Dahms lab in 2008. During that time I taught her how to grow and manipulate *Aspergillus* strains. Biplab Paul is an MSc student in the lab of Tanya Dahms, Mariam and Biplab did the AFM studies at the University of Regina, assisted by T Dahms for the statistical analysis. We supplied their lab with the strains, consumables and expertise for them to culture these for atomic force microscopy. I wrote the part of the manuscript which is related to the work I have done. Editing of the final manuscript was done by Dr. Kaminskyj and Dr. Dahms.

Quantifying the importance of galactofuranose in *Aspergillus nidulans* hyphal wall surface organization by atomic force microscopy.

Biplab C. Paul [a,d], Amira M. El-Ganiny [b,c,d], Mariam Abbas[a], Susan G. W. Kaminskyj [b,e], Tanya E. S. Dahms[*] [a,e]

[a] Department of Chemistry and Biochemistry, University of Regina, 6262 Wascana Parkway, Regina SK S2S 0A2, Canada.

[b] Department of Biology, University of Saskatchewan, 112 Science Place, Saskatoon SK S7N 5E2, Canada.

[c] Microbiology Department, Faculty of Pharmacy, Zagazig University, Egypt.

[d] Contributed equally to the research.

[e] Contributed equally to the writing.

[*] Author to whom correspondence should be addressed. Email: tanya.dahms@uregina.ca; Telephone: 1 306 585 4246

Abstract

The fungal wall mediates cell-environment interactions. Galactofuranose (Gal*f*), the five-member ring form of galactose, has a relatively low abundance in *Aspergillus* walls yet is important for fungal growth and fitness. *A. nidulans* strains deleted for Gal*f* biosynthesis enzymes UgeA (UDP-glucose-4-epimerase) and UgmA (UDP-galactopyranose mutase) lacked immunolocalizable Gal*f,* had growth and sporulation defects, and had abnormal wall architecture. We used atomic force microscopy and force spectroscopy to image and quantify cell wall viscoelasticity and surface adhesion of *ugeA*Δ and *ugmA*Δ strains. We compared them with a wild type (AAE1) and the *ugeB* deletion strain, which has wild type growth and sporulation. Our results suggest that UgeA and UgmA are important for cell wall surface subunit organization and wall viscoelasticity. The *ugeA*Δ and *ugmA*Δ strains had significantly larger surface subunits and lower cell wall viscoelastic moduli than those of AAE1 or *ugeB*Δ hyphae. Double deletion strains, [*ugeA*Δ, *ugeB*Δ] and [*ugeA*Δ, *ugmA*Δ], had more disorganized surface subunits than single deletion strains, and changes in wall surface structure correlated with changes in its viscoelastic modulus for both fixed and living hyphae. Wild type walls had the largest viscoelastic modulus, while those of the double deletion strains had the least. The *ugmA*Δ and particularly the [*ugeA*Δ, *ugmA*Δ] strains were more adhesive to hydrophilic surfaces than wild type, consistent with changes in wall viscoelasticity and surface organization. We propose that Gal*f* is necessary for full maturation of *A. nidulans* walls during hyphal extension.

1. Introduction

The fungal wall supports and shields the hyphal cytoplasm, and mediates interactions between the cell and its environment. Fungal walls are typically about 30 % of cell dry weight (7, 10), and a similar portion of the fungal genome is thought to contribute to cell wall biosynthesis and/or maintenance (11, 17). Fungal walls are composed of a variety of carbohydrate polymers (7, 11, 15), however, deleting many wall biosynthesis genes appears to be compensated by genetic redundancy and/or by induction of the cell wall integrity pathway (6, 7, 23).

The *Aspergillus* wall is reinforced by chitin fibrils, and has a matrix containing alpha- and beta-glucans, other sugars including galactomannans, and proteins. Galactofuranose (Gal*f*) is the five-member ring form of galactose that is found in the cell walls of *Aspergillus* (6, 7, 23), other fungi (reviewed in (15)), and certain other microbes (3). Deletion of UDP-galactopyranose mutase in several *Aspergillus* species has shown that Gal*f*, despite its relatively low abundance, is important for wild type fungal growth, cell morphogenesis, hyphal adhesion, wall architecture, and spore development (6, 8, 9, 14, 16, 25) and may mediate pathogenesis (1, 21-23).

The *A. nidulans* gene products UgeA (UDP-glucose-4-epimerase) (8), and UgmA (UDP-galactopyranose mutase) (9) catalyze sequential steps in Gal*f* biosynthesis (Figure 1). The *ugeA*Δ and *ugmA*Δ deletion strains have similarly compact colonies, aberrant hyphal growth and reduced sporulation. The hyphal walls of these strains differ from wild type and with each other as visualized using transmission electron microscopy (TEM) (8).

Atomic force microscopy (AFM) imaging uses a fine-tipped probe mounted on a flexible cantilever to raster scan the surface of an object generating a topographic map. An approach-retract cycle of the AFM probe, called force spectroscopy (FS), can be used to calculate the viscoelastic modulus of the whole organism or its cell surface, and surface adhesion. Previously we used AFM to show that *A. nidulans* cell walls of growing hyphal tips differ from those of mature regions (18), and to document changes associated with spore swelling, germination and the non-polarized hyphal growth of temperature sensitive mutants (19). Here, we compare the hyphal walls of wild type and a suite of Gal*f* biosynthesis pathway deletion strains using TEM, AFM and FS to gain a better understanding of the role played by Gal*f* in *Aspergillus nidulans* cell wall organization.

2. Materials and Methods

2.1 Strains and culture conditions

Aspergillus nidulans Escherichia coli strains were grown as described in (8, 9). Deletion strain construction followed procedures described in (8, 9) using *nkuA*Δ strains, plasmids and primers listed in supplemental Table SA. AN2951 (*ugeB*) was deleted from A1149 using Af*pyroA* as selectable marker (amplified from pTN1) to generate AAE9. Thereafter, *ugeA* was deleted from AAE9 using *AfpyrG* as selectable marker (amplified from pAO18) to create the [*ugeA*Δ, *ugeB*Δ] double deletion strain AAE10. Construction of AAE8 [*ugeA*Δ, *ugmA*Δ] was described in (8). All *Aspergillus nidulans* strains were cultured in either liquid or solid complete medium (CM), as described in (13).

One litre of CM contains 10 g D-glucose, 2 g peptone, 1 g yeast extract, 1 g casamino acids, 50 mL 20 x nitrate salts (formulation follows), 1 mL trace elements (formulation follows), and 1 mL of vitamin solution (formulation follows). The pH of the CM was adjusted to 6.5 with KOH solution. When required, CM was solidified with 18 g/L Bacto agar. One litre of the 20 x nitrate salts solution contains: 120 g $NaNO_3$, 10.4 g KCl, 10.4 g $MgSO_4 \cdot 7H_2O$, 30.4 g KH_2PO_4. One hundred millilitres of trace element solution contains: 2.2 g $ZnSO_4 \cdot 7H_2O$, 1.1 g H_3BO_3, 0.5 g $MnCl_2 \cdot 4\ H_2O$, 0.5 g $FeSO_4 \cdot 7\ H_2O$, 0.17 g $CoCl_2 \cdot 6\ H_2O$, 0.16 g $CuSO_4 \cdot 5\ H_2O$, 0.15 g $Na_2MoO_4 \cdot 2\ H_2O$, 5 g Na_4EDTA. The pH of the trace elements solution was adjusted to pH 6.5 with KOH. One hundred millilitres of vitamin solution contains: 100 mg each of biotin, pyridoxin, thiamine, riboflavin, p-aminobenzoic acid, nicotinic acid, and 2 drops of chloroform added as preservative. The vitamin solution was stored in a dark bottle, since riboflavin is light sensitive. The 20 x nitrate salts, trace elements, and vitamin solutions were autoclaved for 20 min at 121 °C, cooled to room temperature, then stored at 4 °C. For growth of *A. nidulans* auxotrophic strains (see Table SA), CM was supplemented with the appropriate nutrient as described in (13).

2.2. Confocal fluorescence and transmission electron microscopy (TEM)

Samples were prepared for light microscopy as described in (9). Briefly, freshly harvested spores were grown on coverslips for 16 h at 28 ºC in complete medium (CM) liquid, fixed and stained with Hoechst 33258 (for nuclei) Calcofluor (for cell walls), then imaged by

confocal microscopy. Hyphal width and basal cell length were measured at septal positions in mature regions (~ 40μm from the tip) for 50 cells per strain using LSM examiner.

For TEM, wild type and gene deletion strains were grown on dialysis tubing laid over complete medium agar for 1 d at 28 °C, then fixed, embedded, and sectioned for as described previously (9). Hyphal wall thickness was measured on TEM cross-sections of ten hyphae per strain, typically three measurements per hypha, at places where the cell membrane was crisply focussed.

2.3. Atomic force microscopy (AFM)

Samples for imaging fixed hyphae were prepared for AFM as previously described (18, 19). Briefly, conidia were germinated in liquid growth medium between two glass coverslips for 16 h. The top coverslip was carefully removed, and the hyphae were fixed with 3.7 % formaldehyde in 50 mM phosphate buffer, pH7.0, containing 0.2 % Triton X-100, followed by rinsing with distilled water and air drying. For live cell AFM imaging, hyphae were grown on dialysis tubing (Spectrapor, 12-14 kDa) overlaying agar medium. After 16 h growth, the dialysis tubing was transferred to a glass coverslip. Sterile Whatman #4 filter paper placed beneath the dialysis tubing was used to deliver liquid growth medium by capillary action, ~ 20 μL at a time.

An Explorer^{TM} AF microscope (Veeco http://www.veeco.com/) with a dry scanner (Veeco, model 5460-00) was used for contact mode imaging and force spectroscopy (FS), as previously described (18, 19). Hyphae were visualized by CCD camera (200 ×) and imaged first at low resolution (200 × 200 lines per scan). All topographic and lateral force data were collected from high-resolution images (500 × 500 lines per scan) of fixed and live (scan rate = 1 and 2 Hz, respectively) cells using Si_3N_4 probe tips (Veeco model #1520-00, k = 0.05 nN/nm, nominal resonance n = 17 kHz). Images represent typical results. AFM tip size and shape was calibrated using gold spheres according to (27).

2.4. Force spectroscopy (FS)

Cantilever spring constants, k_c, were determined prior to each force measurement using resonance frequencies according to (5). Tip-sample interaction was tracked by cantilever deflection as a function of Z piezo elongation during probe approach and retraction. For soft materials, meaningful FS comparisons often depend on the velocity of the surface approach (4).

In this case, the approach velocity did not significantly affect the hyphal spring constant (data not shown), but this parameter was kept constant (100 nm/s) to facilitate comparison of viscoelastic moduli between samples. Repeated measurements of individual sites on mature walls gave consistent values, and images obtained before and after FS were unchanged (data not shown), indicating that the walls were not damaged during data collection. Values were averaged from force curves collected in triplicate at ten separate points on the surface of mature hyphal walls (≥ 40 μm from the tip) for five hyphae per sample and typically three different samples.

Force approach curves measure the unit force (nN) required to indent a surface at a given distance (nm), so the slope corresponding to the b-c segment of the approach cycle (refer to Figure 5A) was used to examine the relative cell wall elasticity. FS data were plotted as deflection (nA) versus distance (nm), converted to force (nN) versus distance (nm) curves using the piezo sensor response, and the slope of the line b-c (m) in nN/m used to determine the spring constant k_w of the cell wall according to:

$$k_w = m_s k_c / m_h - m_s \quad (1)$$

where m_s is the sample slope and m_h is the slope for a hard surface (mica). The value of k_w was used for the subsequent determination of Young's modulus according to the equation (28):

$$E \sim 0.80\, k_w/h\, (R/h)^{1.5} \quad (2)$$

where E is the cell wall viscoelastic (Young's) modulus, R is the hyphal radius measured by either Confocal or AFM, and h is the thickness of the cell wall measured by TEM. Surface adhesion values were measured from the last segment of the retraction cycle (Figure 5A, segment e–f). If there is a chemical attraction between the sample and the Si_3N_4 AFM probe, which is hydrophilic, segment e–f will be a measure of its intensity in nN.

2.4. Data Processing and Analysis

AFM images were processed using horizontal levelling, with the maximal height adjusted for optimum contrast (SPMLab version 6.0 software, Veeco). Hyphal widths at mature regions

(~ 40 μm from the tip) and surface feature dimensions from topography and lateral force images were measured at the FWHM of the peak height. AFM data are presented as mean ± standard deviation or as ranges of values. TEM and confocal data are presented as mean ± standard error of the mean. Differences in the mean subunit sizes of wild type and deletion strain hyphae were tested by a one-way ANOVA (InStat 3, GraphPad Prism). Standard errors propagated through equations 1 and 2 were calculated for viscoelastic moduli, and a Student's *t*-test (two-tailed) was used to assess significant difference between values (InStat3, GraphPad Prism).

3. Results

Building on our previous experience using AFM to study *A. nidulans* hyphae (18, 19) we compared a suite of *A. nidulans* strains deleted for Gal*f* biosynthesis enzymes UgeA and UgmA, the near-isogenic wild type strain AAE1, a strain deleted for an epimerase (UgeB) that did not affect hyphal morphogenesis, and double deletion strains [*ugeA*Δ, *ugeB*Δ] and [*ugeA*Δ, *ugmA*Δ]. Double mutants were used to further explore the function of individual gene products. Even enzymes that mediate a known biochemical function may have collateral defects in a deletion strain based on protein-protein interactions, for example if the protein is part of a scaffold for a multi-enzyme.

3.1. Characterization of *Aspergillus nidulans ugeB*

Aspergillus nidulans ANID2951.4 (which we named UgeB) shares 38 % amino acid sequence identity with UgeA (8), and had been annotated as a UDP-glucose/galactose-4-epimerase (www.broadinstitute.org/annotation/genome/aspergillus_group/). The ugeB genomic sequence has a single exon that encodes a 428 amino acid peptide. The *ugeB* cDNA could not be amplified (three attempts), unlike *ugmA* (7) and *ugeA* (8). We deleted *ugeB* (Figure SA) as described in (9), and confirmed the deletion using PCR (Table SA, Figure SA). A [*ugeA*Δ, *ugeB*Δ] strain was generated and confirmed (Figure SB) as described in (8). The *ugmA*Δ strain was described in (9) and the *ugeA*Δ and [*ugeA*Δ, *ugmA*Δ] strains were described in (8). UgeB was expressed *in vitro* using the genomic sequence, which does not contain introns, purified, and shown to convert UDP-galactose into a product that is not UDP-glucose, following the procedure shown in (8, and data not shown). This unknown product awaits conclusive identification.

The *ugeB* sequence was put under the control of the *AlcA* promoter and also tagged with red fluorescent protein (El-Ganiny and Kaminskyj, *in preparation*), then over-expressed by culturing on CM containing 100 mM threonine (CMT). Under these conditions, p*AlcA-ugeB-rfp* was expressed, albeit weakly, in conidia and to a lesser extent in mature hyphae (Figure SC), but was not detectable in hyphal tips (data not shown).

3.2. Morphology of *Aspergillus nidulans* strains deleted for Gal*f* biosynthesis genes

Confocal microscopy images showing the hyphal morphology of the suite of *Galf* biosynthesis deletion strains examined in this study (AAE1, *ugeA*Δ, *ugeB*Δ, [*ugeA*Δ, *ugeB*Δ], *ugmA*Δ, [*ugeA*Δ, *ugmA*Δ]) are shown in Figure 2. Strain morphometry is described in Table 1. Unlike the previously described *ugeA*Δ and *ugmA*Δ deletion strains, which had wide and highly branched hyphae and reduced sporulation (8, 9), the *ugeB*Δ strain had wild type morphology hyphae and growth rate, and abundant sporulation (Table 1; Figure 2; data not shown). The [*ugeA*Δ, *ugeB*Δ] strain was viable when grown on media containing glucose as carbon source, but it did not form colonies on media containing galactose as the sole carbon source (due to *ugeA*Δ), and its hyphae were wide and branched like those of *ugeA*Δ (Table 1; Figure 2).

Transmission electron micrographs of hyphal cross-sections showed that the walls of *ugeA*Δ and *ugmA*Δ strains were two-fold and four-fold thicker, respectively, than those of AAE1 (Table 1, Figure 3) (8, 9). Given the general correlation between hyphal morphology and wall thickness (e.g. 8, 9, 11, 12, 20, 24), we expected that the hyphal wall thickness of *ugeB*Δ might be similar to AAE1. Instead, the *ugeB*Δ strain hyphal walls were almost two-fold thicker than AAE1 (Table 1, Figure 3). Also unexpectedly, the [*ugeA*Δ, *ugeB*Δ] strain hyphal walls were about twice as thick as either single deletion strain, even thicker than those of the [*ugeA*Δ, *ugmA*Δ] strain (Table 1, Figure 3).

TEM images of the *ugeA*Δ (Supplementary Figure **Cb in 8**) and *ugeB*Δ (data not shown) strains grown in liquid shake culture accumulated debris, not observed for the same strains grown on dialysis tubing (Figure 3) or for the [*ugeA*Δ, *ugeB*Δ] strain (data not shown).

3.3. Atomic force microscopy imaging of wild type and Gal*f* gene biosynthesis deletion strains

We used AFM imaging to acquire high-spatial resolution information about the hyphal wall surfaces of two wild type and four Gal*f* biosynthesis gene deletion strains. AFM imaging provides quantitative depth resolution, thus facilitating surface subunit measurements (18, 19). Our previous work demonstrated that for the wild type strain, A28, the walls of hyphal tips and tips of lateral branches had matured by 3 µm behind the apex, at which point their surfaces resembled unbranched regions 20 µm and 40 µm behind the tip (18). To ensure that wall surfaces were mature for all strains, we chose analysis sites that were at least 40 µm behind the hyphal tips, expecting that wall maturation might be slower in the Gal*f* biosynthesis gene deletion strains. AFM data can be collected from living or fixed cells (e.g. (18)). We present images of fixed hyphae for comparing wall surfaces amongst the suite of Gal*f* biosynthesis gene deletion strains, since hyphal wall subunit size and distribution were similar to living cells but were more clearly defined (18).

Contact mode AFM imaging simultaneously collects topography and lateral force information. The latter represents a convolution of topography and tip-sample interactions for rough samples, thus producing relief images with more clearly defined edge features (18). High resolution images of fixed wild type (AAE1) and Gal*f* biosynthesis gene deletion strain hyphae (Figure 4) show distinct differences in their surface subunit size (Table 1) and packing. AAE1 hyphae had small rounded subunits with a consistent size and even packing. In contrast, both the *ugeA*Δ and *ugmA*Δ strain hyphae had substantially larger and more variable-sized hyphal wall surface subunits than AAE1, and also had more disorganized subunit packing. The hyphal wall of the *ugeB*Δ strain most closely resembled that of AAE1, but with slightly elongated subunits. The [*ugeA*Δ, *ugeB*Δ] hyphal surface was notable in that its surface appeared fibrillar in the topographic images, hence maximum subunit sizes were not measured. Thus, both UgeA and UgeB appear to be important for wild type hyphal wall surface formation. The [*ugeA*Δ, *ugmA*Δ] strain hyphal wall surface subunits were similar in size to *ugmA*Δ. Taken together, each member of the suite of Gal*f* deletion strains produced a distinctive wall phenotype.

3.4. Cell wall viscoelasticity and adhesion of wild type and Gal*f* biosynthesis gene deletion strains

Viscoelasticity is the property describing materials such as hyphal walls, which exhibit both viscous (fluid-like) and elastic mechanical properties. Cell wall spring constants measured by FS (Figure 5A, segment b-c) were used to calculate their viscoelastic modulus for both fixed and live hyphae of AAE1 and the suite of Gal*f* gene deletion strains (Table 1). Cell wall viscoelastic moduli for the single deletion strains, UgeAΔ and UgeBΔ, were significantly lower than that of AAE1 (Table 1). Viscoelastic moduli of *ugmA*Δ and the double deletion strains [*ugeA*Δ, *ugeB*Δ] and [*ugeA*Δ, *ugmA*Δ] were at least an order of magnitude smaller than AAE1 (Table 1).

Notably, viscoelastic moduli of fixed hyphal walls were typically three-fold higher than that of live ones (Table 1). Hyphal wall viscoelasticity for the suite of Gal*f* deletion strains exhibited the same trend for fixed and live hyphae.

The Si_3N_4 AFM probes used in this study have hydrophilic surfaces. We used the e-f segment of the FS curve (Figure 5A) to quantify adhesion between *A. nidulans* wall surfaces and the AFM tip during the retraction phase. AAE1 wall surface adhesion to Si_3N_4 is shown in (Table 1). The *ugmA*Δ and [*ugeA*Δ, *ugmA*Δ] hyphae had significantly ($p < 0.05$) stronger adhesion to the hydrophilic tip than wild type hyphae.

4. Discussion

Our most notable finding is that perturbing *A. nidulans* cell wall maturation by deleting genes in the Gal*f* biosynthesis pathway, has profound effects on wall surface subunit size and packing that are directly associated with cell wall viscoelasticity. This is despite the fact that none of these genes is essential for growth in culture. Previously, we used AFM and FS to show for the first time that growing hyphal tips of a wild type *A. nidulans* strain, A28 (18), had wall surface characteristics that were consistent with long-accepted models of wall deposition and maturation (2, 26) that had yet to be quantitatively tested.

El-Ganiny et al. (8, 9) had shown using molecular biology, fluorescence microscopy and TEM that the *ugeA*Δ and *ugmA*Δ deletion strain hyphal morphogenetic defects appeared to be correlated with a lack of immunolocalizable wall Gal*f* and to aberrant hyphal wall architecture.

Now, we have used high spatial resolution AFM imaging and FS to directly quantify wall defects in this suite of Gal*f* biosynthesis gene deletion strains and to compare them to wild type strains.

4.1. Gal*f* is required for wild type *Aspergillus nidulans* hyphal wall formation

This AFM study is the first to make quantitative measurements of cell wall surface subunit features, wall viscoelasticity and adhesive properties of *A. nidulans* strains that had been deleted for enzymes having roles in Gal*f* biosynthesis. Strong but circumstantial data in El-Ganiny et al (9) showed that *A. nidulans* strains lacking UgmA had defective hyphal morphogenesis, colony growth, and spore development deficits that correlated with lack of immunodetectable wall Gal*f*. Using TEM cross sections, El-Ganiny et al (9) showed that hyphal walls of the *ugmA*Δ strain were more than four times the thickness of AAE1 and had poorly consolidated surfaces suggesting that Gal*f* may play a role in wall organization.

Previously, we showed using AFM imaging that growing tips of wild type *A. nidulans* had ellipsoidal surface subunits that were larger and more variable in size than the round subunits found 3 μm or further back (Fig 3. in 18). Consistent with the decrease in subunit size and improved organization as a function of maturation, we showed an increase in surface hydrophobicity (Fig. 6D in 18) attributed to decreased exposure of sugar hydroxyl groups. El-Ganiny's study (9) suggested that the *ugmA*Δ strain walls were weaker than wild type since this phenotype was partially remediated by growth on 1 M sucrose.

Our present study shows that both *ugeA*Δ and *ugmA*Δ strains had substantially larger surface subunits than AAE1. In contrast, the *ugeB*Δ strains, which had wild type colony phenotype and growth rate, had subunit sizes very similar to AAE1. Thus, it appears that *A. nidulans* surface subunit size is inversely correlated with cell wall maturation in A28 (18) and a suite of deletion mutants in the Gal*f* biosynthetic pathway. Our data also show that wall surface organization correlates with wall viscoelastic moduli, and that these data are mirrored by the thickness and surface layer characteristics visualized in hyphal cross sections using TEM.

Viscoelastic moduli of fixed and living cell walls had a strong positive correlation, demonstrating the value of comparing fixed strains, thus reducing data collection time. The viscoelastic moduli of fixed hyphal walls were consistently larger, revealing the relationship between chemical cross-linking of the cell wall and its viscoelasticity. The data offer insight into

the enzymatic cross-linking of hyphal wall components as an integral step in wall maturation, where cross-linking likely contributes to wall integrity by increasing viscoelasticity.

The A4 (28), A28 (18) and AAE1 (current work) are morphological wild type strains. The cell wall viscoelastic modulus of the fixed AEE1 strain was lower than that determined for fixed, rehydrated A4 by Zhao and coworkers (28). Although both studies used the same method to determine cantilever spring constants (5), it is only an estimate and can account for the difference in viscoelastic moduli. The viscoelastic modulus of live AEE1 cell walls (Table 1) was lower than that reported previously for A28 (115 ± 31 MPa; 18). However, since the latter study compared viscoelastic moduli in different regions along single hyphae, cantilevers were not calibrated.

We used Zhao's model (18), which assumes the indentation of a contiguous layer (cell wall) surrounding a large cylinder (hyphae; Figure 5B), to calculate cell wall viscoelastic moduli. A plot of the dimensionless unit Eh/k_w versus $(R/h)^{1.5}$ (data not shown) suggests this model fits AEE1, *ugeA*Δ and *ugeB*Δ strains, better than it does the poorly ordered walls of the *ugmA*Δ, [*ugeA*Δ *ugeB*Δ] and [*ugeA*Δ *ugmA*Δ] strains. Differences can at least in part be attributed to the composition and organization of cell wall components (Figure 5B), whereas viscoelastic moduli for *ugmA*Δ, [*ugeA*Δ *ugeB*Δ] and [*ugeA*Δ *ugmA*Δ] strains suggests the AFM tip may penetrate the loosely packed cell wall surface. The Si_3N_4 AFM tips used in this study have tips that are about 5 nm wide (18). The subunits of the *ugmA*Δ and [*ugeA*Δ *ugmA*Δ] strains are 20-fold larger (Table 1), so the AFM tip could possibly pierce an individual subunit. The surface of the [*ugeA*Δ *ugeB*Δ] strain has a fibrillar appearance (Figure 5C), so its interaction with the AFM tip could be unlike the other deletion strains we studied.

4.2. Gal*f* appears to mediate *Aspergillus nidulans* hyphal wall surface and hyphal adhesion

Lamarre et al (14) suggested that hyphal wall Gal*f* plays a role in *A. fumigatus* hyphal wall surface properties, which they showed qualitatively by the accumulation of material on *Afugm1Δ* hyphal walls using SEM, and by hyphal adhesion to substrates including glass and plastic coverslips, latex beads and epithelial respiratory cells.

We quantified the adhesion between the hydrophilic Si_3N_4 AFM tip and walls of living AAE1, *ugmA*Δ and [*ugeA*Δ, *ugmA*Δ] hyphae. The increasing hyphal wall surface disorder in

*ugmA*Δ and [*ugeA*Δ, *ugmA*Δ] strains correlates with effects on hyphal wall viscoelasticity and adhesion. The loose packing of hyphal walls surfaces observed by AFM imaging of Gal*f* mutants would expose polar groups normally masked during wall maturation, increasing hydrophilic character of the wall surface and resulting in greater adhesion. Consistent with Lamarre et al (14) the *ugmA*Δ and [*ugeA*Δ, *ugmA*Δ] strains tended to adhere to microscope coverslips compared to AAE1 and *ugeB*Δ (data not shown). Adhesion values between the Si_3N_4 tip and *ugmA*Δ and [*ugeA*Δ, *ugmA*Δ] walls were comparable to those previously reported for A28 hyphae at growing tips, where the wall is newly deposited and not yet mature (~ 9 nN, (18)). Thus, surface subunit size, wall viscoelasticity, and wall adhesion to hydrophilic surfaces show consistent trends for wild type and Gal*f* gene deletion strains.

Schmalhorst et al. (23) provided data to suggest that the *A. fumigatus glfA*Δ (homologous to *A. nidulans ugmA* (9)) strain had attenuated virulence in a murine model for systemic aspergillosis. However, scanning electron microscopy of cross-fractured *glfA*Δ hyphal walls were half the thickness of wild type *A. fumigatus* walls, the opposite trend to our study that deserves further attention.

By combining gene deletion characterizations with TEM, AFM, and FS, we have shown that Gal*f* is important for *Aspergillus* hyphal wall maturation. However, despite the strong correlation between our results and those of Lamarre et al (14) we are not yet able to determine the likely location(s) of Gal*f*-containing molecules in *Aspergillus* walls. Indeed, Latgé's 2010 model (16) discusses these molecules without indicating many details relating to their deployment in the three-dimensional wall architecture.

We have shown that perturbing wildtype Gal*f* cell wall deposition has substantial effects on the surface ultrastructure and viscoelasticity of the *Apergillus nidulans* cell wall. Gal*f* appears to have crucial and multiple roles in *Aspergillus* hyphal cell wall maturation and integrity. Studies addressing potential roles of mannose in *A. nidulans* wall structure and adhesive properties, and potential roles of Gal*f* in pathogenicity are underway.

Acknowledgements

This research was supported by Natural Science and Engineering Research Council of Canada Discovery grants to TESD and SGWK, a Canadian Institutes of Health Research/Regional Partnership Program grant to SGWK, and by an Egyptian Ministry of Higher

Education grant to AME. BCP was partially supported by the Department of Chemistry and Biochemistry in the Faculty of Science, University of Regina.

References

1. **Bar-Peled, M., C. L. Griffith, J. J. Ory, and T. L. Doering.** 2004. Biosynthesis of UDP-GlcA, a key metabolite for capsular polysaccharide synthesis in the pathogenic fungus *Cryptococcus neoformans*. Biochem. J. **381:**131-136. doi: 10.1042/BJ20031075.
2. **Bartnicki-Garcia, S., C. E. Bracker, G. Gierz, R. Lopez-Franco, and H. Lu.** 2000. Mapping the growth of fungal hyphae: orthogonal cell wall expansion during tip growth and the role of turgor. Biophys. J. **79:**2382-2390. doi: 10.1016/S0006-3495(00)76483-6.
3. **Beverley, S. M., K. L. Owens, M. Showalter, C. L. Griffith, T. L. Doering, V. C. Jones, and M. R. McNeil.** 2005. Eukaryotic UDP-galactopyranose mutase (*GLF* gene) in microbial and metazoal pathogens. Eukaryot. Cell. **4:**1147-1154. doi: 10.1128/EC.4.6.1147-1154.2005.
4. **Cappella, B., and G. Dietler.** 1999. Force-distance curves by atomic force microscopy. Surf Sci Rep. **34:**5-104.
5. **Cleveland, J. P., and S. Manne.** 1993. A nondestructive method for determining the spring constant of cantilevers for scanning probe microscopy. Rev Sci Instrum. **64:**403-405.
6. **Damveld, R. A.** 2008. A novel screening method for cell wall mutants in *Aspergillus niger* identifies UDP-galactopyranose mutase as an important protein in fungal cell wall biosynthesis. Genetics. **178:**873.
7. **de Groot, P. W., B. W. Brandt, H. Horiuchi, A. F. Ram, C. G. de Koster, and F. M. Klis.** 2009. Comprehensive genomic analysis of cell wall genes in *Aspergillus nidulans*. Fungal Genet. Biol. **46 Suppl 1:**S72-81.
8. **El-Ganiny, A. M., I. Sheoran, D. A. Sanders, and S. G. Kaminskyj.** 2010. *Aspergillus nidulans* UDP-glucose-4-epimerase UgeA has multiple roles in wall architecture, hyphal morphogenesis, and asexual development. Fungal Genet. Biol. **47:**629-635. doi: 10.1016/j.fgb.2010.03.002.
9. **El-Ganiny, A. M., D. A. R. Sanders, and S. G. W. Kaminskyj.** 2008. *Aspergillus nidulans* UDP-galactopyranose mutase, encoded by *ugmA* plays key roles in colony growth, hyphal

morphogensis, and conidiation. Fungal Genetics and Biology. **45:**1533-1542. doi: DOI: 10.1016/j.fgb.2008.09.008.

10. **Gastebois, A.** 2009. *Aspergillus fumigatus*: cell wall polysaccharides, their biosynthesis and organization. Future Microbiology. **4:**583.
11. **Harris, S. D.** 2009. Morphology and development in *Aspergillus nidulans*: a complex puzzle. Fungal Genetics and Biology. **46:**S82.
12. **Kaminskyj, S. G., and J. E. Hamer.** 1998. hyp loci control cell pattern formation in the vegetative mycelium of *Aspergillus nidulans*. Genetics. **148:**669-680.
13. **Kaminskyj, S. G. W.** 2001. Fundamentals of growth, storage, genetics and microscopy of *Aspergillus nidulans*. Fungal Genet. Newsl. 25.
14. **Lamarre, C., Beau, R., Balloy, V., Fontaine, T., Hoi, J. W. S., Guadagnini, S., Berkova, N., Chignard, M., Beauvais, A., and J.-P. Latgé.** 2009. Galactofuranose attenuates cellular adhesion of *Aspergillus fumigatus*. Cell. Microbiol. **11:**1612.
15. **Latgé, J.-P.** 2009. Galactofuranose containing molecules in *Aspergillus fumigatus*. Med. Mycol. **47 Suppl 1:**S104-9. doi: 10.1080/13693780802258832.
16. **Latgé, J.-P.** 2010. Tasting the fungal cell wall. Cell. Microbiol. **12:**863-872. doi: 10.1111/j.1462-5822.2010.01474.x.
17. **Lesage, G., and H. Bussey.** 2006. Cell wall assembly in *Saccharomyces cerevisiae*. Microbiol Mol Biol Rev. **70:**317-343.
18. **Ma, H., L. A. Snook, S. G. Kaminskyj, and T. E. S. Dahms.** 2005. Surface ultrastructure and elasticity in growing tips and mature regions of *Aspergillus* hyphae describe wall maturation. Microbiology. **151:**3679-3688. doi: 10.1099/mic.0.28328-0.
19. **Ma, H., L. A. Snook, C. Tian, S. G. Kaminskyj, and T. E. S. Dahms.** 2006. Fungal surface remodelling visualized by atomic force microscopy. Mycol. Res. **110:**879-886. doi: 10.1016/j.mycres.2006.06.010.
20. **Momany, M., P. J. Westfall, and G. Abramowsky.** 1999. *Aspergillus nidulans* swo mutants show defects in polarity establishment, polarity maintenance and hyphal morphogenesis. Genetics. **151:**557-567.
21. **Moyrand, F.** 2008. UGE1 and UGE2 regulation of the UDP-glucose/UDP-galactose equilibrium in *Cryptococcus neoformans*. Eukaryotic Cell. **7:**2069.

22. **Perfect, J. R.** 2005. Nuances of new anti-*Aspergillus* antifungals. Med. Mycol. **43 Suppl 1:**S271-6.

23. **Schmalhorst, P. S., S. Krappmann, W. Vervecken, M. Rohde, M. Muller, G. H. Braus, R. Contreras, A. Braun, H. Bakker, and F. H. Routier.** 2008. Contribution of galactofuranose to the virulence of the opportunistic pathogen *Aspergillus fumigatus*. Eukaryot. Cell. **7:**1268-1277. doi: 10.1128/EC.00109-08.

24. **Shi, X., Y. Sha, and S. Kaminskyj.** 2004. *Aspergillus nidulans* hypA regulates morphogenesis through the secretion pathway. Fungal Genet. Biol. **41:**75-88.

25. **Wallis, G. L., F. W. Hemming, and J. F. Peberdy.** 2001. Beta-galactofuranoside glycoconjugates on conidia and conidiophores of *Aspergillus niger*. FEMS Microbiol. Lett. **201:**21-27.

26. **Wessels, J. G.** 1999. Fungi in their own right. Fungal Genet. Biol. **27:**134-145. doi: 10.1006/fgbi.1999.1125.

27. **Xu, S., and M. F. Arnsdorf.** 1994. Calibration of the scanning (atomic) force microscope with gold particles. J. Microsc. **173:**199-210.

28. **Zhao, L., D. Schaefer, H. Xu, S. J. Modi, W. R. LaCourse, and M. R. Marten.** 2005. Elastic properties of the cell wall of *Aspergillus nidulans* studied with atomic force microscopy. Biotechnol. Prog. **21:**292-299.

Table 1. Morphological characteristics, maximum dimension of surface subunits, and cell wall viscoelastic moduli of wild type and Gal*f* biosynthesis enzyme gene deletion strains.

Strain	Hyphal width[a] (µm) ± SE	Wall thickness[b] (nm) ± SE	Subunit maximum dimension (nm) ± SD	Viscoelastic moduli of fixed hyphal wall (MPa)[c] ± SD	Viscoelastic moduli of live hyphal wall (MPa)[c] ± SD	Adhesion (nN) ± SD
Wild type (AAE1)	2.4 ± 0.0	54 ± 2	35 ± 5	211 ± 15	82.3 ± 12.9	5.7 ± 1.6
***ugeA*Δ**	3.6 ± 0.1	104 ± 10	63 ± 10	99 ± 48	24.6 ± 13.7	ND
***ugeB*Δ**	2.5 ± 0.0	95 ± 11	39 ± 8	74 ± 22	22.5 ± 8.6	ND
***ugeA*Δ, *ugeB*Δ**	3.5 ± 0.1	217 ± 62	ND[d]	38 ± 21	9.8 ± 5.1	ND
***ugmA*Δ**	3.1 ± 0.1	204 ± 10	108 ± 35	14± 2	3.1 ± 0.4	8.1 ± 0.3
***ugeA*Δ, *ugmA*Δ**	3.2 ± 0.4	162 ± 8	97 ± 23	0.05 ± 0.02	0.03 ± 0.01	17.3 ± 3.9

[a] There was no significant difference in hyphal width for fixed or live hyphae measured either by confocal microscopy or AFM

[b] Measured from TEM hyphal cross-sections. See Materials and Methods section.

[c] SD was calculated from errors propagated through equations 1 and 2. See Materials and Methods section.

[d] Not determined. See Results section.

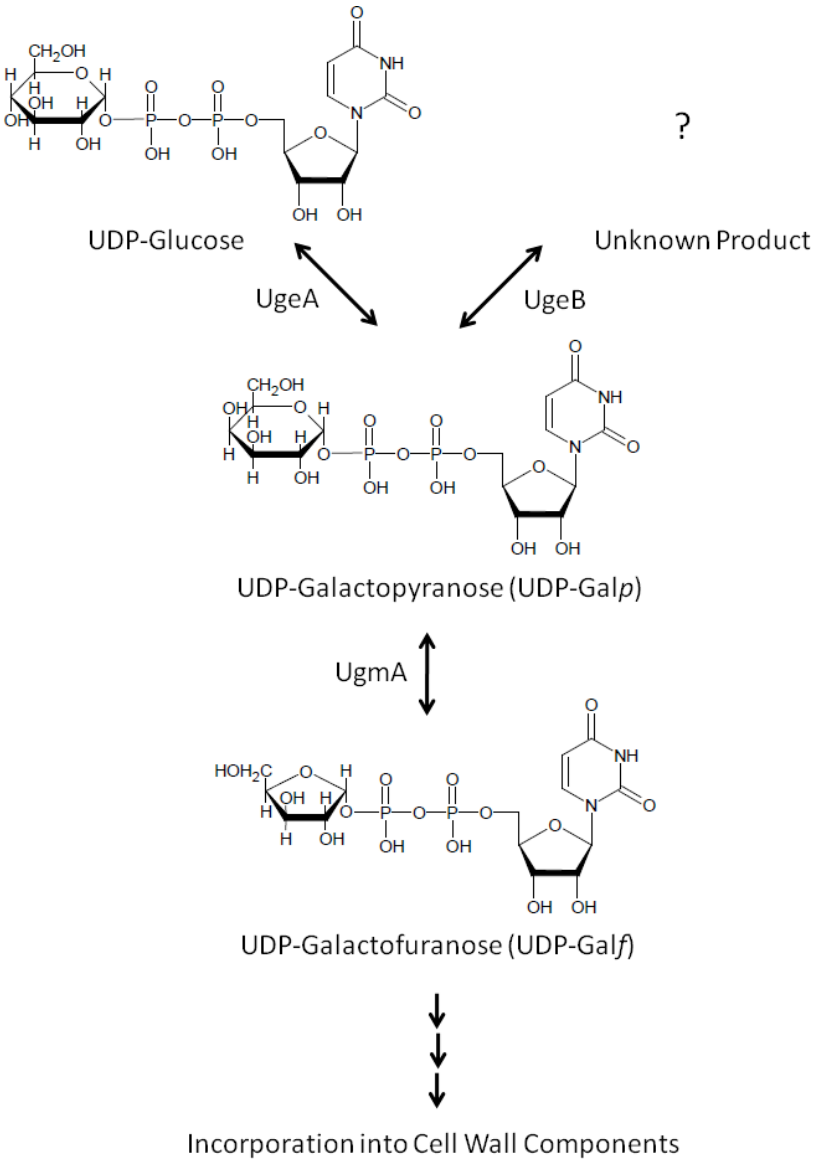

Figure 1: Biosynthesis of Gal*f* from UDP-Glucose. UDP-glucose is converted to UDP-galactopyranose by UDP-glucose 4-epimerase (UgeA). In the reaction shown, UDP-galactopyranose is converted to the final product UDP-galactofuranose by UDP-galactopyranose mutase (UgmA). These two enzymes are localized in the cytoplasm, and then UDP-galactofuranose is transported to the fungal Golgi equivalent, which is the site of incorporation into other cell wall components.

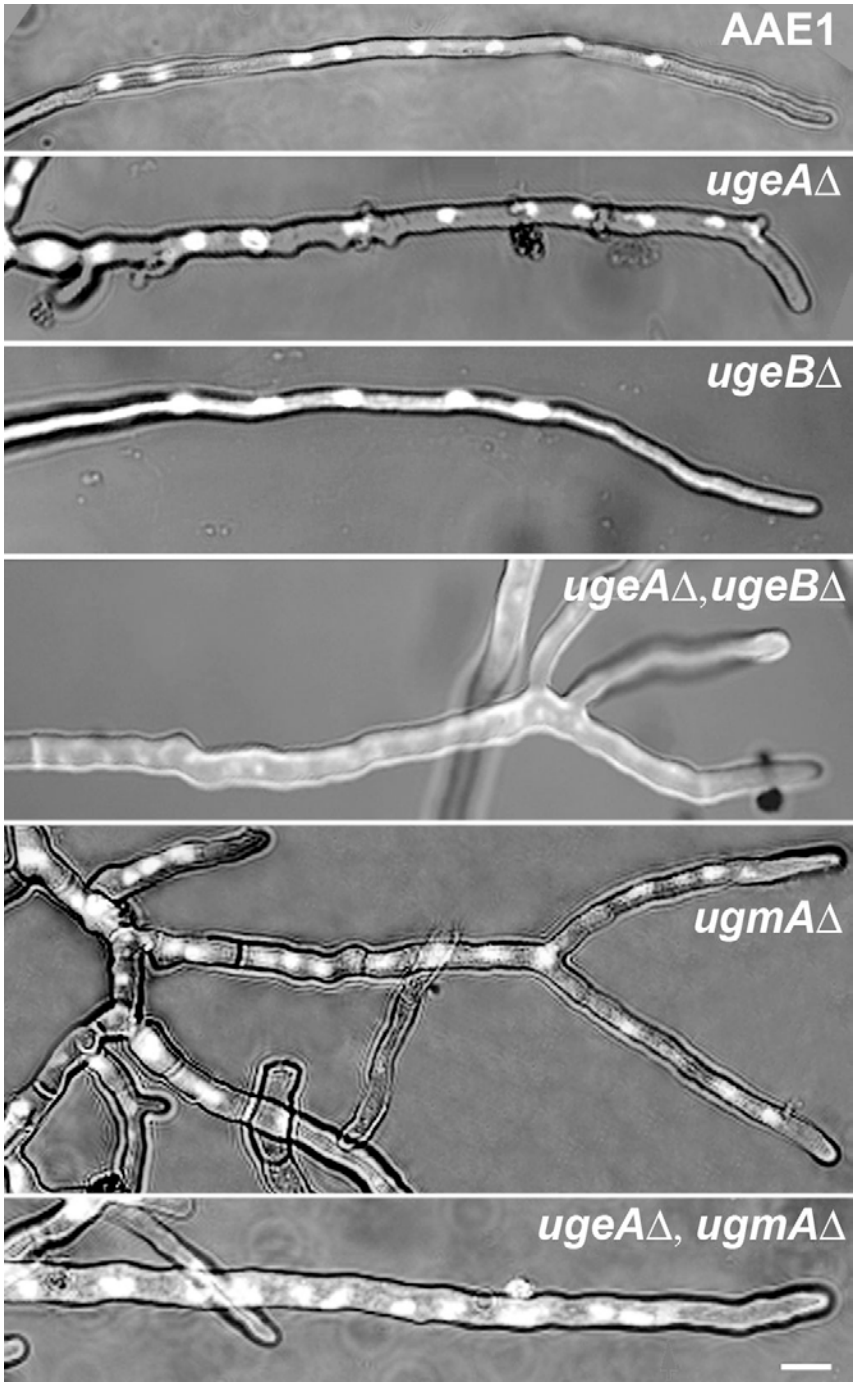

Figure 2. Appearance of the wild type and Gal*f*-biosynthesis deletion strain hyphae use in this study. Strains were grown for 16 h, then fixed and stained with Hoechst 33258 to visualize nuclei. Images are combined fluorescence and transmitted light. Bar = 5 μm (for all images).

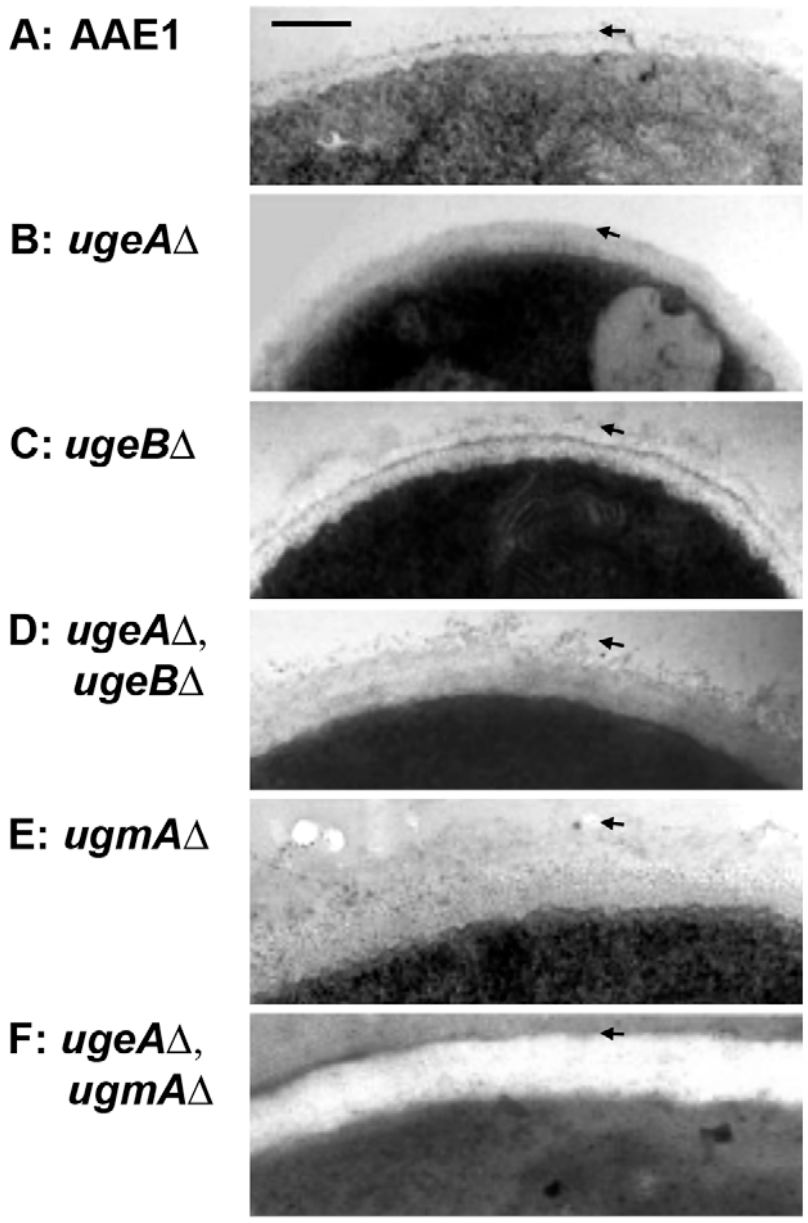

Figure 3. Transmission electron micrographs of hyphal wall cross-sections of AAE1 and Gal*f*-biosynthesis deletion strains used in this study. Bar = 100 nm (in A, wild type image, for all parts). Impressions regarding the relative hyphal diameter as assessed by curvature may be misleading, because some hyphal cross sections were not perpendicular to the hyphal axis. Images have been contrast adjusted to highlight wall structure; the cytoplasm is dark because wall carbohydrates stain poorly for TEM. Arrows indicate the outer boundaries of cell wall thickness measurements.

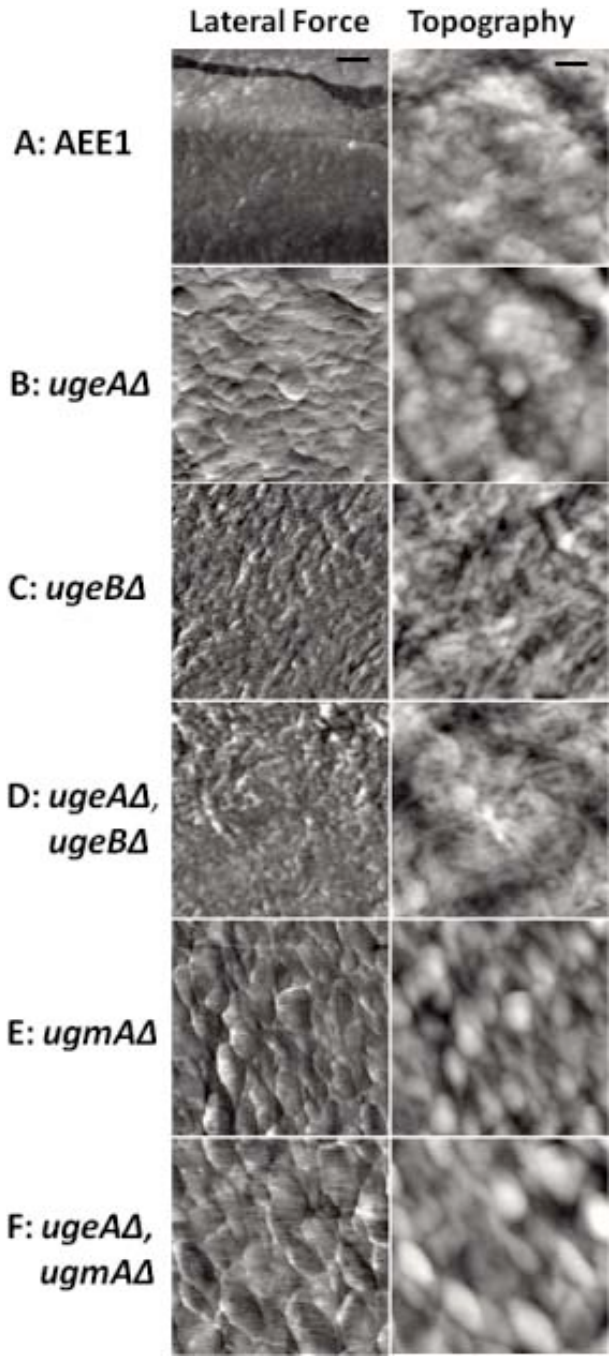

Figure 4: Atomic force microscopy images of wild type and Gal*f*-biosynthesis deletion strains used in this study. Grey scale for lateral force images is ~ 2 nA and for topography images ranges from 50-70 nm. Bar in A = 200 nm, and is valid for all images.

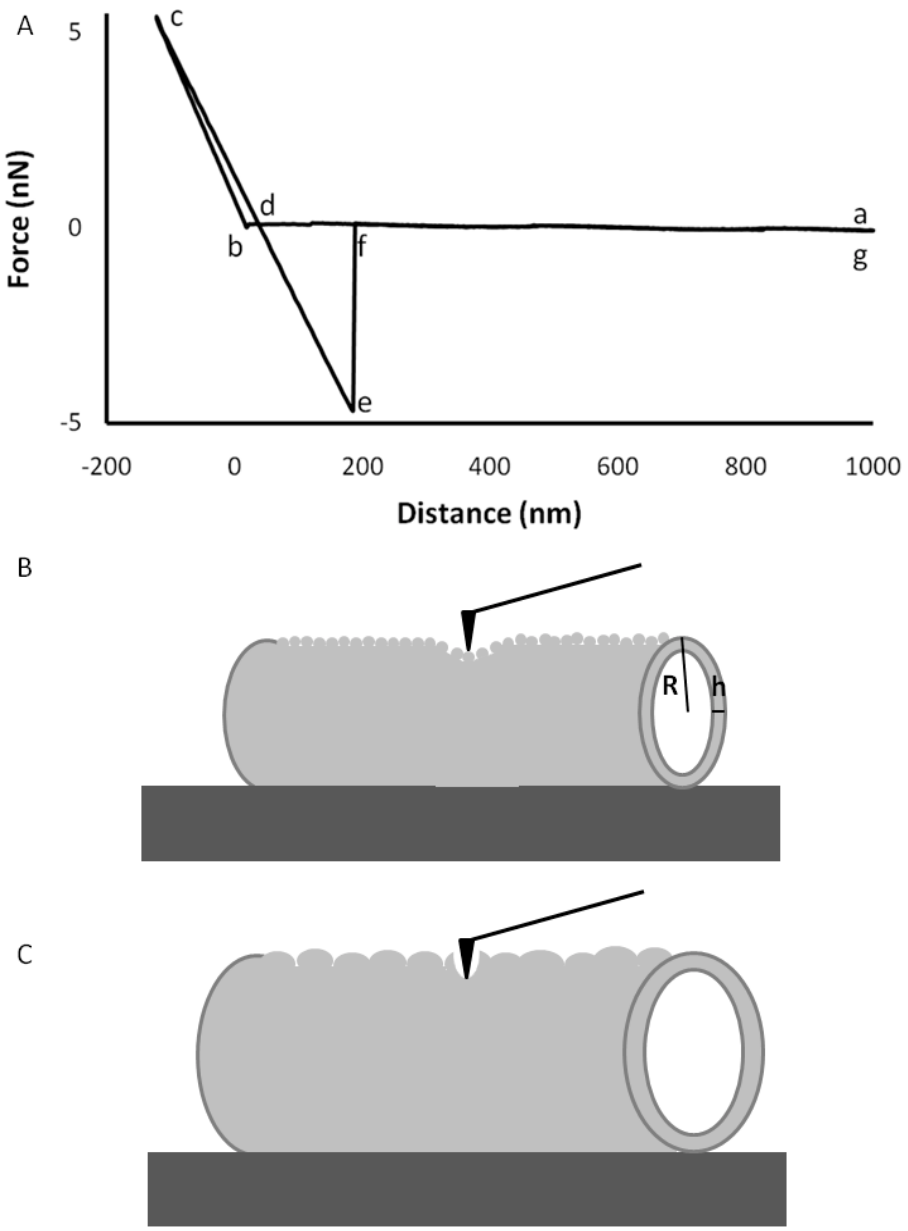

Figure 5: A) Representative force curve shows tip approach (a-c) with jump into contact (b) and tip retraction (c-g). The slope of b-c was used to calculate sample viscoelastic modulus and segment f-e represents tip-sample adhesion. Schematic representation of the AFM tip (black) interacting with the hyphal surface (grey) of B) AEE1, *ugeAΔ*, *ugeBΔ*, in which the entire cell wall is deformed by tip indentation, compared to that of C) *ugmAΔ*, [*ugeAΔ,ugeBΔ*] and [*ugeAΔ,ugmAΔ*] in which the tip likely deforms the loosely packed, larger individual subunits or penetrates the space between.

Supplemental materials:

Supplemental Table SA: Strains, plasmids and primers used in this study

Strains and plasmids

A1149 (wild type)[a]	*pyrG89; pyroA4; nkuA::argB*
AAE1 (wild type)[b]	*pyrG89::Ncpyr4+; pyroA4; nkuA::argB*
AAE2 (*ugmA*Δ) [b]	AN3112::*AfpyrG; pyrG89; pyroA4; nkuA::argB*
AAE5 (*ugeA*Δ) [c]	AN4727::*AfpyrG; pyrG89; pyroA4, nkuA::argB*
AAE8 (*ugeA*Δ, *ugmA*Δ)[c]	AN4727::Af*pyrG*; AN3112::Af*pyroA*; *pyrG89*; *pyroA4*; *nkuA*::*argB*
AAE9 (*ugeB*Δ) [d]	AN2951::*AfpyroA*, *pyrG89*; *pyroA4*; *nkuA*::*argB*
AAE10 (*ugeA*Δ, *ugeB*Δ) [d]	AN4727::*AfpyrG*; AN2951::*AfpyroA*; *pyrG89*; *pyroA4*, *nkuA*::*argB*
pAO18 [a]	S-TAG, AfpyrG, Kan^R
pTN1 [a]	AfpyroA, Amp^R

Primers	5' → 3'	
***ugeB* deletion**		
Ame 9	PyroA F	ATGGCTTCCAACGGTACCA
Ame 10	PyroA R	TTACCATCCTCTCTTGGCCA
Ame 71	upugeB F	GAGCAGGGTACACATAGAGAGGG
Ame 72	upugeB R	TGGTACCGTTGGAAGCCATTGTTGATGGCACTTCAAACAAG
Ame 75	down ugeB F	TGGCCAAGAGAGGATGGTAATGCTGTTAAAAACTGAGCCCG
Ame 76	down ugeB R	GTCCACATTAAAGCTTCTGAGTCCA
Ame 80	ugeBd fus F	TAGTTGAATGACAGAGATCGGTCC
Ame 81	ugeBd fus R	CTCTACCAGCACTGCATCTGAA
Confirmation PCR		
Ame 8	Mid pyrG F	CACATCCGACTGCACTTCC
Ame 16	Mid pyroA R	TCAACAACATCTCCGGTACC
Ame 41	up ugeA F	CTCCTATGGTATGTCTCTTCCAACTT

a Fungal Genetics Stock Center www.fgsc.net.

b El-Ganiny et al. (2008).

c El-Ganiny et al. (2010).

d This study.

A

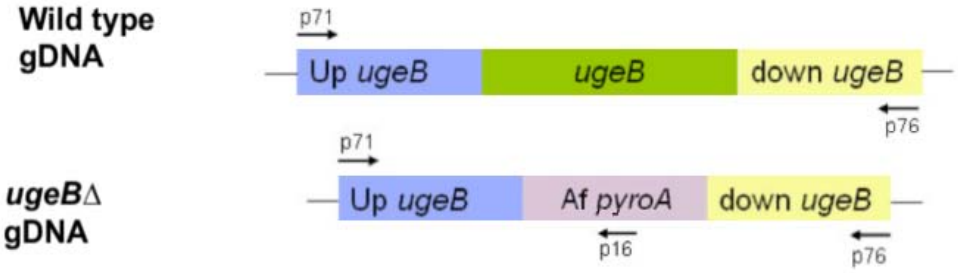

Expected band size (kb)

	p71 & p76	p71 & p16
Wild type	3.3	No band
*ugeB*Δ	2.9	1.5

B

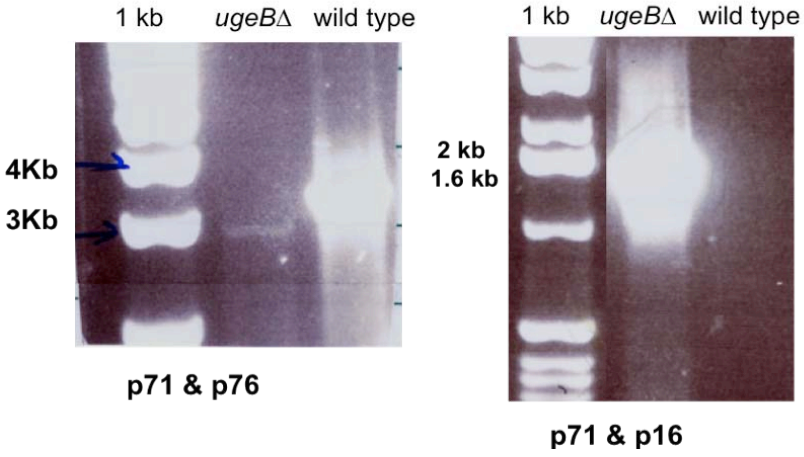

Supplemental Figure SA. Confirmatory PCR for *ugeB*Δ strain

A) Cartoons of wild type (A1149) and *ugeB*Δ (AAE9) genomic DNA, and primer binding sites. Expected amplicon sizes for combinations of genomic DNA template and primer pairs.

B) Agarose gels showing the expected amplicon sizes for these template-primer combinations.

A

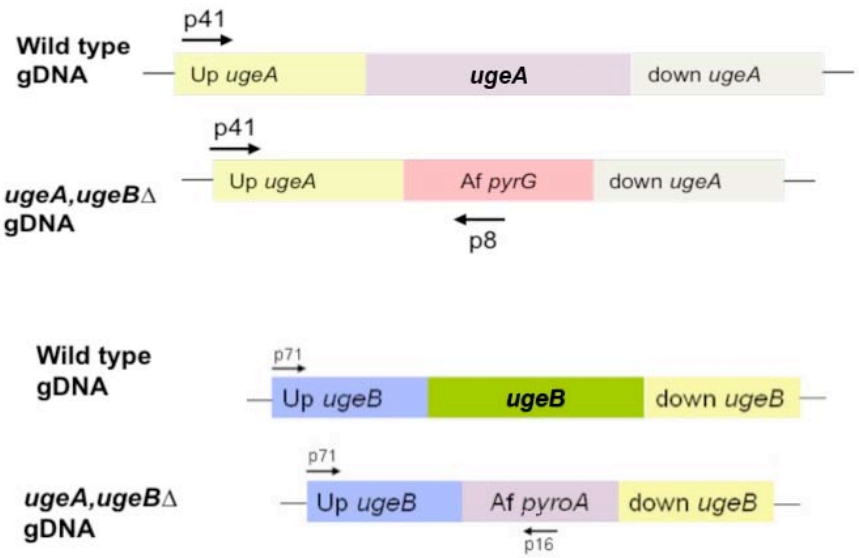

B

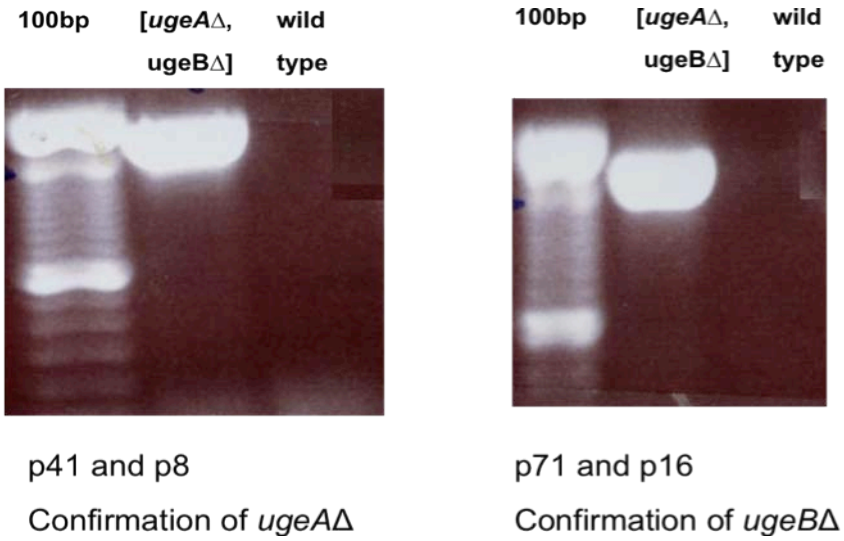

Supplemental Figure SB. Confirmatory PCR for [*ugeA*Δ, *ugeB*Δ] strain

A) Cartoons of wild type and [*ugeA*Δ, *ugeB*Δ] (AAE10) genomic DNA at the *ugeA* and *ugeB* loci, and primer binding sites. For each locus, PCR with wild type template and primers specific for the selectable marker (p8, p16) is not expected to amplify a product.

B) Agarose gels showing the expected amplicon sizes for these template-primer combinations.

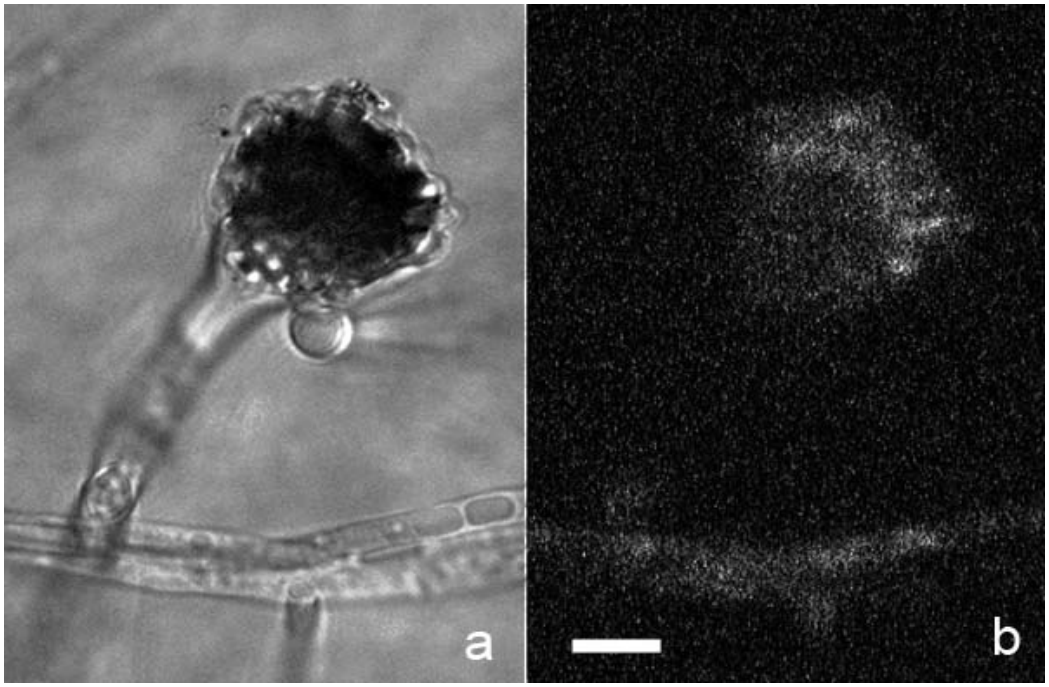

Supplemental Figure SC. Localization of *Aspergillus nidulans ugeB*, Gene expression is under the control of *alcA(*p*)*, which is strongly induced by growth on CM containing 100 mM threonine (CMT). The p*AlcA-ugeB-rfp* fluorescence was imaged using confocal microscopy (a and b are transmitted and fluorescence images respectively). Bar = 10 µm.

Chapter 6

Exploring the Goldilocks effect: effects of changing the level of expression of *Aspergillus nidulans* UDP-galactopyranose mutase

In the previous chapters we used gene deletion strategy to study the biological function of Gal*f* biosynthesis enzymes. In this chapter we are using promoter exchange strategy to investigate the effect of changing the level of expression of Gal*f* biosynthesis enzymes on drug sensitivity and morphogenesis of *Aspergillus nidulans*. This chapter will be submitted for publication as "Exploring the Goldilocks effect: level of expression of Gal*f* biosynthesis enzymes affects antifungal drug sensitivity as well as hyphal and colony morphogenesis in *Aspergillus nidulans*". **El-Ganiny, Sanders and Kaminskyj, *in preparation***

The objectives of the research in this chapter are

1) To study the effects of *ugmA* repression and overexpression on colony and hyphal morphogenesis of *A. nidulans* (Goldilocks effect)
2) To assess the sensitivity of *alcA*(p)-*ugmA* strains and *ugmAΔ* towards commercially available antifungal drugs.

In this chapter I did all the experimental design, the practical work and data analysis. I wrote the first draft of the paper (current version) which will be edited by my supervisor Dr. Kaminskyj after submission according to the reviewer comments.

Exploring the Goldilocks effect: level of expression of Gal*f* biosynthesis enzymes affects antifungal drug sensitivity as well as hyphal morphogenesis in *Aspergillus nidulans*.

Amira M. El-Ganiny [a b], David A.R. Sanders [c], and Susan G.W. Kaminskyj [a d]

[a] Department of Biology, University of Saskatchewan, 112 Science Place, Saskatoon SK S7N 5E2, Canada.

[b] Department of Microbiology, Faculty of Pharmacy, Zagazig University, Egypt.

[c] Department of Chemistry, University of Saskatchewan, 110 Science Place, Saskatoon SK Canada S7N 5C9

[d] Author to whom correspondence should be addressed. Email: susan.kaminskyj@usask.ca Telephone: 1 (306) 966 4422.

Key words: *Aspergillus nidulans*, galactofuranose, UDP-galactopyranose mutase, *alcA* promoter, sporulation, hyphal morphometry, drug sensitivity.

Abbreviations: *alcA*p, promoter of alcohol dehydrogenas I; AmB, Amphotericin B; CM, complete media (1% glucose); CM3G, complete media with 3% glucose; CMT, complete media with 100 mM threonine; CMFT, complete media with 100mM threonine and 0.1% fructose; Gal*f*, galactofuranose; Gal*p*, galactopyranose; qRT-PCR, quantitative real time polymerase chain reaction; SEM, scanning electron microscopy; TEM, transmission electron microscopy; UDP, uridine diphosphate, UgmA, UDP-galctopyranose mutase;

Abstract

The fungal cell wall is essential for the fungus and absent from humans. Galactofuranose (Gal*f*) is about 5 % of the *Aspergillus fumigatus* cell wall carbohydrate, where it decorates certain carbohydrates and lipids. In systemic aspergillosis, Gal*f* has been shown to be a virulence determinant. Previously, we characterized genes in the *A. nidulans* Gal*f* biosynthesis pathway, and showed that Af*glfA* and Af*glfB* were functionally homologous to their *A. nidulans* counterparts *ugmA* and *ugtA* respectively. Gene deletions of those and another member of this pathway; *ugeA* caused substantially reduced growth and sporulation. As part of our ongoing program to assess members of the Gal*f* biosynthesis pathway as targets for antifungal drug development, we generated conditional *A. nidulans* strains using the alcohol dehydrogenase promoter *alcA*(p), qRT-PCR was used to select the suitable media for induction and repression of *ugmA*. We characterized our *alcA*(p)-*ugmA* strain under overexpression and repression conditions using fluorescence microscopy and SEM. As expected, repression of *ugmA* phenocopied the knockout strains. Although *ugmA* overexpression colonies had wild type morphology and sporulation, the hyphae of *alcA*(p)-*ugmA* strain hyphae was wide and highly branched. These results showed that decreasing or increasing *ugmA* expression perturbed several aspects of *A. nidulans* growth and that balanced expression of *ugmA* is required to have a wild type phenotype, which we called the Goldilocks effect. We examined the sensitivity of the *alcA*(p)-*ugmA* strain under repression and overexpression conditions towards four commercially available antifungals in different drug classes: polyenes, azoles, allylamines and echinocandins. Our data showed that overexpression of *ugmA* caused slight decrease in sensitivity to terbinafine (allylamine), whereas its repression increased the sensitivity to caspofungin (echinocandin), and amphotericin B (polyene), but not the other drug classes. Drugs that target Gal*f*–biosynthesis (once developed) could be useful in combination with some other antifungals to improve antifungal therapy.

1. Introduction

Human invasive fungal infections are increasing dramatically due to many reasons including: the improved medical technology leading to increase in the number of immunosuppressed patients and the overuse of antibacterial antibiotics. *Aspergillus* species are second only to *Candida species* as a cause of systemic fungal infections (Erjavec et al., 2009).

Systemic fungal infections are a significant cause of morbidity and mortality despite treatment (Lass-Florl, 2009). Treatment of these infections is challenging because fungi are eukaryotes and hence they share many biochemical pathways with mammals. Echinocandins are the only antifungal drugs that inhibit an aspect of fungal wall synthesis, β-1,3-glucan synthesis (Espinel-Ingroff, 2009). There is a pressing need to develop additional antifungals (Mircus et al., 2009) particularly against different aspects of fungal physiology. We are exploring new targets in the fungal cell wall.

The cell wall is essential for fungal growth. It protects the cell from external damage and stress, and mediates the interaction between the fungus and its environment. If the cell wall is removed or weakened, the fungal cell cannot survive in natural environments (Aimanianda and Latgé, 2010). About 90% of the fungal cell wall is composed of polysaccharides that are not found in human hosts (Latge, 2007). Galactofuranose (Gal*f*) is the five-membered ring form of galactose that is found in the cell wall of many microorganisms including fungi but not in mammals. Gal*f* residues form the side chains of many glycoconjugates including galactomannan; an indicator of invasive aspergillosis. Gal*f* is essential for the virulence of protozoa and fungi including *Aspergillus fumigatus* (Schmalhorst et al., 2008). Because Gal*f* is both a cell wall component and plays a role in virulence, Gal*f* metabolism is thought to be a promising target for drug development (Pedersen and Turco, 2003). New antifungal strategies are focusing on reducing virulence of the pathogen and minimizing its harm to the host rather than killing the pathogen (Gauwerky et al., 2009).

UDP-galactopyranose mutase (UGM) is a key enzyme in Gal*f* biosynthesis. UGM catalyzes the synthesis of UDP-galactofuranose (UDP-Gal*f*) from UDP-galactopyranose (UDP-Gal*p*). UGM is encoded by a single gene in both *Aspergillus nidulans* and *A. fumigatus* (*ugmA*/*glfA)* (El-Ganiny et al., 2008; Schmalhorst et al 2008). Although gene deletion studies showed that *UGM* was not essential for survival *in vitro*, loss of UGM was shown to result in

loss of virulence of *A. fumigatus* (Schmalhorst et al., 2008). El-Ganiny et al. (2008) also showed that *A. fumigatus* and *A. nidulans* UGM genes were functionally homologous.

A complementary approach to study gene function is the use of conditional gene expression strains, where the endogenous promoter is replaced by regulatable promoter to control gene expression (Ichinomiya et al., 2002). In *A. nidulans* the alcohol dehydrogenase promoter *alcA*(p) has been used to study the function of many genes. Generally, *alcA*(p) is induced by alcohols, including threonine, and repressed by glucose (Romero et al., 2003; Tribus et al., 2010).

We generated a conditional *alcA*(p)-*ugmA* strain, and used it to study the effect of induction or repression of *ugmA* on morphogenesis of *A. nidulans,* and its sensitivity to antifungal drugs. Threonine was used for induction of *ugmA* and glucose was used for its repression. Expression levels were confirmed using qRT-PCR. The colony and hyphal characteristics of the *alcA*(p)-*ugmA* strain were studied using confocal microscopy and SEM. Our results showed that the colony characters and sporulation resemble the wild type under induction conditions and phenocopies the deletion mutants when *ugmA* is repressed. Unexpectedly the hyphae of *AlcAp-ugmA* strain were wide, highly branched with frequent septa under repression and induction conditions which is similar to *ugmA*Δ phenotype indicating that increasing *ugmA* concentration is not totally benign. Under gene repression conditions, the *alcA*(p)-*ugmA* strain was more sensitive to the wall targeting agent caspofungin and the cell membrane targeting agent amphotericin B. Our results suggest that Gal*f* biosynthesis is worth further exploration for antifungal chemotherapy, either alone or in combination with other antifungals.

2. Materials and methods

2.1. Strains, plasmids and culture conditions

Strains, primers and plasmids are listed in Table 1**.** *Aspergillus nidulans* strains were grown on complete media (CM) with required nutritional supplements as described previously (Kaminskyj, 2001). CM was modified as follows to manipulate *alcA*(p)-*ugmA* expression: Maximum repression used CM containing 3% glucose (CM3G). Induction of *alcA*(p)-*ugmA* used CM lacking glucose but containing 100 mM threonine (CMT). CM with 100 mM threonine and

0.1% fructose (CMFT) was used to give intermediate or near wild type expression of *ugmA* in the *alcA*(p)-*ugmA* strain.

2.2. Strain construction and confirmation

Protoplasting and transformation followed procedures in Osmani et al. (2006) and Szewczyk et al. (2007). Long-term storage of competent protoplasts is described in (El-Ganiny et al., 2010). The promoter exchange construct consists of *alcA* promoter plus Af*pyrG* as selectable marker which amplified from plasmid p*alcA*(p). This construct was inserted between the upstream of *ugmA* and the *ugmA* coding sequence using fusion PCR. The construct was transformed into A1149 protoplasts, so that Af*pyrG* would be under the control of *ugmA(*p*)* whereas *ugmA* would be under the control of *alcA*(p). Genomic DNA (gDNA) was isolated from putative strains and wild type and used as template for confirmatory PCR (CPCR). Supplemental figure 1 showed the results of CPCR using two different combinations of primers.

2.3. qRT-PCR

Wild type (AAE1) and *alcA*(p)-*ugmA* (AAE12) spores were inoculated on CMT, CMFT and CM3G media, and incubated at 28°C with shaking for 16 hr. The mycelia were collected by centrifugation, flash frozen in liquid nitrogen then lyophilized. Total RNA was extracted from lyophilized mycelia using an RNeasy plant Kit (Qiagen) following manufacturer instructions. RNA concentration was measured using a Nanodrop, and then diluted to 400-500 ng/µL. gDNA elimination and reverse transcription were done using a QuaniTect reverse transcription kit (Qiagen) following the manufacturer's instructions (Cuero et al., 2003).

Quantitative real time PCR (qRT-PCR) was performed in 96-well optical plates. Each run was assayed in triplicate, using total volume of 20 µL reactions containing cDNA at appropriate dilution and using SYBR green fluorescein (Qiagen), with no template control (NTC) for each gene. Actin was used as a reference gene (Bohle et al., 2007). Primers actF and actR (Table 1) were designed using Invitrogen OligoPerfect™ Designer tool. These primers were used to amplify regions containing one intron in the gene, producing a ~200 bp band from cDNA and a ~400 bp band from gDNA (to detect gDNA contamination). The primers ugmF and ugmR

(Table 1) were designed to amplify a 100 bp band. qRT-PCR amplification was done in IQ Cycler (Biorad) using the following PCR conditions: 95°C/15 min for one cycle, 95°C/15 s, 55°C/40 s and 72°C/30 s for 40 cycles and final extension cycle of 72°C/2 min. Melting curve analysis was done using the following cycle: 15 s at 65°C with increase 0.5°C each cycle till 95°C. The relative expression of *ugmA* were normalized to actin and calculated according to the ΔΔCt method (Livak and Schmittgen, 2001). Two independent biological replicates were performed for each strain/culture condition.

2.4. Colony growth and sporulation

The colony characters were examined as described in El-Ganiny et al. (2008). Briefly, wild type and *alcA*(p)-*ugmA* strains were streaked on CMT, CMFT and CM3G media and incubated for 3 d at 28°C to give isolated colonies (Figure 2). Diameter of these colonies were measured (10 colony/strain). The number of spores /colony were counted by selecting individual colonies that had grown in isolation from single spore, and dispensing spores of each colony in microfuge tube containing 1 mL water. A hemocytometer was used to count the number of spore / colony. Four colonies were assessed for each strain and medium combination; two samples were counted for each colony.

2.5. Microscopy: confocal and SEM

Samples prepared for confocal fluorescence microscopy as described in El-Ganiny et al. (2008). Freshly harvested spores were grown on coverslips at 28 ºC for 16 h in CM media with carbon sources as described above. Hyphae were fixed and stained with Hoechst 33258 (for nuclei) and Calcofluor (for cell walls). Samples were imaged using a Zeiss META510. LSM image browser software was used for the morphometeric analysis. Hyphal width (at septa) and basal cell length (distance between adjacent septa) were measured for 50 cells per strain, from two independent samples.

Scanning electron microscopy (SEM) was used to examine sporulating colonies following El-Ganiny et al. (2008). Wild type and *alcA*(p)-*ugmA* strains were grown on dialysis tubing laid on CM with defined carbon sources for 3 d at 28ºC. Colonies were fixed by immersion in 2 % glutaraldehyde, dehydrated in acetone, critical point dried (Polaron E3000,

Series II), and gold sputter coated (Edwards model S150B). Samples were imaged with a JEOL 840A scanning electron microscope.

2.6. Antifungal susceptibility testing

Antifungal agents and analytical grade solvents were obtained from the following manufacturers: amphotericin B, terbinafine, itraconazole, dimethyl sulphoxide (DMSO) (Sigma Chemicals, USA), ethanol (VWR) and caspofungin (Merck & Co., Inc. USA). These four antifungal drugs represent different antifungal drug classes. Stock solutions were prepared as follows: amphotericin B (20 mg/mL in DMSO), itraconazole (1.6 mg/mL in DMSO), terbinafine (1.6 mg/mL in 50% ethanol) and caspofungin (20mg/mL in sterile water). These stock solutions were aliquoted and stored at -80 ºC.

Wild type (AAE1) and *alcA*(p)-*ugmA* (AAE12) strains were grown under repression (CM3G) and induction (CMT) conditions; wild type and *ugmA*Δ (AAE2) strains were grown on CM. Spores collected from 4 day old plates, because *ugmA*Δ and *alcA*(p)-*ugmA* strains were delayed for sporulation. Spore suspensions were filtered through VWR 413 grade papers to move any hyphae or conidiophores, then counted by hemocytometer and adjusted to the same concentration.

Antifungal susceptibility testing was done by employing a disc diffusion method similar to that described in Kontoyiannis et al. (2003). Briefly, 1 x 10^7 spores were inoculated in 20 mL media (CMT or CM3G) and poured in Petri plates (9 cm diameter). After the medium had hardened, sterile ¼ inch (6mm) paper discs were placed on the agar surface. Antifungal drug stock solutions (described above) were micropipetted onto individual disks: 10 µL of terbinafine and itraconazole, or 20 µL of amphotericin B and caspofungin. The plates were incubated at 28 ºC and assessed after 48 h. The radius of the zone of inhibition in millimeters was quantified as: [diameter with no visible growth – disk diameter] / 2. Four biological replicates were assessed for each strain and medium combination, two measurements were taken for each disk on each plate, at orthogonal orientations. Solvent controls (DMSO and 50% ethanol) showed no zone of inhibition.

2.7. Data processing and analysis

Confocal images were processed using LSM examiner software, other images were processed using Adobe Photoshop 7.1. software. Statistical analysis used Graphpad prism 5 for analysis of variance.

3. Results

The alcohol dehydrogenase I promoter, *alcA*(p) has been used successfully to control the expression of many genes in *Aspergillus* (Romero et al., 2003; Tribus et al., 2010). Previously we deleted *A. nidulans ugmA* to explore its biological roles in morphogensis, conidiation, and wall ultrastructure of *Aspergillus nidulans* (El-Ganiny et al., 2008). In this study we explored the role of UgmA overexpression and repression on hyphal and colony morphogensis and on sensitivity to antifungals using a single strain (*alcAp-ugmA*) in which we can conditionally repress or overexpress *ugmA*. As Gal*f* is an important component of the cell wall, and its lack produces a distinctive colony phenotype and weaker cell walls (El-Ganiny et al., 2008; Paul et al., 2011) we expected that controlling *ugmA* expression would have a profound effect on colony and hyphal morphology. We further hypothesized that overexpression or repression *ugmA* would affect strain sensitivity to antifungal drugs especially the wall targeting agents.

3.1. Construction and validation of *alcAp-ugmA* strain

Fusion PCR was used to generate a construct that replaced the *ugmA* endogenous promoter with the conditional promoter *alcA(*p). Af*pyrG* was used as a selectable marker (Szewczyk et al., 2007). To confirm that the construct integrated at the *ugmA* locus, confirmatory PCR using two sets of primers was performed. Primers Ame1 (upstream F) and Ame23 (ugmA R) amplified 2.9 Kb band from wildtype and 5.2 Kb band from *alcA*(p)-*ugmA* strains. The primers Ame1 and Ame134 (midpromoter R) produced a 2.8 Kb band with *alcA*p-*ugmA* strains and no band with wild type gDNA as expected (Suppl. Figure A).

After promoter replacement, the *alcA*(p)-*ugmA* strain was grown on CM media with different carbon sources to select the most suitable media for overexpression and maximum repression of *ugmA*. Wild type and *alcA(*p)*-ugmA* were streaked on CM media containing

threonine, ethanol, fructose-threonine, glycerol or glucose as sole carbon sources, and on a mixture of carbon sources: YEPD (1% yeast extract, 2% peptone, 2% glucose/dextrose, 2% agar) medium (Zarrin et al., 2005). qRT-PCR was used to assess the ability of CMT, CMFT and CM3G media to induce or repress *ugmA* (Table 2 and Figure 1). We found that threonine containing medium (CMT) give the best induction of *ugmA,* showing more than 5 times increase in *ugmA* expression compared to wild type strain grown under the same conditions (Figure 1a), In comparison, fructose-threonine medium (CMFT) resulted in a slight decrease in *ugmA* expression (about 50% decrease than wild type), Medium with 3% glucose (CM3G) showed maximum repression of *ugmA*; about 100 times decrease in its expression (Figure 1b).

3.2. Repression of *ugmA* leads to compact colonial growth and reduced sporulation

In previous studies, glucose and threonine containing media have been used to repress or overexpress *alcA*(p)-regulated genes, respectively (Tribus et al., 2010). In this study, growing the *alcA*(p)-*ugmA* strain on CM3G (repression) media resulted in a decrease in colony size and in sporulation. On CM3G, the colony size of *alcA*(p)-*ugmA* strain was about 20% that of the wild type strain, and *alcA*(p)-*ugmA* sporulation was less than 2% that of wild type (Table 2 and Figure 2). SEM images showed that reduction in sporulation was due to both the decrease in the number of conidiophores and the aborted formation of some conidiophores (Figure 3). Thus, repression of *alcA*(p)-*ugmA* produced a colony phenotype that was general comparable to that of the *ugmA*Δ strain.

We have shown previously that deletion of *ugmA* had a greater effect on sporulation than its repression did in this study (El-Ganiny et al., 2008). To test whether this was related to growth on CMT or CM3G, wild type and *alcA*(p)-*ugmA* strains were grown on YEPD medium, which has been used by others to modulate expression of *alcA*(p)-regulated strains (Zarrin et al., 2005). Unexpectedly, although, the *alcA*(p)-*ugmA* strain colony and sporulation phenotype were substantially more similar to *ugmA* deletion, however on YEPD the sporulation of wild type strain was also greatly reduced (Suppl Figure B). We found that CMFT medium caused only a slight decrease in *ugmA* expression, and moderate effect on colony size and sporulation was noticed. Colony size of *alcA*(p)-*ugmA* was 2/3 that of wild type, whereas sporulation of *alcA(p)-ugmA* was about 40% of wild type grown on same media. Increasing expression of *ugmA* by

growing on CMT has minor effect on colony size which decreased by 25% and sporulation which has about 30% reduction compared to wild type (Table 2).

3.3. Both overexpression and repression of *ugmA* affect hyphal morphology

Previous work in our group showed that deletion of genes in Gal*f* biosynthesis pathway affect hyphal morphogenesis producing wide, uneven hyphae with increased branching and formation of septa (El-Ganiny et al., 2008; El-Ganiny et al., 2010; Paul et al., 2011; Afroz et al., accepted). In this study we expected that *ugmA* repression would produce hyphae that look similar to the *ugmA* deletion, whereas *ugmA* overexpression would give wild type hyphae, consistent with wild type colony and sporulation. However hyphal examination using confocal microscopy showed that both maximum repression and overexpression of *ugmA* had comparable effects on hyphal morphometry, causing increased hyphal width (23% and 20% increase respectively) and decreased basal cell length (43% and 50% decrease respectively) in comparison to wild type strain grown under the same conditions. The *alcA*(p)-*ugmA* strain grown on CMFT had wild type hyphal width, but had 46% decrease in basal cell length compared with wild type grown on same media (Table 2, Figure 4).

3.4. Repression of *ugmA* increases sensitivity to caspofungin and amphotericin B

Sensitivity of wild type (AAE1), *ugmA*Δ (AAE2) and *alcA*(p)-*ugmA* (AAE12) strains to antifungal drugs from four different target classes was tested using disc diffusion method. Our results showed that there was a small difference in sensitivity of *alcA*(p)-*ugmA* and wild type strain under overexpression condition (CMT), whereas under repression conditions *alcA*(p)-*ugmA* was notably more sensitive to both caspofungin and amphotericin B. For each drug, there was a more than 100% increase in the radius of inhibition zone (Table 3, Figure 5). Other antifungal agents including 5-fluorocytosine (5-FC) and nikkomycin Z (NKZ) were assayed for their antifungal activity towards wild type and Gal*f*-defective strains. However, they did not inhibit the growth of wild type or Gal*f*-defective strains (data not shown). Nikkomycin Z caused slightly higher swelling of the geminated spores of the Gal*f*-defective strain (*ugmA*Δ) in comparison to wild type strain when examined microscopically (Suppl. Figure C).

4. Discussion

The number of immunocompromised patients with invasive fungal infections has been increased dramatically. Treatment of systemic fungal infections is problematic due to the limited treatment options (Lass-Florl, 2009). Four classes of antifungal drugs (polyenes, azoles, allylamines and morpholines) target cell membrane ergosterol and ergosterol biosynthesis. Echinocandins are the only antifungal drugs that target fungal cell wall synthesis by inhibiting β-1,3-glucan synthase. Echinocandins are less toxic to humans but they still have narrow spectrum and emerging cases of resistance. This puts a pressure on the scientific community to find novel antifungal drug targets. Virulence factors of fungi could be new potential drug targets, as new approaches attempt to hinder ability of fungi to cause any harm to the host rather than killing the fungus (Gauwerky et al., 2009).

Gal*f* is a monosaccharide in the fungal cell wall that forms the side chains of many glycoconjugates (Latge, 2009). Galactofuranosyl residues are found to be immunodominant that indicates infections with *Aspergillus* (Bennett et al., 1985; Shibata et al., 2009), and a virulence determinant in *Aspergillus fumigatus* (Schmalhorst et al., 2008). Several studies have documented the importance of *ugmA* (one of the enzymes involved in Gal*f* biosynthesis) in fungal growth and morphogensis, and showed that deletion of *ugmA* is correlated with depletion of Gal*f* residues from *Aspergillus* cell walls (Damveld et al., 2008; El-Ganiny et al., 2008; Schmalhorst et al., 2008; Lamarre, 2009).

Previous studies have used the promoter exchange strategy to explore the role and essentiality of many genes (e.g. Hu et al., 2007; Monteiro and De Lucas, 2010). This study is the first study to explore the roles of Gal*f* biosynthesis enzymes on growth, morphogenesis and drug sensitivity of *Aspergillus nidulans* strains using *alcA* regulated strains. Here we are presenting detailed information on UgmA-regulatable strains. Comparable results were found for UgeA and UgtA which function immediately upstream and downstream of UgmA (data not shown).

4.1. *ugmA* repression affects drug sensitivity, colony and hyphal morphogensis

Our results showed that repression of *ugmA* increased the strain sensitivity to some antifungal drugs including caspofungin and amphotericin B. repression of *ugmA* also caused

compact colonial growth, reduced sporulation, increased hyphal width, branching and septum formation . Similarly, repression of genes that play a role in cell wall formation affected growth and morphogensis in other *Aspergillus* species. For example repression of a chitin synthase, *chsB* showed the importance of class IV chitin synthase on hyphal growth and conidiation of *A. nidulans*: as an *alcA*p-*chsB* strain showed slow growth and produced highly branched hyphae under repressing conditions (Ichinomiya et al., 2002). Repression of *A. fumigatus* O-mannosyltransferase 2 (*Afpmt2*) caused growth retardation, abnormal cell polarity defects, and reduced conidium formation (Fang et al., 2010). Jiang et al (2008) created *A. fumigatus* strains conditionally expressing GDP mannose pyrophosphorylase. When GDP mannose pyrophosphorylase was repressed. these strains showed defective cell wall, impaired polarity maintenance, reduced conidiation and increased sensitivity to wall targeting chemicals.

The *alcA*(p) was used also to study the roles of many genes from the cell wall integrity pathway. The Osherov group used *alcA*(p) to study the roles of protein kinase C (*pkcA*) as one of the cell wall integrity controllers. They found that repression of *pkcA* reduce germination, hyphal growth, conidiation and increase the cell wall thickness and sensitivity to wall targeting agents, however this *alcA-pkcA* strain was as sensitive as wild type to amphotericin B and voriconazole (Ronen et al., 2007). Osherov group also used the *alcA-pkcA* strain to identify new cell wall destabilizing compounds (Mircus et al., 2009). In another study the *alcA-pkcA* strain showed hypersensitivity to the antifungal protein PAF (Binder et al., 2010). Fortwendel *et al* (2009) used *A. fumigatus* strains defective in some cell wall integrity pathway genes (*rasAΔ*, *cnaAΔ* and *crzAΔ* strains), and found that these strains showed higher sensitivity to echinocandins.

Schmalhorst et al (2008) used a gene deletion strategy to create an *A. fumigatus* strain defective in Gal*f* biosynthesis (*glfAΔ*), This *glfAΔ* strain was more sensitive to many antifungal drugs including caspofungin and amphotericin B. Their result is consistent with our current result showing increased antifungal drugs sensitivity the Gal*f*-defective strains *alcA(*p)-*ugmA* strain under repression condition and *ugmAΔ* strain towards caspofungin and amphotericin B.

4.2. *ugmA* overexpression is not completely benign

Our study showed that growing the *alcA(*p)-*ugmA* strain on threonine containing medium to overexpress *ugmA* resulted in wild type colony growth and sporulation. Similar results observed in case of induction of *rpdA* (histone deacetylase) in *Aspergillus nidulans,* using two

conditional promoters (*alcA*(p) and xylP(p), where threonine and xylose were used as inducers for *alcA*(p) and xylP(p) respectively (Tribus et al., 2010). In contrast, increasing FlbE activity, one of the conidiation activator in *A. nidulans* led to disrupted asexual development (Kwon et al., 2010). Induction of *ugmA* expression resulted in slight decrease in sensitivity to terbinafine. Similarly, increasing mycobacterium UGM expression increased the resistance to isoniazid drug (Richards and Lowary, 2009).

Unexpectedly, the hyphae of *alcA*(p)-*ugmA* strain grown on overexpression medium were wider with shorter basal cell and more branching. This phenotype waas similar to *alcA*(p)-*ugmA* strain under repression conditions and also to the *ugmAΔ* strain (El-Ganiny et al., 2008). we think that overexpression of *ugmA* will results in increased synthesis and deposition of Gal*f* in fungal cell, perhaps at the expense of metabolites for hyphal growth. This will require further testing, since until now, only methods that reduced cell growth have been shown to affect cell wall composition and hyphal morphology.

In conclusion we have shown that *alcA*(p) can be used to control the expression of *ugmA* in *A. nidulans*. Repression of *ugmA* increased sensitivity to caspofungin and amphotericin B, decreased sporulation, and disrupted normal hyphal growth. Overexpression of *ugmA* also results in abnormal hyphal morphology and in decrease in sensitivity to terbinafine. These results indicate that even increasing *ugmA* expression is not completely benign. Our data suggest that balanced expression of *ugmA* is required for wild type sporulation and hyphal morphology in *A. nidulans,* and we called this effect the Goldilocks effect. Deletion or repression of *ugmA* expression will affect the cell wall and hence the sensitivity to antifungal drugs. Further investigation is required to validate Gal*f* as a virulence factor which will support the idea of targeting it by antifungal therapy; our future work will explore the roles of *ugmA* in *Aspergillus* pathogenicity using animal's model systems.

Acknowledgements

SGWK is pleased to acknowledge funding from the Canadian Institutes of Health Research Regional Partnership Program and the Natural Sciences and Engineering Research Council (NSERC) of Canada Discovery Grant program. AE would like to thank the Egyptian Ministry of higher Education for her Fellowship. Also we would like to thank Merck Company for supplying caspofungin, Sean Xiaoxiao He for assisting with data statistical analysis, and Tom

Bonli, Geology Department, University of Saskatchewan for SEM technical assistance. The *alcA*(p) containing plasmid was a generous gift from Dr. Loretta Jackson-Hayes, Department of Biology, Rhodes college, Memphis TN.

References

Afroz, S., El-Ganiny, A.M., Sanders, D.A.R., Kaminskyj, S.G.W., 2011. Roles of the *Aspergillus nidulans* UDP-galactofuranose transporter, UgtA in wild type hyphal morphogenesis, conidiation, cell wall architecture and drug sensitivity. Fungal Genetics and Biology accepted.

Aimanianda, V., Latgé, J., 2010. Problems and hopes in the development of drugs targeting the fungal cell wall. Expert Review of Anti-infective Therapy 8, 359-364.

Bennett, J.E., Bhattacharjee, A.K., Glaudemans, C.P., 1985. Galactofuranosyl groups are immunodominant in *Aspergillus fumigatus* galactomannan. Mol. Immunol. 22, 251-254.

Binder, U., Oberparleiter, C., Meyer, V., Marx, F., 2010. The antifungal protein PAF interferes with PKC/MPK and cAMP/PKA signalling of *Aspergillus nidulans*. Mol. Microbiol. 75, 294-307.

Bohle, K., Jungebloud, A., Gocke, Y., Dalpiaz, A., Cordes, C., Horn, H., Hempel, D.C., 2007. Selection of reference genes for normalisation of specific gene quantification data of Aspergillus niger. J. Biotechnol. 132, 353-8.

Cuero, R., Ouellet, T., Yu, J., Mogongwa, N., 2003. Metal ion enhancement of fungal growth, gene expression and aflatoxin synthesis in *Aspergillus flavus*: RT-PCR characterization. J. Appl. Microbiol. 94, 953-9561.

Damveld, R.A., Franken, A., Arentshorst, M., Punt, P.J., Klis, F.M., van den Hondel, C.A., Ram, A.F., 2008. A novel screening method for cell wall mutants in *Aspergillus niger* identifies UDP-galactopyranose mutase as an important protein in fungal cell wall biosynthesis. Genetics 178, 873-881.

El-Ganiny, A.M., Sanders, D.A.R., Kaminskyj, S.G.W., 2008. *Aspergillus nidulans* UDP-galactopyranose mutase, encoded by *ugmA* plays key roles in colony growth, hyphal morphogensis, and conidiation. Fungal Genet. Biol. 45, 1533-1542.

El-Ganiny, A., Sheoran, I., Sanders, D.A.R., Kaminskyj, S.G.W., 2010. *Aspergillus nidulans* UDP-glucose-4-epimerase UgeA has multiple roles in wall architecture, hyphal morphogenesis, and asexual development. Fungal Genet. Biol. 47: 629-635.

Erjavec, Z., Kluin-Nelemans, H., Verweij, P.E., 2009. Trends in invasive fungal infections, with emphasis on invasive aspergillosis. Clin. Microbiol. Infect. 15, 625-633.

Espinel-Ingroff, A., 2009. Novel antifungal agents, targets or therapeutic strategies for the treatment of invasive fungal diseases: a review of the literature (2005-2009). Revista iberoamericana de micología 26, 15-22.

Fang, W., Ding, W., Wang, B., Zhou, H., Ouyang, H., Ming, J., Jin, C., 2010. Reduced expression of the O-mannosyltransferase 2 (AfPmt2) leads to deficient cell wall and abnormal polarity in *Aspergillus fumigatus*. Glycobiology 20, 542-552.

Fortwendel, J.R., Juvvadi, P.R., Pinchai, N., Perfect, B.Z., Alspaugh, J.A., Perfect, J.R., Steinbach, W.J., 2009. Differential effects of inhibiting chitin and 1,3-{beta}-D-glucan synthesis in Ras and calcineurin mutants of *Aspergillus fumigatus*. Antimicrob. Agents Chemother. 53, 476-482.

Gauwerky, K., Borelli, C., Korting, H.C., 2009. Targeting virulence: a new paradigm for antifungals. Drug Discov. Today 14, 214-222.

Hu, W., Sillaots, S., Lemieux, S., Davison, J., Kauffman, S., Breton, A., Linteau, A., Xin, C., Bowman, J., Becker, J., Jiang, B., Roemer, T., 2007. Essential gene identification and drug target prioritization in *Aspergillus fumigatus*. PLoS Pathog. 3, e24 doi:10.1371/journal.ppat.0030024 .

Ichinomiya, M., Motoyama, T., Fujiwara, M., Takagi, M., Horiuchi, H., Ohta, A., 2002. Repression of *chsB* expression reveals the functional importance of class IV chitin synthase gene *chsD* in hyphal growth and conidiation of *Aspergillus nidulans*. Microbiology 148, 1335-1347.

Jiang, H., Ouyang, H., Zhou, H., Jin, C., 2008. GDP-mannose pyrophosphorylase is essential for cell wall integrity, morphogenesis and viability of *Aspergillus fumigatus*. Microbiology 154, 2730-2739.

Kaminskyj, S.G., 2000. Septum position is marked at the tip of *Aspergillus nidulans* hyphae. Fungal Genet. Biol. 31, 105-113.

Kaminskyj, S.G.W., 2001. Fundamentals of growth, storage, genetics and microscopy of *Aspergillus nidulans*. Fungal Genetics Newsletter 48: 25-31

Kontoyiannis, D.P., Lewis, R.E., Osherov, N., Albert, N.D., May, G.S., 2003. Combination of caspofungin with inhibitors of the calcineurin pathway attenuates growth *in vitro* in *Aspergillus species*. J. Antimicrob. Chemother. 51, 313-316.

Kwon, N., Shin, K., Yu, J., 2010. Characterization of the developmental regulator FlbE in *Aspergillus fumigatus* and *Aspergillus nidulans*. Fungal Genetics and Biology 47, 981-993.

Lamarre, C., 2009. Galactofuranose attenuates cellular adhesion of *Aspergillus fumigatus*. Cell. Microbiol. 11, 1612-1623.

Lass-Florl, C., 2009. The changing face of epidemiology of invasive fungal disease in Europe. Mycoses 52, 197-205.

Latge, J.P., 2009. Galactofuranose containing molecules in *Aspergillus fumigatus*. Med. Mycol. 47 Suppl 1, S104-109.

Latge, J.P., 2007. The cell wall: a carbohydrate armour for the fungal cell. Mol. Microbiol. 66, 279-290.

Livak, K.J., Schmittgen, T.D., 2001. Analysis of relative gene expression data using real-time quantitative PCR and the 2(-Delta Delta CT) Method. Methods 25, 402-408.

Mircus, G., Hagag, S., Levdansky, E., Sharon, H., Shadkchan, Y., Shalit, I., Osherov, N., 2009. Identification of novel cell wall destabilizing antifungal compounds using a conditional *Aspergillus nidulans* protein kinase C mutant. J. Antimicrob. Chemother. 64, 755-763.

Monteiro, M.C., De Lucas, J.R., 2010. Study of the essentiality of the *Aspergillus fumigatus triA* gene, encoding RNA triphosphatase, using the heterokaryon rescue technique and the conditional gene expression driven by the *alcA* and *niiA* promoters. Fungal Genet. Biol. 47, 66-79.

Osmani, A.H., Oakley, B.R., Osmani, S.A., 2006. Identification and analysis of essential *Aspergillus nidulans* genes using the heterokaryon rescue technique. Nat. Protocols 1, 2517-2526.

Paul, B.C., El-Ganiny, A.M., Abbas, M., Kaminskyj, S.G., Dahms, T.E., 2011. Quantifying the importance of galactofuranose in *Aspergillus nidulans* hyphal wall surface organization by atomic force microscopy. Eukaryot. Cell.10, 646-653.

Pedersen, L.L., Turco, S.J., 2003. Galactofuranose metabolism: a potential target for antimicrobial chemotherapy. Cellular and Molecular Life Sciences 60, 259-266.

Richards, M.R., Lowary, T.L., 2009. Chemistry and biology of galactofuranose-containing polysaccharides. Chembiochem 10, 1920-1938.

Romero, B., Turner, G., Olivas, I., Laborda, F., Ramón De Lucas, J., 2003. *The Aspergillus nidulans alcA* promoter drives tightly regulated conditional gene expression in *Aspergillus fumigatus* permitting validation of essential genes in this human pathogen. Fungal Genet. Biol. 40, 103-114.

Ronen, R., Sharon, H., Levdansky, E., Romano, J., Shadkchan, Y., Osherov, N., 2007. The *Aspergillus nidulans pkcA* gene is involved in polarized growth, morphogenesis and maintenance of cell wall integrity. Curr. Genet. 51, 321-329.

Schmalhorst, P.S., Krappmann, S., Vervecken, W., Rohde, M., Muller, M., Braus, G.H., Contreras, R., Braun, A., Bakker, H., Routier, F.H., 2008. Contribution of galactofuranose to the virulence of the opportunistic pathogen *Aspergillus fumigatus*. Eukaryot. Cell. 7, 1268-1277.

Shibata, N., Saitoh, T., Tadokoro, Y., Okawa, Y., 2009. The cell wall galactomannan antigen from *Malassezia furfur* and *Malassezia pachydermatis* contains {beta}-1,6-linked linear galactofuranosyl residues and its detection has diagnostic potential. Microbiology 155, 3420-3429.

Szewczyk, W., Nayak, T., Oakley, C.E., Edgerton, H., Xiong, Y., Taheri-Talesh, N., Osmani, S.A. and Oakley, B.R. 2007. Fusion PCR and gene targeting in *Aspergillus nidulans*. Nat. Protoc. 1, 3111-3120.

Tribus, M., Bauer, I., Galehr, J., Rieser, G., Trojer, P., Brosch, G., Loidl, P., Haas, H., Graessle, S., 2010. A novel motif in fungal class 1 histone deacetylases is essential for growth and development of *Aspergillus*. Mol. Biol. Cell 21, 345-353.

Zarrin, M., Leeder, A.C., Turner, G., 2005. A rapid method for promoter exchange in *Aspergillus nidulans* using recombinant PCR. Fungal Genet. Biol. 42, 1-8.

Tables

Table 1: strains, primer and plasmids used in this study

Strains

Name	Description	Genotype
A1149 [a]	Wild type	*pyrG89; pyroA4; nkuA::argB*
AAE1 [b]	Wild type	*pyrG89:N. crassa pyr4+; pyroA4; nkuA::argB*
AAE2 [b]	*ugmA*Δ	AN3112*::AfpyrG; pyrG89; pyroA4; nkuA::argB*
AAE12 [c]	*AlcA(*p*)-ugmA*	*ugmA*p*::pyrG:alcA*p:*ugmA*; *pyrG89; pyroA4; nkuA::argB*

Primers		Sequence 5`→3`
Promoter exchange primers		
Ame115[c]	*ugmA* F	TCCTATCACCTCGCCTCAAAATGCTTAGTCTAGCTCGCAAGAC
Ame 23 [b]	*ugmA* R	GCCTGCACCAGCTCCCTGCGCCTTATTCTTAGCAAA
Ame 1 [b]	Upstream F	GACTCTTGAGATTTGCTTGGGTCTC
Ame114[c]	Upstream R	TCAGTGCCTCCTCTCAGACAGAGAAGAGAGCGAAGCTGCAG
Ame118 [c]	Promoter F	CTGTCTGAGAGGAGGCACTGA
Ame119 [c]	Promoter R	TTTGAGGCGAGGTGATAGGA
Ame116 [c]	Fusion F	GTAGTTGACAAGCATACGGAGTACTC
Ame117 [c]	Fusion R	GGACCAGTAGGGACCTTCCT
Ame134 [c]	Midpromoter F	GTGTTTGGTGTTGCCAAAGAC
qRT-PCR primers		
Ame 84 [c]	*ugm* F	CGTTCCCAGCTTTCAGGATA
Ame 85 [c]	*ugm* R	CTTTGCAGCACCCAATCC
Ame100 [c]	*act* F	T T C G G G T A T G T G C A A G G C
Ame101 [c]	*act* R	T C G T G A C A A C A C C G T G C T
plasmids		
p*alcA*(p)		pGEM+ *alcA*(p)+ Af*pyrG*

[a] Fungal Genetics Stock Center www.fgsc.net.

[b] El-Ganiny et al. 2008.

[c] This study.

Table 2: Colony and hyphal characters of wild type (AAE1) and *alcA*(p)-*ugmA* (AAE12) strains grown under induction and repression conditions. Values presented as mean ± SE [d]

Media	Strain	Colony diameter (mm) [a]	Number of spores/ colony *10^{6} [b]	Hyphal width (µm) [c]	Basal cell length (µm) [c]
	wild type	22.5 ± 0.5	12.4 ± 1	2.5 ± 0.03	27.2 ± 1.3
CMT	*alcA*(p)-*ugmA*	16.8 ± 0.6e	8.2 ± 1e	3 ± 0.04f	13.7 ± 0.6f
	wild type	18 ± 0.4	21 ± 5	2.6 ± 0.05	32.7 ± 2.9
CMFT	*alcA*(p)-*ugmA*	12 ± 0.7e	8.4 ± 3e	2.5 ± 0.05	17.9 ± 1.1f
	wild type	16 ± 0.4	38 ± 11	3.1 ± 0.05	30.3 ± 1.6
CM3G	*alcA*(p)-*ugmA*	3.6 ± 0.2f	0.6 ± 0.1f	3.7 ± 0.1f	17.2 ± 1f

[a] 10 coloniess / strain (from three biological replicates)

[b] 3 colonies (each colony counted twice) from three different plates (biological replicates)

[c] 50 measurements / strain, from two independent biological replicates. Hyphal width measured at septa, and basal cell length measured the distance between two subsequent septa.

[d] One-way ANOVA plus Tukey test are used to compare wild type and *alcA*(p)-*ugmA* strains grown on the same media. Values for *alcA*(p)-*ugmA* strains followed by letter if they are significantly different from wild typ, 'e' means significantly different at $P<0.05$; and 'f' means significantly different at $P<0.001$,

Table 3: Sensitivity of wild type, *ugmAΔ*, and *alcA*(p)-*ugmA* strains to antifungal drugs, assessed using disk diffusion method [a, b].

Media	Strain	Terbinafine	Itraconazole	Caspofungin	Amphotericin B
CMT	wild type	16.1 ±0.2	8.3 ± 0.3	4.3 ± 0.2	1.5 ± 0.2
	alcA(p)-*ugmA*	15 ± 0c	8 ± 0.2	4.5 ± 0.1	1.6 ± 0.2
CM3G	wild type	18.3 ± 0.3	7 ± 0.2	3.4 ± 0.1	1.1 ± 0
	alcA(p)-*ugmA*	18 ± 0.2	7.6 ± 0.1	6.8 ± 0.2d	2.3 ± 0.1d
CM	wild type	16 ± 0.5	7 ± 0.3	3.5 ± 0.05	1.7 ± 0.2
	*ugmA*Δ	15 ± 0.8	7.8 ± 0.2	6.3 ± 0.2d	2.5 ± 0.4d

a Drug sensitivity is measured as the radius (mm) of the clear zone with no visible growth. Data presented as mean ± SE (n = 4, four different biological replicates).

b Statistical analysis used unpaired t-test to compare wildtype (AAE1) and Gal*f* defective strains (AAE2 or AAE12) grown on the same media for each tested drug.

c One-way ANOVA plus Tukey test was used to compare wild type and *alcA*(p)-*ugmA* strains grown on the same media. Values for *alcA*(p)-*ugmA* strains followed by 'c' are significantly different from wild type at $P<0.05$, and values followed by 'd' are significantly different at $P<0.001$.

Figures

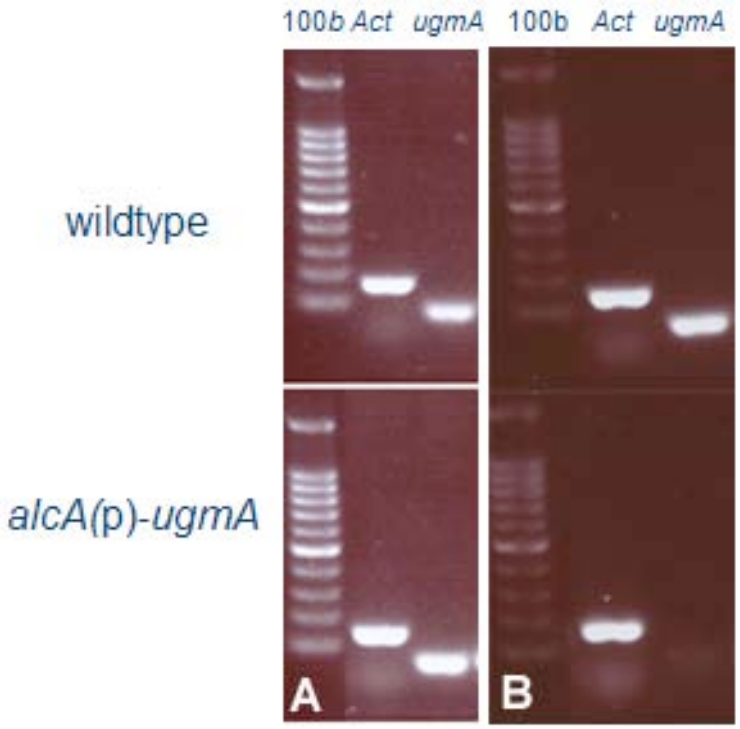

Figure 1: representative gels of the qRT-PCR products, showing the change in *ugmA* expression after induction on CMT (A) and repression on CM3G (B). Actin was used as a reference gene.

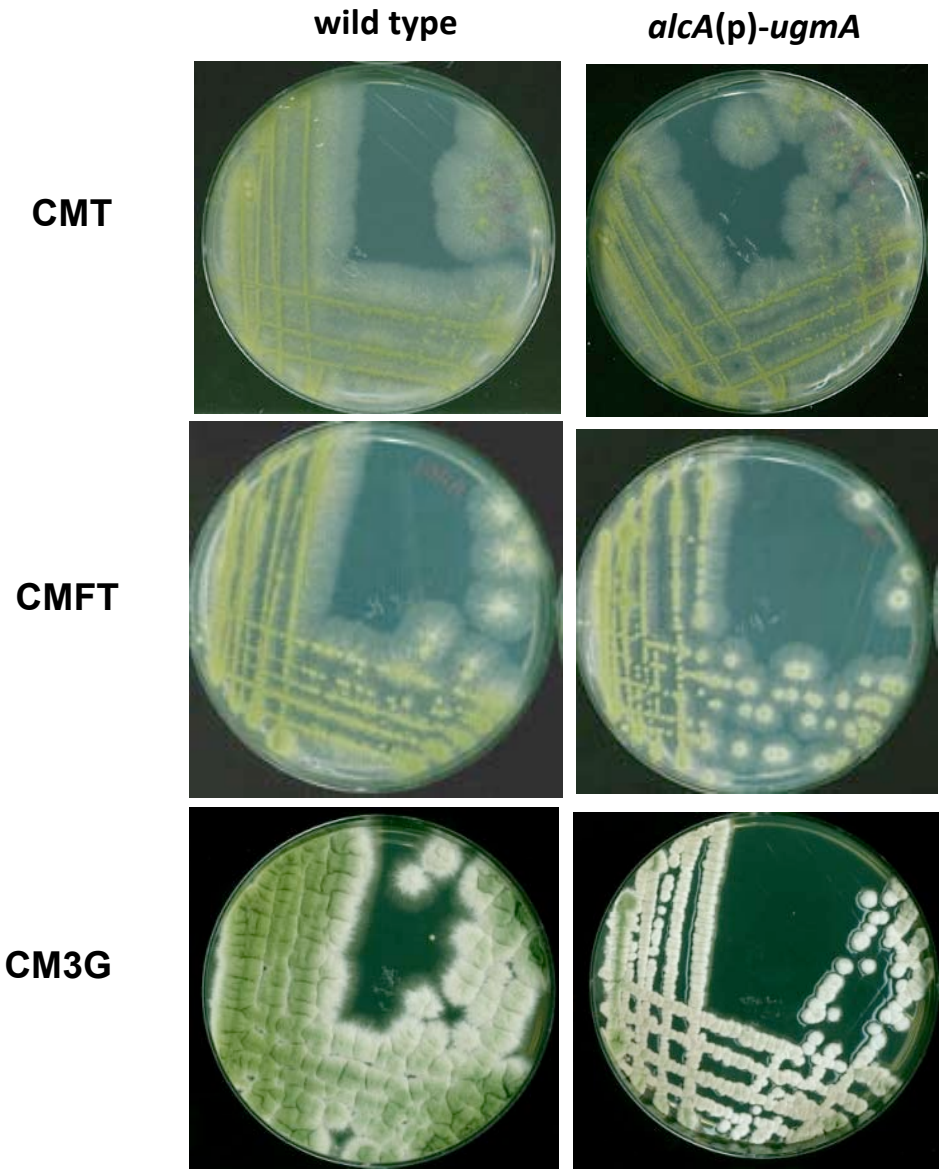

Figure 2: Colony morphology of wild type and *alcA*(p)-*ugmA* strains grown on CM media with different carbon source. *alcA*(p)-*ugmA* strain has wild type colony and sporulation when grown on CMT and CMFT media, and resemble *ugmA*Δ phenotype when grown on CM3G media.

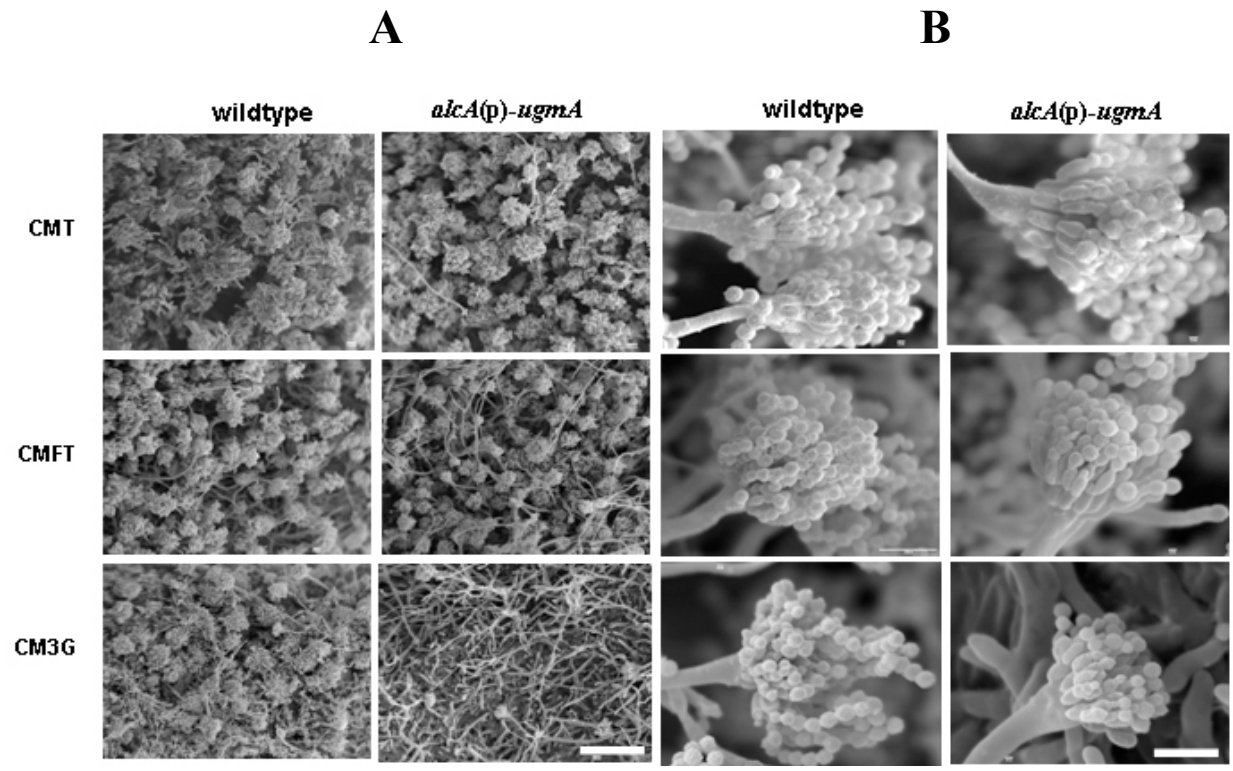

Figure 3: SEM micrographs showing: colony (A), and conidiophore (B) wild type and (*alcA*(p)-*ugmA* strains grown on CM with different carbon source. On CMT and CMFT media, *alcA*(p)-*ugmA* strain has abundant conidiophores with long chains of spores similar to wild type strain. On CM3G media, *alcA*(p)-*ugmA* produced very few conidiophores with short chains of spores. Scale bar is 100µm for A, and 10 µm for B.

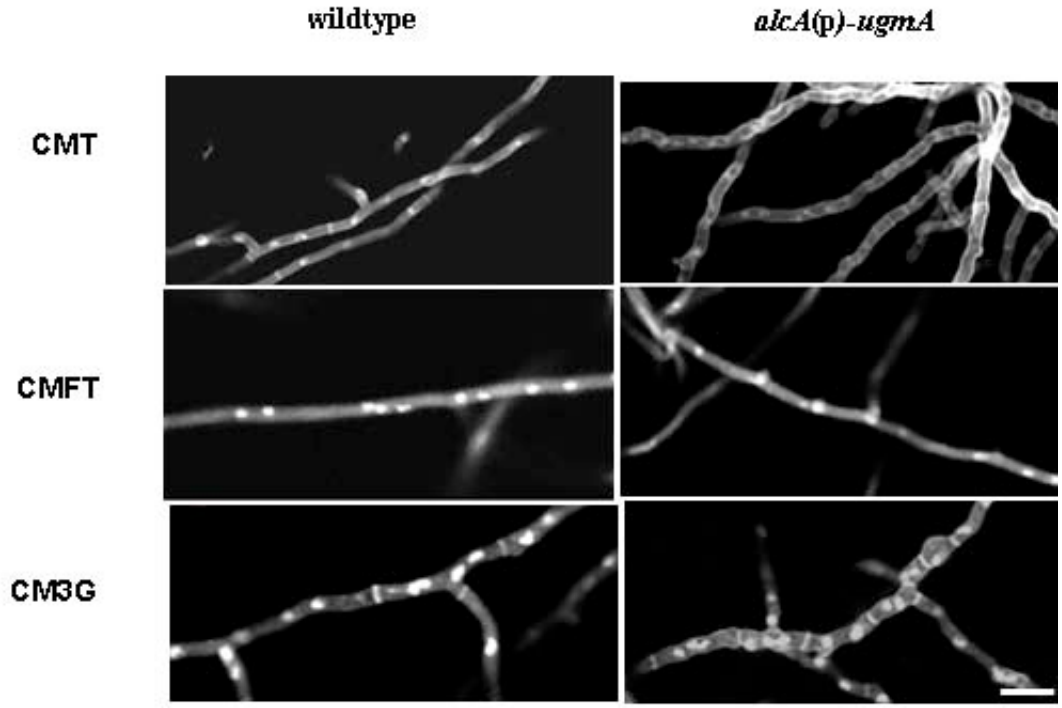

Figure 4: Hyphal morphology wild type and *alcA*(p)-*ugmA* strains grown on CM with different carbon source and stained with Hoechst and Calcofluor. The *alcA*(p)-*ugmA* strain has wild type hyphae only on CMFT media and have wide, highly branched hyphae with shorter basal cells when grow on CMT (overexpression) and CM3G (high repression) media. Scale bar = 10 μm.

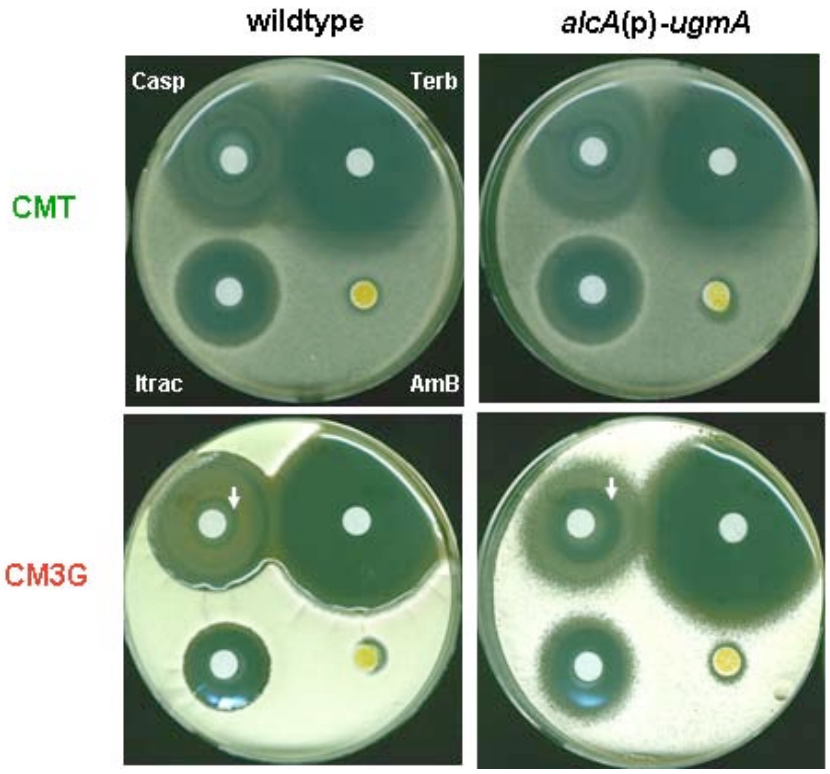

Figure 5: Sensitivity of wild type and *alcA*p-*ugmA* strains grown under induction (CMT) and repression (CM3G) conditions towards four antifungal drugs: caspofungin (Casp), itraconazole (Itrac), terbinafine (Terb) and amphotericin B (AmB). Arrows indicate the edge of the zone of inhibition (zone with no visible growth).

Supplemental materials

a.

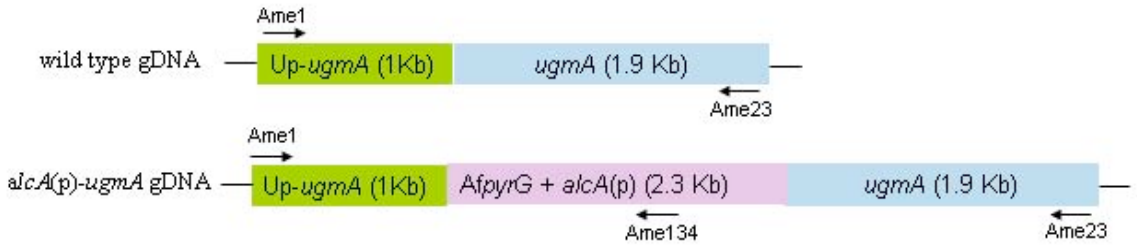

b.

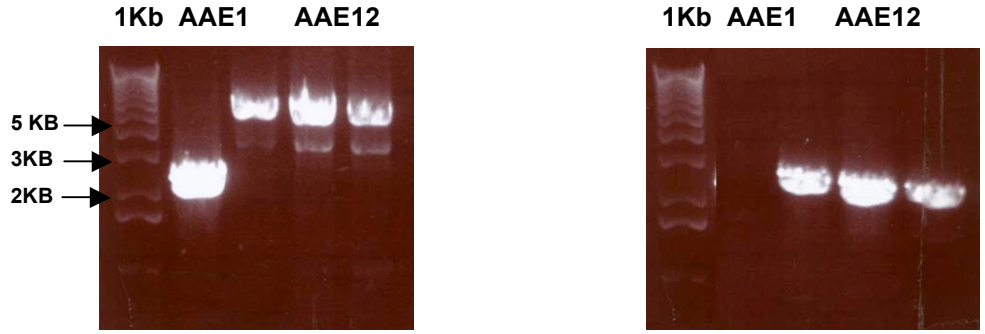

Ame1 & Ame23 Ame1 & Ame134

c.

Primer pair	AAE1	AAE12
Ame1&Ame23	2.9	5.2
Ame1 & Ame134	No band	2.8

Supplemental figure A: Confirmatory PCR for promoter exchange.

a) Diagram showing where the primers bind in the gDNA of wild type and *alcA*(p)*-ugmA* strains
b) Electrophoresis gels for wild type (AAE1) and *AlcA*p-*ugmA* (AAE12) strains using two sets of primers.
c) Expected amplicon size for both AAE1 and AAE12 with two primer pairs.

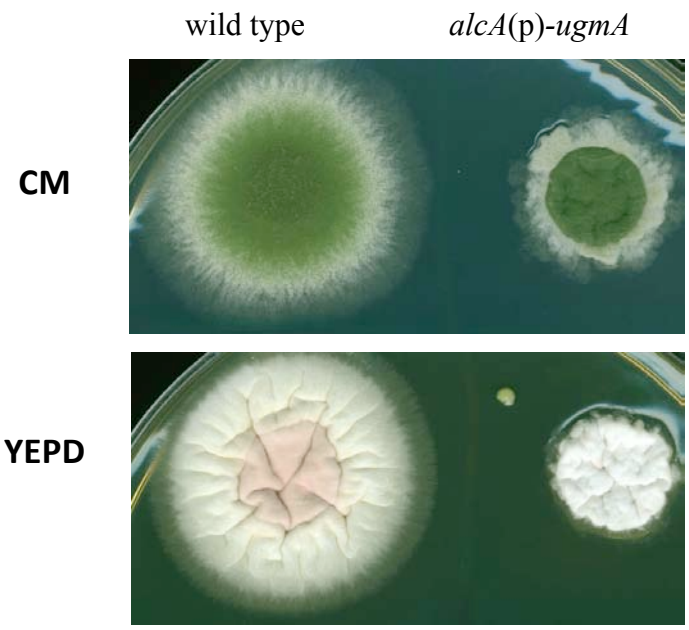

Supplemental Figure B: Colony morphology of wild type and *alcA*(p)-*ugmA* strains grown on CM (1% glucose) and YEPD media. Plates were incubated for 3 days at 28C.

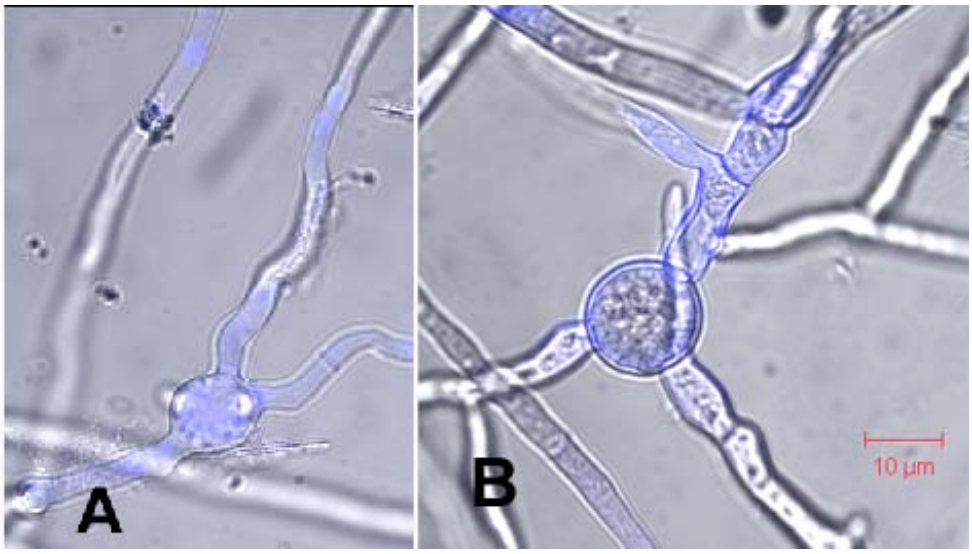

Supplemental figure C: The growth of wild type (A) and *ugmA*Δ strain (B) in liquid CM* + nikkomycin Z (32 µg/ml). Strains are grown for 16 hr. at 28°C, then fixed and stained with Calcofluor and examined using confocal microscopy, Bar 10 µm.

Chapter 7

General discussion

Is the galactofuranose biosynthesis pathway in *Aspergillus* still a possible drug development target?

Invasive fungal infections have increased dramatically since the mid-20th century, in parallel with the increased population of immunocompromised patients (Lass-Florl, 2009). Fungal infections are difficult to diagnose, and following diagnosis there are few therapeutic options, so they cause high morbidity and mortality (Chen et al., 2010; Denning and Hope, 2010). Emerging antifungal resistance against current drugs makes treatment of fungal infections even more difficult (Carrillo-Muñoz et al., 2006). Taken together, there is considerable need to identify new antifungal targets for drug development (Ostrosky-Zeichner et al., 2010).

Cell walls are essential for fungal survival and virulence, and since many of their polysaccharide components are not found in humans, so fungal walls are considered to be promising targets for drug development (Arana et al., 2009). Unfortunately, the fungal wall is composed of multiple interacting components , also the cell wall is produced and maintained by highly redundant suites of genes whose products have overlapping functions. Currently, there is only one class of antifungal drug in clinical use (echinocandins) that targets synthesis of the fungal wall polysaccharide, β-1,3-glucan (Denning, 2003). To date, inhibitors targeting other fungal wall structural components have not been effective in clinical use (Aimanianda and Latgé, 2010). Other compounds which target fungal wall components (e.g. Calcofluor White and Congo Red) that are somewhat effective *in vitro* (Chapters 5) but are not useful clinically.

Galactofuranose (Gal*f*) is the 5-member ring isomer of galactose that forms short side-chains on galactomannans and other glycoconjugates (Latge, 2009). Gal*f* is a cell wall component whose precise roles in cell wall architecture have not yet been well characterized, Gal*f* is considered to be a fungal virulence factor in fungi as well as in pathogenic protozoa. In addition, Gal*f* residues appear to form part of the secreted antigens in invasive aspergillosis infections (Leitao, 2003). However, this is still very preliminary. Loss of Gal*f* in *A. fumigatus* strains has been associated with reduced virulence in one experimental study on a mouse model system (Schmalhorst et al 2008). In addition, Gal*f*-containing glycoconjugates appear to have a

role in invasion of *Trypanosoma cruzi* into mammalian cells (De Arruda et al., 1989). Both being part of the cell wall and playing a role in virulence in at least some studies suggests that the Gal*f*-biosynthesis pathway could be an excellent target for new antifungal drugs. Human serum Gal*f* levels can be detected by the Platelia® monoclonal antibody (EBA2) that binds many forms of Gal*f* epitope, and hence is used to monitor therapy progress in systemic aspergillosis patients (Wheat, 2003). However, Lamarre et al (2009) discussed evidence suggesting that EBA2, fails to recognize all forms of Gal*f* conjugate as it binds only β 1,5 linked Gal*f* residues. Engel et al. (2009) used the MEST-1 monoclonal antibody thoat detects the β 1,6 Gal*f* residues.

My Ph.D. research has explored the function of three enzymes that act sequentially in the *Aspergillus nidulans* Gal*f* biosynthesis pathway: UgeA, UgmA and UgtA. Collectively these enzymes generate UDP-Gal*f* from UDP-glucose in the cytoplasm, then transport it to the fungal Golgi equivalent for incorporation in cell wall Gal*f*-containing glycoconjugates. The research I have described in Chapters 2-6 clearly shows that deletion or down-regulation of any of the three genes whose protein products mediate independent steps in wall Gal*f* biosynthesis causes roughly comparably deficits in fungal growth, cell wall architecture, asexual sporulation, and response to antifungal drugs. Although deletion of any of these genes shows they are not essential, comparable to the effect of echinocandins on *Aspergillus* growth *in vitro*, there are reasons that support considering Gal*f* biosynthesis as promising drug development target

7.1. Each step in Gal*f* biosynthesis controlled by single functional gene

My research shows that the Gal*f* biosynthesis pathway is a promising target for antifungal drug development. Although UgeA, UgmA, and UgtA are not essential for viability, single gene deletions have crippling effects on fungal growth and sporulation. Notably, the *A. nidulans* gene deletion strain phenotypes for UgmA and UgtA were fully complemented by their *A. fumigatus* orthologues (GlfA for UgmA, and GlfB for UgtA) showing that these enzumes are functionally homologous. This provides a substantial resource for future research: *A. fumigatus* is a Biosafety level 2 organism, whereas *A. nidulans* is Biosafety level 1. Thus it will be possible to study the structure and function of mutations in these *A. fumigatus* gene products when they are expressed in *A. nidulans*. Ultimately, these results must also be confirmed in *A. fumigatus*.

Both UDP-galactopyranose mutase (UgmA) and the UDP-Gal*f* transporter (UgtA) are encoded by single gene sequences in *A. nidulans*, which makes targeting these genes an efficient strategy. Although there are two sequences (*ugeA* and *ugeB*) encoding putative UDP-glucose/galactose epimerases, only UgeA was demonstrated biochemically to have this epimerase function and *ugeAΔ* strains had a defective phenotype (chapter 4). In contrast, strains deleted for *ugeB* had wild type morphology, and the UgeB was detected only following overexpression and then only in conidiophores. In addition although UgeB consumes UDP-galactopyranose, it does not generate UDP-glucose (chapter 5). This is strong evidence that UgeA main functional enzyme that can convert UDP-glucose into UDP-galactose in *A. nidulans.* Similarly Damveld et al. (2008) showed that *A. niger* has two sequences encoding UDP-galactopyranose mutase (Ang-*ugmA* and Ang-*ugeB*). Deletion of Ang *ugmA* gave a defective phenotype, while deletion of *ugmB* had no effect on phenotype.

Enzymatic functions that are encoded by single genes cannot readily be compensated by genetic redundancy, and thus have higher likelihood of being drug targets. For example, synthesis of *Aspergillus* β-1,3-glucan is catalyzed by only one enzyme that is encoded by single gene, *fksA* (Kelly et al., 1996). In contrast chitin synthesis uses a suite of at least eight genes with overlapping functions (Mellado et al., 1995). Consistent with this, the echinocandins (β-1,3-glucan synthesis inhibitors) are clinically useful, whereas chitin synthase inhibitors have not proven to be effective drugs in clinical use (Latge, 2007). Consistent with this, nikkomycin Z (a chitin synthase inhibitor) caused morphological defects in wildtype *A. nidulans* hyphae, but was not able to inhibit the growth of either the wild type or the Gal*f*-defective strains, when assessed using disc diffusion method (chapter 6).

None of the Gal*f* biosynthesis enzymes (UgeA [El-Ganiny et al., 2010], UgmA [El-Ganiny et al., 2008], and UgtA [Afroz et al., *in press*]) that I characterized during my research program is essential for viability of *A. nidulans*. However, each of these gene deletion strains has a similar phenotype and each is seriously compromised for growth in culture. These deletion strains have low growth rates with compact colonies and hyphal abnormalities, and severely decreased sporulation. Schmalhorst et al. (2008) showed that an *A. fumigatus* strain deleted for its UgmA homologue had a similar phenotype to our strains and showed reduced pathogenicity in animal models. Although targeting Gal*f* biosynthesis would not be fungicidal, reducing fungal capacity to invade and proliferate in host tissue would potentially slow disease

progress. Consistent with this, it has been shown previously that echinocandins including caspofungin do not kill *Aspergillus* (Denning, 2003) but in experimental animal studies these drugs induce morphological changes that decrease fungal pulmonary injury (Petraitiene et al., 2002) and so they are clinically effective. Stated another way, fungicidal activity does not necessarily translate to improved drug efficacy in clinical use (Chapman et al., 2008). As a result, some recent antifungal therapeutic strategies are no longer trying to kill pathogens but rather to reduce its ability to cause disease (Gauwerky et al., 2009).

7.2. Increased sensitivity of Gal*f*-biosynthesis defective strains to antifungal drugs

As one aspect of testing Gal*f* biosynthesis enzyme pathway enzymes as potential targets for antifungal drug development, I compared Gal*f*-biosynthesis defective strains (*ugmA*Δ or *alcA*(p)-*ugmA* repressed by growth on 3 % glucose) with wild type strains for their sensitivity towards four classes of commercially available antifungals. Gal*f*-biosynthesis defective strains were more sensitive to caspofungin and amphotericin B than wild type strains. This is consistent with Schmalhorst et al. (2008) who showed that the Af*glfA*Δ strain was more sensitive to several antifungal drugs including caspofungin. When the *alcA*(p)-*ugmA* strain was grown on over-expression medium, it was slightly less sensitive to terbinafine than wild type strain, consistent with increased resistance of *Mycobacterium* overexpressing UGM to the cell wall targeting drug isoniazid (Richards and Lowary, 2009).

Also the sensitivity of the *ugtA*Δ strain was assayed using disc diffusion methods towards the fungal wall targeting agents Calcofluor White (CFW) and Congo Red (CR), both of which inhibit fungal growth, but are not clinically useful. The *ugtA*Δ strain showed slight increase in sensitivity to CFW. Both the *A. nidulans ugmA*Δ strain and the A. *niger ugmAΔ* strain were also more sensitive to high concentrations of CFW (30 µg/mL or more) than the wild type strains (Damveld et al., 2008; El-Ganiny et al., 2008). However, the CFW results must be interpreted with some caution, and possibly explored further, since El-Ganiny et al. (2008) also showed that low levels of CFW (10 µg/mL) partially remediated the *ugmA*Δ strain phenotype defects.

The increased sensitivity of the Gal*f*-biosynthesis defective strains to caspofungin is consistent with the importance of the cell wall in fungal growth. We indicated that the Gal*f*-defective strains had weaker cell wall than wild type strains (chapter 5). Attacking these strains

with wall targeting drugs was expected to cause easier damage to the already weakened wall, consistent with the increased sensitivity of *cal* mutants to wall targeting agents (Hill et al., 2006).

Somewhat unexpectedly, these strains were also more sensitive to amphotericin B, which targets ergosterol in cell membranes. Similar increased sensitivity to amphotericin B was shown by Schmalhorst et al. (2008) for *A. fumigatus glfA* deletion strains. Szeghalmi et al (2007) and Gough and Kaminskyj (2010) showed that when hyphae from several fungal species including *A. nidulans* were grown under environmentally stressful conditions, they had increased hyphal protein levels that appeared to partially compensate for weaker cell walls. Consistent with this, preliminary evidence from spectroscopic analysis of *A. nidulans* wild type and Gal*f*-defective strains showed that *ugmA*Δ hyphae had different carbohydrate and substantially higher protein content. The cytoskeleton/cell membrane and the cell wall form complementary support systems in fungal hyphae (Kaminskyj and Heath 1995, 1996). Reduced strength of the *ugmA*Δ cell wall (El-Ganiny et al., 2008; Paul et al., 2011) appears to increase dependence on the cell membrane-cytoskeleton system for maintaining hyphal integrity. Notably, this effect was most strongly shown at the chemical level (increased amphotericin B sensitivity) rather than by inhibition of ergosterol biosynthesis (no significant change in sensitivity to azoles and allylamines

7.3. Double mutant analysis reveals additional potential therapeutic targets

In *A. fumigatus*, the hyphal wall surface appears to be enriched for Gal*f,* which masks a layer enriched in mannosyl residues (Lamarre et al. 2009). El-Ganiny et al. (2008) created a double mutant [*ugmAΔ swoA1*] strain. The *swoA1* mutation in a mannosyl transferase (Shaw and Momany, 2002), produced a strain with extremely diminished sporulation at 37 °C. A double mutant [*ugmAΔ swoA1*] strain had very small colonies and suffered from more severe growth defects than single *ugmA* or *swoA* strains. This suggests that treatments targeting both Gal*f* and mannan biosynthesis could be promising for use in antifungal therapy. Similarly, *S. cerevisiae fks1*Δ strains (defective in β-1,3-glucan synthesis) are synthetically lethal with deletion of *cnb1*Δ (calcineurin catalytic subunit). The calcineurin pathway is required for compensation to cell wall defects that result from interference with β-1,3-glucan synthesis (Cowen and Steinbach, 2008).

Paul et al. (2011) characterized and quantified the effect of several individual Gal*f* biosynthesis gene deletion mutants, as well as two double deletion strains, [*ugeA*Δ*, ugeB*Δ] and [*ugeA*Δ*, ugmA*Δ] on hyphal wall structure. Use of atomic force microscopy, force compliance

analysis, and adhesion quantification showed that the UgmA and UgeA strain walls were substantially weaker and more hydrophilic than wild type strains. Notably, both [*ugeA*Δ*, ugeB*Δ] and [*ugeA*Δ*, ugmA*Δ] double deletion strains had substantially more severe defects than the single deletion strains, appearing to entirely lack the outer wall layer. Thus, as suggested by Costanzo et al. (2010) multiple gene deletion analysis can provide more insights into gene function.

The UgmA and UgtA gene sequences are adjacent in the *A. nidulans* genome (ANID 3112 and ANID 3113, respectively), which is consistent with other fungal systems (reviewed in Engel et al 2009). GFP tagging showed that UgmA is cytoplasmic protein (El-Ganiny et al., 2010), whereas cellular distribution of UgtA-GFP has a strong tip-high gradient (Afroz et al, *in press*), consistent with fungal Golgi distribution (Breakspear et al., 2007; Hubbard and Kaminskyj, 2008) and with tip localized hyphal growth. UgtA is Golgi-localized, likely in the membrane rather than the lumen, because hydropathy analysis showed that it appeared to contain 11 membrane-spanning alpha-helices. Loops including the N-terminus and other between alternate membrane-spanning regions are localized in the cytoplasm (chapter 4). This suggests the possibility that there could be an interaction between UgmA and cytoplasmic amino acids of UgtA related to production or transport of Gal*f* residues for wall glycoconjugates. If this were so, then interfering with a putative UgmA-UgtA interaction might be deleterious to Gal*f* deposition in the cell wall and could be an additional possible target for new antifungals.

7.4. Combination antifungal therapy

The fungal cell wall is dynamic in its composition and architecture, changing in response to hyphal growth (Momany et al., 2004), to enviromental stresses (Szeghalmi et al 2007), and to planktonic versus biofilm growth (Loussert et al 2009). The relative inhibition of one type of cell wall polysaccharide can lead to compensatory increase in another component, typically mediated through the cell wall integrity pathway (Fujioka et al., 2007). For example, echinocandin treatment induces upregulation of chitin synthesis in the cell wall of *C. albicans* allowing the cells to escape lethality (Walker et al., 2008). Similarly, exposure of *A. niger* to CFW increases the expression of genes encoding α-glucan synthases (reviewed in Damveld et al., 2008). Inevitably, if a drug treatment is not 100 % lethal, this will result in development of resistance

(Sanguinetti et al., 2010). For antifungal agents that target gene products (unlike polyenes), the development of resistant strains is predictable (Anderson, 2005; Cowen, 2008).

Combination antifungal therapies are a promising strategy for avoiding, or at least delaying, the development of resistance, that have already been used for new types of anti-bacterial treatment (Bassetti et al., 2008). Combination therapy has been used for treatment of cryptococcal infections (Van et al., 1997). Antifungal combination therapy can follow different strategies. For example it can target cell wall and cell membrane (Manavathu et al., 2003); two cell wall components (Luque et al., 2003); or a cell wall target plus cell wall integrity pathway target like calcineurin pathway (Fortwendel et al., 2009). Results presented in Chapter 6 suggest that anti-Gal*f* drugs (once developed) can be used in combination with echinocandins and/or with polyenes. Results presented in El-Ganiny et al (2008) and discussed in §7.3 suggest that targeting Gal*f* and mannan synthesis could also be therapeutically useful.

Ideally, we can predict how fungal cells can compensate for Gal*f* loss using microarrays or PCR arrays. This will give a better idea about which drug combination would be more useful. Also it will be possible to detect and document synergistic drug interactions in animal models prior to testing in mammalian systems (currently under development by others in Kaminskyj research group).

7.5. Future directions

Given that Gal*f* residues have long been known or suspected to be important or essential for survival, growth, and pathogenicity of several microorganisms (reviewed in Beverley et al. 2005), and since it is increasingly clear that new anti-fungal drug targets must now be selected amongst non-essential pathways for fungal metabolism, why has the Gal*f*-biosynthesis pathway not received more widespread research attention for future drug development studies? Two factors have been extremely important.

Unambiguous chemical analysis of Gal*f* residues is expensive and extremely time consuming, compared to galactose. In solution, galactose is in equilibrium in the pyranose and furanose forms (95:5). These forms are stabilized by conjugation at carbon-1. Under appropriate conditions, purified Af*glfA* will convert UDP-Gal*p* to UDP-Gal*f in vitro*. However, there is no commercially available source of UDP-Gal*f*. Also the EBA2 monoclonal antibody used clinically

in the Platelia kit is not readily available to researchers, and can only be purchased in a 96-well microtitre plate dish for ELISA assays.

Until recently, the protein crystal structure of AfGlfA had not been solved at high resolution, despite ongoing and intense research effort. The structure of the prokaryotic UGM had been solved a decade previously (Sanders et al. 2001), but even for the prokaryote version the precise catalytic mechanism has not been completely clarified. As a result, it had not been possible to develop testable hypotheses about the catalytic mechanism of AfGlfA that could be used to predict and test a possible inhibitor compounds. Till now drugs that can target fungal Gal*f* biosynthesis are not developed.

Although Gal*f* localization in the fungal wall remains incompletely characterized, the recent high spatial resolution crystal structure solutions of AfGlfA (van Straaten et al, in preparation), and *A. nidulans* UgeA (Dalrymple et al, submitted) now permit development and testing of specific hypothesis about amino acids that play important roles in these steps in Gal*f* biosynthesis. With the crystal structures of AnUgeA and AfGlfA now available and building on the results presented from my thesis research, the following experimental directions are possible.

1. Preliminary evidence suggests that like UgmA, both UgeA and UgtA deletion and conditional repression strains have increased sensitivity to antifungal drugs that are currently in clinical use. In addition to characterizing these drug sensitivities more fully, it will be useful to determine whether genes known to be involved in cell wall integrity are upregulated in response to perturbing the Gal*f* biosynthesis pathway. Cell wall integrity pathway genes have previously been characterized in *Aspergillus nidulans* (e.g. Fujioka et al., 2007). If regulation of cell wall integrity pathway genes is altered in Gal*f*-biosynthesis pathway deletion strains, they could be useful targets for combination therapy.
2. Hydropathy analysis of UgtA has identified regions that are located on the cytoplasmic face of this transmembrane protein. Coupled with recent solutions for UgeA (Dalrymple et al, submitted) and UgmA structures (van Straaten et al, *in preparation*) this will allow for prediction of amino acid residues that could be involved in UgeA-UgmA and UgmA-UgtA interactions. If these interactions occur, blocking them might create a phenotype similar to a gene deletion. This suggestion can be tested with site-directed mutagenesis.
3. This research used a suite of methods that can be adapted for rapid throughput analysis of chemical libraries that might potentially have antifungal activity. In particular, the disc

diffusion assay can be adapted to screen and compare the effect of candidate compounds for effect against wild type strains as well as those deleted for individual Gal*f* biosynthesis genes. If the latter show increased effect compared to wild type, this will suggest potential synergies in combination with Gal*f*-targeting compounds, assuming these are developed.

4. The pathogenicity of different Gal*f*-defective strains should be tested in tissue culture or animal model systems in comparison to wild type. There is controversy about the pathogenicity of *ugmA*Δ strains in animal models which needs to be resolved. Due to the cost and time involved in mouse model studies, a complementary strategy is to use animal tissue culture cells to study their response to wild type and Gal*f*-biosynthesis defective strains. Preliminary results, through collaboration with our group, showed that *ugmA*Δ strains cannot grow in tissue culture plates although the wild type can, suggesting that *ugmA*Δ strains will be less able to cause disease. Future developments in this area will include development of new animal pathogenicity model systems.

In summary, the research described in this thesis has presented a comprehensive study of three critical genes required for Gal*f* biosynthesis in the model experimental fungal system *Aspergillus nidulans*. The results clearly show that Gal*f* plays important roles in hyphal wall architecture, in cell growth, in surface-mediated interactions, and also in responses to currently available antifungal drugs. Although compounds that could inhibit function of these enzymes have yet to be generated, there is considerable reason for continuing to work in this area. In particular, the function of specific amino acids in the catalytic site of UgmA and UgeA will be assessed for function. This will be possible for two reasons. The deletion strain defects have been thoroughly described using cell morphometry and ultrastructure analysis, and their responses to antifungal drugs that are in clinical use. The *A. fumigatus* UgmA homologue GlfA and UgtA homologue GlfB were shown to functionally complement their respective *A. nidulans* deletion phenotypes. This will permit rapid characterization of the *in vivo* functions and interactions of these enzymes in a safe and environmentally tractable fungal model species.

References

Afroz, S., El-Ganiny, A., Sanders, D.A.R., Kaminskyj, S.G.W., 2011. Roles of the *Aspergillus nidulans* UDP-galactofuranose transporter, UgtA in wild type hyphal morphogenesis, conidiation, cell wall architecture and drug sensitivity. Fungal Genetics and Biology in press YFGBI2357.

Aimanianda, V., Latgé, J., 2010. Problems and hopes in the development of drugs targeting the fungal cell wall. Expert Review of Anti-infective Therapy 8, 359-364.

Anderson, J.B., 2005. Evolution of antifungal-drug resistance: mechanisms and pathogen fitness. Nat. Rev. Microbiol. 3, 547-556.

Arana, D.M., Prieto, D., Roman, E., Nombela, C., Alonso-Monge, R., Pla, J., 2009. The role of the cell wall in fungal pathogenesis. Microb. Biotechnol. 2, 308-320.

Bassetti, M., Righi, E., Viscoli, C., 2008. Novel beta-lactam antibiotics and inhibitor combinations. Expert Opin. Investig. Drugs 17, 285-296.

Beverley, S.M., Owens, K.L., Showalter, M., Griffith, C.L., Doering, T.L., Jones, V.C., McNeil, M.R., 2005. Eukaryotic UDP-galactopyranose mutase (*GLF* gene) in microbial and metazoal pathogens. Eukaryot. Cell. 4, 1147-1154.

Breakspear, A., Langford, K.J., Momany, M., Assinder, S.J., 2007. CopA:GFP localizes to putative Golgi equivalents in *Aspergillus nidulans*. FEMS Microbiol. Lett. 277, 90-97.

Carrillo-Muñoz, A.J., Giusiano, G., Ezkurra, P.A., Quindós, G., 2006. Antifungal agents: mode of action in yeast cells. Rev. Esp. Quimioter. 19, 130-139.

Chapman, S.W., Sullivan, D.C., Cleary, J.D., 2008. In search of the holy grail of antifungal therapy. Trans. Am. Clin. Climatol. Assoc. 119, 197-215

Chen, S.C., Playford, E.G., Sorrell, T.C., 2010. Antifungal therapy in invasive fungal infections. Current Opinion in Pharmacology 10, 522-530.

Costanzo, M., Baryshnikova, A., Bellay, J., Kim, Y., Spear, E.D., Sevier, C.S., Ding, H., Koh, J.L.Y., Toufighi, K., Mostafavi, S., Prinz, J., St. Onge, R.P., VanderSluis, B., Makhnevych, T., Vizeacoumar, F.J., Alizadeh, S., Bahr, S., Brost, R.L., Chen, Y., Cokol, M., Deshpande, R., Li, Z., Lin, Z., Liang, W., Marback, M., Paw, J., San Luis, B., Shuteriqi, E., Tong, A.H.Y., van Dyk, N., Wallace, I.M., Whitney, J.A., Weirauch, M.T., Zhong, G., Zhu, H., Houry, W.A., Brudno, M., Ragibizadeh, S., Papp, B., Pál, C., Roth, F.P., Giaever, G., Nislow, C., Troyanskaya, O.G., Bussey, H., Bader, G.D., Gingras, A., Morris, Q.D., Kim,

P.M., Kaiser, C.A., Myers, C.L., Andrews, B.J., Boone, C., 2010. The genetic landscape of a cell. Science 327, 425-431.

Cowen, L.E., 2008. The evolution of fungal drug resistance: modulating the trajectory from genotype to phenotype. Nature Reviews.Microbiology 6, 187-198.

Cowen, L.E., Steinbach, W.J., 2008. Stress, drugs, and evolution: the role of cellular signaling in fungal drug resistance. Eukaryot. Cell. 7, 747-764.

Damveld, R.A., Franken, A., Arentshorst, M., Punt, P.J., Klis, F.M., van den Hondel, C.A., Ram, A.F., 2008. A novel screening method for cell wall mutants in *Aspergillus niger* identifies UDP-galactopyranose mutase as an important protein in fungal cell wall biosynthesis. Genetics 178, 873-881.

De Arruda, M.V., Colli, W., Zingales, B., 1989. Terminal β-D-galactofuranosyl epitopes recognized by antibodies that inhibit *Trypanosoma cruzi* internalization into mammalian cells. Eur. J. Biochem. 182, 413-421.

Denning, D.W., 2003. Echinocandin antifungal drugs. The Lancet 362, 1142-1151.

Denning, D.W., Hope, W.W., 2010. Therapy for fungal diseases: opportunities and priorities. Trends Microbiol. 18, 195-204.

El-Ganiny, A.M., Sanders, D.A.R., Kaminskyj, S.G.W., 2008. *Aspergillus nidulans* UDP-galactopyranose mutase, encoded by *ugmA* plays key roles in colony growth, hyphal morphogensis, and conidiation. Fungal Genetics and Biology 45, 1533-1542.

El-Ganiny A.M., Sheoran I., Sanders D.A.R., Kaminskyj S.G.W., 2010. *Aspergillus nidulans* UDP-glucose-4-epimerase *ugeA* has multiple roles in wall architecture, hyphal morphogenesis, and asexual development. Fungal Genetics and Biology 47: 629-635

Engel, J., Schmalhorst, P.S., Dörk-Bousset, T., Ferrières, V., Routier, F.H., 2009. A single UDP-galactofuranose transporter is required for galactofuranosylation in *Aspergillus fumigatus*. J Biol. Chem. 284, 33859-33868.

Fortwendel, J.R., Juvvadi, P.R., Pinchai, N., Perfect, B.Z., Alspaugh, J.A., Perfect, J.R., Steinbach, W.J., 2009. Differential effects of inhibiting chitin and 1,3-β-D-glucan synthesis in Ras and calcineurin mutants of *Aspergillus fumigatus*. Antimicrob. Agents Chemother. 53, 476-482.

Fujioka, T., Mizutani, O., Furukawa, K., Sato, N., Yoshimi, A., Yamagata, Y., Nakajima, T., Abe, K., 2007. MpkA-dependent and -independent cell wall integrity signaling in *Aspergillus nidulans*. Eukaryotic Cell 6, 1497-1510.

Gauwerky, K., Borelli, C., Korting, H.C., 2009. Targeting virulence: a new paradigm for antifungals. Drug Discovery Today 14, 214-222.

Gough K.M., Kaminskyj S.G.W., 2010. sFTIR, Raman and Surface enhanced Raman spectroscopic imaging of fungal cells. In: *Vibrational Spectroscopic Imaging for Biomedical Applications* Gokul Srinivasan, Editor.

Hill, T.W., Loprete, D.M., Momany, M., Harsch, M., Livesay, J.A., Mirchandani, A., Murdock, J.J., Vaughan, M.J., Watt, M.B., 2006. Isolation of cell wall mutants in *Aspergillus nidulans* by screening for hypersensitivity to Calcofluor White. Mycologia 98, 399–409.

Hubbard, M.A., Kaminskyj, S.G., 2008. Rapid tip-directed movement of Golgi equivalents in growing *Aspergillus nidulans* hyphae suggests a mechanism for delivery of growth-related materials. Microbiology 154, 1544-1553.

Kaminskyj S., Heath I.B., 1996. Studies on *Saprolegnia ferax* suggest the importance of the cytoplasm in determining hyphal morphology. Mycologia 88: 20-37.

Kaminskyj S., Heath I.B., 1995. Integrin and spectrin homologues, and cytoplasm-wall adhesion in tip growth. Journal of Cell Science 108: 849-856.

Kelly, R., Register, E., Hsu, M., Kurtz, M., Nielsen, J., 1996. Isolation of a gene involved in 1, 3-β-glucan synthesis in *Aspergillus nidulans* and purification of the corresponding protein. J. Bacteriol. 178, 4381-4391.

Lamarre, C., Beau, R., Balloy, V., Fontaine, T., Sak Hoi, J. W., Guadagnini, S., Berkova, N., Chignard, M., Beauvais, A., Latgé, J., 2009. Galactofuranose attenuates cellular adhesion of *Aspergillus fumigatus*. Cell. Microbiol. 11, 1612-1623.

Lass-Florl, C., 2009. The changing face of epidemiology of invasive fungal disease in Europe. Mycoses 52, 197-205.

Latge, J.P., 2009. Galactofuranose containing molecules in *Aspergillus fumigatus*. Med. Mycol. 47 Suppl 1, S104-109.

Latge, J.P., 2007. The cell wall: a carbohydrate armour for the fungal cell. Mol. Microbiol. 66, 279-290.

Leitao, E.A., 2003. β-Galactofuranose-containing O-linked oligosaccharides present in the cell wall peptidogalactomannan of *Aspergillus fumigatus* contain immunodominant epitopes. Glycobiology 13, 681-692.

Loussert C., Schmitt C., Prevost M., Balloy V., Fadel E., Phillippe B., Kaufmann-Lacroix C., Latge J.P., Beauvais A., 2009 *In vivo* biofilm composition of *Aspergillus fumigatus*. Cel Microbiol doi: 10.1111/j.1462-5822.2009.01409.x

Luque, J.C., Clemons, K.V., Stevens, D.A., 2003. Efficacy of micafungin alone or in combination against systemic murine aspergillosis. Antimicrob. Agents Chemother. 47, 1452-1455.

Manavathu, E.K., Alangaden, G.J., Chandrasekar, P.H., 2003. Differential activity of triazoles in two-drug combinations with the echinocandin caspofungin against *Aspergillus fumigatus*. J. Antimicrob. Chemother. 51, 1423-1425.

Mellado, E., Aufauvre-Brown, A., Specht, C.A., Robbins, P.W., Holden, D.W., 1995. A multigene family related to chitin synthase genes of yeast in the opportunistic pathogen *Aspergillus fumigatus*. Mol. Gen. Genet. 246, 353-359.

Momany M., Lindsey R., Hill T.W., Richardson E.A., Momany C., Pedeira M., Guest G.M., Fisher J.F., Hessler R.B., 2004. The *Aspergillus fumigatus* cell wall is organized in domains that are remodelled during polarity establishment. Microbiology 150: 3261-3268.

Ostrosky-Zeichner, L., Casadevall, A., Galgiani, J.N., Odds, F.C., Rex, J.H., 2010. An insight into the antifungal pipeline: selected new molecules and beyond. Nat. Rev. Drug Discov. 9, 719-727.

Paul B.C., El-Ganiny A.M., Abbas M., Kaminskyj S.G.W., Dahms T.E.S., 2010. Quantifying the importance of galactofuranose in *Aspergillus nidulans* hyphal wall surface organization by atomic force microscopy. Eukaryotic Cell. 10, 646-653.

Petraitiene, R., Petraitis, V., Groll, A.H., Sein, T., Schaufele, R.L., Francesconi, A., Bacher, J., Avila, N.A., Walsh, T.J., 2002. Antifungal efficacy of caspofungin (MK-0991) in experimental pulmonary aspergillosis in persistently neutropenic rabbits: pharmacokinetics, drug disposition, and relationship to galactomannan antigenemia. Antimicrob. Agents Chemother. 46, 12-23.

Richards, M.R., Lowary, T.L., 2009. Chemistry and biology of galactofuranose-containing polysaccharides. Chembiochem 10, 1920-1938.

Sanders, D.A., Staines, A.G., McMahon, S.A., McNeil, M.R., Whitfield, C., Naismith, J.H., 2001b. UDP-galactopyranose mutase has a novel structure and mechanism. Nat. Struct. Biol. 8, 858-863.

Sanguinetti, M., Posteraro, P., Posteraro, B., 2010. Echinocandin antifungal drug resistance in *Candida* species: a cause for concern? Curr. Infect. Dis. Rep. 12, 437-443.

Schmalhorst, P.S., Krappmann, S., Vervecken, W., Rohde, M., Muller, M., Braus, G.H., Contreras, R., Braun, A., Bakker, H., Routier, F.H., 2008. Contribution of galactofuranose to the virulence of the opportunistic pathogen *Aspergillus fumigatus*. Eukaryot. Cell. 7, 1268-1277.

Shaw, B.D., Momany, M., 2002. *Aspergillus nidulans* polarity mutant swoA is complemented by protein O-mannosyltransferase pmtA. Fungal Genet. Biol. 37, 263-270.

Szeghalmi A., Kaminskyj S., Gough K.M., 2007. A synchrotron FTIR microspectroscopy investigation of fungal hyphae grown under optimal and stressed conditions. Analytical and Bioanalytical Chemistry, 387: 1779-1789

Van, D.H., Saag, M.S., Cloud, G.A., Hamill, R.J., Graybill, J.R., Sobel, J.D., Johnson, P.C., Tuazon, C.U., Kerkering, T., Moskovitz, B.L., Powderly, W.G., Dismukes, W.E., 1997. Treatment of Cryptococcal meningitis associated with the acquired immunodeficiency syndrome. N. Engl. J. Med. 337, 15-21.

Walker, L.A., Munro, C.A., de Bruijn, I., Lenardon, M.D., McKinnon, A., Gow, N.A., 2008. Stimulation of chitin synthesis rescues *Candida albicans* from echinocandins. PLoS Pathog. 4, e1000040.

Wheat, L.J., 2003. Rapid diagnosis of invasive aspergillosis by antigen detection. Transpl. Infect. Dis. 5, 158-166.

Appendix: Molecular biology techniques used in the thesis

1. DNA extraction and fusion PCR

1.1. gDNA extraction protocol

1. Inoculate 20 ml CM media in Petri plates with *A. nidulans* spores; incubate overnight at 37ºC (until the mycelia fill the plate).
2. Harvest mycelia by filtration through sterile paper towel, squeeze between several layers of paper towel to move extra water
3. Transfer into sterile microfuge tube, freeze in -80 ºC for 30 min then lyophilize overnight.
4. Break the lyophilized mycelia into fine powder using round toothpick
5. Transfer 100 µl of fine powder into fresh microfuge tube
6. Prepare fresh extraction buffer (pH 7.5-8) immediately before use as follow:

500 mM EDTA	100 µl
10% SDS	20 µl
ddH2O	880 µl

   (This will be enough for 2 samples, make more buffer if you have more samples)
7. Ad 500 µl extraction buffer per tube, Mix vigorously and transfer immediately to preheated 68ºC water bath.
8. Incubate at 68ºC for 10 min meanwhile chill KOAc solution on ice (60 ml 5M KOAc, 11.5 ml glacial acetic acid, 28.5 ml ddH2O).
9. Vortex microfuge tubes briefly, centrifuge 5 min at maximum speed
10. Transfer supernatant to fresh microfuge tube (using micropipette)
11. Add 30 µl chilled KOAc solution, leave on ice for 5 min the centrifuge for 5 min
12. Transfer supernatant into fresh microfuge tube
13. Add equal volume of phenol:chloroform:isoamyl alcohol using Pasteur pipette
14. Vortex 30s then microfuge for 2 min.
15. Transfer the upper layer to a fresh microfuge tube (**DO not** transfer the material at the interface).
16. Add equal volume of chloroform to the partially clean supernatant, vortex for 30s the centrifuge for 2 min

17. Transfer the upper layer to a fresh microfuge tube (**DO not** disturb the interface).
18. Add 600 µl isopropanol, vortex well, centrifuge for 5 min.
19. Pour off isopropanol then add 500 µl of 70% ethanol, vortex till the DNA pellet is not stuck, centrifuge for 5 min then decant supernatant and let the pellet dry.
20. Resuspended in 100 µl (containing 5 µl RNAse). May require heating to dissolve
21. Run agarose gel to check quality of DNA (sharp band) before proceeding into other steps.
22. The DNA should be cleaned using Qiagen columns before using it in PCR.

1.2. Fusion PCR

Fusion PCR is a technique that is used to fuse multiple DNA sequences together (typically three) to generate one construct that can be used for gene targeting (deletion, tagging and promoter exchange).

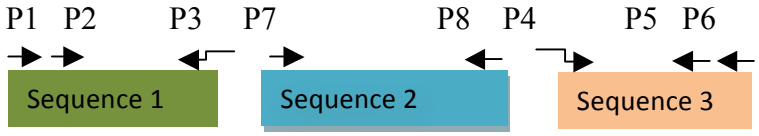

The fused sequences should have overlapping ends, so primers P3 and P4 are usually longer as they have tails (about 40 bases). P3 has a tail similar to reverse complement of P7 and P4 has a tail similar to the reverse complement of P8. The primers P2 and P5 are nested primers that are used in the fusion using Acuiprime high fidelity taq polymerase (Invitrogen) following manufacture instructions.

In case of gene deletion, the construct consists of 1 Kb upstream of the target gene (sequence 1), 1Kb of the downstream (sequence 3) plus the sequence of the selectable nutritional marker (sequence 2). In case of gene tagging with fluorescence protein (XFP), the construct consists of 1 Kb of your target gene, without the stop codon (sequence 1), 1 Kb of its downstream (sequence 3) and a sequence of 5GA-XFP + selectable marker (sequence 2), where 5GA is 5 repeats of glycine and alanine that used as linker between the gene and the XFP. For promoter exchange the construct consists of 1 Kb of the upstream of the target gene (sequence 1), 1 Kb of your target gene starting from ATG (sequence 3) and sequence 3 consists of selectable marker + conditional promoter (e.g. Af*pyrG* + *alcA*p).

When the fused constructs transformed into *A. nidulans* protoplasts, it is inserted in the genome by homologous recombination as sequence 1 & 3 were amplified from gDNA so they are identical to genomic sequences. Sequence 2 usually amplified from plasmid

Recipe for fusion PCR

DNA	1x3 µl
Primers (10µm)	1x2 µl
Taq polymerase	0.2 µl
Buffer (10x)	5 µl
Water	39.8 µl
Total	50 µl

2. RNA manipulation and qRT-PCR

2.1. RNA extraction

RNeasy plant kit (Qiagen) was used for RNA extraction from *A. nidulans* lyophilized mycelia, following the manufacturer instructions (everything should be RNase-free)

1. Inoculate *A. nidulans* spores in liquid CM media (2x 10^5 spores/ mL media), incubate at 37°C with shacking for 16 hr
2. Collect mycelia by centrifugation, remove supernatant and flash froze the pellet in liquid nitrogen. Lyophilize the mycelia overnight
3. Transfer the lyophilized hyphae to RNase free centrifuge tube (start with similar weight for all samples).
4. Broke the mycelia completely into fine powder using small pestle.
5. Add 450 µl RLC buffer (to which β-Mercaptoethanol was added), vortex vigourously
6. Transfer the lysate to QIAshredder spin column and centrifuge for 2 min at maximum speed.
7. transfer the supernatant to a new micro-centrifuge tube without disrupting the pellet
8. Add 0.5 volume 100% ethanol and mix immediately by pipetting, transfer directly to RNeasy spin column, centrifuge for 15s at 8000xg, discard the flow-through
9. Add 700 µl buffer RW1 to the column, close the lid gently and centrifuge for 15s at 8000xg, discard the flow-through.

10. Add 500 µl buffer RPE to the column, centrifuge for 15s at 8000xg, and discard the flow-through.
11. Add 500 µl buffer RPE to the column, centrifuge for 2 min at 8000xg, discard the flow-through
12. place the column in a new 2m collection tube, centrifuge for 1 min at maximum speed
13. place the RNeasy column in a new 1.5 micro-centrifuge tube, add 50 µl RNase-free water directly to the membrane, centrifuge for 1 min at 8000 xg
14. The eluted solution contains total RNA, measure the RNA concentration with Nanodrop and dilute to the appropriate concentration, aliquot and store in -20°C.

2.2. gDNA elimination and cDNA synthesis

Quantitect reverse transcription kit (Qiagen) was used to remove gDNA contamination and synthesize DNA first strand. This protocol is optimized to be used for up to 1 µg RNA. RNA should be diluted up to 500 ng/ µl.

For gDNA elimination follow the following steps

1. Thaw template RNA, gDNA Wipeout buffer and RNase-free water on ice
2. Prepare genomic DNA elimination reaction on ice as follow

gDNA Wipeout buffer 7x	2 µl
Template RNA (500 ng/µl)	2 µl
RNase-free water	10µl
Total	14 µl

3. Incubate for 2-3 min at 42°C, then place immediately on ice

For reverse transcription (cDNA synthesis) follow the following steps

4. Thaw Quantiscript Reverse Transcriptase, Quantiscript RT buffer and RT primer Mix on ice.
5. Prepare the reverse-transcription master mix as follow

Quantiscript Reverse Transcriptase	1 µl
Quantiscript RT buffer 5x	4 µl
RT primer Mix	1 µl
RNA from step 3	14 µl
Total	20 µl

6. Incubate for 15-30 min at 42 °C.
7. Incubate at 95°C for 3 min to inactivate the reverse transcriptase.
8. Measure the cDNA concentration, dilute as required (e.g. 1:10), aliquot and store in -20 °C, this cDNA can be used for qRT-PCR or cloning.

2.3. qRT-PCR procedur

QuantiTect SYBR Green kit (Qiagen) and IQ cycler (BioRad) were used for performing qRT-PCR. We determined the relative expression of *ugmA* in *alcA*(p)-*ugmA* strain compared to wild type in case of induction (CMT), intermediate expression (CMFT) and maximum repression (CM3G) using actin as a reference gene and ΔΔct to calculate the fold change in *ugmA* expression.

Procedure

1) Thaw QuantiTect SYBR Green PCR Master Mix, template cDNA, primers and nuclease-free water on ice.
2) The following recipe is used for 1 reaction

QuantiTect SYBR Green PCR Master Mix (2X)	10 µl
Primers (10 µm)	2x0.3
cDNA	3 µl
Nuclease free-water	6.4 µl
Total	20 µl

3) For each gene (Actin or *ugmA*) multiply the above recipe by 10 to make a cocktail for 10 reactions (3 technical replicates for wild type, 3 for mutant strain, 3 No template control (NTC) and 1 extra).
4) Mix all the ingredients (except cDNA) and divide equally into 3 tubes (A, B, C).
5) Add 10 µl cDNA to tube A (wild type) and B (mutant) and 10 µl water to tube C.
6) Mix and dispense 20 µl in the bottom of each well (of the 96-well plate).
7) Place the plastic film over the plate and carefully seal firmly, clean the surface with Kim wipes before putting in the IQ cycler.

3. DNA cloning

3.1. Cloning using restriction digest and ligation

1) The DNA fragment (insert) and the cloning plasmid (vector) should be cut using the same restriction enzymes to generate compatible ends.
2) Set up the following reaction mixtures

	Test	Negative control
Vector DNA	5 µl	5 µl
Insert DNA	5 µl	-
5X ligase buffer	4 µl	4 µl
Water	5 µl	10 µl
T4DNA ligase	1 µl	1 µl

3) Leave at room temperature at least for 2 hours or ligate overnight
4) Transform 10 µl of the rection mix into *E. coli* comptent cells, shake at 37°C for 1 hr
5) Spread 50-100 µl on LB plates + suitable antibiotics, incubate overnight at 37°C
6) Colonies on test plates can be used for plasmid extraction, negative control plates should have no colonies.

3.2. Cloning using TA TOPO cloning kit (Invitrogen)

TOPO cloning does not require restriction digest or ligation, the following steps are used (following the manufacturer's instructions)

1) Amplify the DNA fragment by PCR, end PCR reaction with a final 7-10 min extension step.
2) Set up the following 2 reactions

	Test	Negative control
Fresh PCR product	1 µl	-
Salt solution	1 µl	1 µl
Water	3 µl	4 µl
TOPO Vector	1 µl	1 µl

3) Mix gently and incubate both reactions for 5 min at room temperature
4) Place tubes on ice, and thaw One Shot *E. coli* cells
5) Add 2 µl of the TOPO cloning reaction to *E. coli* cells and mix gently

6) Incubate on ice for 30 min then heat-shoch the cells for 30 sec at 42°C
7) Add 250 µl of room temperature SOC medium to the *E. coli* cell
8) Cap the tubes and shake at 37°C for 1 h
9) Spread 40 µl of 40 mg/ml X-gal onto LB/ampicillin plates and incubate at 37°C to dry
10) Spread 50 µl transformed E. coli cells on the LB plates prepared in the previous step
11) Incubate plates overnight at 37°C, in the next day transformed colonies (white colonies) can be used for plasmid extraction, negative control plates should have blue or no colonies.